Computing and Artificial Intelligence

ACADEMIC
ACADEMIC PUBLISHING PTE LTD

2023 VOLUME 1 ISSUE 1
ISSN: 3029-2786 (Online)

https://ojs.acad-pub.com/index.php/CAI

1

Editorial Board

Editor-in-Chief

Associate Editor

Editorial Board Members

Volume 1 Issue 1 • 2023

Computing and Artificial Intelligence

Editor-in-Chief

Prof. Shaohua Wan

University of Electronic Science and Technology of China, China

ACADEMIC
ACADEMIC PUBLISHING PTE LTD

2023 | Volume 1 | Issue 1

Computing and Artificial Intelligence

https://ojs.acad-pub.com/index.php/CAI/index

Contents

Original Research Articles

Review Articles

Computing and Artificial Intelligence 2023; 1(1): 99.
Original Research Article

LINGO Profiles Fingerprint and Association Rule Mining for drug-target interaction prediction

Muhammad Jaziem Mohamed Javeed, Azwaar Khan Azlim Khan, Nurul Hashimah Ahamed Hassain Malim*

School of Computer Sciences, Universiti Sains Malaysia, Pulau Pinang 11800, Malaysia

*** Corresponding author:** Nurul Hashimah Ahamed Hassain Malim, nurulhashimah@usm.my

ARTICLE INFO

Received: 27 June 2023
Accepted: 18 July 2023
Available online: 22 August 2023

doi: 10.59400/cai.v1i1.99

ABSTRACT: The prediction of drug-target interactions (DTIs) using machine learning techniques together with the proper representation of compounds can speed up the time-consuming experimental work in predicting DTIs especially when a large dataset is used. Hence, in this paper, we have proposed a new molecular descriptor based on LINGO Profiles known as LINGO Profiles Fingerprint (LPFP). LPFP is used together with machine learning to predict DTIs on a ChEMBL dataset. Dimensionality reduction using Association Rule Mining (ARM) is also introduced to overcome the high dimensionality suffered by LPFP. LPFP managed to reach an equal accuracy reading to the state-of-the-art descriptor called ECFP4 (Δ0.18%), but it suffers in the time taken (Δ27 mins) due to the dimensionality problem mentioned. Hence, three new smaller size LPFPs (s = 60%, s = 70%, s = 80%) were constructed by only extracting the important fragments using ARM and then a benchmark analysis with the original LPFP and ECFP4 fingerprints was done. This study not only solved the dimensionality problem, but also managed to excel in both the accuracy and time taken when predicting DTIs. An increase in the accuracy of over 250 times faster than the original LPFP was observed after the benchmark analysis is performed. Furthermore, an accuracy of over 80% was achieved in three new activity classes that are acquired from ChEMBL, further proving the promising performance of ARM which has made it favourable for LPFPs to be used in DTI prediction and in other drug discovery problems.

KEYWORDS: LINGO Profiles Fingerprint (LPFP); Association Rule Mining (ARM); machine learning; dimensionality reduction; ECFP4; drug-target interactions

1. Introduction

During the past centuries, effort to discover new types of drugs was initiated because there were diseases or clinical conditions which required curable drugs to tackle the immediate menace as there was a shortage in the market for these medical products[1,2]. Due to the conventional methods of drug discovery as explained in the research of Hann and Green[3] are costly and time-consuming, the use of in silico methods to predict the interactions between drugs and target proteins provide a crucial leap for drug repositioning, as it can remarkably reduce wet-laboratory work and lower the cost of the experimental discovery of new drug-target interactions (DTIs)[4,5]. Tools such as machine learning created from the cheminformatics domain provide a

huge potential to go further in the drug design and discovery realm, as they serve the integration of information in several levels to enhance the reliability of data outcomes[4–7]. Generally, machine learning is used to develop classification models and these were used to distinguish active and inactive pairs of drug-like small molecule ligands and their respective target proteins with a higher accuracy[8]. The most common machine learning methods used in drug discovery are typically binary classifiers such as the Naïve Bayes classifiers used by Glick et al.[9] to predict DTIs, Artificial Neural Networks (ANNs) as depicted by Wen et al.[10] and Prado-Prado et al.[11], Support Vector Machines (SVM) by Nasution et al.[12] and Rodríguez-Pérez et al.[13], and Random Forests (RF) as observed by Riddick et al.[14] and Shi et al.[15].

In the works mentioned above[9–15], the use of the molecular descriptor, ECFP4 or Extended Connectivity Fingerprints of bond diameter 4 is very common. When the machine learning methods are evaluated, the superiority of ECFP4 can be seen clearly. In the SVM and Naïve Bayes classifiers, accuracy greater than 80% were recorded[9,12,13] while in ANN, the models developed with the use of ECFP4 managed to outperform other classification techniques such as Decision Trees and Random Forests[10]. The nature of ECFP4, which contains features that are significant to any type of compounds, allow the prediction of a drug to a protein target being made correctly. The convincing performance of ECFP4 makes other researchers in this field to use it as their main compound representation especially for the purpose of DTI prediction. However, in most chemical databases the compounds are usually represented in the SMILES format, or Simplified Molecular Input Line Entry System which is a string that represents a compound structure in the form of text[16]. SMILES is the most extensively used representation in drug discovery as it is easier to use and comprehend compared to other representations. The SMILES notation can be further converted into molecular descriptors such as ECFP4 for the purpose of drug-target interaction prediction, as briefly discussed above.

LINGO is also another representation of chemical compounds that was introduced in the study of Vidal et al.[16]. LINGO is a simple text-based method that calculates the molecular similarities and predicts the structure-related properties using the SMILES representation of a compound[17]. The LINGO method breaks down the canonical SMILES string into a set of substrings of defined length of four characters in which they are called LINGO Profiles or LINGOs[17]. Recently, LINGO Profiles have come into view of the drug discovery community as it provides the simplicity when retrieving the molecules from a database[16]. Hence, in this paper, we will be proposing a new molecular representation based on LINGO Profiles called LINGO Profiles Fingerprint (LPFP). LPFP is a binary vector of 0 s and 1 s whereby each position in the vector indicates the absence (0) or presence (1) of features predetermined in the design of the fingerprint of a specific compound.

Nonetheless, not much work has utilized LINGO Profiles in the prediction of DTIs, mainly due to the superiority of ECFP4. However, based on our previous work[18], we found out that LINGO Profiles gave a comparable performance to ECFP4 in the virtual screening experiment. Hence, we foresee the potential of LINGO Profiles to give a good accuracy in DTI prediction as well. The only drawback of the LINGO Profiles is that the number of LINGO Profiles generated depends on the length of the SMILES representation of a compound. Usually the longer the SMILES string, more LINGO Profiles are generated. Thus, the amount gets bigger when a greater number of compounds is used which will then burden the machine learning model even more as it had to process a huge number of fragments to predict DTIs. Therefore, it is often beneficial to reduce the dimension of the data that is being fed into the learning algorithms such as

adopting the Association Rule Mining (ARM) technique not only for reasons of computational efficiency but also to improve the accuracy of the analysis when high dimensional data is being used, as depicted in the studies of Siswanto et al.[19], Li et al.[20] and Malavika et al.[22]. Furthermore, dimensionality reduction can also help to deduce important facts and to discover new findings that might be useful for the drug discovery community in future[22–25].

Hence, in this paper we will benchmark our proposed molecular descriptor called LINGO Profiles Fingerprint (LPFP) with ECFP4 when performing DTI prediction and evaluate the performance of LPFP in terms of the accuracy and time taken as to how efficient LPFP works with the use of the Association Rule Mining (ARM) technique to reduce the dimension of LPFP to only include significant features for efficient prediction of drug-target interactions.

2. Proposed methodology

The proposed methodology is depicted in **Figure 1**.

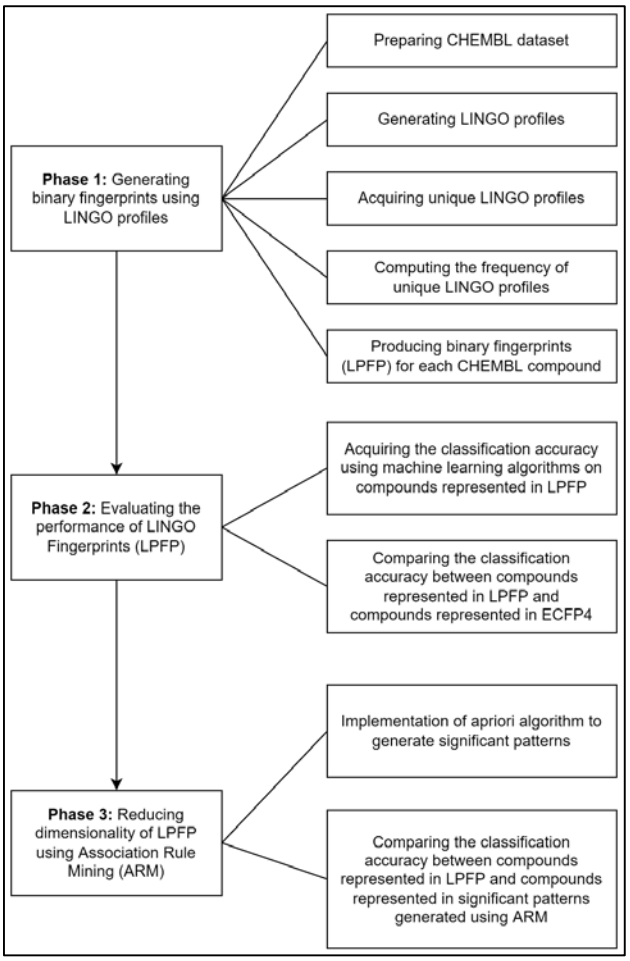

Figure 1. The overall framework of the three main phases involved in all the experiments conducted in this study in generating LPFPs and using ARM to reduce the dimensionality of the fingerprints.

2.1. Phase 1: Generating Binary Fingerprints (LPFP) using LINGO Profiles

The general idea of creating binary fingerprints using LINGO Profiles is to encode the structural information of a chemical compound into bit strings and then splitting the molecule into multiple fragments. If a fragment is present in the chemical compound, the corresponding bit will be assigned to '1' and if a fragment is absent, the bit will be assigned to '0' as depicted in **Figure 2**. The occurrence of a fragment determines the bit, not the number of times the same fragment occurs in the structure. For instance, a fragment will be set only to bit '1' no matter if it is present once or ten times. Therefore, the number of different types of fragments decide the number of bits set in the binary fingerprints. The fragment here is referring to one LINGO Profile. From the LINGO Profiles generated, the duplicated ones are first removed. Then, we sorted the fragments based on the number of occurrences in a decreasing order. This is important as the fragment with a higher frequency sits on the lower bit position while the fragment with a lower frequency sits on the higher bit position of the respective fingerprint. The process of generating LPFPs are discussed in detail in the subsections that follow.

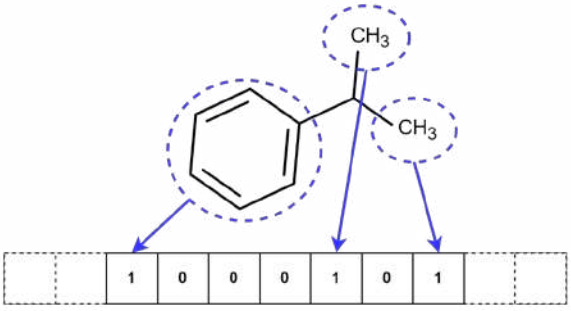

Figure 2. Encoding a chemical compound structure into bit strings of 0 s and 1 s.

2.1.1. Preparing ChEMBL dataset

The first step in Generating Binary Fingerprints called LINGO Profiles Fingerprints (LPFPs) is to prepare the dataset. In this study, we have decided to use the ChEMBL database[26]. The database contains a huge number of drug-like compounds, including over 2.3 million compounds and over 15,000 target proteins and activity classes as well as information on the compounds that were tested and its structures and abstracted bioactivities. The special characteristics possessed by the activity classes in ChEMBL are due to the ligands within it that interacts with certain target proteins.

There are two main categories to which a particular activity class can be classified into and they are known as homogenous and heterogenous. Classes whose compounds share a large number of common fragments are called homogenous. Whereas on the contrary, classes with fewer common fragments that are shared between their compounds are described as heterogeneous. The structure of the compounds within a particular activity class decides which category an activity class belongs to. Since it is a difficult task to observe and analyse each and every compound structure, we have calculated the Mean Pairwise Similarity (MPS) value for each activity class, which can be computed using Equation (1) that is also found and used in the study of Arif et al.[27]:

$$MPS = \frac{Similarity\ Value}{Number\ of\ Actives\ in\ the\ Activity\ Class} \quad (1)$$

The MPS value can be defined as the similarity of chemical structures within each activity class. The MPS reading for an activity class can be obtained by performing pairwise similarity between one random reference structure and every other compound in the activity class using the Tanimoto coefficient. A higher MPS value indicates homogenous activity classes while a lower MPS value indicates heterogeneous activity classes. Six activity classes with different number of compounds were selected and their respective MPS values were computed and they are shown in the table below.

Table 1 shows the homogeneous and heterogeneous activity classes with their respective MPS values that were calculated. It is also important to note that intermediate activity classes refer to activity classes in which their MPS values ranges between the homogenous and heterogenous activity classes. After categorizing the activity classes into homogeneous, intermediate and heterogeneous classes, it is time for us to generate the LINGO Profiles for each compound in all the activity classes.

Table 1. Homogenous and heterogeneous activity classes together with their respective number of compounds and MPS values.

ID	Type	Activity classes	Number of compounds	MPS value
12659	Homo	Prostanoid DP receptor	204	0.21355893
117		Somatostatin receptor 2	62	0.21584493
20174	Inter	G protein-coupled receptor 44	1244	0.17281741
130		Dopamine D3 receptor	1540	0.17229444
52	Hetero	Alpha-2a adrenergic receptor	420	0.15204343
11365		Cytochrome P450 2D6	534	0.15767914

2.1.2. Generating LINGO Profiles

The SMILES representation of each compound for each activity class, as depicted in **Figure 3**, is important for us in order to generate LINGO Profiles.

```
1  CCc1cccc2c3CCOC(CC)(CC(=O)O)c3[nH]c12
2  CSc1ccc(cc1)C(=O)c2[nH]c(=O)[nH]c2C
3  COc1cccc2C(=O)c3c(O)c4CC(O)(CC(OC5CC(N)C(OC6CCCCO6)C(C)O5)c4c(O)c3C(=O)c12)C(=O)CO
4  COC1CN(CCCOc2ccc(F)cc2)CCC1NC(=O)c3cc(Cl)c(N)cc3OC
5  CC(CSC(=O)C)C(=O)N1CCCC1C(=O)NC(Cc2ccccc2)C(=O)O
6  NCCCNCCCCNC(=O)C(O)NC(=O)CCCCCCNC(=N)N
7  CCCOC1C(O)C(OCC)OC1C(COCc2ccc(Cl)cc2)OCc3ccc(Cl)cc3
8  CCC(NC(C)C)C(O)c1ccc(O)c2[nH]c(=O)ccc12
9  CC(N)C(=O)OC(C(=O)NC1C2SCC(=C(N2C1=O)C(=O)OCc3oc(=O)oc3C)CSc4nnc(C)s4)c5ccccc5
10 CN1CC(Cn2nc(C)c3CCCc32)C=C4C1Cc5c[nH]c6cccc4c56
11 CCn1c(cc(=Nc2c(C)cc(C)cc2C)n(C)c1=O)c3ccc(OC)c(OC)c3
12 CC(C)COc1ccccc1Nc2ncc(C(=O)O)c(=O)[nH]2
13 CCOc1ccccc1Nc2ncc(C(=O)O)c(=O)[nH]2
14 CCCOc1ccccc1Nc2ncc(C(=O)O)c(=O)[nH]2
15 CC(C)Oc1ccccc1Nc2ncc(C(=O)O)c(=O)[nH]2
16 CCCCOc1ccccc1Nc2ncc(C(=O)O)c(=O)[nH]2
17 CCOC(=O)Cc1nc(oc1c2ccco2)c3ccc(Cl)cc3
18 Oc1cc(O)c2cc(O)c([o+]c2c1)c3ccc(O)c(O)c3
19 Nc1cc(Cl)ccc1N2CCSC2=N
20 CC(C)NCC(O)c1ccc(N)c(C#N)c1
21 CC(C)C1NC(=O)C(CCCCN)NC(=O)C(Cc2c[nH]c3ccccc23)NC(=O)C(Cc4ccc(O)cc4)NC(=O)C(C)N(C)C(=O)C(Cc5ccccc5)NC1=O
22 CC(C)(C1CC1)C(O)(Cn2cncn2)c3ccc(Cl)cc3
23 CC(NC(=O)C(S)Cc1ccccc1)C(=O)N2CCCC2C(=O)O
24 COc1ccc(cc1OC)C(O)CN2CCN(CC2)C(c3ccccc3)c4ccccc4
25 CCC(OC(=O)CC)c1nc2c(cccc2c(O)c1C(=O)Nc3nccs3)C(F)(F)F
26 CC(CCc1ccc(cc1)C(=O)N)N(CC(O)c2ccccc2)CC(O)c3ccccc3
27 CCCC12Cc3cc(OCC(=O)O)c(Cl)c(Cl)c3C2=CC(=O)CC1
```

Figure 3. An example of several compounds in our ChEMBL dataset with their respective SMILES notation.

With SMILES, we are able to fragment it into overlapping substrings of a fixed size known as LINGOs. In other words, LINGO Profiles are the hologram of the SMILES representation of a molecule in which they are generated by fragmenting the SMILES notation into a fixed size. Before fragmenting the SMILES notation, all element names composed of two characters in the original SMILES are substituted by the names of one character[17]. For example, the 'Cl' and 'Br' present in the SMILES notations are replaced with 'L' and 'R' respectively and the ring numbers are set to '0'. For instance, 'c1ccccc1' and 'c2ccccc2' will be represented as 'c0ccccc0'. The reason for this normalization of the SMILES string is to reduce the number of possible LINGOs to be generated and it prevents, in general, a unique reconstruction of the original SMILES representation from its holographic representation (LINGOs).

After the normalization process is completed, the simplified SMILES strings will then undergo the fragmentation phase. A total number of $n - (q - 1)$ substrings (fragments) of length q is extracted from a SMILES string of length n. The length of q that we will be using is 4, as it is optimal and as every ASCII character can be encoded into 8 bits, a LINGO of size 4 can be encoded into 32 bits of information, which is precisely the size of a word on common hardware. A q-LINGO is a q-character string, including letters, numbers and symbols such as '(', ')', '[', ']' and '#' and it is obtained by stepwise fragmentation of a canonical SMILES representation of all the compounds. This process was done using Java programming and at the end of the fragmentation process, the compounds in each of the activity class will have LINGO Profiles assigned to them in the output file as depicted in **Figure 4**.

```
162085, COC(, OC(=, C(=O, (=O), =O)C, O)C(, )C(N, C(NC, (NC(, NC(=, C(=O, (=O), =O)C, O)C(, )C(N, C(NC, (NC(, NC(=, C(=O,
168103, CC(C, C(C), (C)(, C)(C, )(C), (C)N, C)NC, )NC(, NC(=, C(=O, (=O), =O)C, O)C0, )C0C, C0CC, 0CC0, CC0C, C0CC, 0CCC,
173595, CC(C, C(C), (C)(, C)(C, )(C), (C)O, C)OC, )OC(, OC(=, C(=O, (=O), =O)N, O)NC, )NC(, NC(C, C(Cc, (Cc0, Cc0c, c0cc,
187239, NC(=, C(=O, (=O), =O)C, O)CC, )CC(, CC(N, C(NC, (NC(, NC(=, C(=O, (=O), =O)c, O)c0, )c0c, c0cc, 0ccc, ccc0, cc0c,
187249, CC(C, C(C), (C)C, C)CN, )CN(, CN(C, N(CC, (CC(, CC(O, C(O), (O)C, O)C(, )C(C, C(Cc, (Cc0, Cc0c, c0cc, 0ccc, cccc,
188524, CSCC, SCC(, CC(N, C(NC, (NC(, NC(=, C(=O, (=O), =O)C, O)CO, )COc, COc0, Oc0c, c0cc, 0ccc, cccc, ccc0, cc0c, c0cn,
193112, CC(C, C(C), (C)(, C)(C, )(C), (C)N, C)NC, )NC(, NC(=, C(=O, (=O), =O)c, O)c0, )c0c, c0cc, 0ccc, cccc, cccc, ccc0,
194144, CC(C, C(C), (C)C, C)C(, )C(N, C(NC, (NC(, NC(=, C(=O, (=O), =O)C, O)C(, )C(C, C(Cc, (Cc0, Cc0c, c0cc, 0ccc, cccc,
194611, CC(C, C(C), (C)C, C)C=, )C=C, C=CC, =CC(, CC(=, C(=O, (=O), =O)C, O)C(, )C(C, C(CC, (CC(, CC(O, C(O), (O)C, O)C(,
194658, OC(C, C(CC, (CC(, CC(C, C(Cc, (Cc0, Cc0c, c0cc, 0ccc, cccc, cccc, ccc0, cc0), c0)C, 0)C(, )C(=, C(=O, (=O), =O)N,
194899, CCCC, CCCC, CCCC, CCCC, CCCC, CCCC, CCCC, CCC0, CC00, C0OC, 0OC0, OC0C, C0C(, 0C(=, C(=O, (=O), =O)N, O)N0, )N0C,
194953, COc0, Oc0c, c0cc, 0ccc, ccc(, cc(C, c(CC, (CC(, CC(C, C(CC, (CC(, CC(O, C(O), (O)C, O)C(, )C(C, C(Cc, (Cc0, Cc0c,
195387, CC(C, C(C), (C)C, C)C(, )C(N, C(NC, (NC(, NC(=, C(=O, (=O), =O)O, O)OC, )OCc, OCc0, Cc0c, c0cc, 0ccc, cccc, cccc,
195644, OC(C, C(CC, (CC(, CC(C, C(Cc, (Cc0, Cc0c, c0cc, 0ccc, cccc, cccc, ccc0, cc0), c0)C, 0)C(, )C(=, C(=O, (=O), =O)N,
196026, COc0, Oc0c, c0cc, 0ccc, ccc(, cc(C, c(CN, (CNC, CNC(, NC(C, C(C(, (C(O, C(O), (O)C, O)C(, )C(C, C(Cc, (Cc0, Cc0c,
196618, COc0, Oc0c, c0cc, 0ccc, cccc, ccc(, cc(C, c(CN, (CNC, CNC(, NC(C, C(C(, (C(O, C(O), (O)C, O)C(, )C(C, C(Cc, (Cc0,
196619, COc0, Oc0c, c0cc, 0ccc, ccc(, cc(C, c(CN, (CNC, CNC(, NC(C, C(C(, (C(O, C(O), (O)C, O)C(, )C(C, C(Cc, (Cc0, Cc0c,
196620, CC(C, C(C), (C)C, C)C(, )C(N, C(NC, (NC(, NC(=, C(=O, (=O), =O)O, O)OC, )OCc, OCc0, Cc0c, c0cc, 0ccc, cccc, cccn,
196621, CC(C, C(C), (C)C, C)C(, )C(N, C(NC, (NC(, NC(=, C(=O, (=O), =O)C, O)C(, )C(N, C(NC, (NCc, NCc0, Cc0c, c0cc, 0ccc,
196622, CC(C, C(C), (C)C, C)C(, )C(N, C(NC, (NC(, NC(=, C(=O, (=O), =O)C, O)C(, )C(N, C(NC, (NCc, NCc0, Cc0c, c0cc, 0ccc,
196623, CC(C, C(C), (C)C, C)C(, )C(N, C(NC, (NC(, NC(=, C(=O, (=O), =O)O, O)OC, )OCc, OCc0, Cc0c, c0cc, 0ccc, cccc, cccc,
196624, CC(C, C(C), (C)C, C)C(, )C(N, C(NC, (NC(, NC(=, C(=O, (=O), =O)O, O)OC, )OCc, OCc0, Cc0c, c0cc, 0ccc, cccc, cccc,
196625, CC(C, C(C), (C)C, C)C(, )C(N, C(NC, (NC(, NC(=, C(=O, (=O), =O)C, O)C(, )C(N, C(NC, (NCc, NCc0, Cc0c, c0cc, 0ccc,
196723, CC(C, C(C), (C)C, C)CC, )CCC, CCC(, CC(=, C(=O, (=O), =O)C, O)C(, )C(C, C(CC, (CC(, CC(O, C(O), (O)C, O)C(, )C(C,
196724, CC(C, C(C), (C)(, C)(C, )(C), (C)O, C)OC, )OC(, OC(=, C(=O, (=O), =O)N, O)NC, )NC(, NC(C, C(Cc, (Cc0, Cc0c, c0cc,
196725, CC(C, C(C), (C)(, C)(C, )(C), (C)O, C)OC, )OC(, OC(=, C(=O, (=O), =O)N, O)NC, )NC(, NC(C, C(Cc, (Cc0, Cc0c, c0cc,
196896, CC(C, C(C), (C)(, C)(C, )(C), (C)N, C)NC, )NC(, NC(=, C(=O, (=O), =O)C, O)C0, )C0C, C0CC, 0CC0, CC0C, C0CC, 0CCC,
197916, CC(C, C(C), (C)C, C)C(, )C(C, C(CC, (CC(, CC(O, C(O), (O)C, O)C(, )C(C, C(CC, (CC0, CC0C, C0CC, 0CCC, CCCC, CCCC,
```

Figure 4. An example of several compounds in our ChEMBL dataset together with their respective LINGO Profiles and ID.

2.1.3. Acquiring unique LINGO Profiles

After generating LINGO Profiles for all the compounds in all activity classes, unique LINGO Profiles must be acquired. A Java program was developed for the purpose of extracting unique LINGO Profiles per compound. The unique LINGO Profiles in this context means that there will be no duplicates that will be generated at a different output file. These unique LINGO Profiles that will be produced are in distinct format as we have already removed an identical version of a specific LINGO Profile earlier. This procedure is important as the information obtained here will be used as an input when calculating the frequency of

occurrences for all the unique LINGO Profiles generated in order to create binary fingerprints of LINGO Profiles called LPFPs.

2.1.4. Computing the frequency of unique LINGO Profiles

The next step is to compute the frequency of the occurrences of each unique LINGO Profile because this will act as a template for us to generate the fingerprints. Besides, the information obtained here will allow us to determine specifically which LINGO Profiles are the most significant in the ChEMBL dataset. In order for us to compute the frequency of unique LINGO Profiles, two output files are compared whereby the list of LINGO Profiles obtained for all compounds in our ChEMBL dataset are considered as one file (refer to Section 2.1.2) and the other file contains only the unique LINGO Profiles for all compounds in our ChEMBL dataset (refer to Section 2.1.3). The final output file produced is a sorted list of unique LINGO Profiles based on their computed frequency. The results of the frequency of occurrences of all the unique LINGO Profiles are discussed in the results section later.

2.1.5. Producing binary fingerprint for each compound in ChEMBL dataset

The final step is to finally produce the binary fingerprints. The binary fingerprints will be of length 10,000 and they consist of 0 s and 1 s, whereby the '0' bit represents the absence of the unique LINGO Profile while the '1' bit represents the unique LINGO that is present in the compound. The sample output of the LPFPs generated are as shown in **Figure 5**.

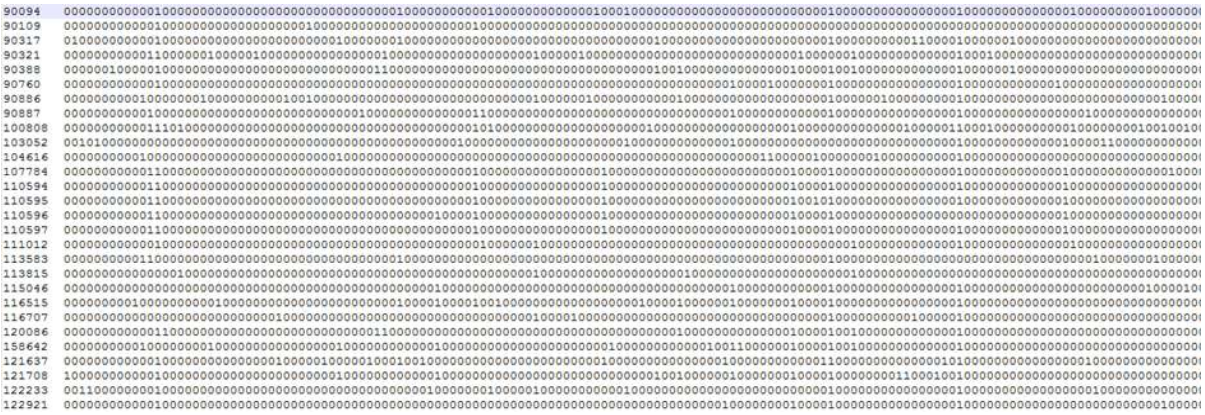

Figure 5. Part of the ChEMBL dataset which display LINGO Profiles Fingerprints (LPFP) and its respective index number for several compounds.

2.2. Phase 2: Evaluating the performance of LINGO Profiles Fingerprints (LPFPs)

2.2.1. Selecting an appropriate machine learning model

In this phase, four machine learning models are developed based on Artificial Neural Networks (ANN), Support Vector Machine (SVM), Naïve Bayes (NB) and Random Forest (RF).

Table 2 shows the size of the machine learning models created when the two molecular descriptors, ECFP4 and LPFP are used. From **Table 2**, it is observed that when ECFP4 is used, we have managed to build all the four predictive models. SVM recorded the lowest model size of about 15 to 30 MB, while ANN registered the highest model size of over 1000 MB. Furthermore, the NB and RF classifiers both have a similar range of model size of about 100 to 200 MB.

Table 2. The comparison of the all the machine learning models' size created using the molecular descriptors ECFP4 and LPFP.

Machine learning models	Size of the model when using ECFP4 (MB)	Size of the model when using LPFP (MB)
ANN	>1000	N/A
SVM	15–30	700–800
NB	100–200	N/A
RF	100–200	N/A

On the other hand, it is interesting to note that only the SVM model was able to be developed using the compounds represented in LPFP. The huge number of features in LPFP, which is ten times more than the features of ECFP4, hindered us to develop the ANN, NB and RF models despite having a large storage space (1 TB) and a competent amount of memory (8 GB) in our machine. Upgrading our machine to a better specification might help us to overcome the problem. However, if the size of the ChEMBL dataset grows bigger, the number of features in the LPFP-represented compounds will also increase.

In other words, the increase in the number of features in LPFP will result in the same problem whereby the machine learning models could not be built due to its huge size in MB. Thus, to perform the DTI prediction using our proposed molecular descriptor, LPFP, we should have a model which is available for this purpose. The unavailability of the ANN, NB and RF models in LPFP and the convincing performance of the SVM classifier in the studies of Nasution et al.[12], Rodríguez-Pérez et al.[13] and that of Heikamp and Bajorath[28] in terms of DTI prediction and drug discovery has convinced us to use the latter for later experiments. Additionally, from **Table 2**, it is also observed that the SVM classifier is the only classifier in which it could be developed for both ECFP4 and LPFP. Hence, SVM is our model of choice

2.2.2. Measuring the performance of ECFP4 and LPFP

To measure the performance of ECFP4 and LPFP in terms of drug-target interaction prediction, the ChEMBL dataset is split into training and testing sets respectively, whereby 70% off the dataset is put aside for training while the remaining 30% is for testing. Furthermore, *k*-fold cross-validation was also applied to the SVM model when performing DTI prediction with the value of *k* is 10 to avoid overfitting. The classification accuracy and the time taken for the compounds represented in LPFP will be recorded per activity class and this process is repeated six times to accommodate all the six ChEMBL activity classes selected as observed in **Table 1**.

Since we have already converted the original SMILES notation of all compounds in our ChEMBL dataset to LINGO Profiles Fingerprints as proposed, it is also vital for us to convert the original SMILES notations of all the compounds in our dataset into ECFP4 fingerprints to be compared with LPFP. Hence, the Chemistry Development Kit (CDK)[29] was used to convert SMILES to ECFP4 and the classification accuracy and the time taken for the compounds represented in ECFP4 will also be recorded separately. Then, at the end of the experiment, the results of the performance and time taken for the compounds represented in LPFP will be benchmarked with the performance and time taken for the compounds represented in ECFP4 respectively.

2.3. Phase 3: Reducing dimensionality of LPFP using Association Rule Mining (ARM)

2.3.1. Implementation of the Apriori algorithm to generate significant patterns

In data mining, association rules are rules that relate one thing to another thing in which two things are closely interrelated[19]. In the context of our work, drug-target interaction prediction is an association-based task in which we are to find drug-target pairs from a list of compounds. Since we have already represented the compounds of all six activity classes in our ChEMBL database as LINGO Profiles in Phase 1, we will now generate significant rules using the Association Rule Mining (ARM) technique. To do so, we have set the *minsupp* and *minconf* parameter to 0.6 and 0.8 respectively before implementing the algorithm on each of the activity class. It is also important to remember that each rule generated is not represented with their ID, since we have already removed the ID from each LINGO Profiles in Phase 1, before performing the experiment. Each LINGO Profile is then inserted into their respective vector space without their ID. Furthermore, rules that pass the threshold level are chosen at the end of the experiment because we believe that it may contain important knowledge in the prediction of DTIs. The rules obtained for each activity class are used to represent all the compounds available in the respective activity class. Additionally, the rules that meet the minimum support and confidence level are then divided into three main categories.

The first category gathers all the rules that have a support level of over 60% ($s = 60\%$). Then, it is followed by the second category whereby it gathers all the rules that have a support level of over 70% ($s = 70\%$) and finally rules that have a support level of 80% ($s = 80\%$) are accumulated together. From each category, fragments are filtered accordingly to eliminate duplicates, and then the unique fragments are used to represent all the compounds in the ChEMBL dataset by encoding them in a binary format. Once the unique fragments are encoded in a binary format, the data is separated into training and testing sets of proportion 70:30, similar to the previous phase and the data is fed into a machine learning algorithm (SVM) in order to predict DTIs. The performance of the model is evaluated in terms of its accuracy and it is then compared with the accuracy of the compounds represented in LPFP which was recorded in Phase 2. In other words, the comparison is done between the compounds represented in significant patterns generated using ARM and the compounds represented in LPFPs.

3. Results and discussion

3.1. Frequency of occurrences of unique LINGO Profiles

The results in this section pertains to the output file obtained from the sorted list of unique LINGO Profiles based on their computed frequency (refer to Section 2.1.4) and they are divided into two categories; the Higher Category and Lower Category. In **Figure 6**, we discovered high frequency (Higher Category) fragments that are frequently present in almost all of the compounds in the ChEMBL dataset.

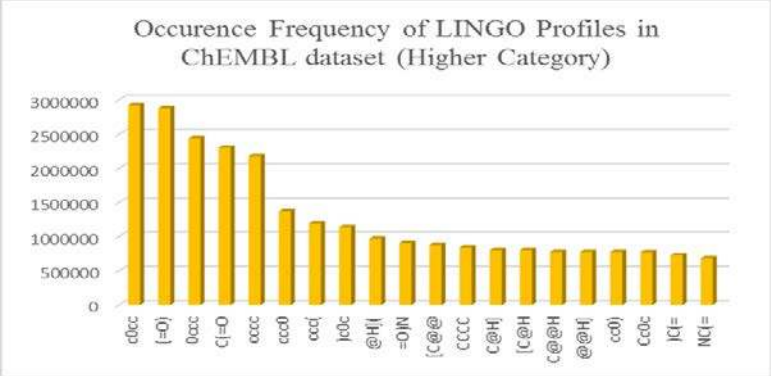

Figure 6. The frequency of occurrences of LINGO Profiles in the ChEMBL dataset (Higher Category).

In addition, repeated occurrence of a particular fragment can be seen in a compound. The fragment with highest frequency of occurrences is 'c0cc', which occurs 2,923,854 times. It was then followed by the fragments '(=O)', '0ccc', 'C(=O' and 'cccc' appearing exactly 2,878,863, 2,436,870, 2,299,177 and 2,176,560 times respectively. A significant change can be observed in the figure wherein the difference between one fragment to another is between the range of 100,000 to 400,000. Nonetheless, there are still other fragments that are in the million range and they are 'ccc0', 'ccc(' and ')c0c' occurring at 1,367,947, 1,194,443 and 1,137,386 times respectively. Going down the list are the fragments that exist in the hundred-thousand range. The '@H](' fragment is the highest in this sub-category appearing 965,532 times followed by the fragments '=O)N', '[C@@', 'CCCC', 'C@H]', '[C@H', 'C@@H', '@@H]', 'cc0)', 'Cc0c', ')C(=' and 'NC(=', whereby the differences between them are recorded at a range of 100,000 to 300,000. Thus, we can simply conclude that the fragments in this category are gradually changing at a very high rate.

Next, **Figure 7** visualises the frequency of occurrences of the Lower Category fragments or fragments that appear less frequently in all the compounds in our ChEMBL dataset. In other words, the fragments that belongs to this category does not occur as much as those fragments in the Higher Category did. In fact, the probability of the presence of these fragments in any of the compounds in ChEMBL are very low. There are certain compounds which do not even have the fragments depicted in **Figures 6** and **7**. Apart from this, it is also observed that there are no repeated occurrences involving fragments from this category. The fragments from this category are '[Hg+', 'Hg+]', 'g+]c', '(O[H', '-]B0', ']B0O', 'O=[F', '=[Fe', 'Fe]O', 'e]O[', ']O[F', 'O[Fe', 'Fe]=', '[Au-', 'Au-]', 'u-]S', '-]SS', ']SS(', '.O[H', 'Hg]C' and 'g]C0'. Interestingly, they all share the same occurrence frequency which is '1'. This means that the fragment only appears once in any of the compounds in the dataset and once they appear in any of the compounds in the dataset, they will not appear again in the remaining compounds. The difference in the occurrence frequency between the fragments in this category (Lower Category) and the fragments from the Higher Category is very large.

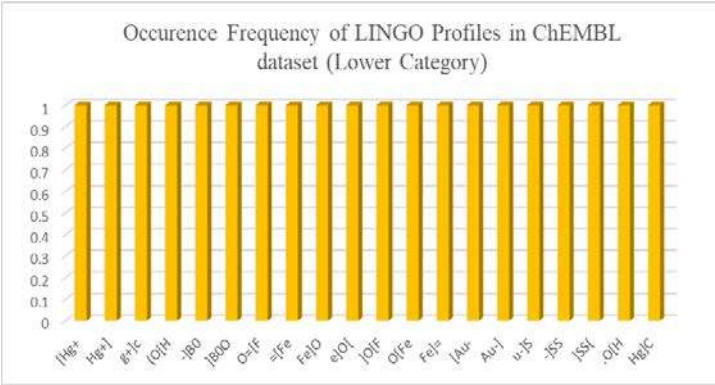

Figure 7. The frequency of occurrences of LINGO Profiles in the ChEMBL dataset (Lower Category).

Moreover, the fragments with a higher frequency of occurrence (Higher Category) tells us that despite the extensive diversity of the ChEMBL dataset, they are present in the majority of the compounds, thus, they play a crucial role in determining the behaviours and characteristics of the compound itself. For example, one of the techniques in virtual screening called similarity searching requires the comparison between a reference structure and the compounds from the database to be done in order to determine the properties of the reference structure. In this case, the fragments that exist in both the reference structure and the database compound plays a huge role as higher coefficient scores between both of them proves that they share certain chemical properties together. Besides, the majority of the compounds in the activity classes that we have selected in this study contains those fragments. This means that the interaction between the compounds with a particular target protein (activity class) are affected by the presence of these fragments.

For the fragments with a lower frequency of occurrence (Lower Category), the extremely low probability of their occurrence in the compounds proof that these fragments did not play a part in determining the behaviour or characteristics of a compound in the ChEMBL dataset. In addition, the lower number of repeated fragments from this category in a particular compound gives us the evidence that those fragments do not solely involve in determining the behaviour or characteristics of a specific compound as it is constantly outnumbered by the fragments from the Higher Category. In terms of drug-target interactions, some activity classes do not even have the fragments from this category in their compounds. The absence indicates that some compounds do not even need those fragments in order to establish an interaction with a particular target protein. Hence, we can conclude that, the fragments from the Higher Category are much more important than the fragments in the Lower Category. From the information that we have obtained above, we have created binary fingerprints or LPFP which consists of unique fragments ranging from the Higher and the Lower categories as to represent the compounds involved in the predicting DTIs and assessing their performance using LPFPs.

3.2. LINGO Profiles Fingerprints (LPFPs) generated

As discussed in Section 2.1.5, binary fingerprints of length 10,723 are generated at the end of Phase 1 (refer to **Figure 5**). The binary fingerprints consist of 0 s and 1 s, in which the '0' bit indicates the absence of a unique LINGO Profile while the '1' bit indicates the presence of a unique LINGO Profile. A sample portion of the LPFP of a compound with the presence and absence of a unique LINGO Profile is visualised in the figure below (refer to **Figure 8**).

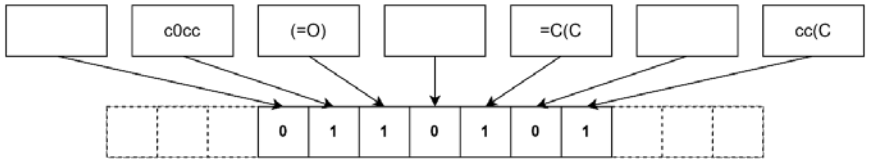

Figure 8. A portion of a LINGO Profile Fingerprint (LPFP) obtained from a compound from our ChEMBL dataset.

3.3. Comparison between the performance of ECFP4 and LPFP

As discussed in Section 2.2, the results of the performance and time taken for the compounds represented in LPFP will be benchmarked with the performance and time taken for the compounds represented in ECFP4. In this section, the said results will be compared, discussed and analysed thoroughly.

From **Table 3**, it is evident that different categories of activity classes (homogenous, heterogeneous and intermediate) produce distinct accuracy values for both descriptors, ECFP4 and LPFP. When LPFP is used, the activity class, Somatostatin receptor 2, recorded the highest accuracy value of 99.01% while Dopamine D3 receptor managed to only achieve 62.81% accuracy (the lowest among all the six activity classes) when SVM was used for its classification purposes. Further investigation led us to the observation of the pattern created among all the activity classes. It turns out that the SVM classifier together with the proposed LPFP representation of the compounds work best on homogenous activity classes, followed by heterogeneous activity classes and finally the intermediate activity classes. There was only a small difference between the average accuracy of heterogeneous and homogenous activity classes. However, a huge gap was recorded between the intermediate activity classes and the homogeneous and heterogeneous activity classes when LPFP was used, as shown in **Table 4**.

Table 3. The classification accuracy and time taken between the compounds represented in LPFP and ECFP4 for each activity class.

Activity class	Accuracy (LPFP)	Time taken for LPFP (mins)	Accuracy (ECFP4)	Time taken for ECFP4 (mins)
Cytochrome P450 2D6	0.8669	33.5629	0.8711	6.1744
Alpha-2a adrenergic receptor	0.8926	33.8055	0.8967	6.5885
G protein-coupled receptor 44	0.6926	33.7916	0.7099	6.4987
Dopamine D3 receptor	0.6281	33.8152	0.6132	6.2299
Somatostatin receptor 2	0.9901	33.0538	0.9901	6.88
Prostanoid DP receptor	0.9554	33.3866	0.9554	6.5764
Average	83.76%	33.5692	83.94%	6.3878

Table 4. The differences in classification accuracy between three categories of activity classes when compounds are represented using LPFPs and ECFP4.

Type of activity classes	Difference in accuracy (ECFP4)	Difference in accuracy (LPFP)
Homogenous	0.000	0.000
Heterogenous	−0.089	−0.093
Intermediate	−0.311	−0.312

Table 4 shows that the SVM classifier used did not perform well when compounds from intermediate classes were used with the LPFP representation. We identified that the main factor which led to this drawback was the nature of the activity classes chosen for this experiment. The majority of the compounds in the ChEMBL dataset belongs to either the heterogeneous or intermediate activity classes. To be specific, the Dopamine D3 receptor contains the highest number of compounds (1540 compounds) followed by the G protein-coupled receptor 44 (1240 compounds), as shown in **Table 1** and both of these activity classes have lower accuracy values (refer to **Table 3**). These activity classes contain compounds that are also present in other activity classes as well. In other words, the group of fragments that are necessary to determine the interactions is not unique to one target protein (activity class), but to various other targets as well. When the machine learning experiment was conducted, the rules inside the SVM model that were generated were not accurate enough to predict the interactions since the rules were made up of fragments that were mixed with other target proteins. For example, in an attempt to predict the accuracy of the Dopamine D3 activity class, the rules to create the model should not be made up of fragments that are solely unique to this activity class. There is no specific target protein or a 'set of fragments' that the model can use to create the rules to determine the interaction between them when using heterogeneous and intermediate activity classes in our experiment. As expected, a much lower accuracy was observed in the intermediate activity classes as they are made up of compounds from homogeneous and heterogeneous classes. On the other hand, homogeneous activity classes, which have a lower number of compounds, managed to obtain a very high accuracy value. This is due to the compounds in this category are unique only to its activity class whereby they do not contain compounds similar to other activity classes. Moreover, the rules created by the model are solely based on fragments derived from those unique compounds itself. When the SVM classifier model was used for DTI prediction, a high accuracy was recorded because the necessary fragments to predict the interactions were present in the rules. Based on this insight, it can be concluded that the nature of the ChEMBL dataset affects the accuracy value of a specific activity class when it is used in predicting DTIs using the SVM classifier.

Furthermore, there were not much of a difference among all the activity classes in terms of the time taken in predicting DTIs using LPFPs. On an average, 33.57 mins was needed to build one classifier model (SVM) using compounds represented in LPFPs and to predict DTIs for each activity class. The heterogeneous activity class, Dopamine D3 receptor took the longest time to build the model and predict DTIs with the total time of 33.8152 mins while the Somatostatin receptor 2 took the fastest to build the model and predict DTIs, totalling to 33.0538 mins. As mentioned earlier, the difference is very minimal, hence, it is apparent that the nature of the ChEMBL dataset does not affect the total time taken. However, it is definitely a possibility that the descriptor used is a factor in the total time taken recorded. The proposed LPFP contains a huge number of features (10,763) which then affects the predictive model to generate a high number of rules for predicting DTIs for each activity class. This is reflected in **Table 2**, where the size of the SVM classifier model built is between the size of 700 to 800 MB. Thus, many rules were generated due to the high number of features present in LPFP. Additionally, some fragments which were not involved in the prediction were necessarily eliminated, leaving only the chosen set of fragments (that were significant) for the prediction to be made for all the compounds in all the six activity classes in our ChEMBL dataset.

In terms of the usage of ECFP4, the Somatostatin receptor 2 activity class recorded the highest accuracy value of 99.01% while the Dopamine D3 receptor managed to only achieved an accuracy value of 61.32%, which is the lowest value among all the other activity classes (refer to **Table 3**). Similar to the case of using

LPFP, the SVM model worked the best with homogeneous activity classes as well, followed by the heterogeneous activity classes and then the intermediate activity classes. A similar pattern was also recorded for the huge difference in the accuracy between the intermediate activity classes and the homogenous and heterogeneous activity classes (refer to **Table 4**). However, the average time taken recorded for the prediction of DTIs for all the activity classes when using ECFP4 is recorded at 6.3878 mins, which is almost five times faster than LPFP. This is probably due to the lower number of features in ECFP4 (1024) which is about ten times less than LPFP's number of features (10,723). Based on **Table 3**, the heterogenous activity class Alpha-2a adrenergic receptor took the longest time to build the SVM model and predict DTIs while the Cytochrome P450 2D6 activity class managed to complete the classification task the fastest with just 6.1744 minutes in predicting DTIs. From the observations, it is obvious that the nature of the ChEMBL dataset do not affect the time taken. The ECFP4 descriptor used, as mentioned above, is of a smaller size in comparison to LPFP, which is the reason why when ECFP4 is used, the average time taken is five times lesser than the average time taken when LPFP is used. This is also reflected in **Table 2**, whereby the size of the SVM model built is only within the range of 15 to 30 MB, meaning that lesser rules were generated when the model was built and DTIs were predicted.

To summarise, the performance of LPFP fell short in comparison to ECFP4 by 0.18% in terms of the accuracy. This small difference proves that LPFPs are able to represent and hold important information pertaining to the compounds that will be used in the next experiment. However, for both homogeneous activity classes, LINGO Profiles Fingerprints managed to achieve the same accuracy values as when ECFP4 was used. Additionally, the accuracy of the Dopamine D3 receptor activity class using LPFP surpassed the accuracy when ECFP4 was used by about 1.49%. It is believed that the differences occur due to the mechanism that was used to encode the fragments that were present in a particular compound. Unlike LPFP, ECFP4 constitutes compound structures by methods of circular atom neighbourhoods. This method allows it to represent both the existence and the non-existence of functionality since both are circumstantial in examining molecular activity. Moreover, the excellence of ECFP4 when performing DTI prediction was also due to their ability to represent an essentially infinite number of different molecular features (including stereo chemical information) and this is crucial in creating an accurate SVM model. On the other hand, LPFP fell slightly in terms of the accuracy scores to ECFP4 due to containing some fragments which were not significant for purpose of DTI prediction. We have taken into account on all the fragments that exist in the ChEMBL dataset and this led to the creation of a SVM model which was less accurate due to the mixture of significant and insignificant features. In terms of the time taken, it was discussed above that there was a huge difference between the LPFP and ECFP4 representation of compounds whereby LPFP took almost five times longer than ECFP4 to predict DTIs for each activity class in the ChEMBL dataset. This is due to the number of features present in the fingerprints with LPFP containing 10,723 features and ECFP4 with 1024 features. In simpler words, the higher the number of features, the longer it takes to predict DTIs. Thus, in the next section, we will be discussing the results on the effects of dimensionality reduction of LPFP using ARM, to improve the performance of our proposed molecular descriptor.

3.4. Dimensionality reduction of LPFP using ARM

As discussed in Phase 3, significant rules for all the compounds in all of the six activity classes are generated using the Association Rule Mining (ARM) technique. The rules generated by ARM possesses

information about known DTIs and they are adhered by the minimum support and confidence level whereby the support level values are categorized into three main categories; 60%, 70% and 80% respectively. In other words, the minimum support level set for the experiment is 60% (s = 60%). The support variable reflects on how frequent a particular item set appears in a transaction meanwhile the confidence variable is used to further highlight how important a frequent item set is by taking into account the specific fragments into the frequent item set. Furthermore, the fragments within the generated significant rules from LPFP were then used to create a new, compact molecular representation which is lower in size compared to the original LPFP in order to overcome the dimensionality problem in the latter. From the rules generated, the significant ones are agglomerated and the unnecessary rules are removed. This is because the significant rules are the ones containing important fragments which may determine the interaction of a compound with a particular target protein. Moreover, the unnecessary or insignificant rules contain fragments which are also found in the significant rules. Thus, they can be eliminated accordingly as well. By adopting this idea, it is believed that the important fragments chosen can improve the accuracy value and overcome the time consumption problem of LPFP when it is used to represent the compounds in an activity class.

For example, **Figure 9** shows the significant group of fragments generated using ARM that were interacting with the Prostanoid DP receptor activity class with their respective values of support and confidence levels.

There were 162 rules generated in total, but many of them were filtered out since only the significant fragments that are present in the frequent itemset shown in **Figure 9** are considered. Two of the fragments in **Figure 9** managed to achieve a support level higher than 70% while the remaining fragments surpass the minimum support level value of 60%. The fragments such as '0ccc', 'C(=O', 'c0cc', '(=O)', 'ccc(', ')c0c', '0)c0', ')cc0' and '=O)O' appeared frequently among the compounds available in this activity class. Furthermore, it is also important to note that the maximum length for all the significant rules is 4 (refer to Section 2.1.2). Hence, three of the fragments exist as antecedents and the remaining fragment exists as a consequent. Since the significant rules that were identified consist of fragments which are only significant to the Prostanoid DP receptor activity class, we can conclude that the presence of any one of the group of fragments shown in **Figure 9** in an unknown ligand will most probably interact with the Prostanoid DP receptor activity class. The same process of generating significant fragments using ARM was also applied to all the other activity classes (Cytochrome P450 2D6, Alpha-2a adrenergic receptor, G protein-coupled receptor 44, Dopamine D3 receptor and Somatostatin receptor 2) and the analysis on the significant group of fragments generated that were interacting with these activity classes were also comprehensively discussed in the supplementary materials provided (refer to Supplementary Materials).

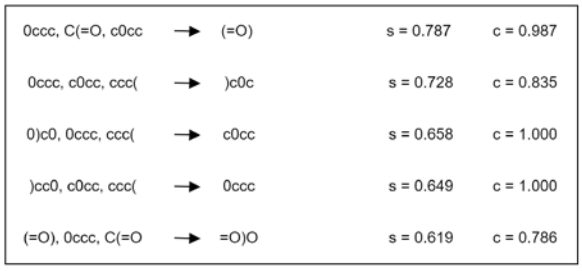

Figure 9. The group of fragments (rules) observed in the Prostanoid DP receptor activity class with the support level higher than the minimum value of 6.0.% ($s \geq 60\%$).

3.4.1 Comparison between the performance of LPFP, ECFP4 and the new and compact representation of compounds using ARM

From the significant fragments obtained earlier for each activity class (refer to **Figure 9** and Supplementary Materials), they were classified into three different groups. The first group contains fragments which have a support level value of above 60% while the second group contains fragments support level value of above 70% and finally, the third group comprises of fragments that have a support level value of at least 80%. These categorisations were made in an attempt to reduce the dimensions of the original LPFP representation. By encoding the compounds using these fragments, an alternative compound representation that met our objective was created and the results of their performance are depicted in **Tables 5** and **6**.

Table 5. The comparison of the accuracy between ECFP4, LPFP and LPFP with a support level value of at least 60%, 70% and 80%.

Activity class	Accuracy of LPFP (s = 80%)	Accuracy of LPFP (s = 70%)	Accuracy of LPFP (s = 60%)	Accuracy of ECFP4	Accuracy of LPFP
Cytochrome P450 2D6	0.8669	0.8835	0.8909	0.8711	0.8669
Alpha-2a adrenergic receptor	0.8943	0.9099	0.9124	0.8967	0.8926
G protein-coupled receptor 44	0.7661	0.9149	0.9281	0.7099	0.6926
Dopamine D3 receptor	0.7008	0.8579	0.8727	0.6132	0.6281
Somatostatin receptor 2	0.9884	0.9884	0.9884	0.9901	0.9901
Prostanoid DP receptor	0.9554	0.9554	0.9587	0.9554	0.9554
Average	86.20%	91.83%	92.52%	83.94%	83.76%

Table 6. The comparison of the time taken between ECFP4, LPFP and LPFP with a support level value of at least 60%, 70% and 80%.

Activity class	Time taken for LPFP (s = 80%) (mins)	Time taken for LPFP (s = 70%) (mins)	Time taken for LPFP (s = 60%) (mins)	Time taken for ECFP4 (mins)	Time taken for LPFP (mins)
Cytochrome P450 2D6	0.1238	0.1519	0.1640	6.1744	33.5629
Alpha-2a adrenergic receptor	0.0965	0.1291	0.1425	6.5885	33.8055
G protein-coupled receptor 44	0.2038	0.1168	0.1305	6.4987	33.7916
Dopamine D3 receptor	0.2563	0.1659	0.1850	6.4987	33.8152
Somatostatin receptor 2	0.0505	0.0536	0.0670	6.4987	33.0538
Prostanoid DP receptor	0.0765	0.0890	0.1000	6.5764	33.3866
Average	0.1346	0.1177	0.1315	6.3878	33.5692

3.4.2. Analysing compacted LPFPs generated using ARM (s = 80%)

The compounds that are represented with the refined LPFPs with a support level of over 80% (s = 80%) performed better than ECFP4 and LPFP, as shown in **Table 5**. Similar to the situation observed in Section 3.3, the SVM classifier model together with the refined and compact LPFP generated using ARM worked the best on homogeneous activity classes, followed by heterogeneous and intermediate activity classes respectively. Similar to the discussion in Section 3.3 as well, the nature of the activity classes is the factor that affects the outcome of the accuracy regardless of the classification technique used and the type of

compound representation implemented. However, the compounds represented using the refined LPFP (*s* = 80%) managed to outperform other descriptors in both the intermediate activity classes. In addition, the refined LPFP also managed to achieve similar accuracies with the rest in the Prostanoid DP receptor activity class. Overall, in terms of the average accuracy, this refined and compact LPFP is better than ECFP4 and LPFP in terms of its classification accuracy whereby it is 2.24% better than ECFP4 and 2.44% better than LPFP. The improvement in terms of accuracy is due to the significant features that were derived from the significant rules that were used to encode the compounds. Despite having a much lower number of features than ECFP4 when performing the classification task, those significant features predicted the outcome accurately. In other words, the features contained in this group of fragments were sufficient to determine the interaction between a compound and a target in any of the six activity classes in our ChEMBL dataset. Furthermore, it is also observed that ECFP4 fell slightly behind the refined LPFP because it contained insignificant features that were not essential for the prediction of DTIs.

On the other hand, this refined LPFP (*s* = 80%) took lesser time to predict DTIs as shown in **Table 6**. For every activity class involved, it took only less than a minute for the model to classify and predict DTIs. When compounds from the Somatostatin receptor 2 activity class were used, the SVM model only took 3.034 s to complete the whole classification process which was the fastest among all the other activity classes involved. Subsequently, the model took the longest time when compounds from the Dopamine D3 receptor were used. Nonetheless, this new and compact LPFP was 47 times much faster than ECFP4 and 249 times much faster than the original LPFP when both of them were put into implementation. It is believed that the important features (fragments) of the compounds that were encoded using this new and compact-sized fingerprints attributed in achieving a higher accuracy value and a shorter time taken in predicting DTIs.

3.4.3. Analysing compacted LPFPs generated using ARM (*s* = 70%)

Unlike the new LPFP (*s* = 80%) as discussed above, the compounds that are represented with the refined LPFPs with a support level of over 70% (*s* = 70%) contained 13 fragments (7 more than LPFP (*s* = 80%)). From **Table 5**, LPFP (*s* = 70%) managed to outperform ECFP4 and LPFP by 7.89% and 8.07% respectively. Additionally, this new LPFP also managed to achieve a higher accuracy reading in each activity class with an exception for the Somatostatin receptor 2, which differs from ECFP4 and LPFP by 0.17%. In addition to that, LPFP (*s* = 70%) performed better than LPFP (*s* = 80%) by 5.63%. The increase in the number of significant features in LPFP (*s* = 70%) has caused the accuracy to be higher than LPFP (*s* = 80%). This means that there were more significant features that was being used in order to encode the compounds and when these compounds were used to predict the interactions, they were able to predict more accurately.

Alternatively, similar to the LPFP (*s* = 80%), LPFP (*s* = 70%) also took a shorter time to predict DTIs, which was approximately 7.062 s on an average to complete the whole classification process as shown in **Table 6**. In fact, it was also much faster than LPFP (*s* = 80%) by 1.014 s. For each of the activity class, LPFP (*s* = 70%) took merely a minute to build the classifier model and accurately predict DTIs. Similar to the situation observed previously, when compounds from the Somatostatin receptor 2 activity class were used, SVM only took 3.213 s to complete the whole classification process, which was the quickest among all the other activity classes involved. Furthermore, SVM when set aside took the longest time to finish the entire procedure when compounds from the Dopamine D3 receptor were utilised. In general, LPFP (*s* = 70%) was

54 times considerably quicker than ECFP4 and 285 times significantly faster than LPFP when two of them were inculcated into usage.

3.4.4. Analysing compacted LPFPs generated using ARM (*s* = 60%)

Moving on, another LPFP was also created based on the rules that had a support level value of above 60%. In this new LPFP (*s* = 60%), a total of 17 fragments were extracted (4 more than LPFP (*s* = 70%) and 11 more times than LPFP (*s* = 80%). The increase in the number of fragments was attributed by the increased number of rules that belonged to this category. As shown in **Table 5**, LPFP (*s* = 60%) overcame the accuracy values of ECFP4 and LPFP by 8.58% and 8.76% respectively. Additionally, LPFP (*s* = 60%) also managed to accomplish a higher accuracy value for each activity class with the exception of the Somatostatin receptor *2* which differs from the other two descriptors (ECFP4 and LPFP) by 0.17%, similar to the case observed in LPFP (*s* = 70%). Besides, LPFP (*s* = 60%) is also deemed superior to LPFP (*s* = 70%) and LPFP (*s* = 80%) by 0.69% and 6.32% respectively. The improvement in terms of accuracy is due to the increase in the number of significant features that were derived from the significant rules that were used to encode the compounds earlier. Despite having a much lower number of features than ECFP4, LPFP, LPFP (*s* = 80%) and LPFP (*s* = 70%), when performing the classification task, those significant features extracted predicted the outcome accurately, resulting in a higher accuracy value.

In terms of the time taken, from **Table 6**, LPFP (*s* = 60%) took 7.89 s on average to complete the whole classification process. It was also much faster than LPFP (*s* = 80%) by 0.186 s, but it is slower than LPFP (*s* = 70%) by 0.828 s. For every activity class involved, it also took merely s to build the classifier and precisely predict DTIs. Similar to the circumstances illustrated by the previous two new LPFPs, when compounds from the Somatostatin receptor 2 activity class were utilised, SVM only took 4.02 s to complete the whole classification process. This was the fastest among all the other activity classes involved. In addition, Dopamine D3 receptor took the longest time to complete its predictions. All in all, LPFP (*s* = 60%) was 48 times impressively faster than ECFP4 and 255 times faster than LPFP when two of them were implemented. Hence, it is prominent that the vital features (fragments) of the compounds that were encoded using this unique smaller size fingerprint accomplished higher accuracy values and reduced the time taken in predicting DTIs. Henceforth, by presenting LPFP (*s* = 60%), this study has successfully figured out on how to beat the dimensionality issues as specified before.

3.4.5. Testing the performance of LPFP on three new activity classes

As thoroughly discussed in the earlier sections of this paper, the convincing performance of the three new LPFPs generated (*s* = 60%), (*s* = 70%) and (*s* = 80%) for all the six activity classes previously has led us to further test and investigate their performance in three new activity classes obtained from ChEMBL, which are the Urotensin II receptor, Focal adhesion kinase 1 and Vanilloid receptor activity classes. These activity classes are selected and categorized into their homogenous, intermediate and heterogeneous nature respectively and the results of the testing are summarized in the table below.

As observed in **Table 7**, all the three new activity classes achieved an accuracy of over 80%. However, in terms of the average, LPFP (*s* = 60%) outperformed the other LPFPs (*s* = 70% and *s* = 80%) by 0.79% and 2.15% respectively. When the homogeneous activity class Urotensin II receptor was used, the accuracy recorded for all the three LPFPs were the highest (over 98%), while the lowest accuracy recorded was when

the heterogeneous activity class Vanilloid receptor was utilized. The difference in terms of the results is due to the nature of the activity class itself whereby variations in terms of the number of compounds and the property associated with each activity classes causes the classification accuracy to be different than one another. Conclusively, it is proven that these new LPFPs (s = 60%), (s = 70%) and (s = 80%) were not only able to overcome the high dimensionality problem, but they can also be used to accurately predict the outcome of any activity class with an average classification accuracy of over 90%.

Table 7. The comparison of the classification accuracy of three new activity classes using the three new LPFPs generated earlier.

Type of activity class	Activity class	Accuracy for LPFP (s = 60%)	Accuracy for LPFP (s = 60%)	Accuracy for LPFP (s = 80%)
Homo	Urotensin II receptor	0.9885	0.9872	0.9866
Inter	Focal adhesion kinase 1	0.9643	0.9643	0.9617
Hetero	Vanilloid receptor	0.8787	0.8564	0.8188
Average		94.38%	93.59%	92.23%

4. Conclusion

To conclude, LINGO Profiles can be used to perform DTI prediction by representing the compounds in a binary fingerprint format called LINGO Profiles Fingerprint or LPFP. LPFP is developed by considering all the unique fragments available in the compounds of all the activity classes in the ChEMBL dataset. From the experiments conducted on all six target proteins (activity classes) using the SVM classifier, LPFP was observed to perform quite well alongside the state-of-art ECFP4 fingerprints. However, there is a slight difference in terms of the accuracy and the time taken is much longer when DTIs were predicted using the compounds that are represented using LPFP. This is due to high number of features (high dimensionality) of LPFP that are associated with the compounds in the activity classes. These features are made up of significant and insignificant features respectively. To solve this problem, Association Rule Mining or ARM was used to overcome the dimensionality problem in LPFP. ARM provides knowledge pertaining to the prediction of drug-target interactions based on the rules that are generated. The rules generated using ARM contains significant fragments that are believed to hold important information about the compounds that exist in all the activity classes involved. Hence, three new variants of LPFPs were developed using features identified by ARM with support values of 60%, 70% and 80%. As a proof, the accuracy obtained using these three new LPFPs; LPFP (s = 60%), LPFP (s = 70%) and LPFP (s = 80%) managed to surpass the accuracy of the original LPFP as well as the ECFP4 fingerprints (over 80% consistently). Besides, the time taken to build the classifier model are also significantly reduced (250 times faster than ECFP4 and LPFP) when compounds are represented with a lower number of features. To put it briefly, the ARM technique can act as an alternative to other in silico methods when predicting DTIs. In the near future, there are various other experiments that could be conducted as expansions to the ones depicted in this paper. For example, more activity classes from various categories are to be included to assess the performance in terms of the accuracy and the time taken to predict DTIs. Furthermore, the reduced LPFPs can also be benchmarked with different kinds of molecular descriptors such as ECFP2, ECFP6, ECFP8, MACCS as well as FCFP. Since different molecular descriptors have different algorithms in encoding the compounds, the variation in the accuracy scores ranging across different activity classes can be observed accordingly. It is also proven that the

significant fragments contained within the rules are vital because the presence of any group of fragments within a compound will determine the interaction between the said compound with a specified target protein.

Supplementary materials

Figure S1: the group of fragments (rules) observed in the Somatostatin receptor 2 activity class for $s \geq 60\%$; Figure S2: the group of fragments (rules) observed in the Alpha-2a adrenergic receptor activity class for $s \geq 60\%$; Figure S3: the group of fragments (rules) observed in the Cytochrome P450 2D6 activity class for $s \geq 60\%$; Figure S4: the group of fragments (rules) observed in the Dopamine D3 receptor activity class for $s \geq 60\%$; Figure S5: the group of fragments (rules) observed in the G protein-coupled receptor 44 activity class for $s \geq 60\%$.

Author contributions

Conceptualization, MJMJ and NHAHM; methodology, MJMJ; software, MJMJ; validation, NHAHM; formal analysis, MJMJ; investigation, MJMJ; resources, MJMJ, AKAK and NHAHM; data curation, MJMJ; writing—original draft preparation, MJMJ, AKAK and NHAHM; writing—review and editing, AKAK; visualization, MJMJ and AKAK; supervision, NHAHM; project administration, NHAHM; funding acquisition, NHAHM.

Funding

This work is supported by the Ministry of Higher Education (MOHE), Malaysia via the Fundamental Research Grant Scheme (FRGS) FRGS/1/2019/ICT02/USM/02/4-203.PKOMP.6711800.

Conflict of interest

The authors declare no conflict of interest.

References

1. Hughes JP, Rees S, Kalindjian SB, Philpott KL. Principles of early drug discovery. *British Journal of Pharmacology* 2011; 162(6): 1239–1249. doi: 10.1111/j.1476-5381.2010.01127.x
2. Drews J. Drug discovery: A historical perspective. *Science* 2000; 287(5460): 1960–1964. doi: 10.1126/science.287.5460.1960
3. Hann M, Green R. Chemoinformatics—A new name for an old problem? *Current Opinion in Chemical Biology* 1999; 3(4): 379–383. doi: 10.1016/S1367-5931(99)80057-X
4. Hung CL, Chen CC. Computational approaches for drug discovery. *Drug Development Research* 2014; 75(6): 412–418. doi: 10.1002/ddr.21222
5. Agamah FE, Mazandu GK, Hassan R, et al. Computational/in silico methods in drug target and lead prediction. *Briefings in Bioinformatics* 2020; 21(5): 1663–1675. doi: 10.1093/bib/bbz103
6. Katsila T, Spyroulias GA, Patrinos GP, Matsoukas MT. Computational approaches in target identification and drug discovery. *Computational and Structural Biotechnology Journal* 2016; 14: 177–184. doi: 10.1016/j.csbj.2016.04.004
7. Chen R, Liu X, Jin S, et al. Machine learning for drug-target interaction prediction. *Molecules* 2018; 23(9): 2208. doi: 10.3390/molecules23092208
8. Yamanishi Y, Kotera M, Kanehisa M, Goto S. Drug-target interaction prediction from chemical, genomic and pharmacological data in an integrated framework. *Bioinformatics* 2010; 26(12): 10.1093/bioinformatics/btq176
9. Glick NM, Davies JW, Jenkins JL. Prediction of biological targets for compounds using multiple-category bayesian models trained on chemogenomics databases. *Journal of Chemical Information Modeling* 2006; 46(3):

1124–1133. doi: 10.1021/ci060003g
10. Wen M, Zhang Z, Niu S, et al. Deep-learning-based drug-target interaction prediction. *Journal of Proteome Research* 2017; 16(4): 1401–1409. doi: 10.1021/acs.jproteome.6b00618
11. Prado-Prado F, García-Mera X, Abeijón P, et al. Using entropy of drug and protein graphs to predict FDA drug-target network: Theoretic-experimental study of MAO inhibitors and hemoglobin peptides from Fasciola hepatica. *European Journal of Medicinal Chemistry* 2011; 46(4): 1074–1094. doi: 10.1016/j.ejmech.2011.01.023
12. Nasution AK, Wijaya SH, Kusuma WA. Prediction of drug-target interaction on jamu formulas using machine learning approaches. In: Proceedings of 2019 International Conference on Advanced Computer Science and information Systems (ICACSIS); 12–13 October 2019; Bali, Indonesia. pp. 169–174.
13. Rodríguez-Pérez R, Vogt M, Bajorath J. Support vector machine classification and regression prioritize different structural features for binary compound activity and potency value prediction. *ACS Omega* 2017; 2(10): 6371–6379. doi: 10.1021/acsomega.7b01079
14. Riddick G, Song H, Ahn S, et al. Predicting in vitro drug sensitivity using Random Forests. *Bioinformatics* 2011; 27(2): 220–224. doi: 10.1093/bioinformatics/btq628
15. Shi H, Liu S, Chen J, et al. Predicting drug-target interactions using Lasso with random forest based on evolutionary information and chemical structure. *Genomics* 2019; 111(6): 1839–1852. doi: 10.1016/j.ygeno.2018.12.007
16. Vidal D, Thormann M, Pons M. LINGO, an efficient holographic text based method to calculate biophysical properties and intermolecular similarities. *Journal of Chemical Information and Modeling* 2005; 45(2): 386–393. doi: 10.1021/ci0496797
17. Abdo A, Pupin M. LINGO-DL: A text-based approach for molecular similarity searching. *Journal of Computer-Aided Molecular Design* 2021; 35(5): 657–665. doi: 10.1007/s10822-021-00383-9
18. bin Javeed MJ, Malim NHAH. Storage consumption reduction using improved inverted indexing for similarity search on LINGO Profiles. *International Journal of Advanced Computer Science and Applications* 2019; 10(5): 2019. doi: 10.14569/IJACSA.2019.0100505
19. Siswanto S, Liong TH, Shaufiah. Dimensionality reduction for association rule mining with IST-EFP algorithm. In: Proceedings of 2015 3rd International Conference on Information and Communication Technology (ICoICT); 27–29 May 2015; pp. 184–187.
20. Li PH, Lee T, Youn HY. Dimensionality reduction with sparse locality for principal component analysis. *Mathematical Problems in Engineering* 2020; 2020: 1–12. doi: 10.1155/2020/9723279
21. Malavika S, Phil M, Selvam K. Reduction of dimensionality for high dimensional data using correlation measures. Available online: http://www.ripublication.com (accessed on 27 July 2023).
22. Fujiwara T, Kwon OH, Ma KL. Supporting analysis of dimensionality reduction results with contrastive learning. *arXiv* 2019; arXiv:1905.03911. doi: 10.1109/TVCG.2019.2934251
23. Mahmud SMH, Chen W, Jahan H, et al. Dimensionality reduction based multi-kernel framework for drug-target interaction prediction. *Chemometrics and Intelligent Laboratory Systems* 2021; 212: 104270. doi: 10.1016/j.chemolab.2021.104270
24. Terol RM, Reina AR, Ziaei S, Gil D. A machine learning approach to reduce dimensional space in large datasets. *IEEE Access* 2020; 8: 148181–148192. doi: 10.1109/ACCESS.2020.3012836
25. Gardiner EJ, Gillet VJ. Perspectives on knowledge discovery algorithms recently introduced in chemoinformatics: Rough set theory, association rule mining, emerging patterns, and formal concept analysis. *Journal of Chemical Information and Modeling* 2015; 55(9): 1781–1803. doi: 10.1021/acs.jcim.5b00198
26. Gaulton A, Hersey A, Nowotka M, et al. The ChEMBL database in 2017. *Nucleic Acids Research* 2017; 45(D1): D945–D954. doi: 10.1093/nar/gkw1074
27. Arif S, Khan NZS, Malim N, Zainudin S. Retrieval performance using different type of similarity coefficient for virtual screening. *Research Journal of Applied Sciences, Engineering and Technology* 2015; 9(5): 391–395. doi: 10.19026/rjaset.9.1418
28. Heikamp K, Bajorath J. Support vector machines for drug discovery. *Expert Opinion on Drug Discovery* 2014; 9(1): 93–104. doi: 10.1517/17460441.2014.866943
29. Steinbeck C, Han Y, Kuhn S, et al. The Chemistry Development Kit (CDK): An open-source Java library for chemo- and bioinformatics. *Journal of Chemical Information Comput Sciences* 2003; 43(2): 493–500. doi: 10.1021/ci025584y

Computing and Artificial Intelligence 2023; 1(1): 321.
Original Research Article

Exploring cybercrime history through a typology of computer mediated offences: Applying Islamic principles to promote good and prevent harm

Syed Raza Shah Gilani[1], Bahaudin Ghulam Mujtaba[2,*], Shehla Zahoor[3], Ali Mohammed AlMatrooshi[4]

[1] *Abdul Wali Khan University Mardan, Mardan 23200, Pakistan*

[2] *Huizenga College of Business and Entrepreneurship, Nova Southeastern University, Fort Lauderdale, Florida 33314-7796, USA*

[3] *Assistant Professor of Law, Shaheed Benazir Bhutto Women University, Peshawar 25000, Pakistan*

[4] *Dubai Police-General Department of Human Rights, Brunel University of London, UB8 3PN Uxbridge, UK*

*** Corresponding author:** Bahaudin Ghulam Mujtaba, mujtaba@nova.edu

ARTICLE INFO

Received: 11 November 2023
Accepted: 30 November 2023
Available online: 26 December 2023

doi: 10.59400/cai.v1i1.321

ABSTRACT: By the new century, the sheer complexity and number of reported cybercrime incidents had exposed major flaws in the cybersecurity infrastructure of industry giants, as well as governments. For example, there have been numerous attempts to intercept Google's source code for the purposes of extracting confidential commercial data. National authorities were also slow to respond to the distribution of offensive images or copyrighted materials over the internet. While previous threats were mostly localized to certain computer systems, in particular countries, the emergence of the modern financial system has transformed digital crimes into a transnational phenomenon. In the intervening years, several companies, such as Lloyds in 2015, have been targets of financial hacking operations. The loss associated with cybercrime has been escalating annually, with figures indicating that costs borne by companies had quadrupled between the years of 2013 and 2015. The challenge has become worse in the recent years and artificial intelligence applications can create even more complexity and anxiety for professionals in every workplace. So, this trend of cybercrimes growing rapidly in the era of artificial intelligence is likely to affect developing and transnational economies, as more public and private sector banking institutions conduct their services online. Muslim countries must jointly collaborate, discuss, and link their spiritual principles to guard against, discourage, and prevent cybercrimes. Implications for Islamic nations along with their public and private sector leaders are explored in this manuscript.

KEYWORDS: cybercrime; criminal intend; online fraud; transnational cybercrimes; Islamic principles; data espionage; crackers; hackers

1. Introduction

Every day, we see new innovative technologies being introduced and used to fulfill professional goals and personal dreams. Some people use new technologies for efficiency and productivity, while others use them for cybercrimes or to cheat and/or shortcut their assignments[1], since modern artificial intelligence (AI) tools "can generate full documents, summarize historical events, create art—in simple terms, and 'complete your homework for you'". AI tools can mimic human cognitive capabilities and functions

often more quickly than teams of professionals, which means cybercrimes can often go undetected for hours and days. Therefore, modern professionals must be aware of cybercrimes and take proactive measures to prevent it through a multi-pronged approach which can include spiritual values. As such, this article examines the history and definition of cybercrime in contemporary debates as the backdrop against which the study will analyze how such crimes are being combated and prosecuted in various countries, especially in Islamic nations such as Pakistan, Iran, Indonesia, Malaysia, Jordan, Egypt, Nigeria, and others. While the article concludes by returning focus to legal and cultural perspectives on cybercrime, the focus is on key issues, definitions, and challenges associated with emerging cybercrime and identity theft phenomena which are impacting people all over the globe[2]. To this end, and in line with the aim of addressing the effectiveness of a developing nation's cybercrime legislation in tackling the growing trend in identity theft related offences, the paper begins with a brief overview of the legal and policy implications of the world's increased dependency on information technology. We will explore several Islamic principles that can be applied by public and private sector leaders to promote "good" through the cyber environment and prevent harmful activities in the modern tech-savvy world, where "the internet of things" are critically influential.

Of course, artificial intelligence technologies are allowing more tools and opportunities for scammers to take advantage of people in all societies regardless of religion or economic prosperity. Westfall[3] explains that "AI voice-cloning scams are on the rise", and these scams are very disturbing because they work and can confuse people who are tech-savvy. As such, individuals as well as public and private sector leaders must protect themselves and their constituencies. In the United States of America.

The Federal Trade Commission warns that scammers are using artificial intelligence to clone people's voices, and the crimes are leading to distressing situations for people around the country. Criminals are tricking victims into thinking they're talking to a relative who may need money for reasons like paying for damages from a car accident, or paying ransom for a kidnapping. Criminals just need a 20-second clip of someone talking, which is often pulled from social media, and they can make an eerily similar clone of their voice. All the way to the point that a mother can't tell the difference between her own child, and a machine[3].

2. Historical view of cybercrime

The global cybercrime market is a low-risk, high-return criminal enterprise, with goods and services in strong supply and demand. As a matter of fact, anyone aiming to make an illicit profit can purchase infrastructure, delivery mechanisms, coding services, antivirus checking services, exploit kits, communication services, and 'cash out' and money transfer services. The challenge lies in detecting the constantly evolving illicit activity, and determining its motivation, impact, and mitigation strategies in real time since criminals learn and adjust their techniques continuously[4].

The term "cybercrime" was not widely used until the late 1990s. However, the practice and method of interfering with information technologies have been in existence for more than a century. The first hacking incident was recorded in 1878 and involved the interception of phone lines through a device known as phreaking. The first recorded example of computer hacking occurred in the 1950s with the use of large mainframe computer servers. At that time, only 13 computer offences were reported worldwide. Criminal prosecution of these crimes was for the most part focused on offences involving the physical theft and destruction of computer hardware rather than "virtual" crimes affecting computer software and information networks[5].

By the mid 1960's, authorities in the U.S. had begun trials on a new electronic database that would allow for information to pass between governmental agencies. The relevant American authorities recognised that although the creation of a centralised governmental database would allow agencies to obtain and record information more efficiently, it would also generate significant privacy and accessibility concerns[6]. As a result, a newly created data authority proposed that new legislative provisions address the potential misuse of private information. These early policy debates in the 1970s rose to greater prominence in subsequent decades as companies and governments begun to rely on information databases[7].

By the 1980s, the speed and operability of computer processors had vastly improved. Now faster and cheaper, computers were widely used in the private sector. Financial markets were also reliant on predictive software and applications that aimed to eliminate human error. Banks were now a repository of financial data belonging to thousands of customers. It is a small wonder that this period sparked a rise in online fraud, software piracy, and network related crimes. Information networks would emerge as an ideal environment for crime because of the anonymity they provide to would be criminals[4].

This period also brought a paradigm shift in legal discourses, marking a move away from traditional property related conceptions to new conceptions and categories of virtual "crime", including illegal use, manipulation and interference with electronic data and information systems. The terminology of "hacking" was popularised during these periods, as offenders exploited flaws in firewalls to gain unauthorised access to computer networks without having to be physically present at a "crime scene". A single use of malicious software could be used to infect and disrupt globally integrated information and payment systems. Faced with the financial costs and dispersive effects of network-disabling cybercrimes, national legislators were forced to reconsider existing definitions and enforcement strategies. In the United States, once a leader in the push-back against cybercrime, the Comprehensive Crime Control Act (CCCA) was drawn up and passed. Subject to this Act, national security agencies were given new jurisdictional powers over cases of computer and credit card fraud. In 1986, two other cybercrime-related laws were passed in the United States—the Computer Fraud and Abuse Act (CFAA) and the Communications Privacy Act (CPA), each outlawing unauthorised access to computer systems as a criminal act[8].

Despite legislative developments in the United States and the United Kingdom, cybercrime continued to make headlines. In 1988, a self-replicating computer virus known as the I-Love-You Virus, infected over 6000 computers worldwide. These actions prompted crime agencies such as INTERPOL to propose several measures aimed at fostering joint responses on threat and crime detection and enforcement[9]. One of these recommendations called on national governments to establish a local Computer Emergency Response Team (CERTs)—a body assigned with the task of anticipating and notifying global counterparts of large-scale attacks on computer networks. The U.S. and the U.K., as well as many other countries, set up national CERTs in response to these recommendations.

The 1990s culminated in an explosion of the global information highway. The territorial boundaries that had long separated nation states no longer applied in cyberspace now that the publication or use of information in one country could be treated as a criminal offence in another. Hacking incidents also increased in frequency and significance during this period. In 1994, hackers accessed major government servers such as NASA and the Korean Atomic Research Institute. In the same year, an employee of a British Telecom illegally trespassed into a network containing information relating to secret military installations. The year 1995 marked another turning point in joint-level law-enforcement responses to the rise in online financial hacking incidents, culminating with the arrest of Vladimir Levin who was alleged

to have stolen an estimated $3 to $10 million from Citibank. The disruptive power of "hacktivist" organisations such as Wikileaks and the leak of thousands of diplomatic cables would, in years to come, sharpen public awareness of data breaches involving sensitive information[10].

Today, most experts agree that cybercrime can include numerous activities, including phishing, spear phishing, and whaling or using fake email messages to get another individual's personal information from internet users or from corporate data networks[11] by targeting specific individuals. It can also include hacking into corporate databases and even shutting them down or misusing their websites, computers, and employee or customer credit card numbers. As such, all individuals, corporations, and governments must work to prevent these hackers from accessing their sensitive data since cybercrimes are on the rise[12]. In a press release by the U.S. Attorney's Office of Western District of New York, it is mentioned a 24-year-old by the name of Maurice Sheftall from Brooklyn, NY, pleaded guilty to fraud and related activities in connection with hacking of corporate computers and stealing customer data. He was sentenced to three years of probation and paying restitution totalling to $41,441. Apparently, Sheftall illegally obtained the customer credentials, such as logins and passwords, for more than 50 customers that had opened accounts with the supermarket retailer known as Wegman. Sheftall logged into Wegman's customers' accounts and changed their passwords and e-mails, thereby locking customers out of their accounts. He used their credit card information to buy groceries for himself and his employees. During a five-month period in early 2021, Sheftall defrauded Wegmans and many of their customers by placing fraudulent orders, in the amount of approximately $9297. The supermarket's actual losses amounted to $41,441 as they reimbursed their customers, purchased credit monitoring for customers who were victims of this hacker, and "the purchase of dark web monitoring to determine where and how Sheftall obtained the customer account information he used to access the accounts"[13]. The Federal Bureau of Investigation (FBI) investigated this cybercrime which eventually led to the guilty plea by Maurice Sheftall.

The historical review of literature shows that the misuse of information technology is by no means a new or novel problem. Governments have been forced to develop laws and legal measures to address the abuse of technologies since even before the internet was invented. However, these responses have not always been effective at addressing new challenges, due to the evolving ways in which computer and network related offences are committed. This is because the internet makes it possible for a person to attack the integrity, confidentiality and privacy of computers and computer data from virtually any place in the world. The identity of the offender is often difficult to establish, and even when law enforcement agencies have enough evidence to indict a person, they may be unable to establish *personal or in rem* jurisdiction (which is the authority of a court over property) to bring criminal proceedings against the offender.

There is consequently a pressing need for legal concepts and frameworks that can both prevent online risks as well as deter future offenders by the threat of criminal prosecution and punishment. The first relies on effective cooperation between law enforcement, at the domestic and international levels, and industry leaders in the field of cybersecurity. The latter depends on the existence and adaption of outmoded criminal law definitions to reflect enforcement challenges. The next section will delve more deeply into these issues as viewed through the prism of identity theft offences[14].

2.1. Definition of cybercrime

There is no singular or universal definition of cybercrime, and the term has attracted broad and narrower definitions. Cybercrime describes any illicit activity performed using electronic operations that

violate the confidentiality, integrity, and availability of computer systems, including the data stored on digital devices[15]. As digital methods become ever-more sophisticated, the definition and ambit of legal regulations have been expanded to include offences that are made possible only with the use of computers, or what we might call computer-centric crimes. The broadest definitions of cybercrimes are drawn expansively to include crimes against the person, property, and national governments. Crimes against internet activities do attract global condemnation and punishment, such as the distribution of child pornography and cyberstalking[16] and crimes against government cyber warfare and terrorism[17]. The more well-established category of crimes is against property including intellectual property violations and software piracy, as well as online account takeover. The traditional delineation of crimes breaks down when it comes to certain computer-mediated offences. An offence such as financial identity theft could foreseeably be classified as a crime against a person and as a crime against property, depending on how one defines the property, or assesses the "true" victim of online financial fraud (is it the bank, or the customer?). Moreover, data breaches, including hacking and data interception, described below, cannot be easily accommodated by traditional theories on property theft. These breaches clearly infringe on the privacy of the data owner. To classify such acts as "theft" of the property would, however, involve "stretching" the common meaning and usage of these terms to their legal and linguistic limits[18].

In the age of information, there is a need to continuously assess whether national legislation is suitably adapted to take account of these a-typical crimes, where traditional definitions no longer work. The next section will consider these issues in the context of attempts to develop a new taxonomy of data related offences.

2.2. Criminal intent in cybercrime

As alluded to above, the emergence of new and increasingly obscure forms of computer-based crimes has challenged our traditional understandings of criminal activity and intent. Under the usual tests of criminal law, a crime can only be sanctioned by law when the a) subjective element of criminal intent (*mens rea*) can be demonstrated beyond a reasonable doubt, in conjunction with b) the objective test of having committed, or been complicit in, an act or conduct (*actus reus*) proscribed as a criminal offence under the relevant laws of a given legal system. What then counts as criminal intent in the context of "computer crime"?[19].

The evolving categories of the computer-mediated crime described above may be difficult to reconcile with traditional conceptions of a crime done to a "thing" or person. While there is sufficient case law on both sides of the Atlantic to support the notion that the theft of intangible information is prohibited in the same way theft of physical property is, jurisdictions such as Saudi Arabia apply different legal principles to these issues. Under Saudi Arabia's Islamic law governed system, certain conditions must be fulfilled before an offence can be classified as theft. One of these is that the property stolen must be capable of physical ownership. It is quite plausible to argue that this is a proper application of the law given that criminal law and penalties should be reserved for serious offences which produce substantial harm, loss, or injury to an individual or the public[20].

The conceptual challenge of redefining criminal law to "fit" new types of computer crimes is not a problem that is unique to Islamic legal systems. In the age of big data, where more and more of our private information is stored online, there is a burgeoning debate around the illegality of data breaches, raising questions around the dividing line between the mishandling of personal information and deliberate acts of destruction, trespass, theft, and deception for financial gain. In this regard, the motivation of cybercrime offenders varies greatly. Some offenders seek to gain notoriety by

circumventing the cybersecurity systems of governmental agencies or tech giants such as Google. Other organisations such as Wikileaks profess more noble aspirations that include improved transparency, democracy, and accountability of governments to the general public. How far should these issues of establishing intent and liability, therefore, be left to the discretion of national legislators and courts? On the broader issue of adapting to criminal law definitions to the new digital landscape, it has been noted that.

Generally, legislators will only prohibit human acts if that is consistent with existing laws and the penal philosophy responsible for them. Most of the computer crimes are consistent with existing legal prohibitions and the penal philosophy responsible for them. Illegal access is the electronic version of trespass. Illegal interception can be seen as an electronic invasion of privacy or burglary offence. And data interference is an electronic property damage offence. System interference and the misuse of devices are entirely new offences that have no analogue in traditional crime, however, system interference protects an entirely new legal interest that has been brought about by the advent of computer systems: the interest of operators and users of computer systems to be able to have them function properly[21].

The above quote raises a fundamental question: whose interests should cybercrime legislation serve: business operators, governments, or individuals? After all, the legal interest of an individual whose credit card details may have been "stolen" can conflict with the credit card company that has suffered a system breach. Normatively speaking, one could also criticise the claim that the legal interest being served by emerging computer crime legislation is to "have them function properly". This seems to be an overly narrow conceptualisation of the law's potential role in regulating the uses and misuses of technology. Moreover, why should certain offences be treated as analogues of traditional crimes, while others are framed in more functional, neutral, and technical terms, as though system or data offences do not also implicate highly contentious matters of national law and policy?

There are conflicts between how the law should balance among competing interests, for instance, the website operator's ability to maintain access to commercial and communications networks and the customer's legal rights to own and control data identifying them. How regulators draw these legal distinctions reflect policy, rather "neutral, choices on matters of criminality, privacy, and security". It is also not entirely clear that these offences can be treated as discrete offences, and indeed there is a significant overlap between computer-mediated offences. At the same time, the divide between traditional and anomalous methods of online crime can be overstated, since modern forms of cybercrime involve elements of both[22].

3. Computer centric crimes

There have been several attempts to formulate a definition of cybercrime that goes beyond the usual penal categories of national criminal law. To this end, Article 1.1 of the Stanford Draft International Convention to Enhance Protection from Cyber Crime and Terrorism (the "Stanford Draft") offers a broad definition as any action that involves an illicit use or trespass on a "cyber system". The Council of Europe Convention on Cybercrime goes further to develop a typology of computer and network related offences. Under this framework, four main categories of crimes are identified and differentiated as punishable offences. These are offences against the integrity and accessibility of computer systems and data, computer related offences, copyright related offences, and content related offences. As noted in a report by the International Telecommunications Union, these categories overlap in several ways since they are not "based on a sole criterion to differentiate between categories". The next section will briefly

describe the main variants of computer-mediated offences with a view of examining the relationship between data offences and the broader definition of identity theft[23].

3.1. Illegal access

The unauthorised or illegal access to a computer is the oldest and perhaps most immediately recognisable form of cybercrime. This category would include hacking and related offences involving unlawful access to a computer system[24]. As indicated above, hacking is one of the most common and destructive types of cybercrimes. Legally, hacking is defined as a mode of trespass or intrusion on computer systems and network resources through the exploitation of network security vulnerabilities. Hacking may be carried for the purposes of acquiring personal information to commit a crime, to deface websites, to conduct an attack to an entity, and for other criminal purposes including financial fraud.

From the perspective of criminal law, it is necessary to bear in mind that hacking offences are rarely an isolated event. Hacking offences are usually accompanied by preparatory acts such as the use of malware. The use of corrupt hardware or software is intentionally implemented or transferred to the targeted computer so that the hacker can gain access to, or override, security related applications such as password prompts. Cracking has been identified as a new variant of hacking related offences. In essence, cracking describes a technique whereby offenders use their skills to reverse engineer software programs, thereby exposes the computer system to malicious elements such as viruses, which may be inserted into the computer's signature code. System crackers are those who have special expertise in targeting operating systems to exploit network vulnerabilities. For example, system crackers carry out interactive searches to find defects in the security of operating systems and network protocols.

An analysis of different jurisdictions highlights divergences in regulatory approaches. Some jurisdictions confine criminal law sanctions for illegal access related offence to the most severe cases. Relatively minor cases of hacking lacking the intent to bypass security protections, cause harm, or destroy data do not meet the threshold of criminal liability under the applicable national law. Other legal systems adopt a strict liability approach and criminalise any form of unauthorised access[25].

3.2. Illegal data acquisition and data espionage

Closely related to the offence of illegal access is the overlapping "crime" of illegal data acquisition. Data espionage refers to any deliberate act of acquiring personal or sensitive data without the owner's consent. Trade secrets and other commercial data are a frequent target of data espionage offences. Corporate espionage is also recognised as a sub-category cybercrime, whereby rival companies and criminal networks illegally access and trespass on closed private networks to acquire trade secrets or exploit copyrighted works.

Data espionage can be accomplished through viruses and spyware, collectively known as malware. There are numerous types of spyware available on the market, for instance, keylogging applications. Once installed on a computer, key logger applications can record important security information such as passwords. Keylogging software can also be attached to computer hardware, namely the keyboard, enabling sensitive data to be recorded and transmitted to third parties.

Overall, hardware-based spyware is more difficult to install since the offender must physically attach it to the victim's computer. On the other hand, remote forms of spyware are exceedingly hard to detect. This points to the general obstacles faced by local law enforcers engaged in efforts to locate and successfully prosecute anonymous offenders. In contrast with earlier prototypes, viruses can be circulated to a wider reach of victims through the internet, most commonly through "infected" email attachments

or "downloadable" files. These viruses are rapidly disseminated because offenders can gain remote access to, and subsequently, control, destroy and delete program files[22].

3.3. Data interference

Data interference offences are singled out as another variant of computer-mediated crimes. By modifying or altering computer files, interfaces and system programs, offenders can inflict significant damage to business operations simply by disrupting company access to data in their possession. Businesses will increasingly rely on information systems to rapidly access, retrieve and collect data to effectively administer and manage accounts and track market trends. The volume and availability of data on computer systems, however, risks the integrity of that information. This is because offenders have a greater opportunity to intercept and monitor private communications between users, such as email communications. They can do this by gaining unauthorised access to wireless or fixed-line communication ports, or by finding unsecure routes through chat functions or other virtual communications. Offenders call also intercept non-encrypted information from data transfers stored on cloud computers or other external storage media available on the internet. The offender may use these functions to blackmail individuals or businesses by locking them out of files until a "ransom fee" is paid.

For the above reasons, many legal systems have amended their penal codes to include data acquisition offences. In addition, there have been attempts to enact robust data protection and privacy laws which regulate the conditions under which internet service providers (ISP) or other media platforms store and transfer information relating to individuals. The European Union, for instance, requires companies to obtain the consent of the data subject (the person who the data relates to) before collecting, using, or transferring that information to third parties[26].

3.4. System interference

Scholars have also drawn a nuanced distinction between data and system interference offences. The former describes efforts to delete, alter or deny access to personal files and data. The latter describes attacks against computer systems, including physical attacks on computer hardware. Damage of this kind would fall under traditional definitions of destruction and damage to property. In recent years, system interference offences typically refer to computer systems which are launched remotely, for instance, computer worms and denial of service attacks. Worms inflict damage on computer networks by creating self-replicating programs that disrupt communication channels, for instance, overloading the network with traffic, causing websites to crash. Computer worms can, consequently, result in significant losses to the business that are unable to operate or trade as normal. While worms can be targeted at entire computer networks, "denial of service" attacks are targeted at a specific computer rendering them inaccessible to the intended victim for several hours and days. System interference is most often accomplished through the spread and proliferation of malicious viruses or spyware in the organization's operation[27]. Companies and individual users that have neglected to install up-to-data anti-malware detection and prevention software are soft targets for this type of offence[28].

The key conceptual challenge presented by system and data related computer-mediated offences lies in their 'virtual' and instantaneous nature. With the rise of automated software attacks, offenders no longer need to have physical access to a computer to able to acquire private data. By the time illegal access has been obtained and data extracted without consent, the offender may already have engaged in further offences of fraud or theft. Since these offences occur remotely and often in jurisdictions that do not benefit from robust cybercrime laws and enforcement regimes, the likelihood that offenders will be successfully apprehended and brought to justice is, at times, exceedingly low. Nonetheless, many

employers have instituted policies that specify that employees should not expect privacy in public spaces as all company properties and equipment are being monitored[29].

4. Virtual offences and law

Should virtual offences be brought under the scope of criminal law? The Council of Europe Convention on Cybercrime has attracted the most signatories and consequently can be seen to represent a broad-based political consensus among states around emerging norms and principles of cyber law. Despite its emerging status as customary law, the Convention does not definitively settle debates on what should or should not count as a crime. Instead, cybercrime is defined in circular terms as any unlawful computer related activities which are conducted through global electronic networks. Of course, this only begs the question of what types of activities should be prohibited and are, moreover, sufficiently harmful to justify criminal proceedings and penalties. Moreover, by focusing exclusively on acts committed through "electronic networks", the Convention appears to exclude certain forms of physical theft or destruction. This is problematic because online fraud can occur after a theft of a physical item such as a credit card or documentation containing personal information. Moreover, this definition excludes the use of physical devices used to "export" software that destroys data stored on a computer. This is problematic because the act of storing this virus and transferring it to another person's physical property clearly implies malicious intent on the part of the offender[30].

Other legal instruments provide for a technical definition of cybercrime as covering any situation where a computer or information network is used as the tool, or target, of criminal activity. The cybersecurity company Symantec defines a cybercrime as any act of crime committed using a computer, network device or hardware. This definition is clearly formulated with the crimes of data acquisition, illegal access, and data interference in mind. Many of these offences overlap: a hacking offence often precedes or facilitates some further act of data interference or espionage. For example, the use of malware installed through hacking techniques may also be used to aid and abet a more serious act of theft or fraud.

In the broader scheme, there are inherent difficulties with any definition that brings within its scope any activity involving the use of computer or technological tool, no matter how tangentially. The most absurd application of an over-inclusive definition of cybercrime "would, for example, cover traditional crimes such as murder, if perchance the offender used a keyboard to hit and kill the victim". A more sensible criticism, rather than an overly broad definition of cybercrime, is that it sheds no further light on what kinds of uses of a computer are sufficiently serious in purpose and intent to give rise to criminal liability and emotional distress[31]. Put differently, technical, or industry lead definitions place undue emphasis on the methods used to commit "computer-related offences" rather than the object of legal protection or the harm intended. A further difficulty with an imprecise definition of cybercrime is that national authorities are left with a wide margin of discretion to determine what counts as illegal or illicit activities[32–34]. The next section explores how Muslims can mitigate the risk of cybercrimes through their spiritual values.

5. Islamic principles and cyber crime

In the context of contemporary problems like cybercrime in the modern workplace, Islamic teachings do provide instruction on ethical conduct and morality as a source of inspiration. Even though traditional Islamic law (*fiqh*) may not address cybercrime directly, certain basic concepts may be utilized to handle a variety of problems related to cybercrime. The following are some Islamic precepts that may at different times apply to online criminal activity.

Private (*Sitr*): Islam puts a significant emphasis on respecting one's own as well as others' honor and dignity, as well as maintaining one's own privacy. These principles can be violated in several ways, including unauthorized access to personal information, hacking, and cyberstalking. The act of stealing or fraudulently accessing another person's digital assets, financial information, or personal data is forbidden in Islam. This is known as the "*prohibition of theft*", or "*sariqah*". This is in addition to the fact that actual theft is also forbidden in Islam. The act of spreading false information through social media, participating in online defamation, or establishing phony accounts with the intention of misleading others goes against the Islamic values of honesty and truthfulness, and thus it is forbidden (*Tafsir*).

Prohibition of backbiting (*Ghiba*): Contrary to the Islamic prohibition of backbiting and injuring others, engaging in cyberbullying, online harassment, or utilizing technology to insult, slander, or damage people is considered a violation of this ban. Honoring agreements and honoring the terms of service of online platforms and services is consistent with the Islamic ideals of honesty and trustworthiness. This concept is referred to as *amanah*.

Principle of non-injury (*Istislah*): Islam places a strong emphasis on non-injury (the principle of non-injury), both to oneself and to others. This concept is violated when one commits acts of cybercrimes that are harmful to people, organizations, or society.

Promote good and prevent harm (Amr Bil Maruf wa Nahi Anil Munkar): Islam urges people to encourage good activities and discourage bad ones. This concept is known as "promotion of good and prevention of evil". In accordance with this idea, the reporting of cybercrimes and the prevention of harmful online activity is required of all Muslims. Engaging in cyberbullying, sharing personal information without authorization, or propagating nasty stories online may be regarded as a type of gossip, which is forbidden in Islam. Another form of speech that is forbidden in Islam is known as *gheebah*.

Respect for authority and the law (*Ta'a*): Adhering to the laws of the nation, particularly those pertaining to cybercrime, is consistent with Islamic teachings about the need to maintain justice and honor authority. Plagiarism, the unlawful dissemination of copyrighted information, and software piracy are all acts that go against the idea of protecting intellectual property rights, which is referred to as *istihqaq*. It is essential to keep in mind that different Islamic scholars and communities may arrive at different interpretations and implementations of Islamic teachings. It is possible that Muslim countries and experts need to collaborate to update these principles for the modern times and provide recommendations that are particular to cybercrimes. Additionally, measures to prevent and treat cybercrimes should be carried out within the context of existing legal systems and international agreements, taking into consideration the unique characteristics of the digital world.

In closing, it should be noted that addressing modern-day cybercrimes within Muslim nations or diaspora requires a holistic approach that incorporates Islamic principles, legal frameworks, technological advancements, education, and international cooperation. By embracing a comprehensive strategy, Muslim nations can effectively combat cybercrimes while upholding the values and ethics of Islam. Respecting individual privacy, preventing harm, promoting honesty, and upholding justice are key principles that Islam emphasizes and that can guide efforts to combat cybercrimes. Developing and updating legal frameworks to encompass a wide range of cyber offenses while considering Islamic values will help create a strong foundation for law enforcement to tackle these issues effectively.

Public awareness campaigns and educational initiatives that align with Islamic teachings can empower individuals to use digital platforms responsibly and ethically, thereby contributing to a safer online environment. Collaboration with technology companies and international organizations will

enable sharing of expertise, resources, and information to combat transnational cyber threats. Ultimately, the challenge of modern cybercrimes calls for a balanced approach that combines the ethical teachings of Islam, the dynamism of technology, and the cooperation of diverse stakeholders. By embracing these principles and working together, Muslim nations, through public and private sector leaders, can pave the way for a digital landscape that aligns with Islamic values while ensuring the security and well-being of their citizens in the digital age.

6. Summary

In terms of overall value and contributions, this article has offered an exploration of the current definitions and debates on cybercrime, focusing on identity theft offences. In the age of the internet, the integrity, confidentiality, and security of personal data is increasingly at risk. Internet users often exercise little control over how that data is used. These difficulties exist regardless of whether the site of regulation is national, international, or business level. Identity theft offenders have shrewdly deployed social engineering techniques such as phishing to steal personal information. The personal information obtained is then used to further deceive their victims. Perhaps more than other types of cybercrime, identity theft can only be effectively regulated if data protection and security are jointly addressed.

Developing countries often lack the regulatory capacities to effectively address new cyber threats or track down and prosecute criminal operations and networks. Islamic countries may need to revise their cybercrime laws to address these deficiencies, particularly in the areas of data protection and privacy. A priority must be to increase the strength of deterrence through effective policing and enforcement strategies for addressing identity theft. However, the types of identity thefts that have generated most attention in the financial arena are those that have targeted prominent governmental representatives and culturally significant institutions. Moreover, all regulation, in Muslim nations, needs to be evaluated on the backdrop of the Islamic law that governs aspects of criminal law.

Ethical approval

All procedures performed in studies involving human participants were in accordance with the ethical standards of the institutional and/or national research committee and with the 1964 Helsinki declaration and its later amendments or comparable ethical standards.

Informed consent

Informed consent was not applicable in the study.

Author contributions

Conceptualization, SRSG; methodology, SRSG; software, SRSG; validation, SRSG, BGM, SZ and AMA; formal analysis, SRSG, BGM, SZ and AMA; investigation, SRSG; resources, SRSG; data curation, SRSG; writing—original draft preparation, SRSG; writing—review and editing, SRSG, BGM, SZ and AMA; visualization, SRSG, BGM, SZ and AMA; supervision, SRSG; project administration, SRSG, BGM, SZ and AMA; funding acquisition, SRSG. All authors have read and agreed to the published version of the manuscript.

Funding

There was no external funding for this research. It was self-funded by the authors.

Conflict of interest

The study authors declare that they have no conflicts of interest.

References

1. Hoeck T. Artificial intelligence is here. Available online: https://lecnews.nova.edu/mass-mail/artificial-intelligence-is-here/ (accessed on 21 December 2023).
2. Mujtaba B, Cavico F. E-commerce and social media policies in the digital age: Legal analysis and recommendations for management. *Journal of Entrepreneurship and Business Venturing* 2023; 3(1): 119–146. doi: 10.56536/jebv.v3i1.37
3. Westfall A. AI voice-cloning scams are on the rise, here's how you can protect yourself: Experts say the scams are disturbing but they work. Available online: https://www.foxbusiness.com/technology/ai-voice-cloning-scams-rise-heres-how-protect-yourself (accessed on 18 December 2023).
4. Australian Cyber Security Centre. *ACSC Threat Report*. Australian Cyber Security Centre; 2016.
5. Payne BK. Defining cybercrime. In: Holt TJ, Bossler AM (editors). *The Palgrave Handbook of International Cybercrime and Cyberdeviance*. Springer International Publishing; 2020. pp. 3–25.
6. Aggarwal P, Arora P, Ghai R. Review on cyber crime and security. *International Journal of Research in Engineering and Applied Sciences* 2014; 2(1): 48–51.
7. Buil-Gil D, Miró-Llinares F, Moneva A, et al. Cybercrime and shifts in opportunities during COVID-19: A preliminary analysis in the UK. *European Societies* 2020; 23(sup1): S47–S59. doi: 10.1080/14616696.2020.1804973
8. Finklea K, Theohary CA. *Cybercrime: Conceptual Issues for Congress and US Law Enforcement*. Congressional Research Service, Library of Congress; 2015. pp. 214–226.
9. Friend C, Grieve LB, Kavanagh J, Palace M. Fighting cybercrime: A review of the Irish experience. *International Journal of Cyber Criminology* 2020; 14(2): 383–399. doi: 10.5281/zenodo.4766528
10. Holt TJ. Regulating cybercrime through law enforcement and industry mechanisms. *The ANNALS of the American Academy of Political and Social Science* 2018; 679(1): 140–157. doi: 10.1177/0002716218783679
11. Taylor RW, Fritsch E, Liederbach J, et al. *Cyber Crime and Cyber Terrorism*, 4th ed. Pearson; 2018. 464p.
12. The Law Office of Elliott Kanter. Defending against cybercrime charges in California. Available online: https://www.enkanter.com/article/defending-against-cyber-crime-charges-in-california (accessed on 18 December 2023).
13. U.S. Attorney's Office. Brooklyn Man pleads guilty and is sentenced for hacking into online accounts of wegmans customers. Available online: https://www.justice.gov/usao-wdny/pr/brooklyn-man-pleads-guilty-and-sentenced-hacking-online-accounts-wegmans-customers (accessed on 18 December 2023).
14. Kort A. Dar al-Cyber Islam: Women, domestic violence, and the Islamic reformation on the World Wide Web. *Journal of Muslim Minority Affairs* 2005; 25(3): 363–383. doi: 10.1080/13602000500408393
15. Phillips K, Davidson JC, Farr RR, et al. Conceptualizing cybercrime: Definitions, typologies and taxonomies. *Forensic Sciences* 2022; 2(2): 379–398. doi: 10.3390/forensicsci2020028
16. AlMatrooshi AM, Gilani SR, Mujtaba BG. Assessment of mandatory reporting laws to break the silence of child sexual abuse: A case study in the United Arab Emirates. *SN Social Sciences* 2021; 1(8): 209. doi: 10.1007/s43545-021-00216-4
17. Lallie HS, Shepherd LA, Nurse JR, et al. Cyber security in the age of COVID-19: A timeline and analysis of cyber-crime and cyber-attacks during the pandemic. *Computers & Security* 2021; 105: 102248. doi: 10.1016/j.cose.2021.102248
18. Lusthaus J, Bruce M, Phair N. Mapping the geography of cybercrime: A review of indices of digital offending by country. In: Proceedings of the 2020 IEEE European Symposium on Security and Privacy Workshops (EuroS&PW); 7–11 September 2020; Genoa, Italy. doi: 10.1109/EuroSPW51379.2020.00066
19. McGuire M, Dowling S. *Cyber Crime: A Review of The Evidence*: *Summary of Key Findings and Implications: Home Office Research Report 75*. Home Office; 2013.
20. Monteith S, Bauer M, Alda M, et al. Increasing cybercrime since the pandemic: Concerns for psychiatry. *Current Psychiatry Reports* 2021; 23: 18. doi: 10.1007/s11920-021-01228-w
21. Radoniewicz F. International regulations of cybersecurity. In: Chałubińska-Jentkiewicz K, Radoniewicz F, Zieliński T (editors). *Cybersecurity in Poland*. Springer; 2022. pp. 165–179. doi: 10.1007/978-3-030-78551-2_5
22. Rani S, Kataria A, Sharma V, et al. Threats and corrective measures for IoT security with observance of cybercrime: A survey. *Wireless Communications and Mobile Computing* 2021; 2021: 579148. doi: 10.1155/2021/5579148
23. Reep-van den Bergh CMM, Junger M. Victims of cybercrime in Europe: A review of victim surveys. *Crime Science* 2018; 7(1): 5. doi: 10.1186/s40163-018-0079-3

24. Mujtaba BG. Cybercrimes and safety policies to protect data and organizations. *Journal of Crime and Criminal Behavior* 2024; in press.
25. Saini H, Rao YS, Panda TC. Cyber-crimes and their impacts: A review. *International Journal of Engineering Research and Applications* 2012; 2(2): 202–209.
26. Gilani SRS, Rehman HU, Khan I. The conceptual analysis of the doctrine of proportionality and, its role in democratic constitutionalism. *Journal of Education & Social Research* 2021; 4(1): 204–210. doi: 10.36902/sjesr-vol4-iss1-2021(204-210)
27. Mujtaba BG. Operational sustainability and digital leadership for cybercrime prevention. *International Journal of Internet and Distributed Systems* 2023; 5(2): 19–40. doi: 10.4236/ijids.2023.52002
28. Gilani SR, Khan I, Zahoor S. The historical origins of the proportionality doctrine as a tool of judicial review: A critical analysis. *Research Journal of Social Sciences and Economics Review* 2021; 2(1): 251–258. doi: 10.36902/rjsser-vol2-iss1-2021(251-258)
29. Mujtaba BG. Ethical implications of employee monitoring: What leaders should consider. *Journal of Applied Management and Entrepreneurship* 2003; 8(3): 22–47.
30. Gilani SRS. *The Significance of the Doctrine of Proportionality in the Context of Militant Democracy to Protect the Freedom of Expression* [PhD thesis]. Brunel University London; 2019.
31. Cavico F, Mujtaba B, Lawrence E, Muffler S. Examining the efficacy of the common law tort of intentional infliction of emotional distress and bullying in the context of the employment relationship. *Business Ethics and Leadership* 2018; 2(2): 14–31. doi: 10.21272/bel.2(2).14-31.2018
32. Buil-Gil D, Miró-Llinares F, Moneva A, et al. Cybercrime and shifts in opportunities during COVID-19: A preliminary analysis in the UK. *European Societies* 2021; 23(S1): S47–S59. doi: 10.1080/14616696.2020.1804973
33. Aggarwal G. General awareness of cyber crime. Available online: https://www.semanticscholar.org/paper/General-Awareness-on-Cyber-Crime-Aggarwal/040b800a8a68bc1eb48ca8a655294e61e088b4af (accessed on 21 December 2023).
34. Peelen AAE, van de Weijer SGA, van den Berg CJW, Leukfeldt ER. Employment opportunities for applicants with cybercrime records: A field experiment. *Social Science Computer Review* 2023; 41(5): 1562–1580. doi: 10.1177/08944393221085706

Computing and Artificial Intelligence 2023; 1(1): 383.
Original Research Article

Application of machine vision in drying process modeling of carrot slices

Gourab Basu[1], Kshanaprava Dhalsamant[1], Punyadarshini Punam Tripathy[1,*], Sonu Sharma[2]

[1] *Agricultural and Food Engineering Department, Indian Institute of Technology Kharagpur, West Bengal 721302, India*
[2] *University of Guelph, Ontario, N1G 2W1, Canada*

*** Corresponding author:** Punyadarshini Punam Tripathy, punam@agfe.iitkgp.ac.in

ARTICLE INFO

Received: 4 October 2023
Accepted: 22 December 2023
Available online: 30 December 2023

doi: 10.59400/cai.v1i1.383

ABSTRACT: In this current research, the drying characteristics of carrot slices dried in a convective hot-air dryer are analyzed employing image analysis to determine the most significant factor. From the acquired images, nine parameters viz. redness (*R*), greenness (*G*), blueness (*B*), lightness (*L*), redness (*a*), yellowness (*b*), energy, entropy, and upper surface area of carrot slices were calculated using the algorithm developed in MATLAB 2015a. Boruta feature selection algorithm in the R console showed lightness, redness, and energy were the most significant features among calculated parameters. Additionally, single-layer feed-forward artificial neural network (ANN) architecture with three inputs (hot air temperature, thickness of slices, drying time), and outputs namely lightness, redness, and energy with one hidden layer was used to model input variables to that of responses. Multiple regression models are employed to optimize the drying condition by further assessing the behavior of response variables with hot air temperature and thickness of slices as inputs and lightness, redness, and energy as outputs. The lightness and redness of samples are found to be decreasing with an increase in temperature and a decrease in thickness. Whereas, the effect of these input parameters on energy, the measure of homogeneity of the product surface, is found to be reversed to that of the effect on lightness and redness. Lightness and redness are set to be highest, whereas energy was kept to be lowest. Convective hot air temperature of 60 °C and 7 mm thickness sample was found to provide the best quality product within the experiment range.

KEYWORDS: machine vision; Boruta; optimization; image analysis; carrot slices

1. Introduction

Carrot (*Daucus carota* L.) is the foremost vegetable plant across the globe owing to its large production of greater than 41 million tons (carrot + turnips)[1]. Carrot is used as processed or fresh produce for human consumption and contains around 16 to 38 mg/100 g carotenoids. These carotenoids are found to improve our immune system and decrease the risk of a few types of cancer and cardiovascular disease[2]. It needs to be dried to increase its shelf life, be easy to transport, and assure protected storage due to its perishability[3–5]. Different techniques like osmotic dehydration, tray drying, fluidized bed, etc. were used to reduce the moisture content of carrots up to safe storage moisture level (9%–10% dry basis)[6]. The primary interest in these studies has been an investigation of drying kinetics at different operating

conditions and a suitable model describing the process accurately. Optimization of independent operating variables based on chemical (carotene content) and physical parameters (like bulk density and rehydration ratio) was also investigated[7]. During drying, changes in visual characteristics are prominent[4]. These include a change in color, texture, and morphology of the product. Thus, to assess the effect of drying on the product, quantification of these qualitative attributes becomes very important[8]. The color attributes include redness, lightness, yellowness, etc., whereas the texture of visual properties includes energy, homogeneity, contrast, etc., and the morphological properties include area, perimeter, ferret diameter, etc.

Machine vision is a novel, rapid, non-contact, and non-destructive method of quantitative information procurement technique for the object of interest[5]. The food industry is among the most important sectors where machine vision is employed in a wide range of applications[9]. Machine vision primarily includes an image acquisition system and a computer system for the analysis of acquired data[10]. Depending upon the particular interest images may be acquired by hyperspectral camera or charged couple device (CCD) camera or scanning electron microscope[11], etc. Among all these devices CCD camera-based images are the most widely used[5]. Images are mostly used to classify the different objects in a mixture. These include different varieties of grains, different grades of fruits[9,11], etc. Images are also used to monitor the effect of various unit operations on the products being operated[12]. Batch drying of shrimps, figs, and apples is a few examples of this paradigm of application[13,14]. Another aspect of the application of machine vision in food is a non-destructive chemical analysis using hyperspectral images[15].

Machine vision is a technique for quantification of the aforementioned visual properties. Thus, to meet the requirement for quantification of qualitative visual properties, machine vision can play an inevitable role. There has been increased interest in the past decade in the application of machine vision in the food sector application[5,15–17]. For example, different varieties of wheat grains were classified based on image color, texture, and morphology[18], an algorithm for the classification of different types of fruits[19] using a feed-forward neural network (FNN)[14]. There is another aspect of the application of machine vision that assesses the change of quality attributes like color during an operation. Mass transfer kinetics of osmotically dehydrated kiwi fruits were investigated by Fathi et al.[20], using image analysis. A study on the effect of drying variables on morphological parameters during convective drying showed a statistically significant relationship between drying medium temperature, velocity, and image texture parameters like normalized energy, contrast, and homogeneity[21,22].

Color kinetics during hot air drying of the osmotically dehydrated pumpkin using image analysis suggested that image textural and morphological features should be taken into consideration to describe the effect of drying time on the product more precisely[23]. In another study, the drying condition of apple slices was optimized on the basis of color change, shrinkage, and drying time by image analysis to find out color change and shrinkage[24].

Image processing and analysis is an innovative tool to recognize objects of interest and for extracting computable data from digital images to deliver objective, non-contact quality assessment without destruction[25,26].

In food industries, machine vision is used largely for the classification of fruits, meats, cereals, nutrient determination, and moisture content distribution in food products. There has been an increased interest in the application of machine vision in the food processing sector in the past few decades. Some of the important features like the area and total color change of food products have been widely used for

drying process modeling as response variables[24,27–29]. However, the textural and morphological features should also be taken into account to get a holistic view of the effect of drying on product quality as proposed by Zenoozian et al.[23]. Different varieties of wheat grains were classified in terms of image color, texture, and morphology[18]. For image analysis, texture represents the distribution pattern of intensity values of reflected light from the surface, whereas morphology suggests the shape and size of an object of interest. Fernandez et al.[30] carried out the image analysis of apple discs to assess the impact of laboratory air drying on the color, shrinkage, and texture of the image. They observed that area was reduced during drying whereas the perimeter did not change much. Similarly, redness increased during drying and lightness almost remained the same. Boruta feature selection algorithm is used to choose statistically significant responses from computationally intensive parameters in the simplest form. Poona and Ismail[31], reported that the Boruta algorithm implanted with a random forest classification algorithm provided a precise model for judicious selection of healthy and infected seedlings. Lim et al.[32], used the Boruta wrapper algorithm to select essential features for the analysis in order to verify the authenticity of white rice. According to the Boruta algorithm, 13 lysoglycerophospholipids (GPLs) were essential among 17 lysoGPLs, hence 13 lysoGPLs were considered essential for their study.

Recent technological advances have transformed several sectors, including food processing. Carrot slice drying modelling using machine vision is a breakthrough. This revolutionary drying technology offers unmatched accuracy and efficiency. Machine vision uses advanced algorithms and image processing to monitor and analyze drying dynamics in real time, revealing moisture content, shrinkage, and color changes. Machine vision enables predictive modelling during carrot slice drying, improving process control and product quality. This research discusses how machine vision can optimize drying settings and produce high-quality dehydrated carrot products in carrot slice drying. This paper's technique, findings, and comments illuminate machine vision's many uses and implications in carrot slice drying. In doing so, we aim to contribute to the growing body of knowledge at the intersection of food science, technology, and process optimization.

Though drying operation increases shelf life, it also reduces the quality attributes of products. Quality evaluation is often both a destructive and expensive task. In this regard, machine vision can intervene and offer a reasonably good solution.

The incorporation of machine vision into the modelling of carrot slice drying process is a state-of-the-art development in the ever-changing field of food processing[33]. Utilizing advanced algorithms and real-time picture analysis, machine vision provides an unparalleled degree of accuracy in monitoring and comprehending the drying dynamics[34]. This study explores the significant advancements introduced by machine vision and conducts a thorough comparison with the most advanced techniques currently available. Through comparing the advantages and disadvantages, our aim is to determine the superiority of machine vision in terms of its ability to forecast outcomes, regulate processes, and improve the overall efficiency of drying carrot slices.

2. Materials and methods

2.1. Raw material

Fresh carrots (*Daucus Carota* L.) were brought from the local market of IIT Kharagpur and kept at 4 °C in the refrigerator. During the experiment, carrots were cut using a vegetable cutter and made into slices of 30 mm diameter (3 mm, 5 mm, and 7 mm thicknesses) and dipped into the water. Finally, carrot slices were kept in a convective tray dryer for drying at preset conditions (50 °C, 60 °C, 70 °C). The initial

moisture content of carrot samples was found to be 85% to 89% (wet basis).

2.2. Convective hot air drying

A laboratory-scale convective hot tray dryer was used for drying carrot slices. Prior to drying, the dryer was run for 30 min to bring the drying air condition to the desired condition under a steady state. Carrot slices were put into the top and middle tray. Experiments were carried in different levels of drying air temperature (60 °C, 70 °C, and 80 °C) and different slice thicknesses (3 mm, 5 mm, and 7 mm) in a laboratory-scale tray dryer with an air velocity of 1.3 m/s. During each experimental run, firstly, a tray having 25 slices of carrots was weighed and put into the dryer. After 15 min the next tray having the same number of carrots was further inserted into the dryer. Thus, after four trays were inserted into the dryer consecutively, the first tray was already treated for 45 min. Now within 15 min of time span, the tray was taken out the dyer, carrot slices were weighed by a weighing balance, and the image was taken by the aid of the image acquisition system. Thus, in 15 min, each try was taken out of the dryer and the aforementioned measurements were taken. While image acquisition, it was made sure that each time a particular slice is placed on the same position over and over. Thus, the image of particular slices was taken repeatedly. This process ensures proper representation of the image attributes. Otherwise, these attributes will vary. The endpoint of drying was determined when there was no significant variation in the mass of samples in three successive readings.

2.3. Image acquisition and image processing

This section elaborates the steps involved in the image acquisition system and the different steps involved in image processing in detail.

2.3.1. Image acquisition

The image acquisition system was constructed using thermocol and chart paper. Thermocol sheets having a thickness of 2 cm were brought from the market. Two squares of 41 m × 41 m were cut for the base and ceiling of the box. Another four pieces of thermocol were cut in the size of 41 m × 31 m for the sides of the acquisition box. Thus, the overall dimension of the image acquisition box was 41 m × 41 m × 31 m. Green chart paper was used as the background of the image. It was done since the green background has negligible redness whereas the carrot has high redness compared to that of the background. Thus, the red color channel was used to segment the image from the background. A backlit system of illumination was employed. In this regard, strip LED lights were used for illumination purposes. Motorola E (2nd generation) phone was used to capture the image. The phone was placed at the top of the box. There was a hole on the top of the box through which the image was captured. The camera lens had an exposure time of 1/139 seconds and a focal length of 2 mm with an aperture of *f*/2.2. Both horizontal and vertical resolution of the image was 72 dpi with a pixel size of 1920 × 2560. The image was stored in .jpg format.

2.3.2. Image processing

Image processing is done to improve the quality and interpretability of the acquired image. Noise is removed from the image. Thus, actual and appropriate quantification of image attributes is measured. Image processing involves several steps. The applicability of an algorithm that is steps involved in processing depends upon the case-specific requirement. For example, an algorithm used for the classification of different kinds of fruits will be different from an algorithm involved in the modeling of the dehydration process of shrimps. Thus, before incorporating a particular algorithm, it becomes very essential to understand the problem domain properly. This makes the certainty of steps to be taken

properly to yield the desired outcomes.

The different steps involved in the image processing of carrot slices are shown in a flowchart in **Figure 1**. Steps include image acquisition, image filtering, separation of the red channel, segmentation of the separated image, masking of the segmented binary image on the original color image, and finally conversion of masked color image into the gray image. After the involvement of these steps, the original image can be subjected to be quantified. The required image attributes are derived based on the final processed image. Different stages of the image of fresh carrot slices (5 mm thickness) taken for the experiment resulting from each of the mentioned steps are shown in **Figure 2**.

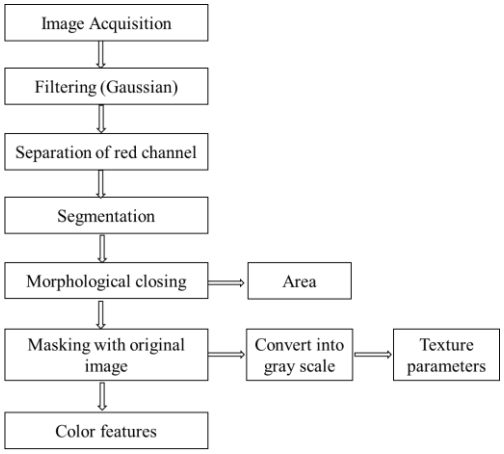

Figure 1. Flowchart of steps involved in image analysis of carrot slices.

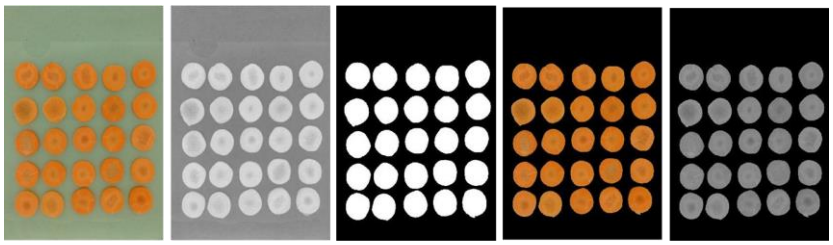

Figure 2. Different stages of an image of fresh carrot slices (5 mm thickness) taken for the experiment, **(a)** original image; **(b)** image in the red channel; **(c)** segmented binary image; **(d)** masked color image; **(e)** gray scale image.

Filtering

Filtering is an essential part of image pre-processing. This reduces the noise in the image. Thus, improves the quality and interpretability of images. In this research, a Gaussian filter was used.

Separation of the red band

The red channel of the acquired image is separated from the other two channels namely R (red) and G (green). This was done to improve the result of the segmentation process. The lower redness value of the background and higher redness value of the object makes it convenient to differentiate between these two.

Segmentation

Through image segmentation, the object of interest is separated from the background and other secondary entities[30]. Then appropriate segmentation method (Otsu method) was used or thresholding operation. Essentially this step separates the object from the background and thus we are left with only an object of interest. This operation results in a binary image with objects assigned with 1 and background

with 0.

Morphological closing

The morphological closing operation is a fundamentally mathematical set operation. It includes firstly erosion and then dilation. These are used for reduction in further noise in the image. Erosion operation removes pixels from the edges of objects in a binary image. While dilation operation fills up the noisy hole within the object of interest. Thus, an image is resulted in removed noises both in boundary and interior. In this particular research disk of the 5-pixel radius was used as a structural element for closing operation.

Area

The area of objects was measured based on the closed foreground of the image. The value returns the total number of pixels, assigned with 1. Now based on the resolution of the image, the returned value was converted into the physical area (mm^2). Here 72 dpi means there are 72 pixels in one inch. Also, the number of pixels in horizontal (1920) and vertical directions (2560) is also known. Thus, the area of each pixel was found and finally, the total areas of objects were determined.

Masking with the original image

The masking operation is done to extract the original color object from its background. It is a matrix multiplication operation. The binary image, having only 1 and 0 is multiplied with each of the R, G, B channels of the original image. Thus, the gray level values of objects remain the same whereas values of other background pixels get zero. To get the original image back, three masked channels are catenated together. Thus, we get the original image back in masked form.

Color feature extraction from masked image

Feature extraction, as the name suggests, essentially means quantification of attributes of the image. Image features are mainly classified as external and internal features. External features are the description of the boundary of a region of interest. Internal image features are attributes related to pixels inside the region of interest. The color feature is one of the widely used internal features. It depicts gray level values of each pixel inside the object.

The camera perceives the image in *RGB* color channels. This channel is device-dependent, which means for different acquisition systems like camera scanners etc. *RGB* values will differ. Thus, to get a reproducible result one must convert this value to such values which are not device-dependent. The "Lab" color space is such a space in which values do not depend on the device which captures the image. So, the masked color image is converted into "Lab" using MATLAB codes. The average values of *RGB* and Lab as well are taken as color features in this research.

Conversion of the masked image into gray scale

The masked color image is then converted into a gray scale. This results in an image containing a weighted average of the gray level of *RGB* values in a particular pixel as given in Equation (1).

$$\text{Gray scale value} = 0.2989 \times R + 0.5870 \times G + 0.1140 \times B \quad (1)$$

where *R*, *G*, *B* represents gray level values of each of the red, green, and blue channel in a particular pixel. The gray level scale value represents the weighted average of the aforementioned values. This is done to compute the image texture features in a convenient way. Otherwise, the texture will be computed in each color plane. It will result in unnecessary computation.

Image texture parameters

Like color features, texture features are also important internal features. The idea of texture in computer vision is completely different than the food industry. In the food industry, food texture, such as gumminess, chewiness, brittleness, adhesiveness, elasticity, viscosity, cohesiveness, and, hardness, is generally discussed while in computer vision discuss image texture as graininess, smoothness, coarseness, and fineness, and is generally characterized by the spatial arrangement of the brightness values of the pixels in a region in images[35]. Texture can reflect the cellular structure of food materials in food images and therefore can be utilized as a food quality indicator up to some extent[36]. There are different methods to calculate these features like statistical, spectral, and structural. Among all these methods, the statistical texture is the most extensively[37] applied method in the food industry for classification or quality grading. One of the widely used statistical texture analysis methods is the grey level co-occurrence matrix, in which the texture feature is extracted by some statistical approaches from the co-occurrence matrix[38]. The relation of pixel gray level intensity with neighboring pixels at a particular distance and direction is computed, called co-occurrence matrix. The statistical relationships of the elements of the co-occurrence matrix are found out. Energy, entropy, homogeneity, etc. are mainly used texture features. Each of these features represents distinct properties of an image.

2.4. Significant feature selection

Extraction of features in large numbers results in so much redundant data. There are many methods, used for data redundancy like filter method, wrapper method, and embedded method. For this current research Boruta algorithm was used[39]. This algorithm is based on the wrapper method. A random forest classifier is used for the selection of significant features among all attributes. It randomly creates many decision trees based on a different number of attributes and thus creates and thus a random forest from a given data set. It also creates shadow variables from the dataset. Each attribute is given an important value as per the classification accuracy. Now the addition of a new branch in the tree that is a new attribute either results in improved or declined accuracy of the tree. Now the change of the importance of an attribute at different trees is computed. If this importance is widely varied the attribute is marked as important otherwise unimportant.

Recently it has found its place in different fields from remote sensing to medicine. Poona and Ismail[31] have applied this algorithm for discrimination between stressed and healthy seedlings using hyperspectral data and Boruta was found to be performing best among other used algorithms. Chen et al.[40] used the Boruta algorithm to find out significant genera of microbes from a pool of microflora causing multiple sclerosis of patients.

2.5. Artificial neural network

Artificial neural network (ANN) is a computing system of interconnected neurons arranged in layers. An input layer, one or more hidden layers, and an output layer are comprised in the feed-forward network. From the outside world, the information is received through the input layer, get processed, and then transmitted to the hidden layers. The predictions get transmitted to the external world by the output layer. "Training" is the iterative process of adjusting the network connection weights in response to a number of examples presented to the network. Training is done to achieve a unique set of connection weights required to compute outputs that are very adjacent to the desired outputs for all the examples used in training[41–44].

ANN models are generally used for classification, prediction, and clustering. This gives an idea

about the effect of independent drying parameters on the quality of carrots, expressed in terms of image features. Drying time, air temperature, and thickness of carrot slices was kept as input variables. The significant features found from the Boruta algorithm were kept as output variables. The total dataset (378) was divided into training (278) and testing (100) datasets. The ranges of responses were different from one another. This results in slower or early stopping of learning the algorithm. To prevent this situation input and output values were normalized between −1 to +1.

Using MATLAB 2015a Neural Network Toolbox, a multilayer feed forward neural network was formed. Levenberg-Marquardt algorithm was used as a training algorithm. A tan-sigmoid function (Equation (2)) was used as the transfer function in the first layer of the network, and a linear (Equation (3)) function was used in the second layer. While training the network, 70% of the data was used for training, 15% was used for validation to prevent overfitting, and the rest 15% was used for testing the model. Once created, the original test data (100) was fed into the network, and output was simulated. Finally, simulated and experimented responses were plotted to find out the goodness of fit of the network architecture to predict the output.

$$\text{Tansig}(x) = \frac{2}{(1 + \text{e}^{-2x})} - 1 \tag{2}$$

$$\text{Purlin}(x) = x \tag{3}$$

Since there is no universally standardized rule for learning rules at input-output layers and the number of hidden layers and neurons at each layer, by trial and error well-performing, suitable architecture was established.

2.6. Data analysis for optimization

All the important responses got from the Boruta algorithm were analyzed. For optimization of processing conditions (hot air temperature and thickness of carrot slice) Design Expert 7.0 (Stat-Ease, USA) software was used, and numerical optimization was employed.

General quadratic second-order polynomial was used for modeling responses with the given set of input variables as shown in (Equation (4)).

$$Y_r = b_{r0} + \sum_{i=1}^{2} b_{ri}x_i + \sum_{i=1}^{2} b_{rii}{x_i}^2 + \sum_{i\neq j=1}^{2} b_{rij}x_i x_j \tag{4}$$

where: Y_r = Responses selected from Boruta algorithm, and b_0, b_i, b_{ii}, b_{ij}—constants, linear, quadratic, and cross-product regression coefficients, respectively. Numerical optimization was used to optimize selected features using a regression model within the experimental range.

3. Results and discussion

3.1. Kinetics of drying

The variation of moisture ratio of carrot slices (3, 5, 7 mm thicknesses) with different levels of hot air temperatures (60 °C, 70 °C, and 80 °C) are shown in **Figure 3**. It can be found that at a fixed temperature of hot air as the thickness of the slices increased, the drying time increased[45,46]. It was also observed that at a higher temperature range the drying time was almost similar to each other at different thicknesses of carrot slices. However, a different type result was reported by Doymaz[47], stating the increase in drying air temperature results in a decrease in the drying time. The observed result in the current study could be attributed to several reasons including the variety of the carrot as it was procured from the local market and could also be thinner thickness selection for the study purpose which led to

faster moisture removal.

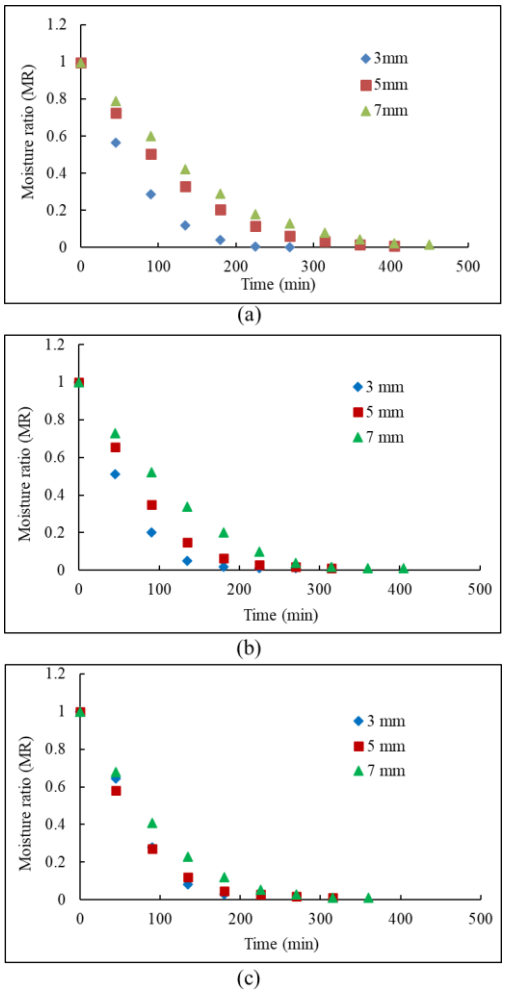

Figure 3. Moisture ratio variation of different thickness carrot slices at hot air temperatures of **(a)** 60 ℃; **(b)** 70 ℃; **(c)** 80 ℃ with time.

3.2. Important feature selection

The dataset on which the Boruta algorithm was applied was generated by taking image features at 45 min intervals at different experimental conditions. Features were combined all together and a larger dataset was produced. The codes are written in the R console to analyze the significant features as shown in **Figure 4**. **Figure 5** represents the several significant image attributes in a graphical manner as obtained from the R console. Representation in this fashion improves the interpretability of the results. It can be seen that all the features are selected as important. This is expected because so far these features like area, total color change have been widely used for modeling as response variables[24,27–29]. But as proposed by Zenoozian et al.[23], the textural and morphological features should also be taken into account to get a holistic view of the effect of drying on product quality. Here, based on mean importance top three important features were selected as energy, lightness, and redness. These features were further used for ANN modeling and used for optimization as well.

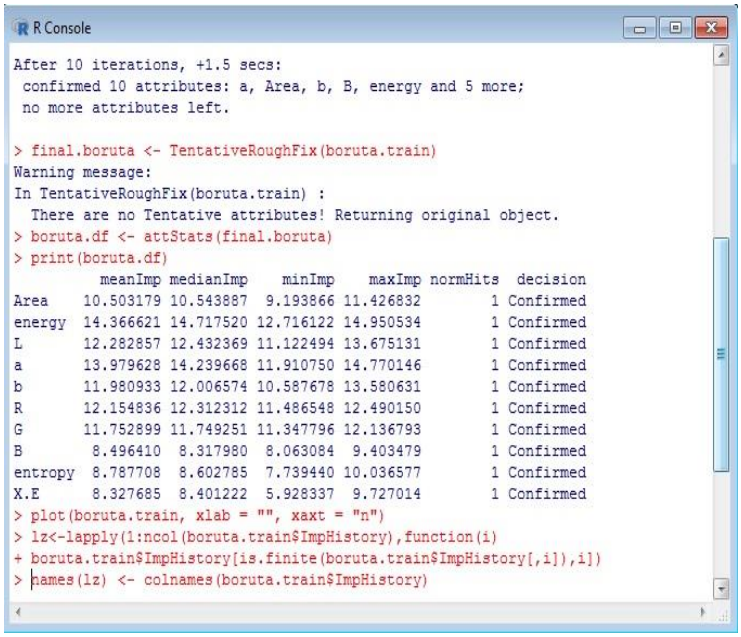

Figure 4. Representation of codes written in R console to analyze the significant features.

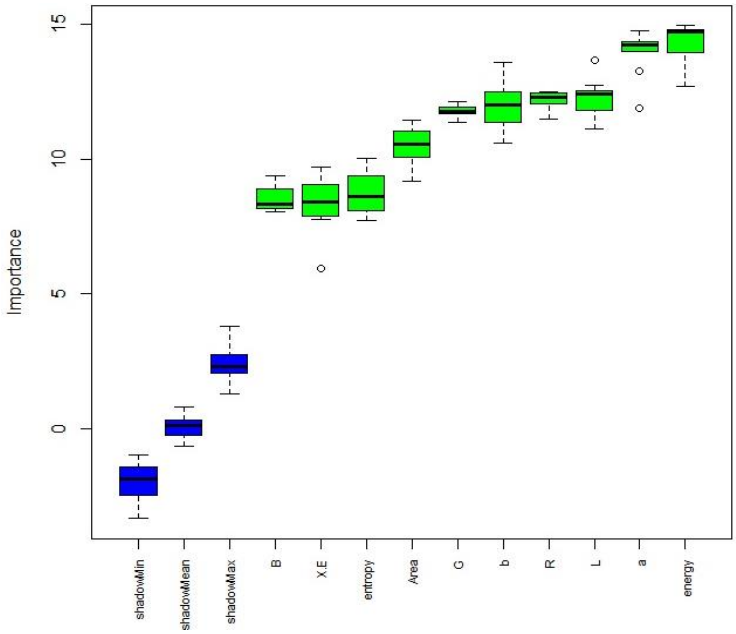

Figure 5. Representation of significant feature attributes in graphical manner as obtained from R console.

3.3. ANN modeling

As mentioned earlier, there is no fixed rule which architecture of the neural network best describes the dataset, the appropriate architecture was figured out by trial and error. Calculation with one hidden layer is less computationally intensive than multiple hidden layers. So, iteration was started with one hidden layer to check it describes the relationship between input and output properly or not. Keeping one hidden layer and transfer function from input fixed number of neurons in the hidden layer was changed. Firstly, the log sigmoid transfer function was used to relate the hidden layer to output. The performance of different neural network architectures with one hidden layer is given in **Table 1**, as observed from the table the simulated output with mean square error (MSE) is around 0.59. As the data is normalized between −1 to +1, MSE in this order cannot be tolerated. Then pure linear transfer function was used to

associate the hidden layer to output. The number of neurons was varied among 3, 5, 7, and 10. The least MSE was found in architecture consisting of 7 neurons. The MSE of the testing set was found to be 0.026. This result is good to be considered. Thus, further hidden layers were not increased. **Table 2** shows the characteristics of selected ANN architecture.

Table 1. Performance of different neural network architectures with one hidden layer.

Simulation	Transfer function from input to hidden layer	Transfer function into the output from the hidden layer	Number of neurons	Mean square error (MSE)	
				Training set	Testing set
1	Tan sigmoid	Log-sigmoid	3	0.256	0.593
2	Tan sigmoid	Log-sigmoid	5	0.260	0.597
3	Tan sigmoid	Pure linear	3	0.014	0.045
4	Tan sigmoid	Pure linear	5	0.012	0.048
5	Tan sigmoid	Pure linear	7	0.015	0.026
6	Tan sigmoid	Pure linear	10	0.016	0.028

Table 2. Structure characteristics of ANN architecture.

Structural characteristics	ANN architecture
Neural network architecture	3-7-3
Total number of hidden layers	1
Number of nodes in input layer	3
Number of nodes in output layer	7
Number of nodes in hidden layer	3
Transfer function from input to hidden layer	Tan sigmoid
Transfer function to output from hidden layer	Pure linear

Simulated results of selected ANN architecture

The simulated values of normalized predicted and experimented outputs are shown in **Figure 6** using neural network architecture with seven neurons in one hidden layer. Outputs of the networks, energy, lightness, redness of dried carrot slices were fairly congruent with experimental values (R^2 = 0.94, 0.94, 0.91) respectively. This is correlating with the capacity of ANN as a modeling tool for nonlinear data.

The weight matrix of the hidden layer (IW) and the output layer (LW) and the bias of hidden layer (b^1) and output layer (b^2) showed the following values in Equations (5–8):

$$IW = \begin{bmatrix} 0.15488 & -0.56547 & -3.9113 \\ -2.0462 & -2.1848 & -1.5131 \\ -0.03037 & -0.85566 & 0.50453 \\ -0.12173 & 0.32794 & -3.0308 \\ 3.232 & 1.6069 & -2.6334 \\ -1.2637 & -2.0799 & 0.73162 \\ 3.3525 & -1.842 & -2.0704 \end{bmatrix} \quad (5)$$

$$LW = \begin{bmatrix} 0.45048 & 0.13598 & -0.52363 & 0.34219 & -0.17151 & -0.27104 & 0.12353 \\ -0.39676 & -0.11841 & 0.42143 & -0.39751 & 0.15787 & 0.31384 & -0.09671 \\ 0.39507 & 0.050292 & -0.32338 & 0.30661 & -0.15527 & -0.26123 & 0.12888 \end{bmatrix} \quad (6)$$

$$(b^1) = \begin{bmatrix} -3.4832 \\ 0.32809 \\ 0.8263 \\ -1.2111 \\ 1.2943 \\ -2.4073 \\ 3.9102 \end{bmatrix} \quad (7)$$

$$(b^2) = \begin{bmatrix} 0.074467 \\ -0.10062 \\ -0.16371 \end{bmatrix} \quad (8)$$

Depending on the developed architecture, the model of neural network which was used for describing the kinetics of drying of carrot slices can be written as the following equation (Equation (9)).

$$\text{Output} = \text{Purelin}\,[\text{LW} \times \text{Tansig}\,(\text{IW} \times \text{inputs} + b^1) + b^2] \quad (9)$$

Equation (9) can be simplified as Equation (10).

$$\text{Output} = \text{LW} \times \left\{ \frac{2}{1 + e^{(-2\times(\text{IW}\times\text{inputs}+b^1))}} - 1 \right\} + b^2 \quad (4)$$

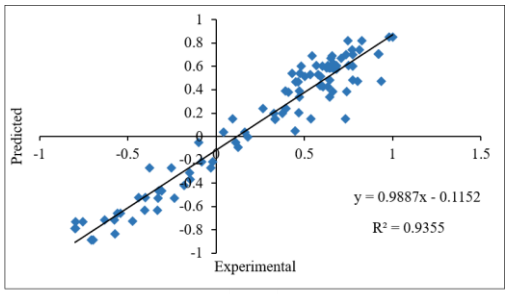

(a)

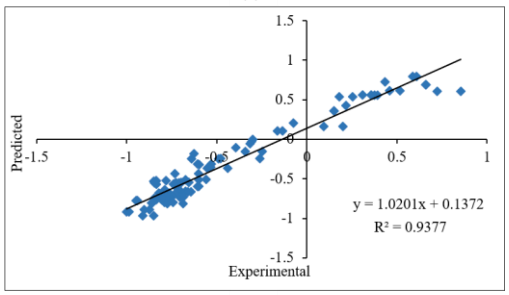

(b)

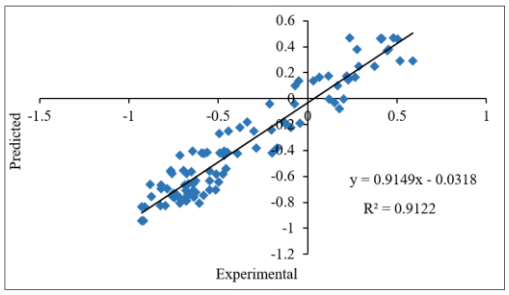

(c)

Figure 6. Predicted vs. experimented plot of **(a)** normalized energy; **(b)** lightness; **(c)** normalized redness values of dried carrot slices.

3.4. Response of the experiments

The effect of convective hot air temperature and thickness of carrot slices on responses such as energy, lightness, and redness are shown in **Table 3**. It can be observed that responses did not vary much

among different operating conditions. The variations in response variables, depending upon the inputs, are discussed in detail.

Table 3. The effect of convective hot air temperature and thickness of carrot slices on responses such as energy, lightness, and redness.

Temperature (°C)	Thickness (mm)	Energy	Lightness	Redness
60	3	0.84	13.79	29.21
60	5	0.82	14.13	29.69
60	7	0.81	14.55	30.14
70	3	0.85	12.91	28.59
70	5	0.83	13.56	29.01
70	7	0.82	13.75	29.21
80	3	0.89	11.67	27.85
80	5	0.86	11.86	28.39
80	7	0.83	12.29	28.65

3.5. Regression modeling of responses

Statistical analysis was performed to find out the significance of independent parameters i.e., convective air temperature and carrot slice thickness on responses, such as Energy, lightness, and redness. Multiple regression was performed, and coefficients of regression were found to assess the behavior of responses as the function of inputs. ANOVA (**Table 4**) was performed on each of the responses on the experimented dataset and significant terms were determined based on *F*-value. Model adequacies were checked by R^2, adjusted-R^2, and predicted-R^2. The coefficient of variation was used to figure out the dispersion of data. CV was found to be below 5. It indicates that drying temperature and slice thickness significantly affect the energy, lightness, and redness in the convective hot air-drying process. Despite the fact that the quadratic model was fitted to all three responses, energy (adjusted-R^2 = 0.89) and lightness (adjusted-R^2 = 0.95) was modeled well in the linear model. Whereas redness was well described as a quadratic model (adjusted-R^2 = 0.98). The coefficients of multiple regression of responses (energy, lightness, and redness) are listed in **Table 5**.

Table 4. Results of ANOVA analysis on response variables such as energy, lightness, redness.

Source	Energy			Lightness			Redness		
	Sum of squares	df	*p*-value prob. > *F*	Sum of squares	df	*p*-value prob. > *F*	Sum of squares	df	*p*-value prob. > *F*
Model	0.0035	2	0.0006	8.2162	2	<0.0001	3.8190	5	0.0018
A—temperature	0.0012	1	0.0029	7.3922	1	<0.0001	2.8805	1	0.0004
B—thickness	0.0022	1	0.0006	0.8239	1	0.0073	0.9115	1	0.0019
AB	-	-	-	-	-	-	0.0043	1	0.5245
A^2	-	-	-	-	-	-	0.0059	1	0.4654
B^2	-	-	-	-	-	-	0.0166	1	0.2568
Residuals	0.0003	6	-	0.3120	6	-	0.0255	3	-
Cor. total	0.0038	8	-	8.5282	8	-	3.8445	8	-
Std. Dev.	0.0072	-	-	0.2280	-	-	0.0922	-	-
Mean	0.8397	-	-	13.1671	-	-	28.9723	-	-

Table 4. (*Continued*).

Source	Energy			Lightness			Redness		
	Sum of squares	df	*p*-value prob. > *F*	Sum of squares	df	*p*-value prob. > *F*	Sum of squares	df	*p*-value prob. > *F*
C.V. %	0.8661	-	-	1.7318	-	-	0.3184	-	-
Press	0.0008	-	-	0.5579	-	-	0.3096	-	-
R^2	0.9172	-	-	0.9634	-	-	0.9933	-	-
Adj-R^2	0.8897	-	-	0.9512	-	-	0.9822	-	-
Pred-R^2	0.7836	-	-	0.9345	-	-	0.9194	-	-
Adeq precision	16.1236	-	-	22.4897	-	-	28.7463	-	-

Note: df—degree of freedom, Prob—Probability, *F*—*F*-value, Cor.—correlation, Std. Dev.—Standard deviation, C.V.—Coefficient of variation, Adj—Adjusted, Pred—Predicted, Adeq—Adequacy.

Table 5. Coefficients of multiple regression of energy, lightness, and redness.

Factors	Energy	Lightness	Redness
	Coefficient estimate	Coefficient estimate	Coefficient estimate
Intercept	0.83973	13.16798	28.99679
A—temperature	0.01431	−1.10998	−0.69289
B—thickness	−0.01954	0.37058	0.38977
AB	-	-	−0.03313
A^2	-	-	0.05442
B^2	-	-	−0.09113

3.5.1. Effect of temperature on energy response

Figure 7a shows the effect of temperature and thickness on energy. It can be found that energy is increases as the temperature increases. It also increases with reduced thickness. The effect of thickness on energy was more pronounced than that of temperature. This increase in energy could be related to smaller pores, leading to a uniform and regular structure.

3.5.2. Effect of temperature on lightness response

The effect of temperature (45–65 °C) in lightness and redness of carrot slices (7 ± 1 mm) thickness was previously investigated by Demiray and Tulek[48]. They have found that at lightness value after drying at 55–65 °C varied between 49.32 and 51. This difference of lightness among different temperatures was decreased at a higher temperature range. In the current study, the experiments were carried even higher range. This results in almost close values of lightness. Although in the literature studied, the effect of thickness on lightness was not investigated, it was found that lightness increased, with increased thickness. The effect of temperature and thickness on lightness is given in **Figure 7b**, demonstrating with greater thickness, the severity of the heating was reduced. The values were close to each other. In this research, lightness values were much lower than the lightness values found by Demiray and Tulek[48], which could be a result due to the variety of carrots.

3.5.3. Effect of temperature on redness response

The decreased redness of carrot slices can be associated with the degradation of *β*-carotene with intensified heating effect. The redness values of carrot slices after drying at 55–65 °C were close to each other, around 31[48]. In this research, it was found to be varying between 28 and 30. With higher temperatures, redness was found to be reduced (**Figure 7c**). In the same time with higher thickness, it was found to be decreased. With greater thickness, the area exposed to heating medium per unit mass was lesser, thus the retention of *β*-carotene was greater. This resulted in greater redness.

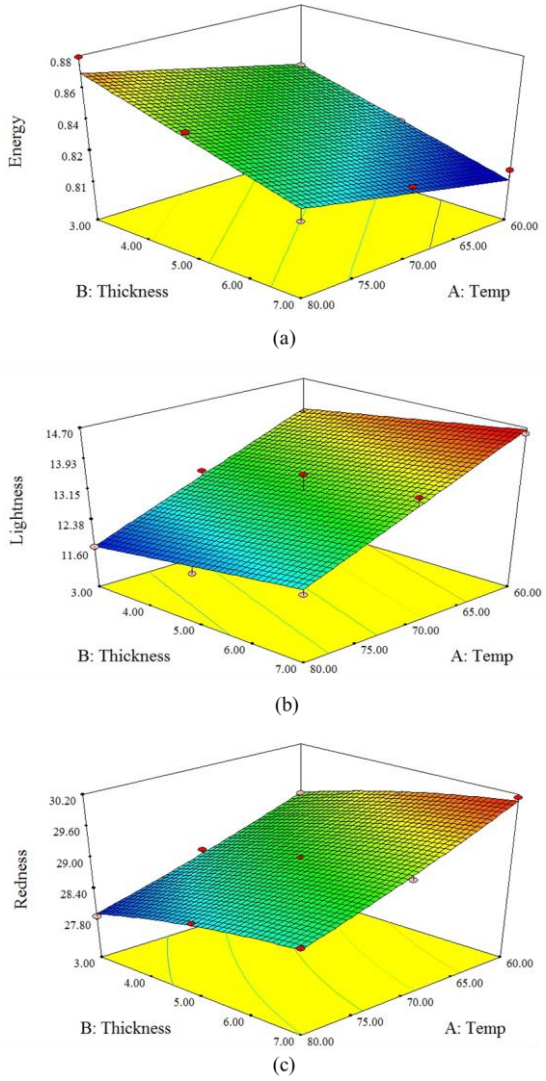

Figure 7. Surface plot of temperature and thickness vs. **(a)** energy; **(b)** lightness; and **(c)** redness of dried carrot slices.

3.6. Optimization of operating conditions of hot air drying

Predictive models of response, energy, lightness, redness was further used to optimize the drying conditions, the thickness of carrot slices, and temperature of convective hot air. These regression models of responses were only valid within experimental limits. Optimization of convective hot air drying for carrots was conducted to minimize energy and maximize lightness and redness. The energy was minimized to lessen the uniformity of the surface of slices. The dried carrot surface has more uniformity thus the energy of the acquired image is higher. The constraints for numerical optimization are given in **Table 6**. The thickness of slices and temperature of convective hot air was kept within limits. The optimal values of hot air temperature and carrot slice thickness were 60 °C and 7 mm with a desirability of 0.87. Besides, the response variables such as energy, lightness, and redness were found to be 0.83, 14.64, and 30.07 respectively.

Table 6. Constrains for numerical optimization for thickness of slices, and temperature of convective hot air, and responses.

Name	Goal	Lower limit	Upper limit	Lower weight	Upper weight	Importance
Temperature	is in range	60	80	1	1	3
Thickness	is in range	3	7	1	1	3
Energy	minimize	0.81	0.88	1	1	3
Lightness	maximize	11.66	14.55	1	1	3
Redness	maximize	27.85	30.14	1	1	3

4. Conclusion

Images of dried carrot slices were taken during the various condition of drying. These were then analyzed and different image features were got. Statistically, significant features among all the analyzed responses were found out using the Boruta algorithm. The artificial neural network was used to assess the effects of drying conditions (drying time, hot air temperature, thickness of carrot slices) on the selected image features (lightness, redness, energy). Predicted outputs of the networks, lightness, energy, redness of dried carrot slices was in good agreement with experimental values (R^2 = 0.94, 0.94, 0.91) respectively. Further drying condition (air temperature and thickness of slice) was optimized based on features. Lightness and redness were set to be maximized whereas energy was to be minimized. Optimized drying condition was found to be 60 ℃ and carrot slice thickness of 7 mm. From the current research findings, it can be observed that the energy, a measure of uniformity of surface increased with an increase in severity of drying conditions. The lightness and redness decreased with an increase in the severity of the drying condition. The lowest temperature of hot air and highest thickness of carrot slice produce the best quality of the product within the experimental range of operation. Therefore, the current research can help the food industries in understanding the distribution of quality attributes of agricultural commodities in a non-destructive way and maintaining them as needed.

Author contributions

Conceptualization, GB and KD; methodology, GB and KD; software, GB; validation, GB and KD; formal analysis, GB and KD; investigation, GB and KD; resources, GB and KD; data curation, GB and KD; writing—original draft preparation, GB and KD; writing—review and editing, KD, PPT, and SS; visualization, GB and KD; supervision, PPT; project administration, GB and KD; funding acquisition, PPT. All authors have read and agreed to the published version of the manuscript.

Acknowledgments

The authors are grateful to the Indian Institute of Technology Kharagpur for financial assistance, infrastructure, and facilities to conduct the research.

Conflict of interest

The authors declare no conflict of interest.

References

1. Food and Agriculture Organization of the United Nations Carrots and Turnips, 2020. Available online: http://www.fao.org/faostat/en/#data/QC/visualize. (Accessed on 10 October 2022).
2. Ahmad T, Cawood M, Iqbal Q, et al. Phytochemicals in Daucus carota and Their Health Benefits. Foods. 2019; 8(9): 424. doi: 10.3390/foods8090424
3. Dhalsamant K, Tripathy PP, Shrivastava SL. Effect of pretreatment on rehydration, colour and

nanoindentation properties of potato cylinders dried using a mixed‐mode solar dryer. Journal of the Science of Food and Agriculture. 2017; 97(10): 3312–3322. doi: 10.1002/jsfa.8181
4. Wang H, Fang XM, Sutar PP, et al. Effects of vacuum-steam pulsed blanching on drying kinetics, colour, phytochemical contents, antioxidant capacity of carrot and the mechanism of carrot quality changes revealed by texture, microstructure and ultrastructure. Food Chemistry. 2021; 338: 127799. doi: 10.1016/j.foodchem.2020.127799
5. Sharma S, Dhalsamant K, Tripathy PP. Application of computer vision technique for physical quality monitoring of turmeric slices during direct solar drying. Journal of Food Measurement and Characterization. 2018; 13(1): 545-558. doi: 10.1007/s11694-018-9968-0
6. Sharma S, Dhalsamant K, Tripathy PP, et al. Quality analysis and drying characteristics of turmeric (*Curcuma longa* L.) dried by hot air and direct solar dryers. LWT. 2021; 138: 110687. doi: 10.1016/j.lwt.2020.110687
7. Mudahar GS, Toledo RT, Floros JD, et al. Optimization of Carrot Dehydration Process using Response Surface Methodology. Journal of Food Science. 1989; 54(3): 714-719. doi: 10.1111/j.1365-2621.1989.tb04688.x
8. Dey D, Dhalsamant K, Tripathy PP. Effect of different pre-treatments on rehydration kinetics of solar and hot-air dried Fuji apple slices. Trends in Horticulture. 2023; 6(2): 3185. doi: 10.24294/th.v6i2.3185
9. Kakani V, Nguyen VH, Kumar BP, et al. A critical review on computer vision and artificial intelligence in food industry. Journal of Agriculture and Food Research. 2020; 2: 100033. doi: 10.1016/j.jafr.2020.100033
10. Jahanbakhshi A, Kheiralipour K. Evaluation of image processing technique and discriminant analysis methods in postharvest processing of carrot fruit. Food Science & Nutrition. 2020; 8(7): 3346-3352. doi: 10.1002/fsn3.1614
11. Tian H, Wang T, Liu Y, et al. Computer vision technology in agricultural automation —A review. Information Processing in Agriculture. 2020; 7(1): 1-19. doi: 10.1016/j.inpa.2019.09.006
12. Zhu H, Yang L, Sun Y, et al. Identifying carrot appearance quality by an improved dense CapNet. Journal of Food Process Engineering. 2020; 44(1). doi: 10.1111/jfpe.13586
13. Mohebbi M, Akbarzadeh-T MR, Shahidi F, et al. Computer vision systems (CVS) for moisture content estimation in dehydrated shrimp. Computers and Electronics in Agriculture. 2009; 69(2): 128-134. doi: 10.1016/j.compag.2009.07.005
14. Aghbashlo M, Hosseinpour S, Mujumdar AS. Application of Artificial Neural Networks (ANNs) in Drying Technology: A Comprehensive Review. Drying Technology. 2015; 33(12): 1397-1462. doi: 10.1080/07373937.2015.1036288
15. El-Mesery H, Mao H, Abomohra A. Applications of Non-destructive Technologies for Agricultural and Food Products Quality Inspection. Sensors. 2019; 19(4): 846. doi: 10.3390/s19040846
16. Ebrahimi E, Mollazade K, Babaei S. Toward an automatic wheat purity measuring device: A machine vision-based neural networks-assisted imperialist competitive algorithm approach. Measurement. 2014; 55: 196-205. doi: 10.1016/j.measurement.2014.05.003
17. Sampson DJ, Chang YK, Rupasinghe HPV, et al. A dual-view computer-vision system for volume and image texture analysis in multiple apple slices drying. Journal of Food Engineering. 2014; 127: 49-57. doi: 10.1016/j.jfoodeng.2013.11.016
18. Majumdar S, Jayas DS. Classification of cereal grains using machine vision: IV. Combined morphology, color, and texture models. Transactions of the ASAE. 2000; 43(6): 1689-1694. doi: 10.13031/2013.3069
19. Zhang Y, Wang S, Ji G, et al. Fruit classification using computer vision and feedforward neural network. Journal of Food Engineering. 2014; 143: 167-177. doi: 10.1016/j.jfoodeng.2014.07.001
20. Fathi M, Mohebbi M, Razavi SMA. Application of Image Analysis and Artificial Neural Network to Predict Mass Transfer Kinetics and Color Changes of Osmotically Dehydrated Kiwifruit. Food and Bioprocess Technology. 2009; 4(8): 1357-1366. doi: 10.1007/s11947-009-0222-y
21. Hosseinpour S, Rafiee S, Mohtasebi SS. Application of Image Processing to Analyze Shrinkage and Shape Changes of Shrimp Batch during Drying. Drying Technology. 2011; 29(12): 1416-1438. doi: 10.1080/07373937.2011.587620
22. Hosseinpour S, Rafiee S, Mohtasebi SS, et al. Application of computer vision technique for on-line monitoring of shrimp color changes during drying. Journal of Food Engineering. 2013; 115(1): 99-114. doi: 10.1016/j.jfoodeng.2012.10.003
23. Zenoozian MS, Feng H, Razavi SMA, et al. Image analysis and dynamic modeling of thin-layer drying of osmotically dehydrated pumpkin. Journal of Food Processing and Preservation. 2008; 32(1): 88-102. doi: 10.1111/j.1745-4549.2007.00167.x
24. Sturm B, Hofacker WC, Hensel O. Optimizing the Drying Parameters for Hot-Air–Dried Apples. Drying Technology. 2012; 30(14): 1570-1582. doi: 10.1080/07373937.2012.698439
25. Jahns G, Nielsen HM, Paul W. Measuring image analysis attributes and modelling fuzzy consumer aspects

for tomato quality grading. Comput. Electron. Agric. 2001; 31(1): 17-29. doi: 10.1016/S0168-1699(00)00171-X
26. Blaschke T. Object based image analysis for remote sensing. ISPRS Journal of Photogrammetry and Remote Sensing. 2010; 65(1): 2-16. doi: 10.1016/j.isprsjprs.2009.06.004
27. Behroozi Khazaei N, Tavakoli T, Ghassemian H, et al. Applied machine vision and artificial neural network for modeling and controlling of the grape drying process. Computers and Electronics in Agriculture. 2013; 98: 205-213. doi: 10.1016/j.compag.2013.08.010
28. Dhalsamant, K., Tripathy, P. P., & Shrivastava, S. L. (2017). Moisture transfer modeling during solar drying of potato cylinders considering shrinkage. International Journal of Green Energy, 14(2), 184-195. doi: 10.1080/15435075.2016.1256290
29. Hosseinpour S, Rafiee S, Aghbashlo M, et al. Computer Vision System (CVS) for In-Line Monitoring of Visual Texture Kinetics During Shrimp (*Penaeus Spp*.) Drying. Drying Technology. 2014; 33(2): 238-254. doi: 10.1080/07373937.2014.947513
30. Fernandez L, Castillero C, Aguilera JM. An application of image analysis to dehydration of apple discs. Journal of Food Engineering. 2005; 67(1-2): 185-193. doi: 10.1016/j.jfoodeng.2004.05.070
31. Poona NK, Ismail R. Using Boruta-Selected Spectroscopic Wavebands for the Asymptomatic Detection of Fusarium Circinatum Stress. IEEE Journal of Selected Topics in Applied Earth Observations and Remote Sensing. 2014; 7(9): 3764-3772. doi: 10.1109/jstars.2014.2329763
32. Lim DK, Long NP, Mo C, et al. Combination of mass spectrometry-based targeted lipidomics and supervised machine learning algorithms in detecting adulterated admixtures of white rice. Food Research International. 2017; 100: 814-821. doi: 10.1016/j.foodres.2017.08.006
33. Min W, Zhou P, Xu L, et al. From Plate to Production: Artificial Intelligence in Modern Consumer-Driven Food Systems. arXiv preprint arXiv:2311.02400
34. Banda T, Farid AA, Li C, et al. Application of machine vision for tool condition monitoring and tool performance optimization–a review. The International Journal of Advanced Manufacturing Technology. 2022; 121(11-12): 7057-7086. doi: 10.1007/s00170-022-09696-x
35. Zheng C, Sun DW, Zheng L. Recent applications of image texture for evaluation of food qualities—A review. Trends in Food Science & Technology. 2006; 17(3): 113-128. doi: 10.1016/j.tifs.2005.11.006
36. Gao X, Tan J. Analysis of expanded‐food texture by image processing part II: Mechanical properties. Journal of Food Process Engineering. 1996; 19(4): 445-456. doi: 10.1111/j.1745-4530.1996.tb00404.x
37. Brosnan T, Sun DW. Improving quality inspection of food products by computer vision—A review. J. Food Eng. 2004; 61: 3-16. doi: 10.1016/S0260-8774(03)00183-3
38. Haralick RM, Shanmugam K, Dinstein I. Textural Features for Image Classification. IEEE Transactions on Systems, Man, and Cybernetics. 1973; SMC-3(6): 610-621. doi: 10.1109/tsmc.1973.4309314
39. Kursa MB, Rudnicki WR. Feature Selection with theBorutaPackage. Journal of Statistical Software. 2010; 36(11). doi: 10.18637/jss.v036.i11
40. Chen J, Chia N, Kalari KR, et al. Multiple sclerosis patients have a distinct gut microbiota compared to healthy controls. Scientific Reports. 2016; 6(1). doi: 10.1038/srep28484
41. Chen CR, Ramaswamy HS, Alli I. Prediction of quality changes during osmo-convective drying of blueberries using neural network models for process optimization. Drying Technology. 2001; 19(3-4): 507-523. doi: 10.1081/drt-100103931
42. Cheng F, Chen FN, Ying YB. Image Recognition of Unsound Wheat Using Artificial Neural Network. 2010 Second WRI Global Congress on Intelligent Systems. Published online December 2010. doi: 10.1109/gcis.2010.220
43. Uhlig S, Colson B, Hettwer K, et al. Valid machine learning algorithms for multiparameter methods. Accreditation and Quality Assurance. 2019; 24(4): 271-279. doi: 10.1007/s00769-019-01384-w
44. Dhalsamant K. Development, validation, and comparison of FE modeling and ANN model for mixed‐mode solar drying of potato cylinders. Journal of Food Science. 2021; 86(8): 3384-3402. doi: 10.1111/1750-3841.15847
45. Dhalsamant K, Tripathy PP, Shrivastava SL. Effect of sodium metabisulfite pretreatment on micrographs, surface roughness and X-ray diffraction analyses of solar dried potato cylinders. Innovative Food Science & Emerging Technologies. 2018; 47: 399-411. doi: 10.1016/j.ifset.2018.03.014
46. Dhalsamant K, Tripathy PP, Shrivastava SL. Heat transfer analysis during mixed-mode solar drying of potato cylinders incorporating shrinkage: Numerical simulation and experimental validation. Food and Bioproducts Processing. 2018; 109: 107-121. doi: 10.1016/j.fbp.2018.03.005
47. Doymaz I. Drying kinetics, rehydration and colour characteristics of convective hot-air drying of carrot slices. Heat and Mass Transfer. 2016; 53(1): 25-35. doi: 10.1007/s00231-016-1791-8
48. Demiray E, Tulek Y. Color Degradation Kinetics of Carrot (*Daucus carota* L.) Slices during Hot Air Drying. Journal of Food Processing and Preservation. 2014; 39(6): 800-805. doi: 10.1111/jfpp.12290

Computing and Artificial Intelligence 2023; 1(1): 409.
Original Research Article

Advanced nonlinear fuzzy observer and robust control design for systems subject to cyber-physical attacks

Souad Bezzaoucha Rebai

Department of Electrical, Computer Engineering and Automation, EIGSI La Rochelle, MIA Lab., La Rochelle 17041, France; souad.bezzaoucha@eigsi.fr

ARTICLE INFO

Received: 18 October 2023
Accepted: 20 December 2023
Available online: 29 December 2023

doi: 10.59400/cai.v1i1.409

ABSTRACT: In the following contribution, the control design of CPSs (Cyber Physical Systems) usually consists of an observer to estimate the state of the physical system and a controller to compute the control commands based on the state estimation studied. Our objective is to design control methods that are robust against attacks in the model, attenuating their effect and ensuring at the same time a reliable state and attack estimation allowing their detection and isolation while maintaining the system stability, integrity, and performance. The considered approach is based on the Lyapunov theory and LMI resolution approach in order to deduce the observers-controller gains. A robust output H_∞ control and quadratic stabilization for nonlinear systems subject to actuator and sensor data deception attacks (cyber-physical-attacks) is proposed. The detection & identification issues are also reconsidered since the system states and the malicious signals will be reconstructed via a Polytopic-based T-S (Takagi-Sugeno) observer. An innovative design method where the attacked system is presented as an uncertain one subject to external disturbances is developed. A robust polytopic state feedback stabilizing controller based on a polytopic observer with disturbances attenuation for the resulting uncertain system is considered. To illustrate our proposed approach, we present a numerical example. An algorithm based on a robust polytopic controller ensuring asymptotic stability despite data deception attacks and external perturbations attenuation guaranteed by the H_∞ norm will be given. Indeed, a PDC (Parallel Distributed Compensation) controller coupled with a polytopic observer to estimate the unmeasurable state variables and actuator/sensor attack signals will be designed for nonlinear systems subjected to data deception attacks.

KEYWORDS: polytopic fuzzy representation; cyber-physical-systems; state and attack reconstruction; robust stabilizing control; disturbances attenuation

1. Introduction

In recent years, many scholars have presented reliable control strategies against various cyberattacks, such as false data injection attacks, time-delay switch attacks, and denial-of-service attacks. Indeed, since there are numerous physical sensors, complex interaction mechanisms, and massive signals, the security of cyber-physical systems (CPSs) is inevitably threatened. In order to tackle these threats, we need advances in detection, feedback control, and estimation with built-in resilience to cyber-attacks, to

maintain system integrity and reliability at all times, by providing uninterrupted, equipment-safe, and controlled operation.

The development of control and estimation algorithms resistant to faults and failures is a longstanding challenge. In fault detection and isolation, the goal is to identify one or more components that have malfunctioned within a system. Conventionally, this involves comparing sensor measurements with a model and generating what is known as a residual signal. The resulting signal is subsequently examined to ascertain the occurrence of a fault. One of the interesting approaches, based on both model-based, nonlinear modeling, robust control, and state and unknown parameters estimation, isolation, and reconstruction is the so-called polytopic one. This approach is the one to be considered in the following contribution.

This class of systems can indeed represent numerous nonlinear systems. Furthermore, it shows in the technical development similarities with the well-studied linear models where it extends existing results established for linear systems into the nonlinear domain.

2. Literature review

Cyber-Physical security extends beyond the scope of cyber-security, offering an additional layer of defense. As an extension of the previous contribution[1], where an event-based approach was considered; in the following paper, a robust control design is developed by applying a fuzzy robust control and attack resilient estimation algorithm for nonlinear system stabilization. Indeed, neutralizing attacks through resilient estimation and control enhances the system's ability to withstand damage and sustain operation, even in the presence of adversarial threats. The domain of cyber-security and resilience encompasses various stages, including detection (discerning if an attack has occurred), isolation (identifying the elements under attack, such as sensors, actuators, or control nodes), identification/estimation, and resilience[2].

In order to tackle this threat, we need advances in detection, feedback control, and estimation with built-in resilience to cyber-attacks, to maintain system integrity and reliability at all times, by providing uninterrupted, equipment-safe, and controlled operation[2,3].

Numerous approaches for detecting attacks found in the literature rely on classical fault detection techniques[4–9]. Viewed from a physical process standpoint, cyber-attacks can be perceived as stealthy and malicious disturbances. Addressing cyber-physical attacks requires surpassing traditional methods derived from fault diagnosis such that novel techniques become imperative to handle attacks that appear in mathematical models. Consequently, to overcome the conservative mathematical conditions, there is a growing interest in merging advanced nonlinear approaches with conventional control theory-based techniques; this method is gaining a lot of interest as a promising approach and interesting solution.

Applying robust control and attack-resilient estimation algorithms seems to be of great interest in recent research. Indeed, Zhu et al.[10] considered an L2 state estimation issue for a class of discrete time-invariant systems subjected to both randomly occurring switching topologies and deception attacks over wireless sensor networks. Lu et al.[11] tried to compensate DoS attacks and save network bandwidth resources by combining event triggered mechanisms and the Lyapunov function method. Zhu and Basar[12] proposed a set of coupled optimality criteria for a holistic robust and resilient design for cyber physical systems with an application to power systems. A model-based approach coupled with deep neural network was also proposed by Moazeni and Khazaei[13] where a cyberattack detection procedure was applied on the tank's level measurements of a water distribution system.

Developing control and estimation algorithms resilient against faults and failures is a well-established challenge. In fault detection and isolation, the goal is to identify if one or more components of a system have failed. Conventionally, this involves comparing sensor measurements with an analytical model of the system and generating a residual signal. This residual signal is then analyzed in order to determine if a fault has occurred.

Nevertheless, in these algorithms, typically, there is one residual signal per failure mode. In certain problem formulations, the number of failure modes can be extensive, making it impractical to generate and analyze a residual signal for each possible failure mode[13]. For instance, in a study by Bezzaoucha Rebai[14], a novel detection criterion based on state residuals, utilizing real-time observed state data, was applied to an intelligent transportation system. To expedite detection, an adaptive detection threshold was introduced to replace the pre-existing computed threshold.

One of the interesting approaches, based on both model-based, nonlinear modeling, robust control, and state and unknown parameters estimation, isolation, and reconstruction is the so-called polytopic one. This approach is the one to be considered in the following contribution.

To address challenges introduced by various nonlinearities, such as time-varying parameters, saturation, hysteresis, and sine and cosine functions, among others, the concept behind Fuzzy Takagi-Sugeno Polytopic models is to extend the well-established linear results/approaches into the nonlinear domain. The polypotic Takagi-Sugeno approach was already applied for state and stealthy attack estimation[1,14–16]. In the present contribution, as a natural extension of research work, the robust control side will be considered.

Impact and contribution

The present article addresses the stability, estimation, and control aspects of cyber-physical systems subject to false-data injection attacks from a pure automation and control point of view. The proposed approach is based on the so-called Model-based Attack Detection Identification and Isolation strategy, which incorporates a system model in the processes of detecting, isolating, and identifying.

In the following paper, the control design of CPSs computing the control commands based on the state estimation is studied. Our objective is to design control methods that are robust against attacks in the model, attenuating their effect and ensuring at the same time a reliable state and attack estimation allowing their detection and isolation while maintaining the system stability, integrity, and performance. The considered approach is based on the Lyapunov theory and LMI resolution approach in order to deduce the observers-controller gains. A robust output H_∞ control and quadratic stabilization for nonlinear systems subject to actuator and sensor data deception attacks (cyber-physical-attacks) is proposed. The detection & identification issues are also reconsidered since the system states and the malicious signals will be reconstructed via a Polytopic-based T-S (Takagi-Sugeno) observer. An innovative design method where the attacked system is presented as an uncertain one subject to external disturbances is developed. A robust polytopic state feedback stabilizing controller based on a polytopic observer with disturbances attenuation for the resulting uncertain system is considered.

The paper is organized as follows: After a brief introduction with a short literature review of related works and impact and contribution sections, presented in section 1; the Polytopic representation is applied to the malicious attacks, the system modeling with the actuator and sensor data deception attacks, followed by the uncertain system representation are then detailed respectively in section 2, i.e., Materials and Methods. Section 3 is about the main Results of the following paper, presenting the robust output

H_∞ observe-based T-S controller. Sections 4 and 5 are about the approach illustration through a numerical example, discussion, and conclusion.

3. Materials and methods

The design of control and estimation algorithms resilient to faults and failures is an important challenge in control engineering. In prior works, Teixeira et al.[19] and Oudghiri et al.[20] delved into fault detection and identification, focusing on detecting component failures by comparing measured output signals with expected ones. In our current study, our objective goes beyond mere detection; we aim to not only identify attacks but crucially to estimate them. This estimation is used for fault/attack-tolerant control design that is robust and stable. Without effective detection and estimation strategies, attacks can lead to undesirable consequences, potentially harming the physical plant.

We focus in this paper on deception attacks or false-data injection attacks. In control systems, various types of detectors can be developed to defend against such malicious attacks. Here, we aim to adapt the approach developed by Bezzaoucha et al.[16] to achieve an exact and simultaneous reconstruction of both the system state and the time-varying attack signal.

In our scenario, we assume that the attacker manipulates the gains of the sensors and/or actuators in the control system, constituting the injection of false information from sensors or controllers. Mathematically, explicit equations for both sensor and actuator signal attacks are derived, representing time-varying multiplicative faults/attacks. The Polytopic T-S approach is then employed to achieve real-time reconstruction of these signals.

3.1. Polytopic modeling of attacked systems

Let us consider the nonlinear system described by Equation (1), wherein the vector of time-varying parameters is denoted as $\theta(t)$, $\theta(t) \in \mathbb{R}^n$ is defined by $\theta(t) = \begin{pmatrix} \theta^u(t) \\ \theta^y(t) \end{pmatrix}$ where $\theta^u(t) \in \mathbb{R}^{n_{\theta_u}}$ and $\theta^y(t) \in \mathbb{R}^{n_{\theta_y}}$ correspond respectively to the actuator and sensor attacks ($n = n_{\theta_u} + n_{\theta_y}$). Denoting $x(t) \in \mathbb{R}^{n_x}$, $y(t) \in \mathbb{R}^m$ and $u(t) \in \mathbb{R}^{n_u}$ as the system state, output, and control, respectively. The nonlinear system is characterized by a Polytopic representation with r sub-models. This representation can be readily obtained using the Sector Nonlinearity Transformation (SNT). The formulation of System (1) is as follows:

$$\begin{cases} \dot{x}(t) &= \sum_{i=1}^{r} \mu_i\big(x(t)\big)\big(A_i x(t) + \mathcal{B}_i u(t)\big) \\ y(t) &= C(t)x(t) \end{cases} \tag{1}$$

with the time-varying matrices $B_i(t)$ and $C(t)$ defined by follow:

$$\begin{cases} B_i(t) = B_i + \sum_{j=1}^{n_{\theta_u}} \theta_j^u(t)\overline{B}_{ij} \\ C(t) = \big(I_m + F(t)\big)C \end{cases} \tag{2}$$

s.t. B_i, $\overline{B}_{ij}$ are constant matrices and $\theta_j^u(t)$ time-varying unknown parameters corresponding to the multiplicative actuator attacks. $F(t) = diag(\theta^y(t)) \in \mathbb{R}^{m\times m}$ is defined by:

$$F(t) = \sum_{j=1}^{n_{\theta_y}} \theta_j^y\,(t) F_j \tag{3}$$

$diag(\theta^y(t))$ corresponds to a diagonal matrix with the terms $\theta_j^y(t)$ (sensor attacks) on its diagonal with $n_{\theta_y} = m$ and F_j matrices of dimension $\mathbb{R}^{m\times m}$ and where the element of coordinate (i,i) is equal to 1 and 0 elsewhere, i.e.,

$$F_j = \begin{pmatrix} 1 & 0 & 0 \\ \vdots & 1 & \vdots \\ 0 & \dots & 1 \end{pmatrix} \tag{4}$$

3.2. Polytopic representation of malicious attacks

The actuator data deception, or false data injection are modeled thanks to the time-varying parameters $\theta_j^u(t)$. These attacks are of course unknown but bounded $\theta_j^u(t) \in \left[\theta_j^{2u}, \theta_j^{1u}\right]$, with supposed known limits. From the SNT transformation, the $\theta_j^u(t)$ are rewritten as:

$$\theta_j^u(t) = \tilde{\mu}_j^1\left(\theta_j^u(t)\right)\theta_j^{1u} + \tilde{\mu}_j^2\left(\theta_j^u(t)\right)\theta_j^{2u} \tag{5}$$

with

$$\begin{aligned} \tilde{\mu}_j^1\left(\theta_j^u(t)\right) &= \frac{\theta_j^u(t) - \theta_j^{2u}}{\theta_j^{1u} - \theta_j^{2u}} \\ \tilde{\mu}_j^2\left(\theta_j^u(t)\right) &= \frac{\theta_j^{1u} - \theta_j^u(t)}{\theta_j^{1u} - \theta_j^{2u}} \\ \tilde{\mu}_j^1\left(\theta_j^u(t)\right) + \tilde{\mu}_j^2\left(\theta_j^u(t)\right) &= 1,\ \forall t \end{aligned} \tag{6}$$

In a similar manner $\theta_j^y(t)$ is expressed as:

$$\theta_j^y(t) = \overline{\mu}_j^1\left(\theta_j^y(t)\right)\theta_j^{1y} + \overline{\mu}_j^2\left(\theta_j^y(t)\right)\theta_j^{2y} \tag{7}$$

with

$$\begin{aligned} \tilde{\mu}_j^1\left(\theta_j^y(t)\right) &= \frac{\theta_j^y(t) - \theta_j^{2y}}{\theta_j^{1y} - \theta_j^{2y}} \\ \tilde{\mu}_j^2\left(\theta_j^y(t)\right) &= \frac{\theta_j^{1y} - \theta_j^y(t)}{\theta_j^{1y} - \theta_j^{2y}} \\ \tilde{\mu}_j^1\left(\theta_j^u(t)\right) + \tilde{\mu}_j^2\left(\theta_j^u(t)\right) &= 1,\ \forall t \end{aligned} \tag{8}$$

Replacing (5) and (7) in (2), we obtain:

$$\begin{cases} B_i(t) = B_i + \sum_{j=1}^{n_{\theta_u}} \sum_{k=1}^{2} \tilde{\mu}_j^k\left(\theta_j(t)\right)\theta_j^{ku}\overline{B}_{ij} \\ C(t) = \left(I + \sum_{j=1}^{n_{\theta_y}} \sum_{k=1}^{2} \overline{\mu}_j^k\left(\theta_j^y(t)\right)\theta_j^{ky} F_j\right) C \end{cases} \tag{9}$$

3.3. Polytopic representation of physical plant subjected to data deception attacks

To ensure uniform weighting functions, and to express $C(t)$ as a straightforward polytopic matrix, we leverage the convex sum property of $\tilde{\mu}_j\left(\theta_j^u(t)\right)$ and $\overline{\mu}_j\left(\theta_j^y(t)\right)$ of each parameter $\theta_j^u(t)$ and $\theta_j^y(t)$. Consequently, Equation (9) is reformulated as:

$$\begin{aligned} B_i(t) &= B_i + \sum_{j:1}^{2^{n_{\theta u}}} \tilde{\mu}_j\left(\theta^u(t)\right)\bar{B}_{i_j} \\ C(t) &= \left(I + \sum_{j=1}^{2^n\theta^y} \bar{\mu}j^{(\theta^y(t))\overline{F}_J}\right) C \end{aligned} \tag{10}$$

with

$$\begin{cases} \widetilde{\mu_J}\left(\theta^u(t)\right) = \prod_{k=1}^{n_{\theta u}} \tilde{\mu}_k^{\sigma_j^k}\left(\theta_k^u(t)\right) \\ \overline{\mathcal{B}}_{ij} = \sum_{k=1}^{n_{\theta u}} \theta_k^{u\sigma_j^k}\overline{B}_{ik} \end{cases} \tag{11}$$

and

$$\begin{cases} \overline{\mu_j}\left(\theta^y(t)\right) = \prod_{k=1}^{n_{\theta y}} \overline{\mu}_k^{\sigma_j^k}\left(\theta_k^y(t)\right) \\ \overline{F}_j = \sum_{k=1}^{n_{\theta y}} \theta_k^{y\sigma_j^k} F_j \end{cases} \tag{12}$$

where the global weighting functions $\widetilde{\mu_J}\left(\theta^u(t)\right)$ and $\overline{\mu_j}\left(\theta^y(t)\right)$ satisfy the convex sum property where indices are expressed by:

$$j{=}2n\theta u{-}1\sigma j1{+}2n\theta u{-}2\sigma j2{+}\ldots{+}20\sigma jn\theta u{-}(21{+}22{+}\ldots{+}2n\theta u{-}1) \tag{13}$$

for the actuator, and for the sensor.

$$j = 2^{n_{\theta y}-1}\sigma_j^1 + 2^{n_{\theta y}-2}\sigma_j^2 + \cdots + 2^0\sigma_j^{n_{\theta y}} - (2^1 + 2^2 + \cdots + 2^{n_{\theta y}-1}) \tag{14}$$

Finally, using Equations (10), the nonlinear LPV system (1) becomes:

$$\begin{cases} \dot{x}(t) &= \sum_{i=1}^{r}\sum_{j=1}^{2^{n_{\theta u}}} \mu_i\left(x(t)\right)\widetilde{\mu_j}\left(\theta^u(t)\right)\left(A_i x(t) + \mathcal{B}_{ij}u(t)\right) \\ y(t) &= \sum_{k=1}^{2^{n_{\theta y}}} \overline{\mu_k}\left(\theta^y(t)\right)\tilde{C}_k x(t) \end{cases} \tag{15}$$

$$\begin{aligned} \mathcal{B}_{ij} &= B_i + \overline{\mathcal{B}}_{ij} \\ \tilde{C}_k &= C + \overline{F}_k C \end{aligned} \tag{16}$$

3.4. Uncertain system representation

Utilizing Equation (15), we formulate a state and actuator/sensor data deception observer. Employing an $\mathcal{L}_2$ attenuation approach, our objective is to minimize the impact of attacks on both the state and the estimation error of malicious inputs.

The considered observer is described by:

$$\begin{cases} \dot{\hat{x}}(t) = \sum_{i=1}^{r}\sum_{j=1}^{2^{n_{\theta_u}}} \mu_i(\hat{x}(t))\widetilde{\mu_j}\left(\widehat{\theta^u}(t)\right) \\ \qquad \left(A_i x(t) + \mathcal{B}_{ij}u(t) + L_{ij}(y(t) - \hat{y}(t))\right) \\ \dot{\widehat{\theta^u}}(t) = \sum_{i=1}^{r}\sum_{j=1}^{2^{n_{\theta_u}}} \mu_i(\hat{x}(t))\widetilde{\mu_j}\left(\widehat{\theta^u}(t)\right) \\ \qquad \left(K_{ij}^u(y(t) - \hat{y}(t)) - \alpha_{ij}^u\hat{\theta}^u(t)\right) \\ \dot{\widehat{\theta^y}}(t) = \sum_{i=1}^{r}\sum_{k=1}^{2^{n_{\theta_y}}} \mu_i(\hat{x}(t))\overline{\mu_k}\left(\widehat{\theta^y}(t)\right) \\ \qquad \left(K_{ik}^y(y(t) - \hat{y}(t)) - \alpha_{ik}^y\widehat{\theta^y}(t)\right) \\ \hat{y}(t) = \sum_{k=1}^{2^{n_{\theta_y}}} \overline{\mu_k}\left(\widehat{\theta^y}(t)\right)\tilde{C}_k\hat{x}(t) \end{cases} \tag{17}$$

where $L_{ij} \in \mathbb{R}^{n_x \times m}$, $K_{ij}^u \in \mathbb{R}^{n \times m}$, $\alpha_{ij}^u \in \mathbb{R}^{n \times n}$, $K_{ik}^y \in \mathbb{R}^{m \times m}$ and $\alpha_{ik}^y \in \mathbb{R}^{m \times m}$ are the observer gains to be calculated, ensuring at the same time the state and attacks estimation (convergence to zero of the estimation errors) and robust control constraints (to be developed in details in the following section). Let's establish the errors in state and data deception estimation as follows: $e_x(t)$, $e_{\theta^u}(t)$ and $e_{\theta^y}(t)$ as:

$$\begin{aligned} e_x(t) &= x(t) - \hat{x}(t) \\ e_{\theta^u}(t) &= \theta^u(t) - \hat{\theta}^u(t) \\ e_{\theta^y}(t) &= \theta^y(t) - \hat{\theta}^y(t) \end{aligned} \tag{18}$$

The system Equation (15) are reformulated to facilitate the computation of the dynamics of estimation errors. The modified representation is as follows:

$$\begin{cases} \dot{x}(t) = \sum_{i=1}^{r}\sum_{j=1}^{2^{n_{\theta_u}}} [\,\mu_i(\hat{x}(t))\widetilde{\mu_j}\left(\widehat{\theta^u}(t)\right)\left(A_i x(t) + \mathcal{B}_{ij}u(t)\right) + \\ \qquad \delta_{ij}(t)\left(A_i x(t) + \mathcal{B}_{ij}u(t)\right)] \\ y(t) = \sum_{k=1}^{2^{n_{\theta_y}}} \left[\overline{\mu_k}\left(\widehat{\theta^y}(t)\right)\tilde{C}_k x(t) + \overline{\delta_k}(t)\tilde{C}_k x(t)\right] \end{cases} \tag{19}$$

with $\delta_{ij}(t)$ and $\overline{\delta_k}(t)$ are defined by the following equations:

$$\delta_{ij}(t) = \mu_i(x(t))\widetilde{\mu_j}(\theta^u(t)) - \mu_i(\hat{x}(t))\widetilde{\mu_j}\left(\widehat{\theta^u}(t)\right) \tag{20}$$

$$\overline{\delta_k}(t) = \overline{\mu_k}(\theta^y(t)) - \overline{\mu_k}\left(\widehat{\theta^y}(t)\right) \tag{21}$$

and satisfying:

$$-1 \le \delta_{ij}(t) \le 1, -1 \le \overline{\delta_k}(t) \le 1 \tag{22}$$

Let us define now:

$$\Delta A(t) = \sum_{i=1}^{r} \sum_{j=1}^{2^{n_{\theta_u}}} \delta\, ij(t) A_i = \mathcal{A}\Sigma(t) E_A \tag{23}$$

$$\Delta B(t) = \sum_{i=1}^{r} \sum_{j=1}^{2^{n_{\theta_u}}} \delta_{ij}\,(t) \mathcal{B}_{ij} = \mathcal{B}\Sigma(t) E_B \tag{24}$$

$$\Delta C(t) = \sum_{k=1}^{2^{n_{\theta_y}}} \overline{\delta_k}\,(t) \tilde{C}_k = C\overline{\Sigma}(t) E_C \tag{25}$$

with

$$\mathcal{A} = \begin{bmatrix} A_1 & \dots & A_1 & \dots & A_r & \dots & A_r \\ \underbrace{\qquad}_{2^{n_{\theta_u}} times} & & & & \underbrace{\qquad}_{2^{n_{\theta_u}} times} & & \end{bmatrix} \tag{26}$$

$$\mathcal{B} = [\mathcal{B}_{11} \quad \dots \quad \mathcal{B}_{r2^n}] \tag{27}$$

$$\sum(t) = diag(\delta_{11}(t), \dots, \delta_{r2^n}(t)) \tag{28}$$

$$\bar{\Sigma}(t) = diag\left(\bar{\delta}_2(t), \cdots, \overline{\delta_{2^{n_{\theta_y}}}}(t)\right) \tag{29}$$

$$\begin{gathered} E_A = [I_{n_x} \quad \dots \quad I_{n_x}]^T,\ E_B = [I_{n_u} \quad \dots \quad I_{n_u}]^T \\ E_C = \left[I_{2^{n_{\theta_y}}} \quad \dots \quad I_{2^{n_{\theta_y}}}\right]^T = [I_{2^m} \quad \dots \quad I_{2^m}]^T \end{gathered} \tag{30}$$

Thanks to (22) and definitions (29), we have:

$$\Sigma^T(t)\Sigma(t) \le I, \quad \overline{\Sigma}^T(t)\overline{\Sigma}(t) \le I \tag{31}$$

Using the above definitions (23)–(30), system (19) is then written as an uncertain system given by:

$$\begin{cases} \dot{x}(t) = \sum_{i=1}^{r} \sum_{j=1}^{2^{n_{\theta_u}}} \mu_i\left(\hat{x}(t)\right) \widetilde{\mu_j}\left(\widehat{\theta^u}(t)\right) \\ \qquad \left(\left(A_i + \Delta A(t)\right)x(t) + \left(\mathcal{B}_{ij} + \Delta B(t)\right)u(t)\right) \\ y(t) = \sum_{k=1}^{2^{n_{\theta_y}}} \overline{\mu_k}\left(\widehat{\theta^y}(t)\right)\left(\tilde{C}_k + \Delta C(t)\right)x(t) \end{cases} \tag{32}$$

4. Results: Robust polytopic H_∞ T-S control

Herein, we shall propose an algorithm in order to calculate the considered observer and controller gains ensuring the fulfillment of the following conditions:

- The system described by Equation (32) attains asymptotic stability despite data deception attacks.
- External perturbations attenuation guaranteed by the H_∞ norm. In other words, the goal is to find an observer Equation (17) and a Parallel Distributed Compensation (PDC) controller Equation (33) for a given scalar $\gamma > 0$ s.t. attenuation condition Equation (40) is met. The resulting conditions to be solved will be detailed in Lemma II.

For the nonlinear system subjected to data deception attacks Equation (1), employing the polytopic

observer to estimate the unmeasurable state variables and actuator/sensor attack signals, as detailed in Equation (17); we define the PDC (Parallel Distributed Compensation) controller as follows:

$$u(t) = -\sum_{l=1}^{r} h_l\left(\hat{x}(t)\right)\Omega_l\hat{x}(t) \tag{33}$$

Let us first express the estimation errors dynamics. From Equations (32) and (18), the estimation errors dynamics are then given by:

$$\begin{cases} \dot{e}_x(t) = \sum_{i=1}^{r}\sum_{j=1}^{2^{n_{\theta_u}}}\sum_{k=1}^{2^{n_{\theta_y}}}\sum_{l=1}^{r} \\ \quad \mu_i(\hat{x}(t))\widetilde{\mu_j}\left(\widehat{\theta^u}(t)\right)\overline{\mu_k}\left(\widehat{\theta^y}(t)\right)\mu_l(\hat{x}(t)) \\ \quad ((A_i - L_{ij}\tilde{C}_k + \Delta B(t)\Omega_l)e_x(t) \\ \quad + \left(\Delta A(t) - \Delta B(t)\Omega_l - L_{ij}\Delta C(t)\right)x(t)) \\ \dot{e}_{\theta^u}(t) = \sum_{i=1}^{r}\sum_{j=1}^{2^{n_{\theta_u}}}\sum_{k=1}^{2^{n_{\theta_y}}}\mu_i\left(\hat{x}(t)\right)\widetilde{\mu_j}\left(\widehat{\theta^u}(t)\right)\overline{\mu_k}\left(\widehat{\theta^y}(t)\right) \\ \quad (-K_{ij}^u\tilde{C}_k e_x(t) - \alpha_{ij}^u e_{\theta^u}(t) \\ \quad -K_{ij}^u\Delta C(t)x(t) + \alpha_{ij}^u\theta^u(t) + \dot{\theta^u}(t)) \\ \dot{e}_{\theta^y}(t) = \sum_{i=1}^{r}\sum_{k=1}^{2^{n_{\theta_y}}}\mu_i\left(\hat{x}(t)\right)\overline{\mu_k}\left(\widehat{\theta^y}(t)\right) \\ \quad (-K_{ik}^y\tilde{C}_k e_x(t) - \alpha_{ik}^y e_{\theta^y}(t) \\ \quad -K_{ik}^y\Delta C(t)x(t) + \alpha_{ik}^y\theta^y(t) + \dot{\theta^y}(t)) \end{cases} \tag{34}$$

By Equations (32), (17) and (34), the following uncertain system with bounded external disturbances is obtained:

$$\begin{aligned} \dot{x}_a(t) = &\sum_{i=1}^{r}\sum_{j=1}^{2^{n_{\theta_u}}}\sum_{k=1}^{2^{n_{\theta_y}}}\sum_{l=1}^{r} \\ &\mu_i(\hat{x}(t))\widetilde{\mu_j}\left(\widehat{\theta^u}(t)\right)\overline{\mu_k}\left(\widehat{\theta^y}(t)\right)\mu_l(\hat{x}(t)) \\ &\left(\Phi_{ijkl}x_a(t) + \Psi_{ijk}\omega(t)\right) \end{aligned} \tag{35}$$

where $x_a(t) = \left(x(t) \quad e_x(t) \quad e_\theta^u(t) \quad e_\theta^y(t)\right)^T$ is the extended state vector and $\omega(t) = (\theta^u(t) \quad \dot{\theta}^u(t) \quad \theta^y(t) \quad \dot{\theta}^y(t))^T$ the exogenous input (attack signals and their derivatives), supposed unknown but bounded. Matrices Φ_{ijkl} and Ψ_{ijk} are defined as follows:

$$\Phi_{ijk} = \begin{pmatrix} \Phi_{ijkl}^1 & \left(\mathcal{B}_{ij} + \Delta B(t)\right)\Omega_l & 0 & 0 \\ \Delta A(t) - \Delta B(t)\Omega_l - L_{ij}\Delta C(t) & A_i - L_{ij}\tilde{C}_k + \Delta B(t)\Omega_l & -K_{ij}^u\tilde{C}_k & 0 \\ -K_{ij}^u\Delta C(t) & -K_{ij}C & -\alpha_{ij}^u & 0 \\ -K_{ik}^y\Delta C(t) & -K_{ik}^y\tilde{C}_k & 0 & -\alpha_{ik}^y \end{pmatrix} \tag{36}$$

with $\Phi_{ijkl}^1 = A_i - \mathcal{B}_{ij}\Omega_l + \Delta A(t) - \Delta B(t)\Omega_l$ and

$$\Psi_{ijk} = \begin{pmatrix} 0 & 0 & 0 & 0 \\ 0 & 0 & 0 & 0 \\ \alpha_{ij}^{u} & I & 0 & 0 \\ 0 & 0 & \alpha_{ik}^{y} & I \end{pmatrix} \tag{37}$$

From Equation (35) and the nominal system output (without sensor data deception attack, i.e. $y_n(t) = Cx(t)$), the resulting closed-loop system becomes:

$$\begin{pmatrix} \dot{x}_a(t) \\ y_n(t) \end{pmatrix} = \sum_{i=1}^{r} \sum_{j=1}^{2^{n_{\theta_u}}} \sum_{k=1}^{2^{n_{\theta_y}}} \sum_{l=1}^{r} \mu_i(\hat{x}(t)) \widetilde{\mu_j}\left(\widehat{\theta^u}(t)\right) \overline{\mu_k}\left(\widehat{\theta^y}(t)\right) \mu_l(\hat{x}(t)) \begin{pmatrix} \Phi_{ijkl} & \Psi_{ijk} \\ \overline{C} & 0 \end{pmatrix} \begin{pmatrix} x_a(t) \\ \omega(t) \end{pmatrix} \tag{38}$$

s.t.

$$y_n(t) = Cx(t) = (C \quad 0 \quad 0 \quad 0)x_a(t) = \overline{C}x_a(t) \tag{39}$$

Let us remember the following definition and lemmas:

Definition 1. For a positive scalar γ, the system Equation (38) is said to be stable with desired H_∞ attenuation level γ if it is exponentially stable with:

$$\int_{\infty}^{0} \{ \left(y_n^T(t)\right)_\infty \left(y_n(t)\right)_\infty - \gamma^2 \omega^T(t)\omega(t) \} dt < 0 \tag{40}$$

Lemma I. From the Lyapunov theory, the system (18) is stable with an H_∞ disturbance attenuation γ if there exists a positive symmetric matrix $P = P^T > 0$ s.t.

$$\begin{bmatrix} \Phi_{ijkl}^T P + P\Phi_{ijkl} & P\Psi_{ijk} & \overline{C}^T \\ * & -\gamma^2 I & 0 \\ * & * & -I \end{bmatrix} < 0 \; i, l = 1, \dots, r, j = 1, \dots, 2^{n_{\theta_u}}, k = 1, \dots, 2^{n_{\theta_y}} \tag{41}$$

In order to relax conditions given in Lemma I, the following formulation is given:

Lemma II. For a given positive scalar γ, if there exist matrices P, Z_{ijkl}, where $P = P^T > 0$ and $Z_{ljki} = Z_{ijkl}^T$, $i \neq k$, $i, l = 1, \dots, r, j = 1, \dots, 2^{n_{\theta_u}}, k = 1, \dots, 2^{n_{\theta_y}}$ fulfilling the matrix inequalities (42)-(43)-(44), then, the controller Equation (33) makes the H_∞ norm of polytopic system Equation (38) under attenuation level γ.

$$\begin{bmatrix} \Phi_{ijki}^T P + P\Phi_{ijki} & P\Psi_{ijk} \\ * & -\gamma^2 I \end{bmatrix} < Z_{ijki}; i, l = 1, \dots, r, j = 1, \dots, 2^{n_{\theta_u}}, k = 1, \dots, 2^{n_{\theta_y}} \tag{42}$$

$$\begin{bmatrix} (*)^T P + P\left(\Phi_{ijkl} + \Phi_{ljki}\right) & 2P\Psi_{ijk} \\ * & 2\Psi_{ijk}^T P \end{bmatrix} < Z_{ijkl} + Z_{ljki}; i \neq l, j = 1, \dots, 2^{n_{\theta_u}}, k = 1, \dots, 2^{n_{\theta_y}} \tag{43}$$

$$\begin{bmatrix} Z_{1jk1} & \dots & Z_{1jkr} & \overline{C}^T \\ \vdots & \ddots & \vdots & \vdots \\ Z_{rjk1} & \dots & Z_{rjkr} & \overline{C}^T \\ \overline{C} & \dots & \overline{C} & -I \end{bmatrix}_{j=1,\dots,2^{n_{\theta_u}}, k=1,\dots,2^{n_{\theta_y}}} < 0 \tag{44}$$

Lemma III: Consider two matrices X and Y with appropriate dimensions, a time-varying matrice

$\Delta(t)$ and a positive scalar ε. The following property is verified:

$$X^T\Delta^T(t)Y + Y^T\Delta(t)X \leq \varepsilon X^T X + \varepsilon^{-1}Y^T Y \tag{45}$$

for $\Delta^T(t)\Delta(t) \leq I$.

Replacing Φ_{ijkl} and Ψ_{ijk} by their expressions, the obtained constraints can be easily solved using convex optimization tools and/or the use of a dedicated resolution tool for bilinear constraints like the PenBMI Matlab toolbox. In the study by Kocvara and Stingl[21,22] we can find some examples.

Calculation details

In the following, a detailed calculation procedure is given in order to solve the matrix inequalities (41–43). For simplicity reasons, let us consider the case where the system is subject to a single actuator attack (i.e., $y(t) = Cx(t)$ and $n_{\theta_y} = 1$). The obtained uncertain system with bounded external disturbances is given by:

$$\dot{x}_a(t) = \sum_{i=1}^{r}\sum_{j=1}^{2}\sum_{k=1}^{r} h_i(\hat{x})\mu_j(\widehat{a^u})h_k(\hat{x})\left(\Phi_{ijk}x_a(t) + \Psi_{ij}\omega(t)\right) \tag{46}$$

s.t. $x_a(t) = (x(t) \quad e_x(t) \quad e_{a^u}(t))^T$ and $\omega(t) = (a^u(t) \quad \dot{a^u}(t))^T$. Matrices Φ_{ijk} and Ψ_{ij} are defined as follows:

$$\Phi_{ijk} = \begin{pmatrix} \Phi_{ijk}^1 & \left(\mathcal{B}_{ij} + \Delta B(t)\right)\Omega_k & 0 \\ \Delta A(t) - \Delta B(t)\Omega_k & A_i - L_{ij}C & 0 \\ 0 & -K_{ij}C & -\alpha_{ij}^u \end{pmatrix} \tag{47}$$

with $\Phi_{ijk}^1 = A_i - \mathcal{B}_{ij}\Omega_k + \Delta A(t) - \Delta B(t)\Omega_k$ and

$$\Psi_{ij} = \begin{pmatrix} 0 & 0 \\ 0 & 0 \\ \alpha_{ij}^u & I \end{pmatrix} \tag{48}$$

Let us now detail the stability condition given by Lemma 1 for this system, i.e.,

$$\begin{bmatrix} \Phi_{ijk}^T P + P\Phi_{ijk} & P\Psi_{ij} & \overline{C}^T \\ * & -\gamma^2 I & 0 \\ * & * & -I \end{bmatrix}_{i,k=1,\ldots,r,j=1,2} < 0 \tag{49}$$

In order to solve this constraint, each term will be replaced by its expression and then we will separate the constant and the time-varying terms. The last one, based on the convex sum property, will be bounded; this will allow to solve the matrix inequalities using the tools mentioned above.

Based on definitions, Equations (47) and (48), and considering the matrix P as a diagonal one (i.e., $P = \begin{pmatrix} P_1 & 0 & 0 \\ 0 & P_2 & 0 \\ 0 & 0 & P_3 \end{pmatrix}$, where P_1, P_2 and P_3 are positive symmetric matrix), the constraint Equation (49) is rewritten as:

$$Qijk+QktQkTt<0,\ i,k=1,\ldots,r,j=1,2 \tag{50}$$

where Q_{ijk} is given by:

$$Q_{ijk} = \begin{pmatrix} Q_{ijk}^1 & P_1\mathcal{B}_{ij}\Omega_k & 0 & 0 & 0 & C \\ * & Q_{ij}^2 & -C^T K_{ij}^T P_3 & 0 & 0 & 0 \\ * & * & -2\alpha_{ij}P_3 & P_3\alpha_{ij} & P_3 & 0 \\ * & * & * & -\gamma^2 I & 0 & 0 \\ * & * & * & * & -\gamma^2 I & 0 \\ * & * & * & * & * & -I \end{pmatrix} \quad (51)$$

with $Q_{ijk}^1 = P_1A_i - P_1\mathcal{B}_{ij}\Omega_k + A_i^T P_1 - \Omega_k^T\mathcal{B}_{ij}^T P_1$ and $Q_{ij}^2 = P_2A_i - P_2L_{ij}C + A_2^T P_2 - C^T L_{ij}^T P_2$ Based on Equations (23), (24) and (25), $\mathcal{Q}_k(t)$ is rewritten as:

$$\begin{aligned} \mathcal{Q}_k(t) = &(\mathcal{A}^T P_1 \quad \mathcal{A}^T P_2 \quad 0 \quad 0 \quad 0 \quad 0)^T \Sigma(t)(E_A \quad 0 \quad 0 \quad 0 \quad 0 \quad 0) \\ &+(\mathcal{B}^T P_1 \quad 0 \quad 0 \quad 0 \quad 0 \quad 0)^T \Sigma(t)(-E_B\Sigma_k \quad -E_B\Sigma_k \quad 0 \quad 0 \quad 0 \quad 0) \\ &+(0 \quad \mathcal{B}^T P_2 \quad 0 \quad 0 \quad 0 \quad 0)^T \Sigma(t)(-E_B\Sigma_k \quad 0 \quad 0 \quad 0 \quad 0 \quad 0) \end{aligned} \quad (52)$$

Based on property (31) and lemma 3, $\mathcal{Q}_k(t) + \mathcal{Q}_k^T(t)$ is bounded as the following:

$$\mathcal{Q}_k(t) + \mathcal{Q}_k^T(t) < \begin{pmatrix} \mathcal{Q}_1 & \mathcal{Q}_3 & 0 & 0 & 0 & 0 \\ \mathcal{Q}_2 & 0 & 0 & 0 & 0 & 0 \\ 0 & 0 & 0 & 0 & 0 & 0 \\ 0 & 0 & 0 & 0 & 0 & 0 \\ 0 & 0 & 0 & 0 & 0 & 0 \\ 0 & 0 & 0 & 0 & 0 & 0 \end{pmatrix} \quad (53)$$

with $\mathcal{Q}_1 = \varepsilon_{A1}^{-1}P_1\mathcal{A}\mathcal{A}^T P_1 + \varepsilon_{A1}E_A^T E_A + \varepsilon_{B1}^{-1}P_1\mathcal{B}\mathcal{B}^T P_1 + \varepsilon_{B1}\Omega_k^T E_B^T E_B\Omega_k + \varepsilon_{A2}E_A^T E_A + \varepsilon_{B1}^{-1}P_1\mathcal{B}\mathcal{B}^T P_1 + \varepsilon_{B2}\Omega_k^T E_B^T E_B\Omega_k$, $\mathcal{Q}_2 = \varepsilon_{A2}^{-1}P_2\mathcal{A}\mathcal{A}^T P_2 + \varepsilon_{B2}^{-1}P_2\mathcal{B}\mathcal{B}^T P_2$, and $\mathcal{Q}_3 = \varepsilon_{B1}\Omega_k^T E_B^T E_B\Omega_k$. Applying now Schur's complement with adequate change of variables, constraints (41), (42) and (43) will be easily solved using the tools (PenBMI) presented above.

5. Discussion: Numerical simulation

In the subsequent sections, the presented approach is employed on a fundamental model of a biological wastewater treatment plant. The mathematical model is defined by two state variables, $x_1(t)$ and $x_2(t)$, corresponding to the biomass and substrate concentrations, respectively. The input $u(t)$ signifies the dwell time in the treatment plant, while the measured output is the biomass concentration ($y(t) = x_1(t)$).

5.1. LPV representation of the process

As a preliminary step, we express the nonlinear system Equations (54) in a polytopic form. As presented by Zhou and Khargonekar[18], and with specific assumptions in place, certain simplifications allow us to represent the nonlinear model as follows:

$$\begin{cases} \dot{x}_1(t) = \dfrac{ax_1(t)x_2(t)}{x_2(t)+b} - x_1(t)u(t) \\ \dot{x}_2(t) = -\dfrac{cax_1(t)x_2(t)}{x_2(t)+b} + \big(d - x_2(t)\big)u(t) \end{cases} \quad (54)$$

where a, b, c and d are known parameters. Let us define:

$$\rho_1(t) = -u(t), \quad \rho_2(t) = \frac{ax_1(t)}{x_2(t)+b} \quad (55)$$

From Equations (54) and (55), the quasi-LPV system Equation (56) is deduced:

$$\dot{x}(t) = \begin{pmatrix} \rho_{1^{(t)}} & \rho_2(t) \\ o & -c\rho_2(t) + \rho_1(t) \end{pmatrix} x(t) + \begin{pmatrix} 0 \\ d \end{pmatrix} u(t) \tag{56}$$

Given that a Linear Parameter-Varying (LPV) representation is derived within a compact set of the state space, we can determine the maximum and minimum values of the terms $\rho_1(t)$ and $\rho_2(t)$ based on knowledge of the domain of variation of $u(t)$, Specifically, $\rho_1(t) \in [-1, -0.2]$ and $\rho_2(t) \in [0.004,15]$. By applying the convex polytopic transformation, two partitions are defined for each premise variable:

$$\begin{cases} \rho_1(t) = \varrho_{11}(\rho_1)\rho_1^2 + \varrho_{12}(\rho_1)\rho_1^1 \\ \rho_2(t) = \varrho_{21}(\rho_2)\rho_2^2 + \varrho_{22}(\rho_2)\rho_2^1 \end{cases} \tag{57}$$

with

$$\begin{aligned} \varrho_{11}(\rho_1) &= \frac{\rho_1(t) - \rho_1^2}{\rho_1^1 - \rho_1^2},\ \varrho_{12}(\rho_1) = \frac{\rho_1^1 - \rho_1(t)}{\rho_1^1 - \rho_1^2} \\ \varrho_{21}(\rho_2) &= \frac{\rho_2(t) - \rho_2^2}{\rho_2^1 - \rho_2^2},\ \varrho_{22}(\rho_2) = \frac{\rho_2^1 - \rho_2(t)}{\rho_2^1 - \rho_2^2} \end{aligned} \tag{58}$$

where the scalars ρ_1^1, ρ_1^2, ρ_2^1 and ρ_2^2 are defined as

$$\begin{aligned} \rho_1^1 &= \max_u \rho_1(t),\ \rho_1^2 = \min_u \rho_1(t) \\ \rho_2^1 &= \max_x \rho_2(t),\ \rho_2^2 = \min_x \rho_2(t) \end{aligned} \tag{59}$$

The sub-models are characterized by the sets (A_i, B_i, C) with $i = 1,2,3,4$. Utilizing the definitions of ρ_1 and ρ_2, all the B_i matrices are set to $B = [0 \quad d]^T$. The output matrix $C = [1 \quad 0]$ and the matrices A_i are expressed as:

$$A_1 = \begin{pmatrix} \rho_1^1 & \rho_2^1 \\ 0 & -c\rho_2^1 + \rho_1^1 \end{pmatrix},\ A_2 = \begin{pmatrix} \rho_1^1 & \rho_2^2 \\ 0 & -c\rho_2^2 + \rho_1^1 \end{pmatrix}$$

$$A_3 = \begin{pmatrix} \rho_1^2 & \rho_2^1 \\ 0 & -c\rho_2^1 + \rho_1^2 \end{pmatrix},\ A_4 = \begin{pmatrix} \rho_1^2 & \rho_2^2 \\ 0 & -c\rho_2^2 + \rho_1^2 \end{pmatrix}$$

The weighting functions $\mu_i(t)$ are defined by the following equations:

$$\begin{aligned} \mu_{1^{(t)}} = g_{11}\big(\rho_1(t)\big)g_{21}\big(\rho_2(t)\big) \big| \mu_{2^{(t)}} = g_{11}\big(\rho_1(t)\big)g_{22}\big(\rho_2(t)\big) \\ \mu_{3^{(t)}} = g_{12}\big(\rho_1(t)\big)g_{21}\big(\rho_2(t)\big) \big| \mu_{4^{(t)}} = g_{12}\big(\rho_1(t)\big)g_{22}\big(\rho_2(t)\big) \end{aligned} \tag{60}$$

5.2. Date deception attacks representation on the actuator/sensor

Two categories of data deception attacks are considered, specifically attacks targeting actuators and sensors. Mathematically, these attacks are assumed to be modeled as bounded multiplicative actuator and sensor time-varying faults.

In the considered example, it is presumed that the parameter d is susceptible to hacking. This actuator attack is represented by $d(t)$, such that:

$$d(t) = d + \Delta d(t) \tag{61}$$

It can alternatively be expressed as:

$$d(t) = d + \theta^u(t)\overline{d}, \quad \theta^u(t) \in \left[\theta^{u2}, \theta^{u1}\right] \tag{62}$$

with $d = 2.5$, $\overline{d} = 2.1$ and $\theta^{u2} = -0.1958, \theta^{u1} = 0.1979$. Parameters a, b, c have been identified and set to $a = 0.5$, $b = 0.07$ and $c = 0.7$. Regarding the actuator attack, the polytopic representation of the input matrix B is subsequently expressed through two sub-models, as follows:

$$B_1 = B + \theta^{u1}\overline{B}, \quad B_2 = B + \theta^{u2}\overline{B} \tag{63}$$

where is defined by $\overline{B} := [0 \quad \overline{d}]^T$. The weighting functions $\widetilde{\mu_j}(\theta^u(t))$ are defined as given in Equations (6) and (11).

Now, in the case of a sensor attack, we assume that a bounded multiplicative sensor fault $\theta^y(t)$ influences the output $y(t)$, such that:

$$y(t) = (1 + \theta^y(t))x_1(t) \tag{64}$$

As previously explained, $\theta^y(t)$ can also be written as:

$$\theta^y(t) = \overline{\mu}_1{}^1(\theta^y(t))\theta^{y1} + \overline{\mu}_1^2(\theta^y(t))\theta^{y2}, \ \theta^y(t) \in [\theta^{y2}, \theta^{y1}] \tag{65}$$

with $\theta^{y2} = 0.125, \theta^{y1} = 0.625$, $\overline{\mu}_1{}^1(\theta^y(t))$ and $\overline{\mu}_1^2(\theta^y(t))$ are defined by Equations (8) and (12). The polytopic form of the output is then given by:

$$y(t) = \sum_{k=1}^{2} \overline{\mu}_k\,(\theta^y(t))\tilde{C}_k x(t) \tag{66}$$

with $\tilde{C}_1 = (1 + \theta^{y2} \quad 0)$, $\tilde{C}_2 = (1 + \theta^{y1} \quad 0)$.

5.3. Simulation results

In the given example, incorporating both actuator and sensor attacks and applying the proposed approach by solving Theorem 1, a simultaneous state and attacks observer is formulated. The initial conditions for the system are taken as $x(0) = (0.1 \quad 1.5)$, and for its observer $\hat{x}(0) = (0.09 \quad 2.3)$. For both attacks, the initial conditions are set to zero, i.e $\hat{\theta}^u(0) = 0$ and $\hat{\theta}^y(0) = 0$.

The state vector, its estimate, and the data deception attack along with their estimates are illustrated in **Figures 1** and **2**, respectively. The plots demonstrate the efficacy of the proposed observer; both system states and the time-varying multiplicative actuator/sensor attacks are accurately estimated, ensuring system stability and attenuating the effects of attacks.

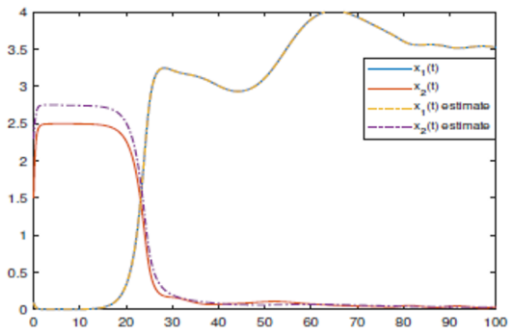

Figure 1. System states and their estimates.

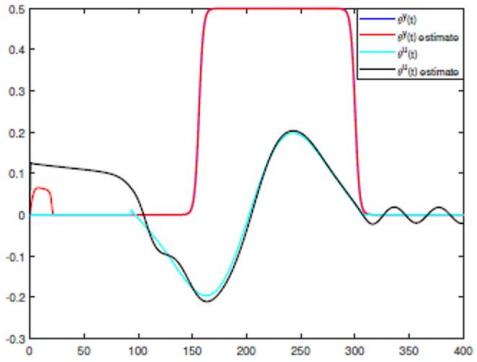

Figure 2. Data deception attacks and their estimates.

6. Conclusion

In the presented contribution, a robust control and quadratic stabilization for nonlinear systems subject to actuator and sensor data deception attacks (cyber-physical-attacks) has been proposed. A new design method based on the rewritten of the attacked system as an uncertain one subject to external disturbances was detailed. Robust polytopic state feedback stabilizing controller based on polytopic observer with disturbance attenuation for the obtained uncertain system was applied. The considered approach gives both controller and observer gain on a single step design and presents less conservative stability conditions than usual approaches. The obtained results are promising and as perspective research work would be on a concrete system (cyber-physical-plant) application.

Conflict of interest

The author declares no conflict of interest.

References

1. Bezzaoucha Rebai S. *A Cyber-Security Contribution to Estimation and Event-Based Control Scheduling Co-Design for Polytopic and T-S Fuzzy Models Using a Lyapunov Approach*. Springer Nature; 2022.
2. Wang R, Sun Q, Ma D, Hu X. Line impedance cooperative stability region identification method for grid-tied inverters under weak grids. *IEEE Transactions on Smart Grid* 2020; 11(4): 2856–2866.
3. Housh M, Kadosh N, Haddad J. Detecting and localizing cyber-physical attacks in water distribution systems without records of labeled attacks. *Sensors* 2022; 22(16): 6035. doi: 10.3390/s22166035
4. Taheri M, Khorasani K, Shames I, Meskin N. Cyber attack and machine induced fault detection and isolation methodologies for cyber-physical systems. *arXiv* 2009; arXiv:2009.06196. doi: 10.48550/arXiv.2009.06196
5. Ye L, Zhu F, Zhang J. Sensor attack detection and isolation based on sliding mode observer for cyber-physical systems. *International Journal of Adaptive Control and Signal Processing* 2020; 34(4): 469–483.
6. Zhang X, Zhu F. Observer-based sensor attack diagnosis for cyber-physical systems via zonotope theory. *Asian Journal of Control* 2020.
7. Karimipour H, Leung H. Relaxation based anomaly detection in cyber-physical systems using ensemble Kalman filter. *IET Cyber-Physical Systems: Theory & Applications* 2019; 5(1): 49–58.
8. Li Q, Bu B, Zhao J. A novel hierarchical situation awarness model for CBTC using SVD entropy and GRU with PRD algorithms. *IEEE Access* 2021.
9. Lukens JM, Passian A, Yoginath S, et al. Bayesian estimation of oscillator parameters: Toward anomaly detection and cyber-physical system security. *Sensors* 2022; 22(16): 6112. doi: 10.3390/s22166112
10. Zhu F, Liu X, Wen J, et al. Distributed robust filtering for wireless sensor networks with markov switching topologies and deception attacks. *Sensors* 2020; 20(7): 1948. doi: 10.3390/s20071948
11. Lu W, Yin X, Fu Y, et al. Observer-based event-triggered predictive control for networked control systems under dos attacks. *Sensors* 2020; 20(23): 6866. doi: 10.3390/s20236866
12. Zhu Q, Basar T. Robust and resilient control design for cyber-physical systems with an application to power systems. In: Proceedings of the 50th IEEE Conference on Decision and Control and European Control

Conference (CDC-ECC); 12–15 December 2011; Orlando, FL, USA.
13. Moazeni F, Khazaei J. Detection of random false data injection cyberattacks in smart water systems using optimized deep neural networks. *Energies* 2022; 15(13): 4832. doi: 10.3390/en15134832
14. Bezzaoucha Rebai S. A cyber-security contribution: Estimation and event-based control scheduling co-design for polytopic & t-s models. In: Proceedings of the 2021 International Conference on Fuzzy Theory and Its Applications (Ifuzzy 2021); 5–8 October 2021; Taitung, Taiwan.
15. Bezzaoucha Rebai S, Voos H. Simultaneous State and False-Data Injection Attacks Reconstruction for NonLinear Systems: An LPV Approach. In: Proceedings of the 2019 3rd International Conference on Automation, Control and Robots; 11–13 October 2019; Prague, Czech Republic.
16. Bezzaoucha S, Marx B, Maquin D, Ragot J. Nonlinear joint state and parameter estimation: Application to a wastewater treatment plant. *Control Engineering Practice* 2013; 21(10): 1377–1385.
17. Blanke M, Kinnaert M, Lunze J, Staroswiecki M. *Diagnosis and Fault-Tolerant Control*. Springer-Verlag; 2003.
18. Zhou K, Khargonekar P. Robust stabilization of linear systems with norm-bounded time-varying uncertainty Control. *Systems and Control Letters* 1988; 10(1): 17–20.
19. Teixeira A, Pérez D, Sandberg H, Johansson K. Attack models and scenarios for networked control systems. In: Proceedings of the 1st International Conference on High Confidence Networked Systems; 17–18 April 2012; Beijing, China.
20. Oudghiri M, Chadli M, El Hajjaji A. One step procedure for robust output fuzzy control. In: Proceedings of the 2007 Mediterranean Conference on Control & Automation; 27–29 June 2007; Athens, Greece. pp. 1–6. doi: 10.1109/MED.2007.4433964
21. Kocvara M, Stingl M. PENNON—A code for convex nonlinear and semidefinite programming. *Optimization Methods and Software* 2003; 18(3): 317–333.
22. Kocvara M, Stingl M. PENBMI, Version 2.0, 2004. Available online: www.penopt.com for a free developer version (accessed on 2 June 2023).

Computing and Artificial Intelligence 2023; 1(1): 100.
Review Article

Harmful algal blooms (HAB) open issues: A review of ecological data challenges, factor analysis and prediction approaches using data-driven method

Nur Aqilah Paskhal Rostam[1], Nurul Hashimah Ahamed Hassain Malim[1,*], Nur Afzalina Azmee[2], Renato J. Figueiredo[3], Mohd Azam Osman[1], Rosni Abdullah[1]

[1] *School of Computer Sciences Universiti Sains Malaysia, Penang 11800, Malaysia*

[2] *Faculty of Science and Mathematics, Universiti Pendidikan Sultan Idris, Tanjong Malim 35900, Perak, Malaysia*

[3] *Department of Electrical and Computer Engineering of the University of Florida, Gainesville, FL 32611, United States*

*** Corresponding author:** Nurul Hashimah Ahamed Hassain Malim, nurulhashimah@usm.my

ARTICLE INFO

Received: 27 June 2023
Accepted: 3 August 2023
Available online: 16 November 2023

doi: 10.59400/cai.v1i1.100

ABSTRACT: Ongoing research on the temporal and spatial distribution of algae ecological data has caused intricacies entailing incomprehensible data, model overfit, and inaccurate algal bloom prediction. Relevant scholars have integrated past historical data with machine learning (ML) and deep learning (DL) approaches to forecast the advent of harmful algal blooms (HAB) following successful data-driven techniques. As potential HAB outbreaks could be predicted through time-series forecasting (TSF) to gauge future events of interest, this research aimed to holistically review field-based complexities, influencing factors, and algal growth prediction trends and analyses with or without the time-series approach. It is deemed pivotal to examine algal growth factors for useful insights into the growth of algal blooms. Multiple open issues concerning indicator types and numbers, feature selection (FS) methods, ML and DL forms, and the time series-DL integration were duly highlighted. This algal growth prediction review corresponded to various (chronologically-sequenced) past studies with the algal ecology domain established as a reference directory. As a valuable resource for beginners to internalize the algae ecological informatics research patterns and scholars to optimize current prediction techniques, this study outlined the (i) aforementioned open issues with an end-to-end (E2E) evaluation process ranging from FS to predictive model performance and (ii) potential alternatives to bridge the literature gaps.

KEYWORDS: data-driven prediction method; harmful algal bloom; time series forecasting; machine learning; deep learning

1. Introduction

The escalation of HAB trends over the past years has caused much global concern. The HABs entail various bloom types that cause harm without exception as HAB toxins adversely impact human, environmental, and economic health while their non-toxic counterparts could prove detrimental to fishery-based resources and tools[1]. Rapid algae generation and growth, which depict its susceptibility to shifts in environmental conditions[2], have been thoroughly examined in ecological informatics as typical ecological data issues. As an emerging field that integrates computational methods for ecological evaluation, ecological informatics regards the intensive nature of ecological data with its valuable content and the necessity to convey empirical outcomes and make research-, conservation-, and resource

management-oriented decisions[3]. The conceptual framework associates ecological components (genomes, organisms, populations, communities, ecosystems, and landscapes) with data management, analysis, and synthesis.

Early prevention and algae growth control were executed as various places were impacted by this natural phenomenon until 2015 and continue to be affected to date. Nevertheless, several prediction-oriented issues resulting from spatial and temporal algae distribution remain unaddressed despite the exertion of time and effort to forecast HAB growth. The rapid generation and growth of algae under favorable environmental conditions could differ on short timescales ranging from several days to weeks or hours[4]. The concentration could shift abruptly as current chlorophyll content could occasionally be five times more concentrated than before and vice versa. This complexity further instigates the non-linearities and ambiguities in ascertaining HAB-favouring conditions, thus complicating the prediction process and causing forecasting errors due to fluctuations and ambiguities[5].

Apart from the nature of algal blooms, highly non-linear data and time-varying processes that remain vague[6] hinder current physical prediction models from establishing a clear coefficient, thus highlighting the correlation between every factor in algal bloom prediction and the multiple variable data sources required for analysis[7]. Such shortcomings are further hampered by prolonged durations and high financial costs and undermine prediction accuracy. Spatial and temporal distributions are impacted by multiple climatic, geographical, and ecological elements. Temporal distribution, which catalyzes the interconnection of indicators, inevitably increases prediction-related intricacies[8]. Summarily, all the aforementioned concerns have rendered prediction to become more complex and imprecise.

Effective algae bloom modeling and prediction in such an intricate system is significantly challenging given the presence of physical, chemical, and biological processes and their subsequent interrelations. Water pollution or eutrophication with algae implies an intricate operation of all potentially impacting factors[9]. The drawbacks could be resolved using ML or artificial intelligence (AI) for insights into the algal community. In line with previous studies, multiple scholars have employed past historical data to forecast algal bloom by integrating ML methods following the successful data-driven approach in algal growth prediction. Essentially, ML methods constituting artificial neural network (ANN), support vector machine (SVM), decision trees (DT), random forest (RF), and regression offer a principled set of mathematical techniques to elicit meaningful features from the data in generating distinctive patterns that could be manipulated for decision-making, estimating, and forecasting purposes.

The necessity to predict future HAB events has resulted in the incorporation of time series, which considers the temporal aspect. Multiple time-series approaches were implemented through the traditional method or integration with ML techniques following past research. Regarding the primary variation between the time series and traditional statistical forecasting, data points in the traditional statistical prediction (classification) could be independent of one another while the counterparts in time series denote a temporal nature that induces interdependence. This time dimension adds an explicit ordering to data points that should be conserved to offer vital information to learning algorithms[10].

Traditional time-series statistical forecasting models resembling auto-regressive integrated moving average (ARIMA) and its variants, such as autoregressive models (AR), moving average (MA), and autoregressive and moving average (ARMA) is extensively employed to make predictions. The models prove inappropriate for non-linear data evaluation despite their capacity to determine temporal behavior and generate satisfactory forecasts for linear time-series data[10] given their function in assuming specific distribution or function types of time series, thus deterring them from ascertaining the intricate

underpinnings of non-linear associations and depicting reality. As most of the models disregarding variable interdependencies in terms of multivariate time series induced low prediction accuracy, initiatives to incorporate DL in environmental study problems have intensified as the DL model reflects optimal performance for time-series data forecasting. Research on DL, such as recurrent neural network (RNN) and its variant, long short-term memory (LSTM), remains scarce given the recent integration of time series with DL in algal growth prediction studies[7].

The input-output variable relationship denotes a crucial study component. Concerning aquatic systems, information involving the impacts of physical, chemical, and biological water quality parameters on algal dynamics is necessary for optimal system internalization and management. Other elements (meteorological) also induce algae growth parallel to the growing data. On practical grounds, an efficient prediction approach denotes intricate algorithms, a holistic understanding of the blooms mechanism, and a reliable dataset with essential components. Determining this relationship by assessing the aforementioned set of information would generate insightful data to unveil the interconnection between factors. It is crucial to review past literature on algae prediction techniques and present complexities in determining an optimal algal growth prediction method from various aspects as precise decision-making arise from a sound interpretation of forecasting in various prediction tasks. The same framework could be generalized across other domains if the dynamics and comprehension of algae are addressed factor-wise. In this vein, the worldwide trend on water resource conservation and protection could be sustained.

The remaining sections are organized as follows: Section 2 provides an overview of the algae ecology, algal growth factor analysis, and research concerns; Section 3 highlights current literature on the data-driven method through ML, traditional time series, and time series with DL; Section 4 elaborates on open issues and future study directions; Section 5 summarizes the research.

2. Background study of algae ecology

Radmer[11] identified two distinct algae types that commonly live in water or damp environments: macroalgae and microalgae. Macroalgae imply bigger algae (seaweed) while microalgae denote the smaller counterpart (phytoplankton or cyanobacteria and green and red algae, red algae). Algae require (i) the sun as its primary source of energy, (ii) water, (iii) conducive temperature, and (iv) nutrients for growth: elements that could be easily found in water. Algae also require carbon dioxide, which is generated from pollutants (smoke, fumes from cars, and a little carbon dioxide) when plants breathe at night in the absence of sunlight, to produce sugar. The HAB implies an excess of harmful algae. Water conditions with nutrient-rich water columns (specifically phosphorus and nitrogen) following regular fish-feeding and fertilizer (or sewage) discharge into an aquatic system catalyze HAB growth. Toxic HAB could prove detrimental to human health and aquatic life (including fishes) in the form of ailments and demise, respectively, whereas non-toxic counterparts could damage fishery resources[1]. Harmful algal blooms could resemble foam, scum, or mats on the water surface in different colors and release life-threatening toxins (microcystin or MC, anatoxin, cylindropermopsin, and saxitoxin). In this regard, HAB has become a serious environmental concern on a global scale[12]. Discolored water could also be a HAB indicator. **Table 1** presents common HABs and their implications on human health following Bui et al.[12].

Table 1. Common HABs and health effect.

Organism	Water type	Color	Toxin	Health effects
Alexandrium sp.	Salt	Red or brown	Saxitoxins	Paralytic shellfish poisoning, paralysis, death
Karenia brevis	Salt	Red	Brevetoxins	Gastrointestinal illness, muscle cramps, seizures, paralysis, respiratory problems
Pseudo-nitzschia	Salt	Red or brown	Domoic acid	Amnesiac shellfish poisoning, vomiting, diarrhea, confusion, seizures, permanent short-term memory loss, death
Microcystis	Fresh	Blue-green	MC	Gastrointestinal illness, liver damage

2.1. Factor analysis affecting algae growth

Past literature demonstrated the severity and essentiality of algae prediction as a means of early prevention. Based on Whigham and Recknagel[13], recent advancements in algal bloom modeling encounter two drawbacks: insufficient ecological information for deductive modeling and inefficient data analysis for inductive modeling. The HAB heterogeneity must be evaluated to derive a comprehensive understanding and control their formation[14]. In other words, algal growth analysis would provide an optimal understanding of the aquatic system. The analysis method is an initial step pre-predictive modeling to gain useful insights and internalize algal ecology factors and interconnections in managing two primary elements: algae interrelationships and dynamics.

Many efforts have been exerted to evaluate algae ecology to comprehend the dynamics, ambiguity, and non-linear nature of algal growth prediction. Several studies solely emphasized this evaluation sans predictive work. The analysis techniques were performed by categorizing the algae. As some algorithms could also be utilized in pre-processing or FS, the algal bloom method analysis requires a thorough examination to internalize the pertinent factors and interrelations in algal ecology.

All algae species depend on light as a fundamental input for photosynthesis and nutrients for growth and reproduction: nitrogen and phosphorus. Factors encompassing water temperature, turbidity, mixing, competition, and grazing also hold relevance to the algae population dynamics. For example, Huang and Zheng[15] listed 20 environmental parameters entailing water temperature (WT), ambient temperature, secchi disk depth (SDD), transparency, turbidity, solar radiation, total phosphorus (TP), total nitrogen (TN), ammonia-nitrogen (NH_3–N), ammonium-nitrogen (NH_4–N), nitrate nitrogen (NO_3–N), ammonium ion concentration, dissolved oxygen (DO), conductivity, alkalinity, calcium concentration, total suspended solids (TSS), silica, pH, salinity, and chlorophyll-a (Chl-a) that catalyze cyanobacteria bloom.

Chlorophyll, the green pigment in leaves, enables plants to create energy from light using photosynthesis. The amount of photosynthesizing plants are implicitly assessed by measuring chlorophyll. Such plants would be algae or phytoplankton in a water sample. Overall, chlorophyll denotes the measure of all (dead or living) green pigments while Chl-a implies the measure of a pigment portion that remains alive. Sunlight, temperature, nutrients, and wind collectively impact both the prevalence of algae and Chl-a concentration. The first algae outbreak or 'bloom' may occur and grow in spring when nutrients are in rich supply and the water temperature and days turn warm. Algae concentration prediction, which could be measured in total chlorophyll form with raw water, was previously executed as a robust algal growth indicator[16].

Tian et al.[17] highlighted water quality, hydrology, and climate conditions as the key determinants of chlorophyll dynamics while Bui et al.[12] indicated that WT, pH, and DO were positively related to cynobacterial community dynamics and MC concentration. Meanwhile, nutrient level, phosphate, and

nitrogen concentration were also identified as fundamental elements. Water quality-oriented research ascertains the chemical and physical attributes of water bodies and potential contaminants that reduce the water quality and forecast algae growth. Notably, Chl-a also constitutes the biological elements in water quality research. **Table 2** lists the most extensively-assessed qualitative water quality parameters following Gholizadeh et al.[18].

Table 2. Common qualitative measures.

Water quality parameter	Abbreviation	Units
chlorophyll-a	Chl-a	mg/L
Secchi disk depth	SDD	m
Temperature	T	˚C
Coloured dissolved organic ma	CDOM	mg/L
Total organic carbon	TOC	mg/L
Dissolved organic carbon	DOC	mg/L
Total suspended matters	TSM	mg/L
Turbidity	TUR	NTU
Sea surface salinity	SSS	PSU
Total phosphorus	TP	mg/L
Total nitrogen	TN	mg/L
Ortho-phosphate	PO_4	mg/L
Chemical oxygen demand	COD	mg/L
Biochemical oxygen demand	BOD	mg/L
Electrical conductivity	EC	Ms/cm
Ammonia nitrogen	NH_3-N	mg/L

Wells et al.'s[14] study extensively covered past and present algal blooms with emphasis on how climate shifts globally impact the marine planktonic system with elaborations on the connection of specific environmental aspects (temperature, stratification, light, ocean acidification, precipitation-induced nutrient inputs, and grazing) that undergo alterations amidst climate change. The 2013 United States Environmental Protection Agency (EPA) analysis summarised the implications of climate change on HABs with multiple mechanisms: warmer WT, altered salinity and rainfall patterns, high carbon dioxide concentration, coastal upwelling, and rising sea levels.

Other elements including microclimates and the thermal, hydric, and radioactive conditions in the first meter above and below the Earth surface may optimize prediction performance despite the paucity of scholarly attention. Microclimates are frequently disregarded in ecology and evolution despite empirical proof of their essentiality in ecosystem dynamics and processes, such as the organism responses to climate change[18] although Kearney and Porter[19] emphasized the importance of understanding microclimates in ecology given its representation of the physical conditions experienced by organisms. Amsler et al.'s[20] initial work that examined algal abundance with microclimate in 1992 aimed to morphologically, physiologically, and behaviourally connote the early germling life-history stages of algal for survival. Resultantly, the planktonic environment is chemically heterogeneous on a macroalgal propagule scale.

Biological oceanographers have come to acknowledge the high variability of nutrient concentration in water columns, which could then be assessed with classical approaches. Following Shi et al.[21], the

cyanobacterial dynamics sensitivity to climate conditions differed across regions based on hydrodynamics, morphology, and specified chemical parameters. This phenomenon exemplifies one of the microclimates examined in this study. Some of the crucial variables were elaborated on throughout the current review. All the aforementioned and additional variables were classified into several categories (see **Table 3**).

Table 3. Categorical variables.

Abbreviation	Variables	Factor category
Chl-a	Chlorophyl-a	Biological factor (BF)
BC	Bloom cases (incident)	
SGR	Specific growth rate	
WT	Water temperature	Physical factor (PF)
Salin	Salinity	
DO	Dissolved oxygen	
Turb	Turbidity	
pH	pH	
SDD	Secchi disk depth	
SS	Suspended solid	
DC	Depth code	
FI	Freshwater inflow	
EV	Estuarine velocity	
SRT	Salinity recovery time	
TIN	Total inorganic nitrogen	Chemical factor (CF)
PO_4	Orthophosphate	
TP	Total phosphorus	
TN	Total nitrogen	
AN	Ammonia nitrogen	
NO_2–N	Nitrite nitrogen	
NO_3–N	Nitrate nitrogen	
COD	Chemical oxygen demand	
Si	Silica	
Hg	Mercury	
Pb	Lead	
Zn	Zinc	
Al	Aluminum	
Rf	Rainfall	Meteorological factor (MF)
T_{min}	Minimum temperature	
T_{avg}	Average temperature	
T_{max}	Maximum temperature	
Hum	Humidity	
SR	Daily solar radiation	
WS	Daily average wind speed	

Algal bloom-oriented research could also include factors constituting population density and algal bloom cases. The elements are explicitly inspired by a distinctive domain, such as the dengue outbreak where population density and dengue cases are key determinants of dengue prediction[21,22]. Shi et al.[21] indicated that population density impacts the dengue outbreak following economic and income variances. Essentially, 'dengue cases' denote one of the key variables recognized by relevant scholars[23–26]. It could prove advantageous to thoroughly examine human factors for algae prediction as high nutrient loading and carbon dioxide concentration is induced by human activities. Careful consideration or adoption of additional determinants with data fusion could provide high-impact outcomes for the prediction process. Extensive research on whether data fusion optimizes prediction performance proves necessary to date.

2.2. Ecological data issue and challenges

Notably, HAB research and management struggle to ascertain species variety, life histories, ecosystems, and subsequent implications. The potentially-harmful algae ecology that does not fall under one distinctive group[1] leads to dynamic growth and complex prediction. Issues concerning dynamics and interconnections frequently appear in ecological modeling parallel to the aforementioned factors catalyzing algal growth.

Frequently correlated algae ecological variables have caused redundant information as high algae data interrelations primarily result from the indicator connections that are highly associated with one another. For example, multiple variables in aquatic environments implicitly or explicitly rely on the amount of oxygen available. Algae prediction needs to consider abiotic factors and their association with WT and nutrient concentration[27]. This occurrence has instigated low data quality, ambiguities, and variabilities. The formation of algal blooms depicts high uncertainty in addition to spatial variation following complex mechanisms.

Kim[28] thoroughly outlined dynamic-related issues. Specifically, dynamic algae growth, which could differ based on short timescales (hours to days), has rendered the identification of favorable HAB conditions a significant empirical effort among scholars. Algae concentration could alter abruptly when the present chlorophyll concentration is five times higher than before and vice versa, thus hampering accurate forecasting. Based on scholarly perspectives, natural factors undeniably induce impromptu changes in algae content. To date, ecological data are ambiguously connoted as expert knowledge following the presence of random variables, incomplete and inaccurate data, and approximate predictions (rather than measurements) that lead to data incomprehensibility[29].

Algae ecological data experience high missing values following their reliance on frequently-maintained monitoring sensors or systems, which could be damaged by the presence of algae. As coral-like algae would attach itself to the utilized equipment and damage all the installed sensors in line with Rostam et al.[30], early algae prediction remain essential given the extended timeframe offered for coastal water facilities to shut down before the equipment is damaged[31,32].

Highly non-linear behavior and dynamics emphasize conventional approaches resembling model-fitting[33]. Regarding aquatic systems, holistic knowledge of the physical, chemical, and biological water quality parameter impacts on algal dynamic proves necessary for optimal system comprehensibility and management. One measure of interest implies the examination of dynamic algae criteria within the algae domain where it is pivotal to disclose the input-output variable link: an essential algae ecological study element, particularly for precise prediction.

Ecological data typically appear in time-series format[34]. Time-series problems add to the order

complexity or frequently encompass temporal dependency, which causes two otherwise identical time points to fall under distinct classes or forecast different behaviors, unlike simpler classification and regression problems[35]. This attribute could prove challenging given the necessity for specialized data management in model fitting and assessment where the time series data need to be formatted or framed as a supervised machine learning pre-forecasting, hence increasing data evaluation complexities.

The ML techniques could function optimally on more intricate time-series forecasting issues with various input variables, intricate non-linear associations, and missing data. Such approaches frequently require hand-engineered features from domain experts or practitioners with domain backgrounds for enhanced performance. To date, time-series forecasting with DL serves to gauge temporal dependence from the data, efficiently determine past pivotal observations, and grasp their relevance to the present prediction process[35]. In this vein, crucial information could be derived from the input and dynamically shift the context as required. Feature engineering also constitutes one of the ML disciplines that could transform and engineer raw data into the fitting format for time-series forecasting.

As this section only highlights current algae ecological data complexities, the aforementioned methods would be extensively reviewed in another section. The current section serves to examine regression problems or concerns involving real-value predictions and empirical works that employ raw numerical static and time-series data. This review does not cover research on spatial data image-processing as the methodology constitutes distinctive terms of feature extraction or selection, which slightly differs from previous descriptions for easier comparison.

3. Data-driven prediction model

The algorithms currently incorporated into algal bloom prediction are categorized into data- and process-driven models. Process-driven model typically requires several parameters, such as initial conditions and ecological variables. The models, which occasionally encounter the uncertainty of kinetic coefficients, require optimal system knowledge[12] although process-driven models reflect highly-precise predictions. Data derivation intricacies in the simulation process have instigated drawbacks in process-driven method implementation.

Past research documented the successful implementation of the data-driven AI-based method. Essentially, data-driven models rely on computational astuteness and ML techniques[36]. An ML algorithm serves to identify the system input-output association with a training dataset that characterizes all system behaviors. The trained model could be subsequently tested with an independent dataset to ascertain the extent to which it could be generalized across unseen data. Algae prediction would be more precise upon identifying the optimal parameter level through past ecological data insights.

Appropriate FS is mandatory in this case. The ML for unsupervised techniques, such as clustering could facilitate data discovery or elicit useful insights rather than merely relying on domain knowledge. As such, unsupervised ML was also reviewed. Sections for the algae prediction model through ML (presented in distinctive parts) are classified into unsupervised and supervised ML and time-series forecasting.

3.1. Algal growth prediction with unsupervised ML

Traditional clustering approaches are unsupervised given the absence of outcome variables and knowledge of the associations between the dataset observations[37]. Ecological data classification facilitates notable pattern and feature identification. Despite the abundance of clustering methods, such as hierarchical clustering, self-organizing map (SOM), and K-means, both SOM and K-means denote the

common clustering technique within this domain. Kohonen's[38] SOM, a useful feature extraction tool with a series of known patterns[39], represents multi-dimensional data in a relatively lower (one or two) dimensional space. Neurons on the grid would eventually merge around areas with high-density data points using multiple iterations. Overall, SOM denotes an efficient instrument in high-dimensional data visualization that proves adequate for the data comprehension stage in the knowledge discovery process.

Following Li et al.'s[40] recent research on SOM implementations in algae analysis and forecasting, the proposed SOM perceivably selects the most influential input variables for Chl-a. The K-means approach was subsequently integrated to define the cluster boundaries. Resultantly, SOM and GA-BPNN functioned as an FS instrument and efficiently performed clustering and predictions. In the study of Malek et al.[41], SOM was also utilized as an analysis tool of limnological time-series in the Putrajaya Lake and wetlands for algae growth identification. An expert system was subsequently established following the rules elicited from SOM for algal growth modeling and prediction.

Generally, K-means clustering is incorporated into datasets where all the variables are quantitative and the distance between observations is evaluated with the squared euclidean distance. **Table 4** presents past studies with SOM and K-means that are applied in this domain and the number of employed features (#F), water source types, method, and factors category connected to **Table 3**.

Table 4. Unsupervised ML prediction method.

Article (s)	#F	Sources	Method	Factors category			
				BF	PF	CF	MF
[27]	5	Lake	SOM-fuzzy	/	/	/	-
[39]	6	Coastal	SOM	/	/	/	-
[40]	24	Lake, reservoir	SOM, K-means GABPN	/	/	/	-
[42]	4	Lake	SOM-FL	-	/	/	-
[43]	13	Lake	RNN-SOM	/	/	/	-
[44]	11	Lake	SOM	/	/	/	-

Coastal dataset clustering is few compared to other water sources (see **Table 4**), thus implying the lack of SOM and K-means application to coastal ecological datasets. The SOM benefits and effectiveness regarding information extraction without background knowledge of the examined ecosystem reflect a potential unsupervised learning approach.

3.2. Algal growth prediction with supervised ML

Supervised learning implies the ML task of learning a function that outlines input to output following sample input-output pairs. A function is inferred from the labeled training data encompassing a set of training samples. Methods involving regression and time-series analysis and AI are implemented to evaluate the historical dataset for algal bloom prediction[27]. Such approaches adequately model the HAB dynamics[45]. This review, which emphasized previous studies on the algal growth prediction model, is sequenced based on ML approaches (fuzzy, ANN, and SVM) and includes hybrid techniques alongside a group of other approaches classified under the 'other' category: genetic algorithm (GA), naïve bayes (NB), RF, evolutionary algorithm (EA), hybrid evolutionary algorithm (HEA), multilayer perceptron (MLP) and DT. Lastly, the TSF method was thoroughly reviewed in a separate section. **Table 5** demonstrates the trend of algae prediction approaches between 2014 and 2020.

Table 5. The trend of algae prediction method (2014–2020).

Article (s)	Fuzzy	ANN	SVM	Hybrid	Other	TSF
[7]	-	/	-	-	-	/
[12]	-	/	-	-	-	-
[15]	-	-	-	-	/	-
[17]	-	/	-	-	/	-
[23]	-	-	-	-	-	/
[28]	/	-	-	-	/	-
[29]	-	-	-	-	-	/
[34]	-	-	-	-	-	/
[41]	-	/	/	-	-	-
[46]	-	-	-	-	/	-
[47]	-	-	-	-	-	/
[48]	-	-	/	-	-	-
[49]	-	/	-	-	-	-
[50]	-	/	-	-	-	-
[51]	-	/	-	-	-	-
[52]	-	/	-	-	-	-
[53]	-	/	-	-	-	-
[54]	-	-	/	-	-	-
[55]	-	/	-	-	-	-
[56]	-	/	-	-	-	/
[57]	-	/	-	-	-	-
[58]	-	/	/	/	/	-
[59]	-	-	-	-	-	/
[60]	-	-	-	-	-	/
[61]	-	-	-	-	-	/
[62]	-	/	-	-	-	/
[63]	-	/	-	-	/	/
[64]	-	-	/	-	/	-
[65]	-	-	-	-	/	-
[66]	-	-	-	-	-	/
[67]	-	-	-	-	-	-
[68]	-	/	/	-	/	/
[69]	-	-	-	/	/	-
[70]	-	/	/	-	-	/
[71]	-	/	-	-	-	/
[72]	-	-	-	-	-	/

3.2.1. Fuzzy approach

The fuzzy approach successfully resolves ecological data ambiguity due to its dynamic nature. Zadeh's[72] fuzzy set theory in 1965 follows an extension of the classical connotation of the term 'set', which enables the processing of fuzzy premises in the 'IF-THEN' form with fuzzy sets in the premise and

conclusive parts. The implementation of algal bloom prediction was scarcely documented despite the theory prevalence in uncertainty analysis. Most of the studies emphasized data clustering into specified classes or categories for pre-prediction rather than actual forecasting. In this regard, the fuzzy approach complements classification as opposed to regression and time-series prediction problems. Nevertheless, this method could establish comprehensible rules or offer useful insights owing to logical descriptions of the FL system action. Only three empirical works have been documented to date.

Chen and Mynett[73] employed nine parameters (pH, conductivity, BOD, DO, NH^{4+}, NO^{3-}, NO^{2-}, TIP, Chl-a) with the fuzzy approach in lakes. The SOM sought appropriate fuzzy set connotations and explicit inference rules that are supported by heuristic knowledge amidst data unavailability. Chen et al.[27] utilized the fuzzy method through SOM to ascertain the multivariate structure and provide insights into the spatial-temporal dynamics of algal blooms. Notwithstanding, both techniques only offered a one-way procedure that focused on understanding instead of actual prediction and disregarded model output feedback for further optimization. The study of Malek et al.[42] highlighted four variables for lake-based research: pH, SD, dissolved oxygen, and nitrate nitrogen. The method might not prove successful for large datasets and intricate features given the absence of empirical evaluation despite its practicality and efficiency in managing insufficient datasets with complex correlations and ambiguous interconnections.

3.2.2. Artificial neural network (ANN)

The ANN implies a computational non-linear model entailing artificial neurons or processing elements that is organized in three interconnected layers: input, hidden layer (middle). Each neuron constitutes weighted inputs (synapses), an activation function (denotes the output given an input), and one output. The weighted input sum generates the activation signal transferred to the activation function in obtaining one neuron output. The extensively employed activation functions encompass linear, step, sigmoid, tanh, and rectified linear unit (ReLu) functions. Backpropagation, which computes the loss function gradient, is the most commonly utilized approach to identify the error contribution of every neuron. In 1997, Recknagel et al.[74] pioneered the modeling of algal blooms in freshwaters through ANNs. Backpropagation was employed in training where inputs and outputs imply palpable water quality parameters and the biomass quantities of particular algal groups, respectively. **Table 6** summarizes other algal growth studies using ANN and its ensuing variants.

Table 6. Supervised ML prediction using ANN.

Article (s)	#F	Sources	Method	Results	Factors category			
					BF	PF	CF	MF
[12]	8	Reservoir	FFBP-ANN	RMSE: 0.108	-	/	/	-
[17]	1	Reservoir	ANN	MSE: 1.303 R: 0.774	/	-	-	-
[49]	9	Reservoir	MLP TDNN	MSE: 1.76	-	/	-	-
[50]	12	River	ANN Sensitivity analysis	R^2: 0.82	/	/	/	/
[52]	11	Coastal	RBMDBN	RSME: 0.0475 MAE: 18.72%	/	/	/	-
[53]	17	Fresh water	ELM	RSME: 0.3013 MAE: 0.2366 R^2: 0.8322	/	/	/	-

Table 6. (*Continued*).

Article (s)	#F	Sources	Method	Results	Factors category			
					BF	PF	CF	MF
[56]	12	Coastal	DBN-ARIMA	RMSE: 0.154 MAE: 0.123 MAPE: 17.21 R: 0.798	/	/	/	-
[57]	1	Lake	DDBN TDBN DBN	RMSE: 1.48 RMSE: 1.53 RMSE: 1.55	/	-	-	-
[62]	7	River	ELM ANFIS LR	RMSE: 13.8 RMSE: 16.7 RMSE: 17.5	/		/	/

3.2.3. Support vector machine (SVM)

The SVM denotes a linear decision boundary that operates by mapping data to high-dimensional feature space for data point classification despite not being linearly isolated. Data would be transformed in such a way that the separator could be drawn as a hyperplane upon identifying a distinction between the categories. In SVR, it serves to forecast the output by fitting the maximum number of output points (from the training data) between the boundary lines and simultaneously remaining as flat as possible[75]. Essentially, SVM regression is a non-parametric approach following its dependence on the function of kernel: the employment of a linear classifier to address a non-linear classification task. Several works recommended SVM application in algae forecasting. Xie et al.[75] suggested an SVM-oriented prediction to internalize and predict a dynamic algae population shift in freshwater reservoirs and resolve the complex non-linearity of water variables with their interactions. Resultantly, SVM generates high prediction accuracy despite utilizing a small sample number. The modeling outcomes demonstrated that SVM outperformed ANN. **Table 7** highlights previous studies on algal growth prediction with SVM.

Table 7. Supervised ML prediction using SVM.

Article (s)	#F	Sources	Method	Results	Factors category			
					BF	PF	CF	MF
[47]	9	Coastal	SVM GRNN	RMSE: 5.436 RMSE: 9.966	/	/	/	-
[54]	10	Fresh water	SVM	R^2: 067	/	/	/	-
[69]	9	Reservoir	SVM	RMSE: 1.04 R^2: 0.71 MAE: 0.40	/	/	/	-
[75]	16	Reservoir	SVM	R^2: 0.863 RMSE: 0.264 MAE: 0.226	-	/	/	-
[76]	11	Lake	SVM BPNN MRS	RMSE: 13.4822 RMSE: 14.8427 RMSE: 15.3446	/	/	/	-

3.2.4. Other approaches to algal growth prediction

The hybrid method integrates multiple algorithms for high performance. Specifically, the incorporation of various ML algorithms could significantly enhance the overall outcome by refining one another, generalizing, or adapting to unknown tasks as most of the algorithms are developed for a

particular dataset or task[76,77]. The NN was integrated with another approach in the study by Wang et al.[78] where a hybrid model constituting BPNN, rough decision model, and decision rule were structured to forecast cyanobacteria bloom. The rough reduction method omits irrelevant characteristics without losing pivotal knowledge by only choosing key neural network determinants. Intriguing results were outlined in the research of Li et al.[61] who recommended an approach to forecast algae bloom with FS: minimum redundancy maximum relevance (mRMR) with RF, which is resistant to overfitting problems. Likewise, the study by Serry et al.[55] primarily employed FS for algae bloom prediction in the improvement phase. Regrettably, the RMSE and correlation coefficient outcomes remained low. The SVM algorithm could be further enhanced with a metaheuristic approach, such as GA in line with Wang et al.[58]. Several other methods as in **Table 8** are also portrayed similar performance.

Table 8. Other supervised approaches in algal growth prediction.

Article (s)	#F	Sources	Method	Results	Factors category			
					BF	PF	CF	MF
[6]	5	Lake	ADHDP-AGM	RMSE: 1.0363	/	/	/	-
[52]	7	Mortar surface	LS-SVR	RMSE: 4.55 R^2: 0.94	-	-	-	-
[55]	4	River	Meta-learning: CFS & GA	RMSE:0.2 MAPE:0.14 Corr.:0.8	-	/	/	-
[57]	8	Freshwater	GA-BP GA-LSSVM BP TS	Error: 40.7 Error: 35.4 Error 64.2 Error:116.9	/	/	/	-
[60]	11	Satellite coastal data	Multi-variate regression	Accuracy 1-day: 65.6 2-day: 72.1 3-day: 71.9	/	/	/	/
[61]	24	Lakes, reservoir	GA-BPNN	RMSE CI: 0.0030 CII: 0.0006 CIII: 0.012 CIV: 0.0040	/	/	/	-
[62]	13	Lake	RF with mRMR (FS)	CE:0.33 RMSE:2.12 MAE:7.57	/	/	/	-
[64]	1	Coastal	Wavelet transform multistep 1–20	RMSE: 2.010-4.696, MAPE:0.375-1.266	/	-	-	-
[65]	14	Lake, reservoir	ABC-RBF-SVM	RMSE:0.0030 MAE: 0.0020 R^2:90	/	/	/	-
[66]	9	Reservoir	DCCPI, PCA, cusp catastrophe	R: 0.873	/	/	/	-
[68]	34	Freshwater	Hybrid moth search algorithm (MSA) (RVFL)	RMSE:0.187 Data Partition (50:50) RMSE: 0.0446 Data Partition (70:30)	/	/	/	-
[79]	8	Lake	SMR-GP	RMSE:37.9	/	/	/	/

The GA denotes an approach to resolving both constrained and unconstrained optimization problems in line with natural selection, which catalyzes biological evolution. This algorithm reiteratively

refines a population of individual solutions and arbitrarily chooses individuals from the present population to be parents at every step to produce children for the next generation. In this regard, the population 'evolves' towards an optimal solution over successive generations. Essentially, GAs could address various optimization problems that do not complement standard optimization algorithms, including counterparts in which the objective function is discontinuous, not differentiable, stochastic, or highly non-linear. Wang et al.[57] incorporated GA to enhance the BP network and least squares SVM generalization capacity. Meanwhile, Wang et al.[57] recommended a prediction method of bloom combined with the time series and intelligent non-linear models to optimize the error caused by time-series analysis. The influencing factors and forecasting data of chlorophyll-a time-series prediction error were modeled by BP, GA-BP, LSSVM, and GA-LSSVM. Consequently, the suggested model optimized time-series prediction. Wang et al.[58] eventually integrated SVM with GA and a relevance vector machine (GA-RVM) to forecast the abundance of phytoplankton in association with algal blooms at a Macau freshwater reservoir and compare their performance with an ANN model. The GA-SVM models outperformed other approaches. Evidently, GA-oriented research is applied to or integrated with SVM. Further studies are necessary to perceive whether GA could still demonstrate a competitive performance for other algal blooms prediction.

3.3. Time series forecasting (TSF)

Although current literature on prediction techniques elaborates on supervised ML, including simple classification or regression problems, the processes could not forecast algal growth beyond or prior to the present period, which is pivotal in the early prevention of HAB disasters or potential outbreaks. Based on the review, the ML models recommended in this domain failed to represent temporal data attributes, which proves essential when the time dimension adds explicit ordering to data points that should be conserved given their provision of additional or vital information to learning algorithms. Furthermore, Xie et al.[75] indicated the forecasting model to demonstrate higher performance than the prediction counterpart. Following the research outcomes, the algal bloom is a complex, non-linear, and dynamic system that is impacted by water variables in previous and current months. Such problems should be resolved with time series.

A time series implies a series of chronologically indexed (listed or graphed) data points. Generally, time series denotes a successive sequence of discrete-time data taken at equally-spaced points in time. Time series encompassing univariate and multivariate forms have evolved across various disciplines, specifically in hydrological and ecological modeling and oceanography. Univariate time series constitutes a series with a single time-dependent variable while the multivariate counterpart depicts multiple single time-dependent variables that rely on past values and other variables. Notably, this dependence serves to predict future values.

Much algae prediction research encompasses various intricate variables. Time series data could be broadly categorized into (i) stationary time series and (ii) non-stationary time series. In stationary time series, statistical components resembling mean value or variance prove constant over time and stay in relative equilibrium based on their corresponding mean values as opposed to their non-stationary counterpart. Time series data could be framed as supervised learning through the value at the previous time-step to forecast the value at the following time-step[80]. The time series forecast horizons are defined as follows: short-, medium-, and long-term forecast ranges from one hour to one week, one week to one year, and over a year, respectively. A one-step prediction only forecasts the training dataset of the following day, whereas multi-step TSF predicts multiple time-steps in the future. Multistep-ahead TSF

enables the prediction of algae growth duration for the following year and the maximum and minimum temperature for algal growth in the following month or years. Typically, multivariate TSF models are sensitive to multi-step (short-, mid-, and long-term) horizons as in-depth predictions lead to the complex modeling of multi-step forecasting following accumulated errors and low performance[81].

Traditional direct, recursive strategies, hybrid and multiple input multiple output (MIMO) strategies were employed for multi-step forecasting[82]. The recursive strategy aims to train a model that exclusively emphasizes a one-step-ahead prediction. The predictions are recursively forecasted post-model training. In other words, intermediate predictions are utilized as inputs to forecasting the following values until the time horizon prediction[83].

The direct strategy establishes a set of different N models for various time steps with the same input data employed to feed all the models, unlike the recursive counterpart that utilizes one model. Meanwhile, MIMO implies a multiple output strategy where the prediction model output denotes a vector of future values forecasted with only one model. The MIMO strategy could conserve the temporal stochastic dependency of sequential data to address the drawbacks of recursive and direct methods given that the objective function during model training simultaneously alleviates the prediction errors on multiple horizons[83]. The computational costs of MIMO are also lower than that of the direct strategy following its prerequisite of only one model to be trained.

Some scholars from other disciplines who compared distinctive multi-type forecasting types[84–86] proved that such variations elicited multiple outcomes. Nevertheless, current forecasting in the algal growth prediction domain typically emphasized a single-step prediction. Research on multi-step forecasting has failed to thoroughly describe the aforementioned approach. Traditional time series and DL in time series would be extensively discussed in the following subsections.

3.3.1. Traditional TSF

Stochastic time series models, such as ARIMA that constitute subclasses of other models (AR, MA, and ARMA) are one of the most renowned and extensively utilized time series techniques. Box and Jenkins suggested a fairly successful variation of the ARIMA model, such as the seasonal ARIMA (SARIMA) for seasonal TSF. This model has garnered much scholarly attention following its versatility in representing several time series variations with simplicity and the associated Box-Jenkins methodology for robust model development. Nevertheless, the models encountered specific drawbacks in terms of pre-assuming a linear form of the associated time-series data, which proves inadequate in various practical circumstances[10], and the inability to determine complex interactions from non-linear data[87]. The AI and DL approaches are becoming increasingly common in empirical studies. Based on the literature review, RNN and LSTM denote two DL techniques that demonstrate a more optimal performance compared to other algorithms in TSF.

3.3.2. Deep TSF

Deep learning is an ML subdiscipline that concerns algorithms, such as ANN that are inspired by the brain structure and function. Several DL model types, such as RNN and its ensuing variant (LSTM) are typically employed in TSF. The RNN, which entails a network with feedback connections from hidden and output layers to the preceding counterparts, is recommended when managing dynamic datasets[83]. In this regard, sequential data dynamics could be ascertained with previous pattern memories retained through network cycles. Meanwhile, LSTM implies a novel form of neural network that performs predictions based on the data derived from previous times.

The LSTM is a specified RNN architecture developed to model temporal sequences and their long-range dependencies more precisely than conventional RNNs. Notably, LSTM does not utilize activation functions in its recurrent components. The stored values are not altered while the gradient is retained during RNN-oriented training. The LSTM units are implemented in 'blocks' with several units with three or four 'gates' (input, forget, and output) that regulate the information flow based on the logistic function.

This architecture facilitates the learning of longer-term dependence. The GRUs resemble LSTMs albeit with a more simplified structure and utilize a set of gates to control information flow despite not employing separate memory cells and incorporating fewer gates[88]. Although the recently-evolved LSTM has been implemented across various disciplines, specifically in TSF, only a few studies adopted the LSTM algorithm for algae prediction. For example, Lee and Lee[7] incorporated the LSTM model involving algal bloom prediction for a short-term (one week) prediction on newly-constructed water quality on 16 rivers. Wang et al.[60] employed the time series non-linear model to rectify the error induced by traditional time series analysis. Although LSTM has reflected much improvement and undergone multiple integrations with other DL approaches (Bi-LSTM, Encoder-Decoder, and CNN-LSTM) to date, the algorithms are yet to be examined in terms of algal prediction. **Table 9** presents past studies within the TSF domain.

Table 9. Time series with DL forecasting.

Author (s)	#F	Sources	Method	Results	Factors Category			
					BF	PF	CF	MF
[7]	10	River	MLP RNN LSTM	RMSE: 9.28 RMSE: 7.93 RMSE: 7.67	/	/	/	-
[22]	10	River	LSTM	RMSE 1-D Pred.: 0.04868 4-D Pred.: 0.08015	/	/	/	-
[28]	6	River	MPUM	RMSE: 16.89 R^2: 0.74	/	/	/	-
[33]	9	Coastal	CCM	MAE: 0.55–0.35	-	/	/	/
[43]	13	Lake	RNN-SOM	RMSE: 19.0 R: 0.7 Accuracy: 87%	/	/	/	-
[56]	12	Coastal	DBN-ARIMA	RMSE: 0.154 MAE: 0.123 MAPE: 17.21 R: 0.798	/	/	/	-
[60]	7	Reservoir	GLM	R: 0.71	/	-	/	-
[66]	12	River	Merge LSTM	RMSE: 0.0459	/	/	/	/
[70]	13	Coastal	RNN	RMSE: 1.269 MAE: 0.79	/	/	/	/
[71]	4	Reservoir	LSTM	RMSE 1–10: 27–16 (decrease)	-	/	-	/

4. Analysis and discussion

This study review has outlined several unresolved concerns and knowledge gaps for optimal prediction performance. The first issue denotes FS where most of the selections are performed arbitrarily or based on domain knowledge following Rahman and Shahriar[89]. Despite the implementation of other

approaches, such as MA, mRMR, and influence matrix, the techniques only emphasized vital FS without insights into the reason underpinning pivotal FS selection. The aforementioned complexities garnered much scholarly attention when some researchers began employing sensitivity analysis or the clustering approach for data discovery with SOM and K-means. Despite a rise in the utilization of other clustering techniques, only two counterparts appear to be extensively employed by relevant researchers. This knowledge gap has led the current research to examine other unsupervised ML approaches.

Features that are regarded as extremely high or low could lead to model fitting intricacies and performance fluctuations following the arbitrary FS. Arguments on model fitting and performance correspond to McGowan et al.[33], Li et al.[40], and Lu et al.[16] where dataset arbitrariness has instigated model overfitting and prediction errors. Inappropriate FS techniques for time series might also hinder or degrade the time-series forecasting performance. The employed features differ in number with a maximum of 34 indicators and a minimum of one. This research classified the number of utilized indicators into the following categories: low (1–11), medium (12–22), and high (over 22). **Figure 1** depicts the percentage of studies under the aforementioned categories. Specifically, a low number of (parameters) or indicators reflected over 50%, followed by the incorporation of a medium number of indicators, and a high number of indicators at 7%.

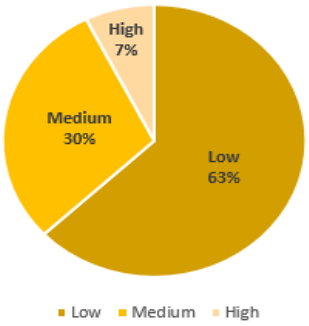

Figure 1. Range of indicators percentage.

Correlational research could be performed between parameter behaviors and the amount of Chl-a or algal growth predictors with an unsupervised method (clustering), which is typically regarded as the fundamental notion in pattern discovery. This conundrum has left a grey area where insights into the forecasting approach based on associations in an intricate ecological time-series data might catalyze forecasting-oriented decision-making.

Based on the current research, most of the water sources included in past studies involved lakes and reservoirs. As such, future works prove necessary for other sources, such as freshwater bodies, coastal areas, and estuaries as presented in **Figure 2**. Most of the studies only emphasized one water source at a time following their distinctive attributes and variations owing to hydrologic, geographic, climatic, morphologic, physical, chemical, geochemical, and biological aspects. Accommodating all water source types would imply the customization of study indicators to specified sources. Assumably, past empirical works were primarily reliant on data availability.

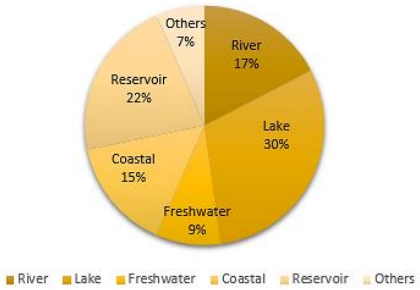

Figure 2. Trend of type of water sources.

Insufficient data following frequency updates would deter the forecasting process. Some high-volume data entail update frequencies that are consistently taken in minutes, hours, or on a daily basis. Nevertheless, sporadic data prevents pattern identification when (i) data is only gathered once a month, (ii) a substantial amount of data is missing, and (iii) the data is on a small scale. Such complexities could be resolved through large-scale data to complement the learning and training process. Concerning the factors category, this review has only observed a few studies that fully employed the four aforementioned factors despite the necessity of climates under the meteorological factor. Several open issues or gaps in managing different data size ranges and integrating data with adequate approaches remain unaddressed.

The third issue denotes algorithm performance where measurements that disregard water source types demonstrated overall or average TSF performance with DL compared to basic ML. Based on the empirical outcomes, current ML data-driven models could not sufficiently extract multi-factor timing data features with most of the models not depicting temporal data attributes. The LSTM has consistently outperformed other approaches with minimal prediction errors.

In terms of analysis method, specific performance measures, such as RMSE, the coefficient of determination (R^2), correlation coefficient (R), the mean absolute error (MAE), mean-square-error (MSE), and mean absolute percentage error (MAPE) were utilized with RMSE as the most favored and extensively utilized counterpart to assess the forecasted model-actual data value variance. The prevalence of past literature that employed RMSE has catalyzed the comparison process across domains. Much research has proven the deep time-series performance with RNN and LSTM to determine and depict temporal data attributes following the reviewed evaluation techniques.

Although data-driven methods offer versatility in FS to make predictions, this liberty to perform variable selection could instigate over-fitting and under-fitting complexities if carelessly ascertained. Discussions on feature engineering were not extensively throughout this review, specifically in the time-series prediction approach, following the need for non-trivial and time-consuming efforts[90] although feature engineering is pivotal in developing lag value and minimum or maximum horizon to forecast in TSF.

The fourth issue concerns improvement. The LSTM was primarily applied to river- and reservoir-oriented data despite its overall efficiency. As such, further works prove crucial to examine other water source types. Fluctuations in LSTM performance following the number of employed indicators and method-based shortcomings could also be observed. Although LSTM is capable of retaining information in the long run, the sequence-to-sequence LSTM architecture can only receive the input sequence to a fixed-length internal representation owing to the categorization of specific knowledge into small parts for easy remembrance. The LSTMs are impacted by multiple random weight initializations and behave akin to the feed-forward neural network where small weight initializations are favored. In this vein, other open issues require examination to resolve current circumstances. Feature engineering with LSTM and a

comprehensive understanding of the temporal aspect entailing algal growth data could induce optimal performance. Additional parameter tuning and learning approaches could similarly enhance present LSTM performance.

The fifth and final concern constitutes the engagement or data integration of various categories as one dataset is a complex task. A different data update and intricacies regarding the frequency taken would also vary. Such differences would result in the incorporation of multiple pre-processing approaches in data cleaning. Future studies should consider different factor categories as data fusion is primarily disregarded based on the aforementioned reasons. Different factors were classified following specific attributes: CF, BF, PF, and MF (see **Table 3**). Although several past studies did not include specific categorical factors, particularly MF, recent research from 2016 has incorporated MF following much scholarly attention. **Figure 3** depicts the overall trend of past studies regarding factor (BF, PF, CF, and MF) usage between 2009 and 2020.

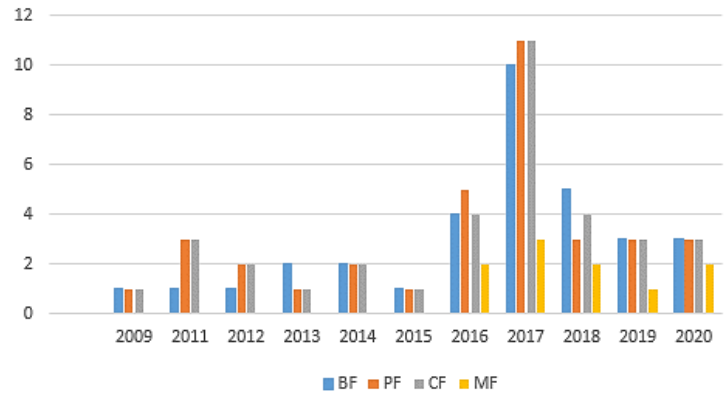

Figure 3. Trend of using categorical factors from 2009–2020.

The MF factor category, which only began considering and employing algae prediction from 2016 onwards, is palpably illustrated in **Figure 3**. Additionally, different predictors or factors began increasing between 2016 and 2020. This phenomenon might be associated with the advent of Internet of Things (IoT), which evolved with the development of sensors and utilization of multiple technologies that catalyze the data acquisition process. Such assumptions corroborated with Ande et al.[91] who disclosed that over 450 organizations have provided IoT platforms specializing in end-to-end solutions, system security, application enablement, device management, analytics, cloud storage, and back-end connectivity in 2017. These reasons further strengthen the notions underpinning multiple factor utilization with large-scale data based on the different factors gathered through various sensors. Overall, most of the employed factors attained the highest peak in 2017 or were significantly regarded from 2016 to 2018.

The benefits of data integration and dataset design are comprehensively performed in feature engineering, which typically requires expert knowledge to develop designs in terms of data and temporal elements, such as minimum or maximum past value prediction. Feature engineering provides such contributions based on the type of information that proves crucial from the input, which is vital for mapping and dynamic shifts as contextually required. Feature engineering implies one of the ML domains that could convert and engineer raw data into a fitting format for the prediction process, particularly in TSF[61].

Previous scholars emphasized single-step multivariate prediction with little research on modeling

the multi-step forecasting technique and no in-depth descriptions of multi-step methodology in their respective works although a long-term forecast could prove advantageous in future outbreak prediction. Various multi-step methods that were performed across different disciplines yielded distinctive outcomes. This inconsistency has resulted in another knowledge gap concerning the most adequate method for multi-step algal growth prediction. This approach proves more challenging as opposed to the normal counterpart given the presence of performance issues, particularly on cumulative errors and low performance in the wake of extended prediction. Multi-step performance in TSH, which is crucial in preventing algal growth, requires further investigation. Specific studies on enhancing the multi-step forecasting approach have been duly identified. Regarding the time-series domain, Venkatraman[92] incorporated several stages (prediction and optimization) in the predictive model build. Relevant works to resolve the aforementioned intricacies remain lacking despite the challenges encountered in advocating this multi-step method.

5. Conclusion

Prediction constitutes the core research concern in HAB-oriented research. Early prevention and awareness are pivotal following the HAB outbreaks and the increase in algae growth. The present prediction process could be enhanced through DL with time series by evaluating specific open issues that must be resolved based on comprehension and prediction performance given the high capacity in managing the non-linearity, ambiguities, and dynamics of algal growth. This method could be optimized by examining the prediction part and considering key features by improving the present selection approach and revealing the factor interconnections between the factors for a robust predictive algorithm. The capacity to forecast blooms (even if just a week in advance) by fully incorporating the multi-step method could enable public health authorities to address human health issues[30,31] and provide adequate time for water facilities to shut down before the equipment is damaged. The current study has holistically reviewed contemporary algal growth forecasting techniques. Particular open issues were also indicated for future research. Summarily, in-depth examination proves necessary to develop workable strategies in the future.

Acknowledgments

This study, which is part of the collaboration between Universiti Sains Malaysia and the University of Florida under the facilitation of the Pacific Rim Application and Grid Middleware Assembly (PRAGMA), is funded by the Malaysian Ministry of Higher Education through the Transdisciplinary Research Grant Scheme (TRGS/1/2018/USM/01/5/4 - 203.PKOMP.67612).

Conflict of interest

The authors declare no conflict of interest.

References

1. Anderson DM. Approaches to monitoring, control and management of harmful algal blooms (HABs). *Ocean & Coastal Management* 2009; 52(7): 342–347. doi: 10.1016/j.ocecoaman.2009.04.006
2. McCormick PV, Cairns J. Algae as indicators of environmental change. *Journal of Applied Phycology* 1994; 6(5–6): 509–526. doi: 10.1007/BF02182405
3. Recknagel F, Michener WK. *Ecological Informatics: Data Management and Knowledge Discovery*. Springer; 2017.
4. Wong KTM, Lee JHW, Hodgkiss IJ. A simple model for forecast of coastal algal blooms. *Estuarine, Coastal and Shelf Science* 2007; 74(1–2): 175–196. doi: 10.1016/j.ecss.2007.04.012
5. Sun Y, Li J, Liu J, et al. Using causal discovery for feature selection in multivariate numerical time series.

Machine Learning 2015; 101(1–3): 377–395. doi: 10.1007/s10994-014-5460-1
6. Zhang H, Hu B, Wang X, et al. An action dependent heuristic dynamic programming approach for algal bloom prediction with time-varying parameters. *IEEE Access* 2020; 8: 26235–26246. doi: 10.1109/ACCESS.2020.2971244
7. Lee S, Lee D. Improved prediction of harmful algal blooms in four major South Korea's rivers using deep learning models. *International Journal of Environmental Research and Public Health* 2018; 15(7): 1–15. doi: 10.3390/ijerph15071322
8. Huo S, He Z, Su J, et al. Using artificial neural network models for eutrophication prediction. *Procedia Environmental Sciences* 2013; 18: 310–316. doi: 10.1016/j.proenv.2013.04.040
9. Yang X, Wu X, Hao H, He Z. Mechanisms and assessment of water eutrophication. *Journal of Zhejiang University SCIENCE B* 2008; 9(3): 197–209. doi: 10.1631/jzus.B0710626
10. Adhikari R, Agrawal RK, Kant L. PSO based neural networks vs. traditional statistical models for seasonal time series forecasting. In: Proceedings of the 2013 3rd IEEE International Advance Computing Conference (IACC); 22–23 February 2013; Ghaziabad, India. pp. 719–725.
11. Radmer RJ. Algal diversity and commercial algal products. *BioScience* 1996; 46(4): 263–270. doi: 10.2307/1312833
12. Bui MH, Pham TL, Dao TS. Prediction of cyanobacterial blooms in the Dau Tieng Reservoir using an artificial neural network. *Marine and Freshwater Research* 2017; 68(11): 2070–2080. doi: 10.1071/MF16327
13. Whigham PA, Recknagel F. An inductive approach to ecological time series modelling by evolutionary computation. *Ecological Modelling* 2001; 146(1–3): 275–287. doi: 10.1016/S0304-3800(01)00313-1
14. Wells ML, Trainer VL, Smayda TJ, et al. Harmful algal blooms and climate change: Learning from the past and present to forecast the future. *Harmful Algae* 2015; 49: 68–93. doi: 10.1016/j.hal.2015.07.009
15. Huang JD, Zheng H. Current trend of metagenomic data analytics for cyanobacteria blooms. *Journal of Geoscience and Environment Protection* 2017; 5(6): 198–213. doi: 10.4236/gep.2017.56018
16. Lu J, Huang T, Hu R. Data mining on algae concentrations (chlorophyll) time series in source water based on wavelet. In: Proceedings of the 2008 Fifth International Conference on Fuzzy Systems and Knowledge Discovery; 18–20 October 2008; Ji'nan, China. pp. 611–616.
17. Tian W, Liao Z, Zhang J. An optimization of artificial neural network model for predicting chlorophyll dynamics. *Ecological Modelling* 2017; 364: 42–52. doi: 10.1016/j.ecolmodel.2017.09.013
18. Zellweger F, De Frenne P, Lenoir J, et al. Advances in microclimate ecology arising from remote sensing. *Trends in Ecology & Evolution* 2019; 34(4): 327–341. doi: 10.1016/j.tree.2018.12.012
19. Kearney MR, Porter WP. NicheMapR-an R package for biophysical modelling: The microclimate model. *Ecography* 2017; 40(5): 664–674. doi: 10.1111/ecog.02360
20. Amsler CD, Reed DC, Neushuli M. The microclimate inhabited by macroalgal propaguies. *British Phycological Journal* 1992; 27(3): 253–270. doi: 10.1080/00071619200650251
21. Shi K, Zhang Y, Zhou Y, et al. Long-term MODIS observations of cyanobacterial dynamics in Lake Taihu: Responses to nutrient enrichment and meteorological factors. *Scientific Reports* 2017; 7(1): 1–16. doi: 10.1038/srep40326
22. Cho H, Choi UJ, Park H. Deep learning application to time-series prediction of daily chlorophyll-a concentration. *WIT Transactions on Ecology and the Environment* 2018; 215: 157–163. doi: 10.2495/EID180141
23. Mathulamuthu SS, Asirvadam VS, Dass SC, et al. Predicting dengue incidences using cluster based regression on climate data. In: Proceedings of the 2016 6th IEEE International Conference on Control System, Computing and Engineering (ICCSCE); 25–27 November 2016; Penang, Malaysia. pp. 245–250.
24. Mustaffa Z, Sulaiman MH, Emawan F, et al. Dengue outbreak prediction: Hybrid meta-heuristic model. In: Proceedings of 2018 19th IEEE/ACIS International Conference on Software Engineering, Artificial Intelligence, Networking and Parallel/Distributed Computing (SNPD); 27–29 June 2018; Busan, Korea (South). pp. 271–274.
25. Zhu G, Hunter J, Jiang Y. Improved prediction of dengue outbreak using the delay permutation entropy. In: Proceedings of the 2016 IEEE International Conference on Internet of Things (iThings) and IEEE Green Computing and Communications (GreenCom) and IEEE Cyber, Physical and Social Computing (CPSCom) and IEEE Smart Data (SmartData); 15–18 December 2016; Chengdu, China. pp. 828–832.
26. Džeroski S. Applications of symbolic machine learning to ecological modelling. *Ecological Modelling* 2001; 146(1–3): 263–273. doi: 10.1016/S0304-3800(01)00312-X
27. Chen Q, Rui H, Li W, Zhang Y. Analysis of algal bloom risk with uncertainties in lakes by integrating self-organizing map and fuzzy information theory. *Science of the Total Environment* 2014; 482–483: 318–324. doi: 10.1016/j.scitotenv.2014.02.096
28. Kim S. A multiple process univariate model for the prediction of chlorophyll-a concentration in river systems. *International Journal of Limnology* 2016; 52: 137–150. doi: 10.1051/limn/2016003
29. Egerton TA, Morse RE, Marshall HG, Mulholland MR. Emergence of algal blooms: The effects of short-

term variability in water quality on phytoplankton abundance, diversity, and community composition in a tidal estuary. *Microorganisms* 2014; 2(1): 33–57. doi: 10.3390/microorganisms2010033
30. Rostam NAP, Ahamed Hassain Malim NH, Abdullah R. Development of a low-cost solar powered & real-time water quality monitoring system for Malaysia seawater aquaculture: Application & challenges. In: Proceedings of the 2020 4th International Conference on Cloud and Big Data Computing; 26–28 August 2020; United Kingdom. pp. 86–91.
31. Caron DA, Garneau ME, Seubert E, et al. Harmful algae and their potential impacts on desalination operations off southern California. *Water Research* 2010; 44(2): 385–416. doi: 10.1016/j.watres.2009.06.051
32. Lewitus AJ, Horner RA, Caron DA, et al. Harmful algal blooms along the North American west coast region: History, trends, causes, and impacts. *Harmful Algae* 2012; 19: 133–159. doi: 10.1016/j.hal.2012.06.009
33. McGowan JA, Deyle ER, Ye H, Carter ML, et al. Predicting coastal algal blooms in southern California. *Ecology* 2017; 98(5): 1419–1433. doi: 10.1002/ecy.1804
34. Pennekamp F, Iles AC, Garland J, et al. The intrinsic predictability of ecological time series and its potential to guide forecasting. *Ecological Monographs* 2019; 89(2): e01359. doi: 10.1002/ecm.1359
35. Gamboa JCB. Deep learning for time-series analysis. *arXiv* 2017; arXiv:1701.01887. doi: 10.48550/arXiv.1701.01887
36. Jung NC, Popescu I, Kelderman P, et al. Application of model trees and other machine learning techniques for algal growth prediction in Yongdam reservoir, Republic of Korea. *Journal of Hydroinformatics* 2010; 12(3): 262–274. doi: 10.2166/hydro.2009.004
37. Bair E. Semi-supervised clustering methods. *Wiley Interdisciplinary Reviews Computational Statistics* 2013; 5(5): 349–361. doi: 10.1002/wics.1270
38. Kohonen T. Self-organized formation of topologically correct feature maps. *Biological Cybernetics* 1982; 43(1): 59–69. doi: 10.1007/BF00337288
39. Wu ML, Zhang YY, Dong JD, et al. Identification of coastal water quality by self-organizing map in Sanya Bay, South China Sea. *Aquatic Ecosystem Health & Management* 2011; 14(3): 291–297. doi: 10.1080/14634988.2011.604273
40. Li X, Sha J, Wang ZL. Chlorophyll-a prediction of lakes with different water quality patterns in China based on hybrid neural networks. *Water* 2017; 9(7): 1–13. doi: 10.3390/w9070524
41. Malek S, Salleh A, Ahmad SMS. Analysis of algal growth using Kohonen self-organizing feature map (SOM) and its prediction using rule based expert system. In: Proceedings of the 2009 International Conference on Information Management and Engineering; 3–5 April 2009; Kuala Lumpur, Malaysia. pp. 501–504.
42. Malek S, Syed Ahmad SM, Singh SKK, et al. Assessment of predictive models for chlorophyll-a concentration of a tropical lake. *BMC Bioinformatics* 2011; 12(Suppl 13): S12. doi: 10.1186/1471-2105-12-S13-S12
43. Malek S, Salleh A, Milow P, et al. Applying artificial neural network theory to exploring diatom abundance at tropical Putrajaya Lake, Malaysia. *Journal of Freshwater Ecology* 2012; 27(2): 211–227. doi: 10.1080/02705060.2011.635883
44. Voutilainen A, Arvola L. SOM clustering of 21-year data of a small pristine boreal lake. *Knowledge and Management of Aquatic Ecosystem* 2017; 418: 36. doi: 10.1051/kmae/2017027
45. Nitin M, Kwok-wing C. Machine-learning paradigms for selecting ecologically significant input variables. *Engineering Applications of Artificial Intelligence* 2007; 20(6): 735–744. doi: 10.1016/j.engappai.2006.11.016
46. Obenour DR, Gronewold AD, Stow CA, Scavia D. Using a Bayesian hierarchical model to improve Lake Erie cyanobacteria bloom forecasts. *Water Resources Research* 2014; 50(10): 7847–7860. doi: 10.1002/2014WR015616
47. Knoll LB, Hagenbuch EJ, Stevens MH, et al. Predicting eutrophication status in reservoirs at large spatial scales using landscape and morphometric variables. *Inland Waters* 2015; 5(3): 203–214. doi: 10.5268/IW-5.3.812
48. Li X, Yu J, Jia Z, Song J. Harmful algal blooms prediction with machine learning models in Tolo Harbour. In: Proceedings of the 2014 International Conference on Smart Computing; 3–5 November 2014; Hong Kong, China. pp. 245–250.
49. Aria SH, Asadollahfardi G, Heidarzadeh N. Eutrophication modelling of Amirkabir Reservoir (Iran) using an artificial neural network approach. *Lakes & Reservoirs: Research and Management* 2019; 24(1): 48–58. doi: 10.1111/lre.12254
50. Guallar C, Delgado M, Diogene J, Fernandez-Tejedor M. Artificial neural network approach to population dynamics of harmful algal blooms in Alfacs Bay (NW Mediterranean): Case studies of Karlodinium and Pseudo-nitzschia. *Ecological Modelling* 2016; 338: 37–50. doi: 10.1016/j.ecolmodel.2016.07.009
51. Tran TH, Hoang ND. Estimation of algal colonization growth on mortar surface using a hybridization of

machine learning and metaheuristic optimization. *Sādhanā* 2017; 42(6): 929–939. doi: 10.1007/s12046-017-0652-6
52. Zhang Z, Peng G, Guo F, et al. The key technologies for eutrophication simulation and algal bloom prediction in Lake Taihu, China. *Environmental Earth Sciences* 2016; 75(18): 1295. doi: 10.1007/s12665-016-6106-3
53. Lou I, Xie Z, Ung WK, Mok KM. Freshwater algal bloom prediction by extreme learning machine in Macau Storage Reservoirs. In: Sun F, Toh KA, Romay M, et al. (editors). *Extreme Learning Machines 2013: Algorithms and Applications. Adaptation, Learning, and Optimization*. Springer, Cham; 2014. Volume 16. pp. 95–111.
54. Fan J, Wu J, Kong W, et al. Predicting bio-indicators of aquatic ecosystems using the support vector machine model in the Taizi River, China. *Sustainability* 2017; 9(6): 892. doi: 10.3390/su9060892
55. Serry H, Hassanien AE, Zaghlou S, Hefny HA. Predicting algae growth in the Nile River using meta-learning techniques. In: Proceedings of the International Conference on Advanced Intelligent Systems and Informatics 2017; 9–11 September 2017; Cairo, Egypt. pp. 745–754.
56. Qin M, Li Z, Du Z. Red tide time series forecasting by combining ARIMA and deep belief network. *Knowledge-Based Systems* 2017; 125: 39–52. doi: 10.1016/j.knosys.2017.03.027
57. Wang L, Wang X, Jin X, et al. Analysis of algae growth mechanism and water bloom prediction under the effect of multi-affecting factor. *Saudi Journal of Biological Sciences* 2017; 24(3): 556–562. doi: 10.1016/j.sjbs.2017.01.026
58. Wang Y, Xie Z, Lou IC, et al. Algal bloom prediction by support vector machine and relevance vector machine with genetic algorithm optimization in freshwater reservoirs. *Engineering Computations* 2017; 34(2): 664–679. doi: 10.1108/EC-11-2015-0356
59. Karki S, Sultan M, Elkadiri R, Elbayoumi T. Mapping and forecasting onsets of harmful algal blooms using MODIS data over coastal waters surrounding Charlotte County, Florida. *Remote Sensing* 2018; 10(10): 1–19. doi: 10.3390/rs10101656
60. Wang H, Zhu R, Zhang J, et al. A novel and convenient method for early warning of algal cell density by chlorophyll fluorescence parameters and its application in a highland lake. *Frontiers in Plant Science* 2018; 9: 1–3. doi: 10.3389/fpls.2018.00869
61. Li X, Sha J, Wang ZL. Application of feature selection and regression models for chlorophyll-a prediction in a shallow lake. *Environmental Science and Pollution Research* 2018; 25(20): 19488–19498. doi: 10.1007/s11356-018-2147-3
62. Yi HS, Park S, An KG, Kwak KC. Algal bloom prediction using extreme learning machine models at artificial weirs in the Nakdong River, Korea. *International Journal of Environmental Research and Public Health* 2018; 15(10): 2078. doi: 10.3390/ijerph15102078
63. Du Z, Qin M, Zhang F, Liu R. Multistep-ahead forecasting of chlorophyll *a* using a wavelet nonlinear autoregressive network. *Knowledge-Based Systems* 2018; 160: 61–70. doi: 10.1016/j.knosys.2018.06.015
64. Nieto PG, García-Gonzalo E, Fernández JA, Muñiz CD. Water eutrophication assessment relied on various machine learning techniques: A case study in the Englishmen Lake (Northern Spain). *Ecological Modelling* 2019; 404: 91–102. doi: 10.1016/j.ecolmodel.2019.03.009
65. Tian Y, Zheng B, Shen H, et al. A novel index based on the cusp catastrophe theory for predicting harmful algae blooms. *Ecological Indicators* 2019; 102: 746–751. doi: 10.1016/j.ecolind.2019.03.044
66. Cho H, Park H. Merged-LSTM and multistep prediction of daily chlorophyll-a concentration for algal bloom forecast. In: *IOP Conference Series: Earth and Environmental Science*, Proceedings of the 2019 International Conference on Advances in Civil and Ecological Engineering Research; 1–4 July 2019; Kaohsiung, Taiwan. IOP Publishing; 2019. Volume 351.
67. Hussein AM, Elaziz MA, Wahed MSA, Sillanpää M. A new approach to predict the missing values of algae during water quality monitoring programs based on a hybrid moth search algorithm and the random vector functional link network. *Journal of Hydrology* 2019; 575: 852–863. doi: 10.1016/j.jhydrol.2019.05.073
68. Hill PR, Kumar A, Temimi M, Bull DR. HABNet: Machine learning, remote sensing-based detection of harmful algal blooms. *IEEE Journal of Selected Topics in Applied Earth Observations and Remote Sensing* 2020; 13: 3229–3239. doi: 10.1109/JSTARS.2020.3001445
69. Mamun M, Kim JJ, Alam MA, An KG. Prediction of algal chlorophyll-a and water clarity in monsoon-region reservoir using machine learning approaches. *Water* 2020; 12(1): 30. doi: 10.3390/w12010030
70. Wang X, Xu L. Unsteady multi-element time series analysis and prediction based on spatial-temporal attention and error forecast fusion. *Future Internet* 2020; 12(2): 34. doi: 10.3390/fi12020034
71. Song C, Zhang H. Study on turbidity prediction method of reservoirs based on long short term memory neural network. *Ecological Modelling* 2020; 432: 109210. doi: 10.1016/j.ecolmodel.2020.109210
72. Zadeh LA. Fuzzy sets. *Information and Control* 1965; 8(3): 338–353. doi: 10.1016/S0019-9958(65)90241-X
73. Chen Q, Mynett AE. Integration of data mining techniques and heuristic knowledge in fuzzy logic modelling

of eutrophication in Taihu Lake. *Ecological Modelling* 2003; 162(1–2): 55–67. doi: 10.1016/S0304-3800(02)00389-7
74. Recknagel F, French M, Harkonen P, Yabunaka KI. Artificial neural network approach for modelling and prediction of algal blooms. *Ecological Modelling* 1997; 96(1–3): 11–28. doi: 10.1016/S0304-3800(96)00049-X
75. Xie Z, Lou I, Ung WK, Mok KM. Freshwater algal bloom prediction by support vector machine in Macau storage reservoirs. *Mathematical Problems in Engineering* 2012; 2012: 397473. doi: 10.1155/2012/397473
76. Abdelrahim M, Merlosy C, Wang T. Hybrid machine learning approaches: A method to improve expected output of semi-structured sequential data. In: Proceedings of the 2016 IEEE Tenth International Conference on Semantic Computing (ICSC); 4–6 February 2016; Laguna Hills, CA, USA. pp. 342–345.
77. Liu J, Zhang Y, Qian X. Modeling chlorophyll-a in Taihu Lake with machine learning models. In: Proceedings of the 2009 3rd International Conference on Bioinformatics and Biomedical Engineering; 11–13 June 2009; Beijing, China. pp. 8–13.
78. Wang Z, Huang K, Zhou P, Guo H. A hybrid neural network model for cyanobacteria bloom in Dianchi Lake. *Procedia Environmental Sciences* 2010; 2: 67–75. doi: 10.1016/j.proenv.2010.10.010
79. Daghighi A. *Harmful Algae Bloom Prediction Model for Western Lake Erie Using Stepwise Multiple Regression and Genetic Programming* [Master's thesis]. Cleveland State University; 2017.
80. Hota HS, Handa R, Shrivas AK. Time series data prediction using sliding window based RBF neural network. Available online: https://www.semanticscholar.org/paper/Time-Series-Data-Prediction-Using-Sliding-Window-Hota-Handa/91037f01fd4b845eadca0b53f5dc00d9f61ac493 (accessed on 22 June 2023).
81. Yin J, Rao W, Yuan M, et al. Experimental study of multivariate time series forecasting models. In: Proceedings of the 28th ACM International Conference on Information and Knowledge Management; 3–7 November 2019; Beijing, China. pp. 2833–2839.
82. Taieb SB, Bontempi G, Atiya AF, Sorjamaa A. A review and comparison of strategies for multi-step ahead time series forecasting based on the NN5 forecasting competition. *Expert Systems with Applications* 2012; 39(8): 7067–7083. doi: 10.1016/j.eswa.2012.01.039
83. Nguyen HP, Liu J, Zio E. A long-term prediction approach based on long short-term memory neural networks with automatic parameter optimization by Tree-structured Parzen Estimator and applied to time-series data of NPP steam generators. *Applied Soft Computing* 2020; 89: 106116. doi: 10.1016/j.asoc.2020.106116
84. An NH, Anh DT. Comparison of strategies for multi-step-ahead prediction of time series using neural network. In: Proceedings of the 2015 International Conference on Advanced Computing and Applications (ACOMP); 23–25 November 2015; Ho Chi Minh City, Vietnam. pp. 142–149.
85. Taieb SB, Sorjamaa A, Bontempi G. Multiple-output modeling for multi-step-ahead time series forecasting. *Neurocomputing* 2010; 73(10–12): 1950–1957. doi: 10.1016/j.neucom.2009.11.030
86. Taieb SB, Hyndman RJ. *Recursive and Direct Multi-Step Forecasting: The Best of Both Worlds.* Monash University; 2012.
87. Divina F, Torres MG, Vela FAG, Noguera JLV. A comparative study of time series forecasting methods for short term electric energy consumption prediction in smart buildings. *Energies* 2019; 12(10): 1–23. doi: 10.3390/en12101934
88. Chung J, Gulcehre C, Cho K, Bengio Y. Empirical evaluation of gated recurrent neural networks on sequence modeling. *arXiv* 2014; arXiv:1412.3555. doi: 10.48550/arXiv.1412.3555
89. Rahman A, Shahriar MS. Algae growth prediction through identification of influential environmental variables: A machine learning approach. *International Journal of Computational Intelligence and Applications* 2013; 12(2): 1–19. doi: 10.1142/S1469026813500089
90. Yin J, Rao W, Yuan M, et al. Experimental study of multivariate time series forecasting models. In: Proceedings of the 28th ACM International Conference on Information and Knowledge Management; 3–7 November 2019; Beijing, China. pp. 2833–2839.
91. Ande R, Adebisi B, Hammoudeh M, Saleem J. Internet of Things: Evolution and technologies from a security perspective. *Sustainable Cities and Society* 2020; 54: 101728. doi: 10.1016/j.scs.2019.101728
92. Venkatraman A, Hebert M, Bagnell JA. Improving multi-step prediction of learned time series models. In: Proceedings of the Twenty-Ninth AAAI Conference on Artificial Intelligence; 25–30 January 2015; Austin, Texas, USA.

Computing and Artificial Intelligence 2023; 1(1): 360.
Review Article

Application of computer vision in livestock and crop production—A review

Bojana Petrovic[1,*], Vesna Tunguz[2], Petr Bartos[1]

[1] *Department of Technology and Cybernetics, Faculty of Agriculture and Technology, University of South Bohemia, 37005 Ceske Budejovice, Czech Republic*

[2] *Faculty of Agriculture, University in East Sarajevo, Sarajevo 71000, Bosnia and Herzegovina*

*** Corresponding author:** Bojana Petrovic, petrovic_bojana@hotmail.com

ARTICLE INFO

Received: 23 November 2023
Accepted: 12 January 2024
Available online: 4 February 2024

doi: 10.59400/cai.v1i1.360

ABSTRACT: Nowadays, it is a challenge for farmers to produce healthier food for the world population and save land resources. Recently, the integration of computer vision technology in field and crop production ushered in a new era of innovation and efficiency. Computer vision, a subfield of artificial intelligence, leverages image and video analysis to extract meaningful information from visual data. In agriculture, this technology is being utilized for tasks ranging from disease detection and yield prediction to animal health monitoring and quality control. By employing various imaging techniques, such as drones, satellites, and specialized cameras, computer vision systems are able to assess the health and growth of crops and livestock with unprecedented accuracy. The review is divided into two parts: Livestock and Crop Production giving the overview of the application of computer vision applications within agriculture, highlighting its role in optimizing farming practices and enhancing agricultural productivity.

KEYWORDS: artificial intelligence; innovation; agriculture automation; computer vision; smart agriculture; smart technology

1. Introduction

The use of artificial intelligence (AI) in the livestock industry is increasing nowadays. Investment in artificial intelligence is expected to increase significantly by 2026, and computer vision is indeed a significant and growing area within the field of AI. Modern computer vision technology helps farmers collect, store, and retrieve data for livestock operations. Managing and analyzing livestock operations is much more difficult than monitoring crops because animals move from one place to another. In commercial production systems, there are barriers to the widespread adoption of computer vision although it is a promising tool for animal care[1]. Digital image analysis, together with digital image processing and computer vision, is often used as a collective term to describe similar processes and applications[2]. Digital image processing with specific algorithms was used to estimate the body length, breast ratios, height, and width of cattle. The exact yield depended on the estimation of the photographic capability of the study parameters[3]. In digital image analysis, the most important factor is image quality. Different scenarios are possible in multimodal biometric systems by using sensors, and feature sets[4]. Nasirahmadi et al.[5] describe the most advanced 3D imaging systems in combination with 2D cameras to effectively identify the behavior of farm animals and present automated approaches to monitor and study the feeding, drinking, lying, movement, aggression, and reproduction behavior of cattle and pigs. The results showed that these technologies can assist the farmer by monitoring normal behaviors and

early detection of abnormal behaviors in large farms[5]. The studies showed that the use of video analysis can detect the possibility of non-intrusive animal monitoring in real time. According to Eduardo et al.[6], it was possible by video and data processing techniques after the ASF virus infection to monitor the changes in animal movement. The results showed that a significant decrease in animal movement can be detected after infection as early as four days after experimental infection with the ASF virus. Nevertheless, other technologies are also important for animal research, such as spectral and hyperspectral imaging, radiography, satellite imagery, and ultrasound. According to Patrício et al.[7], the development of precision solutions for livestock farming is one way to bring animals closer to producers in these expanding systems. Machine vision technology combined with the Internet of Things (IoT) offers benefits for precision livestock farming, such as monitoring the health status of all animals, including cattle, sheep, pigs, and poultry. On the other hand, one of the fundamental branches of agriculture (crop production) supplies the livestock industry with fodder and the human population[8]. Nowadays, with an inadequate level of management work in the field of crop production and a difficult financial and economic situation is necessary to find the best way for improving agricultural enterprises and production. Moreover, the demand for agricultural products is now growing with increasing the human population[9,10]. The intentions of development and progress in agriculture also imply that the vast majority of processes are already digitized and the volume of data. Over the past decade, it was impossible to trace over a wider geographical area, during the production season, where a specific field crop is planted. However, now with a relatively small amount of data from the field, it is possible to train artificial intelligence algorithms to recognize crops using footage. In this way, a map of the sowing structure is obtained, as well as an insight into how much arable land is under a certain culture in a given year, which is important information for state institutions. In the field of agricultural automation, the development of technology plays a key role in future development[11]. The use of the camera instead of the human eye helps in the identification, measurement, and tracking of image processing. Together with image capture by remote cameras, computer vision techniques enable non-contact and scalable sensing solutions in agriculture[12]. Intelligent systems based on machine vision algorithms are becoming an everyday part of agricultural production management, and machine vision-based agricultural automation technology is being used to increase productivity and efficiency in agriculture[13]. In addition, machine vision technology is also used for production management in crop protection, harvesting, and crop monitoring[14]. Year by year, computer vision applies in more and more scientific fields and becoming more and more popular and applicable. Therefore, the purpose of the article is to present the use of computer vision in livestock and crop production.

2. Computer vision in agriculture

Contributions of computer vision-artificial intelligence (AI) are generally known in areas such as analysis of weather conditions, plant health detection, monitoring, planting, and harvesting[15]. Farmers, for example, using simple tools, will receive information about the occurrence of diseases and pests before they happen. Based on the algorithms, it is possible to notice changes in plant growth and make an estimate of how much yield there will be or how much humus there is in the soil. Computer vision models are trained using datasets for processing images, for example, plants. After that, they define algorithms that help them determine the image of the diseases, pests, or weeds. These systems are particularly suitable for the evaluation of properties such as color, texture, scale, surface defects, and impurities, as well as for the classification of food into specific grades and the detection of defects[16]. Various imaging techniques are available to detect complex traits related to growth, yield, and adaptation to biotic or abiotic stress factors (e.g., diseases, insects, water stress, and nutrient deficiencies), including color

imaging (e.g., machine vision), imaging spectroscopy (e.g., multispectral and hyperspectral remote sensing), thermal infrared imaging, planar imaging, fluorescence imaging and 3D imaging and planar imaging[17] (cameras, lights, and communication devices), and CV systems (image processing algorithms)[18]. In addition, since 2012 Convolutional Neural Networks (CNNs) have dominated solutions to CV tasks, showing superior performance over traditional machine-learning methods[19]. Nowadays, drone technologies, remote sensors, and satellite technology are widely used in agricultural production. The application of deep learning technology allows us to utilize the possibilities of merging computer vision and artificial intelligence in agriculture. This leads to an improvement in the yield volume of high-quality scene images that can be effectively processed for intelligent agricultural applications[20]. Computer vision automation helps farmers to achieve data about fields, or gardens, allowing them to track, and evaluate specific objects using visual elements. In addition, machine vision for detection offers numerous tools and algorithms with different performance characteristics that can be used to operate with consumer cameras[21]. The most notable contributions used today are machine learning for crop rotation, pesticide spraying, crop monitoring, phenotyping by computer vision, weed control, smart systems for crop grading and sorting, and yield analysis as well as the application of computer vision in livestock production (**Figure 1**).

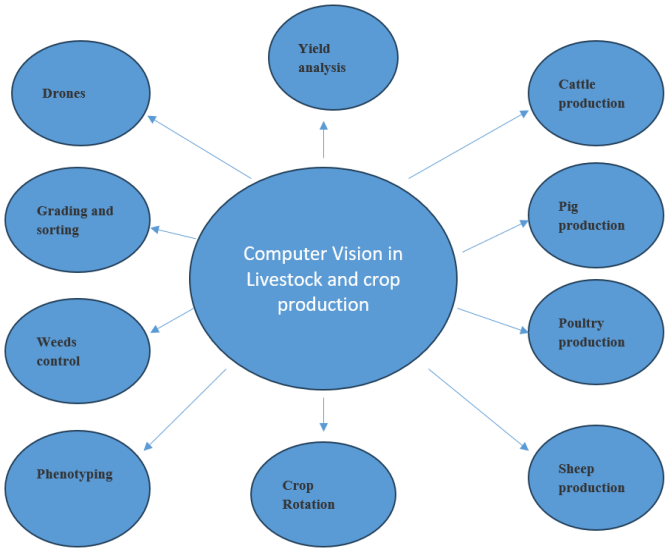

Figure 1. Computer vision in livestock and crop production.

3. Livestock production

3.1. Application of computer vision in cattle production

The Web of Science platform was searched for articles with terms such as computer vision, animal, livestock, poultry, cattle, sheep, pigs, deep learning, and any combination thereof. However, additional literature was also searched on Google and Google Scholar to find more information about livestock in general. Automation of the process of monitoring cattle behavior is becoming increasingly important, so computer vision is playing an important role in cattle production and livestock production in general. Developments in artificial intelligence and computer vision in cow production offer a wide range of solutions in the field of object detection and tracking. A recently proposed approach to cow movement or activity detection is illustrated in **Figure 2**[22]. Some of the non-computer vision solutions could be used for tracking a cow's vital signs and activity in real-time, but they use unique sensors for each cow and they are very expensive. On the other hand, the farmer could use the camera to check the video feed from

his phone while trusting the system to notify him if something happens that requires his attention[23]. CVS can be exploited through breeding programs. For example, Nye et al.[24] used the catalogs of breeding programs to demonstrate a web scraper with an image segmentation algorithm for extracting images and information. They presented how the extracted information can be used to determine genetic parameters related to coat pigmentation and conformation traits in dairy cows. Similar, Moore et al.[25] reported on the use of various cattle data for the prediction of genetic parameters. The results showed that more accurate genetic parameters could be determined with the information from the CVS due to the larger amount of data. Tassinari et al.[1] conducted research on the development of a computer vision system based on Deep Learning aimed at recognizing individual cows in real-time. Results showed that the system successfully identified cows based on coat patterns, assessed their position, tracked movements, and helped understand cows' actions. An image-based model for the recognition of cow breeds was proposed by Gupta et al.[26]. The YOLOv4 algorithm of DL was used for the discriminative feature of cows with a limited training dataset. The results of the comprehensive analysis show that the proposed approach achieves an accuracy of 81.07%, with a maximum kappa value of 0.78 at an image size of 608 × 608 and an overlap over unity (IoU) threshold of 0.75 in the test dataset. However, the improvement using computer vision is achieved by several publicly available datasets: ImageNet[27], PASCAL VOC (Visual Object Classes)[28], and MSCOCO[29]. Some of the datasets developed specifically for use in cuttle computer vision systems are Holstein Cattle Recognition[30], Friesian Cattle 2017[31], Aerial Cattle 2017[32]. Currently, image classification, instance segmentation, semantic segmentation, pose estimation, tracking and object detection are public datasets for computer vision tasks or challenges[33]. Therefore, datasets and technologies for cuttle farming are important for analysis and decision-making.

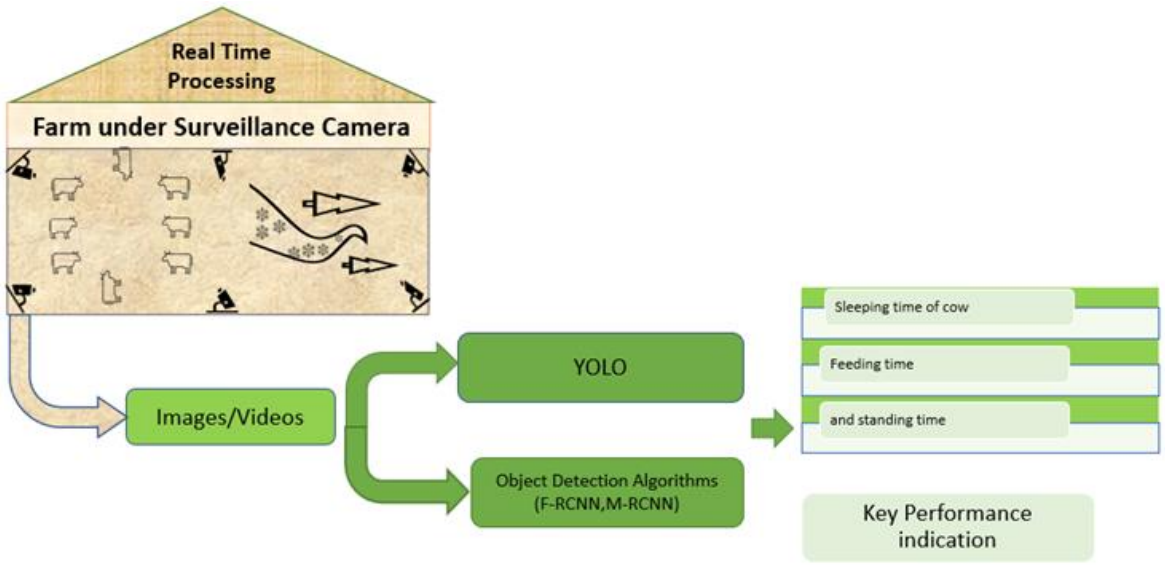

Figure 2. The proposed method for detecting cow movements and activities[22].

3.2. Application of computer vision in pig production

Pork is the meat with the second overall consumption[34] and therefore it is very important to use more advanced methods such as precision livestock management instead of conventional methods to improve production. According to Albernaz-Gonçalves at al.[35], it is currently difficult for swine production to recruit enough skilled labor to provide quality care for pigs given the economic climate and labor shortages. Rauw at all.[36] reported that more intensive care of an individual animal has a positive impact on the welfare and health of the animal. Several animal science studies have been conducted to

determine pig health status[37], comfort and well-being[38], pig drinking behavior[39], posture changes in pigs[40], and live weight[41]. In pig production today, computer vision offers rapidly growing potential to improve production, resulting in improved animal care and reduced labor costs[42]. For example, precision feeding of pigs requires automated measurement devices for data collection, data processing, and calculation methods for estimating nutrient requirements[43]. Technologies such as IoT and AI to monitor the health and welfare of pigs are frequently used in pig farms. Parameters such as humidity and temperature are determined by IoT[18], while feature extraction, modeling, and data analysis are determined by AI[44]. In pig recognition based on computer vision, the importance of networks is becoming increasingly important. Some of the networks used in recognition based on computer vision in swine production are MobileNet[45], DeepLabv3+[46], Xception[47], YOLOv5[40]. AI algorithms also use deep learning models with images or videos to recognize pig behavior[18]. Chen et al.[48] applied the video-based method and obtained good results. On the other hand, for the image, researchers usually used Faster[49], Mask R-CNN[50], YOLO[51]. Although the use of new technologies improves pig production, in practice, the willingness to adopt new technologies is still in progress. Therefore, for farmers who have adopted the technology, government agencies should provide adequate subsidies, which will not only help protect farmers after adopting the risk of the new technology but also encourage more farmers to adopt the technology[44].

3.3. Application of computer vision in poultry production

Today, the use of artificial intelligence can reduce losses due to premature death and the rejection of billions of chickens per year before they are processed into meat[52]. However, poultry has a higher density compared to other animals[53], which leads to limitations or a high degree of uncertainty in monitoring the behavior and distribution of groups of chickens in feeding, drinking, and resting areas. Modern broiler houses with large numbers of chickens are equipped with cameras, and the use of computer vision is one of the methods for continuous remote monitoring of commercial farms[54]. According to Okinda et al.[55], the application of computer vision in poultry farming includes recognition and identification of images, detection of objects, classification of images, segmentation, and recognition of objects. Abd Aziz et al.[56] reported that computer vision works in three basic steps: 1) acquiring an image, 2) processing the image, and 3) understanding the image. Despite the many advantages of vision systems, the performance of any vision system in monitoring livestock is greatly affected by the varying light conditions in the farm environment, color, contrast between background and foreground, and occlusion problems[55]. Recently, researchers reported the efficiency of using computer vision in poultry production, especially for monitoring chicken welfare in terms of weight, lameness, behavior, temperature, activities, and health[57–59]. Some of the Digital technologies for poultry producers are presented in the **Table 1**. The potential of computer vision algorithms using Mask R-CNN for broiler detection and monitoring resource utilization in broilers was investigated by Jerine et al.[54]. They found that in a high stocking density commercial environment, individual broilers can be detected and monitored when it comes to resource utilization. According to Karthikeyan[60], AI could be trained using computers/artificial vision to detect heat stress in birds early using thermal imaging cameras or infrared cameras. Dawkins et al.[61], used cameras to analyze the optical movement patterns of flocks of chickens as they moved around a house. The results confirmed the hypothesis that visual movement patterns of broiler flocks on commercial farms in the United Kingdom and Switzerland are correlated with two important animal welfare outcomes-mortality and fecal burn.

Table 1. Digital technologies for poultry producers.

Technology	Description
3D printing prosthetics	Printing of plastic or metal parts when the farm requires replacing[62].
Robots	Provide farmers to make data-driven decisions regarding broiler production that could result in a healthier, more productive growing environment[63].
Drones	Allow farmers to monitor poultry conditions from the air to keep watch for potential problems and help optimize field management[64].
Sensors	Streamlining data collection for chickens and farmers, enabling cheaper poultry production[65].
Poultry system simulation model	Simulates the water, energy, wastewater, and labor utilization of a poultry processing plant[66].
Block chain technology	Uses predictive analytics and deep learning analysis to display and forecast future performance throughout the supply chain[66].
Automation and digitalization, big data	It is possible to apply various ways to enhance poultry production by improving efficiency, productivity, and overall management[67].
Machine learning: Statistical process control	Accurate identification of changes in variables throughout the food supply chain[68].
Internet of things	Connection between sensors and smartphones or other devices in a hen house[69].

3.4. Application of computer vision in sheep production

For most sheep producers, profit is directly related to the commercial value of the flock and the cost of the bred sheep. In recent years, considerable progress has been made in the field of machine vision and machine learning[70]. Several works with sheep can be found in the literature, aiming at image processing with physiological information (skin temperature, respiratory rate, and heart rate), weight prediction, behavior recognition, sheep breed identification, etc. Fuentes et al.[71] investigated the evaluation of physiological information such as heart rate modeled with machine learning algorithms, skin temperature, and respiratory rate in sheep exposed to thermoneutral and controlled heat stress conditions by automatically tracking the regions of interest from RGB videos and infrared thermal videos of sheep. According to the results obtained, the application of automated computer vision algorithms and machine learning models was proposed to obtain critical biometric data from recorded RGB and infrared thermal videos of sheep to help in the automatic assessment of heat stress. Bhatt et al.[72] proposed an automated sheep weight estimation system for real-time operations using a smartphone. A SegNet-inspired deep network was used for segmentation, and a novel segmentation approach and neural network-based regression model were used to achieve better results for the sheep weight estimation task. A deep learning model based on the YOLO v5 network[73] was used to recognize the behavior of sheep (lying down, drinking, and eating). Nowadays the application of YOLO v7 (**Figure 3**) is becoming more popular for sheep detection behavior providing more accurate data[74].

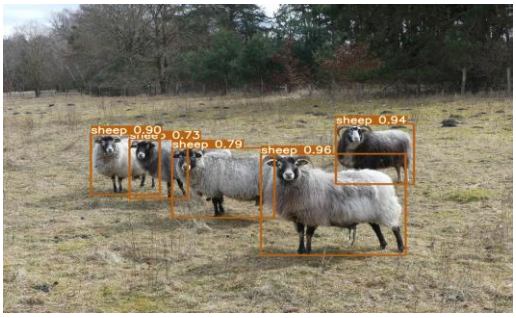

Figure 3. Computer vision to detect sheep with YOLOv7[74].

The application of a deep learning network in a structured environment of intensive farming can provide satisfactory results without the need for large amounts of data if it is ensured that the application and experimental conditions are the same. Sanibel et al.[75] presented the establishment of a prototype computer vision system in a sheep farm, the creation of a database of 1642 sheep images of four breeds taken on a farm and labeled with the respective breed by an expert with its breed, and the training of a classifier for sheep breeds using machine learning and computer vision to achieve an average accuracy of 95.8%. Sarwar et al.[76] used a combination of drone technology and deep learning algorithms to count sheep using convolutional neural networks through video streams captured by drones. They found that capturing top-view images was mainly used for free-range scenarios and could not be extended to indoor sheep rearing. According to the above-mentioned statements from different literature, it can be concluded that there is a need for the development of applications of new technologies in livestock production.

4. Crop production

4.1. Computer vision phenotyping

In the field of agriculture, the integration of cutting-edge technologies has revolutionized traditional agricultural practices. Phenotyping using computer vision is a powerful tool, providing farmers and researchers with unprecedented insights into the health, growth patterns, and overall productivity of plants. Plant phenotyping is one of the biggest bottlenecks in the field of plant science and plant breeding, and further progress requires an interdisciplinary approach and the integration of activities from fields such as plant physiology, sensing, and bioinformatics. Although some methods for phenotyping have drawbacks, such as space-time coverage and limitations in terms of cost, the plant phenotype plays an important role in sciences such as agronomy, botany and genetics[77]. The disadvantages of phenotyping include the structural characteristics of plants and their organs (leaves, fruits, roots etc.) as well as the measurement of size, growth, and 3D surface structure. However, phenotypic information with intelligent perception plays an important role in minimizing agricultural inputs without compromising crop yields and selecting new varieties of high-yielding and high-quality crops[78]. Nowadays, field experiments using aerial phenotyping with thermal and multispectral sensors help to obtain a large number of plant images for crop monitoring and are widely used in crop research[79]. Plant phenotyping frameworks include many sensors with mobile systems, such as motorized gantries[80], tray conveyors[81], and aerial and ground vehicles[82], to collect plant growth and physiology data. Bauer et al.[83] presented the results of combining AirSurf with a deep learning classifier trained with over 100,000 labeled lettuce signals and computer vision algorithms. The results show the significant value of AirSurf-L for pre-harvest plant marketability and precise harvesting strategies. Quantitative evaluation of phenotypic differences throughout the plant's life cycle helps identify genetic factors associated with growth and development[84]. In addition, researchers Choudhury et al.[85] determined stem angle using temporal analysis of plant phenotyping. They found that plant phenotyping analysis summarized the temporal patterns of stem angle into three main groups and contributed to the temporal variation of stem angle, which can be regulated by genetic variation under different environmental conditions. Mochida et al.[86] reported that useful clues for preventive interventions in farming provide a meta-analysis of the spectral signatures of crops associated in association with the environmental conditions, physiological states, and growth stage. The researchers such as Minervini et al.[87] comprehensively discussed the bottlenecks and future trends in the field of image-based plant phenotyping, Toda and Okura[88] for plant stress phenotyping, while Vandenberghe et al. for plant 3D phenotyping. Furthermore, deep learning has become more popular in phenotyping. Thus, RCNN, ZFNet, LeNet18, VGGNet, ResNet, ResNeXt, and

VGGNet[89] have been used successfully in plant phenotyping. This innovative approach leverages advanced image processing techniques to analyze visual data, offering a deeper understanding of plant characteristics that can significantly impact decision-making in agriculture. Computer vision phenotyping stands at the forefront of precision agriculture, providing a transformative approach to crop monitoring and analysis. As technology continues to evolve, the integration of computer vision will likely become a cornerstone in the pursuit of sustainable and efficient farming practices, ultimately contributing to global food security.

4.2. Weeds control

Weed detection and control is another major problem in agriculture and, according to many growers, one of the biggest threats to crop production. Nowadays, farmers tend to use less chemical-intensive systems in order to achieve high yields with good quality. Conventional agriculture combines profitable agricultural production with environmental protection requirements by using reduced tillage, crop rotations, residues, and cover crops to control emerging weeds[90]. Traditional weed control methods often rely on manual labor or the indiscriminate use of herbicides, leading to higher costs and environmental problems. The digitalization of agriculture and new cultivation techniques are some of the possible alternatives for "smart" weed control solutions. For example, self-organizing maps (SOMs) have been used in the past[91], and today they are a powerful, unsupervised machine-learning technique that has proven to be a versatile tool in the field of data analysis. The use of self-organizing maps helps to deal with problems in an unsupervised way and independently of the data[92]. Pantazi et al.[93] used hierarchical map classifiers (SKN, CP-ANN and XY-F) to identify *S. marianum* among other plants in a field, where *Avena sterilis L*. was predominant. The results showed that the identification rates of *S. marianum* reached an accuracy of 98.64% with SKN, 98.87%, with CP-ANN, and 98.64% with XY-F. A precision farming system was proposed by Zhai et al.[94] as a multi-agent system. According to them, this system makes it possible to schedule tasks and allocate scarce resources, as well as spray pesticides only in the exact places where weeds grow. On the other hand, Zhang et al.[95] developed a weed classification model based on the YOLOV3-tiny network. Building a weed classification model based on the YOLOv3-tiny network involves several steps, including data acquisition, preprocessing, training, and evaluation. A study of weed detection and segmentation confirms that CNN shows high performance in accurately detecting and segmenting weeds. In addition, Blue River Technology has developed a robot called See & Spray, which reportedly uses computer vision to monitor and precisely spray weed plants[96,97]. Object recognition algorithms, such as YOLO or Faster R-CNN, can be used to precisely localize and identify individual weed instances.

Precision weed detection robots use advanced technologies such as computer vision, machine learning, and robotics to autonomously identify and control weeds in agricultural fields (**Figure 4**). These robots have been developed to improve efficiency and accuracy in weed detection, contributing to sustainable and precise agricultural practices. In this way, it is possible to significantly reduce weeds and the risk of contamination of crops, humans, animals, and water resources. However, growers should take long-term action to improve crop competitiveness against weeds and maintain soil fertility.

Figure 4. An example of the use of AI in the analysis of aerial images of crops for identification of weeds.

4.3. Smart systems for crop grading and sorting

Nowadays, the food industry contributes the most to the agricultural sector and the automation of vegetable sorting is the order of the day[98]. The main objective of grading in agriculture is to generate more and more income. Therefore, grading has a significant impact on agribusiness to generate more profit[99]. Smart systems for crop classification and sorting play a crucial role in increasing efficiency and accuracy in the agricultural industry. These systems use advanced technologies to automate the process of sorting and grading crops based on various parameters such as size, color, weight, and quality. For farmers sorting and grading crops enables them to separate produce into categories more accurately (**Figure 5**). Many researchers have studied the sorting of a variety of crops using artificial intelligence. Llobet et al.[100] for predicting the degree of ripeness of bananas using electronic nose sensors, Bennedsen et al.[101] for detecting surface defects in apple fruit, Zakaria et al.[102] for assessing the degree of ripeness of mangoes. Nur et al.[103] investigated agricultural products that were classified based on the shape and size of the fruit using support vector machines (SVMs) and whose quality class was determined using fuzzy logic (FL). Different types of fruit and one vegetable were used for the experiment: Oranges, mangoes, carrots, apples, and bananas. Of the five fruits selected, the results were good for three. The working model of the date fruit sorting system, including the hardware and software developed by Yousef[104], uses RGB images of date fruits. The accuracy of the system was 80%. In contrast, Nandi et al.[105] used a CCD camera and a conveyor belt to sort and classify mangoes. RGB color space, edge detection, and boundary tracking were used to determine the color quality and dimension of the mangoes. They note that experts judge the degree of ripeness by firmness and smell and not just by skin color. A new design for an autonomous fruit sorting and classification system that is portable, inexpensive, fast, and customizable by the user was presented by Hadha et al.[106]. Using a test with orange fruit, they showed that the algorithm transforms the (red, green, and blue) color space into the HSV color space (hue, saturation, and value). The size ranged from 25 mm to 75 mm, indicating good results in color classification, sizing, and sorting.

Figure 5. Example of sorting and grading tomato fruit by application of AI[107].

Researchers Paymode et al.[108] used the CNN model with an accuracy of 97.59% for the training images and an accuracy of 92.45% for the test images to determine the size, quality, and shape of the onions. The classification and sorting of dragon fruit were also performed using machine learning algorithms (CNN, ANN, and SVM)[109]. The functioning of these algorithms was based on the shape, size, weight, color, and diseases of the dragon fruit. The use of advanced computer vision algorithms and machine learning models enables the automatic recognition and classification of plants based on various parameters such as size, color, and quality[110]. While the introduction of intelligent crop sorting systems offers many benefits, ongoing research and development is essential to overcome challenges and further refine these technologies. Interdisciplinary collaboration between agronomists, engineers, and technologists is critical to realizing the full potential of smart systems, promoting sustainable agriculture, and ensuring food security in a rapidly evolving global landscape. The use of smart systems for crop sorting increases productivity, reduces labor costs, and ensures a consistently high-quality crop. These technologies contribute to the overall efficiency of the agricultural value chain.

4.4. Using drones in crop production

Drones, also known as Unmanned Aerial Vehicles (UAVs) or Unmanned Aircraft Systems (UAS), are becoming increasingly popular in agriculture, including crop production. They offer various benefits and applications that can improve efficiency, precision, and overall crop management. Spray drones are used for the application of fertilizers, herbicides, pesticides, fungicides, and seeds as they are cheaper, faster, and more accurate compared to traditional methods. In some countries, popular methods for precision agriculture include photogrammetry and remote sensing[111,112], crop monitoring[113] and soil and field analysis[114]. The use of drones in agriculture is useful for monitoring plant growth, increasing yields, and spraying pesticides and fertilizers in the field[115]. Drones equipped with spraying systems can precisely apply fertilizers, pesticides, or herbicides to specific areas, minimizing waste and reducing environmental impact. Today, the ability of unmanned aerial vehicles (UAVs) to, for example, fly over crops and quickly collect crop management data is crucial for precision agriculture, which requires real-time data[116]. Hogan[117] reported that flight duration, ease of use, the ability to better utilize cameras, and reliability through the Global Positioning System (GPS) and customizable apps for smartphones and tablets. According to El Bilali et al.[118] the use of drones together with other information and communication technologies (ICT) opens up a new phase in agriculture, in which we speak of digital agriculture, smart agriculture, e-agriculture, and precision agriculture. Mogili and Deepak[119] have studied the use of drones for crop monitoring and pesticide spraying. They concluded that the UAV spraying

system automatically navigates with the GPS coordinates to spray the pesticides on the infected areas where there is no vegetation identified by the Normalized Difference Vegetation Index (NDVI). NDVI maps created using drone imagery can help farmers identify areas of the field that may be under stress, allowing for targeted interventions. The use of drone-generated variable rate application (VRA) maps makes it possible to determine the level of nutrient uptake in the field. In this way, the farmer can apply 300 kg/ha of fertilizer to problematic areas, 200 kg/ha to medium-quality areas, and 150 kg/ha to healthy areas, thus reducing fertilizer costs and increasing yields[120]. Drones create 3D maps to help farmers analyze the soil. To achieve better plant growth, the use of drones provides data useful for irrigation and nitrogen management via soil analysis[121]. In addition, drones can create detailed topographic maps of fields that help farmers understand the terrain and plan irrigation systems more effectively. Drones with hyper-spectral, multi-spectral, or thermal sensors can be used to count plants and assess their health, allowing farmers to detect areas of lower plant density or signs of disease early[122]. According to Ayamga et al.[123], drones play a critical role in decision-making and the management process by providing plant health imaging, integrated GIS mapping, and minimizing the need to physically enter the field, thus contributing to higher yields and lower costs. In addition, information expert Gerard Sylvester said that drones will help farmers adapt to climate change and tackle other challenges to improve the efficiency of overall farming operations[124]. The data collected by drones can be processed with specialized software to gain actionable insights. This information can support decision-making and enable farmers to make informed decisions about how to manage their crops. While drones offer numerous benefits for crop production, it is important that farmers undergo appropriate training and comply with regulations to ensure safe and effective use. Furthermore, ongoing advances in drone technology are likely to bring even more opportunities and improvements in precision agriculture.

4.5. Computer vision and machine learning for crop rotation

Crop rotation is one of the plant production systems that represent a regular spatial (crop rotation) and temporal (crop rotation) change of crops. Proper crop rotation plays an important role in the production of field crops. The application of crop rotation is important because the continuous cultivation of crops puts a lot of stress on the soil, and since it is the most important resource in agriculture, we must do everything we can to restore it. Nowadays, most methods are used to work only one year compared to annual crop rotations. Many researchers have studied crop classification and have come to the conclusion that PSE + LTAE (Pixel Set Encoder and Lightweight Temporal Attention) is one of the most modern methods[125–127]. Machine learning models can analyze historical data on crop performance and soil conditions to predict the best crop rotation plans for optimal yields. Satellite observations and past reports help classify perennial crops to improve the crops grown in agriculture[128]. Liu et al.[129] proposed a hybrid convolutional neural network (CNN) and long short memory (LSTM) architecture for crop rotation mapping (CRM) to combine the time series of synthetic aperture radar (SAR) and optical data in a crop rotation mapping. According to Shiraly[130], the visual features—such as plant boundaries, plant types, soil texture, etc.—are represented as vectors by neural convolutional networks. These vectors are then fed into the time series prediction model. Algorithms such as random forests, XGBoost, recurrent neural networks, or even transformer networks are then used to predict the new soil variables. Stanhope et al.[131] investigated a webcam-based system to augment mechanical guidance systems for row crop cultivation in the early stages of plant growth, combining computer vision and machine learning. They used a low-cost CCD camera and the Python OpenCV platform. The results show that the system was successfully tested for driving speeds up to 6 km/h in several corn and soybean fields under different ambient light and growing conditions. Braeger and Foroosh[132] proposed a voxel CNN method that

proved successful when applied to the latest voxel CNN Octnet architecture, achieving a 1% increase in overall accuracy on the ModelNet10 dataset. Long Short-Term Memory (LSTM) networks, a type of recurrent neural network (RNN), can be used in the context of crop rotation to model temporal dependencies and make predictions based on historical data[133]. However, according to Niall et al.[134], some of the traditional CV techniques (SIFT, SURF, BRIEF) are still useful and collaboration with agronomists and professionals is essential to ensure that the model's recommendations are consistent with practical farming considerations. Today, a combination of computer vision and machine learning provides farmers with data-driven decisions that improve the efficiency and sustainability of crop rotation practices, resulting in higher yields and long-term soil health.

4.6. Yield analysis

Yield mapping is a precision agriculture technique that involves collecting and analyzing data on crop yields in a field. A yield mapping system in precision agriculture measures and records the number of crops harvested at different points in a field and simultaneously records the position of harvesting machinery[135]. Assessing the quality and quantity of specialty crops during harvest is critical for several reasons, including achieving higher yields and improving overall farming practices[136]. In the 1990s, image classification functions were used to detect fruit moving along the packing line to distinguish between acceptable features (e.g., a stalk and blemishes)[137]. However, Raphael et al.[138] concluded that the application of RGB-recorded images in orchards is associated with difficulties, e.g. the different sizes and colors of apples and the non-diffuse natural light causing strong shading. The integration of computer vision, chemical markers (such as Marker M-2), and other accessories can indeed provide a powerful and efficient solution for determining the location of cold and hot spots after microwave sterilization. This approach combines real-time visual data with chemical indicators to increase accuracy and speed in identifying temperature variations[139]. Patel et al.[140] have looked at the localization of fruit on trees as one of the requirements for an effective fruit harvesting system. The ability to accurately identify the location and ripeness of fruit enables the automation of harvesting processes, reducing waste and optimizing the use of resources. Color and shape analysis was used to segment the images of different fruits taken under different lighting conditions. The results show that the proposed method can accurately segment the occluded fruits with an efficiency of 98%. In addition, it was found that based on the data obtained from the hyperspectral camera at the full pod development stage, the yield of soybeans can be best predicted using multilayer neural networks[141]. The same group of authors showed that the prediction of soybean yield by the VNM model is more accurate at the local level than at the regional or state level. According to Kapach et al.[142], the most important applications of computer vision (CV) in agriculture have been developed for fruit detection. The main goal was to identify individual fruits and leaves, segment them from scenes with branches, and localize them in space, either for yield estimation or for robotic harvesting systems. It is important to note that factors such as soil type, topography, and historical management practices can contribute to yield variability[143]. Yield mapping, when integrated with precision agriculture, can greatly enhance a farmer's ability to optimize resource allocation, improve crop yields, and make more informed decisions for sustainable agricultural practices.

5. Discussion

The use of computer vision is now an integral part of agricultural production. Start-ups are turning to task-specific AI and image-processing solutions to improve yields and achieve the goal of a sustainable food supply by 2050[144]. When it comes to livestock and next-generation farms to manage the greenhouse environment with smart irrigation, start-ups such as cropx aquaspy, hydropoint data systems, alesca life,

aero farms, bright farms, connecterra, farmnote, advanced animal diagnostics are using machine learning and computer vision techniques to capture, analyze, model and predict the factors that can improve yields[145]. As mentioned above, the use of computer vision offers many advantages such as accuracy, efficiency, and cost-effectiveness. Animal welfare is a priority in modern agriculture. Specific applications such as monitoring animal health, behavior, and productivity contribute to better animal welfare, especially by detecting signs of distress or disease. Automated systems can analyze video feeds to detect signs of illness, stress, or anomalies in behavior[146]. Optimizing feeding, breeding, and overall resource management on farms helps farmers and leads to better productivity. By monitoring feeding patterns and behavior, computer vision can help optimize feed distribution and reduce feed waste. The advantages of low cost as well as high efficiency of the application of Computer vision technology were represented by other researchers[11,147]. Overall, these benefits contribute to more efficient, sustainable, and humane livestock farming. Machine vision technology has the potential to revolutionize the industry by providing farmers and ranchers with valuable insights and tools to optimize their operations. However, farmers face technical issues, privacy concerns, and the initial cost of setting up such systems. In addition, 24/7 operation of vision systems can be very energy intensive. High energy consumption can drive up operating costs and may not be environmentally friendly. Despite these drawbacks, the benefits of computer vision in livestock production often outweigh the drawbacks, but it is important to carefully plan and address these challenges to ensure the successful implementation of this technology. In crop production, computer vision technology increases precision and efficiency. It enables precise monitoring, data collection, and management of crops, resulting in less wasted resources and higher yields. Monitoring of crop growth with computer vision enables the detection of subtle changes in crops and provides a reliable and accurate basis for timely regulation[85]. It is combined with other precision farming technologies, such as GPS-guided machines and sensor networks, to create comprehensive and data-driven farming systems. The multi-sensor imaging system attached to the drones makes it easier for the farmer to detect fewer infrared-reflecting patches in the farmland, thus reducing the further spread of the disease[144]. The application of computer vision improves crop production practices, reduces environmental impact, and contributes to more efficient, sustainable, and economically viable agriculture. Computer vision is becoming an essential tool for modern farming, helping farmers meet the challenges of a growing global population and changing environmental conditions. As in livestock production in crop production computer vision algorithms may occasionally produce false positives (incorrectly identifying issues) or false negatives (failing to identify issues). This can lead to unnecessary interventions or missed problems in crop management.

6. Conclusion

Technology and artificial intelligence play a key role in transforming agriculture by enabling efficient resource management, crop monitoring, and improving production quality. Companies in agriculture (as well as other industries) are using computer vision and AI applications to drive new innovations and unlock new efficiencies that help them achieve their goals in the face of modern challenges. In the realm of livestock farming, computer vision plays a pivotal role in monitoring animal behavior, health, and welfare. Automated systems equipped with cameras and image analysis software can detect signs of distress or disease in livestock, enabling prompt intervention and preventing disease outbreaks. These technologies have the potential to increase both productivity and animal welfare, contributing to sustainable and responsible livestock farming. In crop production, computer vision aids in phenotyping, weed control, crop grading and sorting, crop irrigation, crop rotation, as well as yield mapping. It provides real-time monitoring of plant health and growth, allowing for precise irrigation and fertilization,

which in turn conserves resources and improves crop yield. By increasing food demands, the adoption of computer vision in livestock and crop production promises to not only increase yields but also reduce environmental impact and promote animal welfare. The marriage of cutting-edge technology and traditional farming practices represents a promising future for agriculture, ensuring food security in a rapidly evolving world.

Availability of data and material

Not applicable.

Author contributions

The authors contributed equally to the conceptualization, methods, writing, revision, as well as editing of the manuscript.

Conflict of interest

The authors declare no conflict of interest.

References

1. Tassinari P, Bovo M, Benni S, et al. A computer vision approach based on deep learning for the detection of dairy cows in free stall barn. *Computers and Electronics in Agriculture* 2021; 182: 106030. doi: 10.1016/j.compag.2021.106030
2. Fernandes AFA, Dórea JRR, Rosa GJ de M. Image analysis and computer vision applications in animal sciences: An overview. *Frontiers in Veterinary Science* 2020; 7. doi: 10.3389/fvets.2020.551269
3. Pradana ZH, Hidayat B, Darana S. Beef cattle weight determine by using digital image processing. In: Proceedings of the 2016 International Conference on Control, Electronics, Renewable Energy and Communications (ICCEREC); 13–15 September 2016; Bandung, Indonesia. pp. 179–184 doi: 10.1109/iccerec.2016.7814955
4. Önder H, Ari A, Ocak S, et al. Use of image analysis in animal science. *Journal of Information Technology in Agriculture* 2020; 1.
5. Nasirahmadi A, Edwards SA, Sturm B. Implementation of machine vision for detecting behaviour of cattle and pigs. *Livestock Science* 2017; 202: 25–38. doi: 10.1016/j.livsci.2017.05.014
6. Eduardo FC, Marta MA, Benjamin I, et al. Motion-based video monitoring for early detection of livestock diseases: The case of African swine fever. *PLoS One* 2017; 12(9): e0183793. doi: 10.1371/journal.pone.0183793
7. Patrício DI, Chen C, Larsen MLV, Berckmans D. Review: Precision livestock farming: Building 'digital representations' to bring the animals closer to the farmer. *Animal* 2019; 13(12): 3009–3017. doi: 10.1017/S175173111900199X
8. Fernández-Carrión E, Martínez-Avilés M, Ivorra B, et al. Motion-based video monitoring for early detection of livestock diseases: The case of African swine fever. *PLOS ONE* 2017; 12(9): e0183793. doi: 10.1371/journal.pone.0183793
9. Patrício DI, Rieder R. Computer vision and artificial intelligence in precision agriculture for grain crops: A systematic review. *Computers and Electronics in Agriculture* 2018; 153: 69–81. doi: 10.1016/j.compag.2018.08.001
10. Mamai O, Parsova V, Lipatova N, et al. The system of effective management of crop production in modern conditions. *BIO Web of Conferences* 2020; 17: 00027. doi: 10.1051/bioconf/20201700027
11. Tian H, Wang T, Liu Y, et al. Computer vision technology in agricultural automation—A review. *Information Processing in Agriculture* 2019; 7(1): 1–19. doi: 10.1016/j.inpa.2019.09.006
12. Liakos K, Busato P, Moshou D, et al. Machine learning in agriculture: A review. *Sensors* 2018; 18(8): 2674. doi: 10.3390/s18082674
13. Tian H, Wang T, Liu Y, et al. Computer vision technology in agricultural automation—A review. *Information Processing in Agriculture* 2020; 7(1): 1–19. doi: 10.1016/j.inpa.2019.09.006
14. Redmond RS, Coenelia W, Ibrahim AH, et al. Research and development in agricultural robotics: A perspective of digital farming. *International Journal of Agricultural and Biological Engineering* 2018; 11(4): 1–14. doi: 10.25165/j.ijabe.20181104.4278

15. Foglia MM, Reina G. Agricultural robot for radicchio harvesting. *Journal of Field Robotics* 2006; 23(6–7): 363–377. doi: 10.1002/rob.20131
16. Ramin Shamshiri R, Weltzien C, et al. Research and development in agricultural robotics: A perspective of digital farming. *International Journal of Agricultural and Biological Engineering* 2018; 11(4): 1–11. doi: 10.25165/j.ijabe.20181104.4278
17. Vithu P, Moses JA. Machine vision system for food grain quality evaluation: A review. *Trends in Food Science & Technology* 2016; 56: 13–20. doi: 10.1016/j.tifs.2016.07.011
18. Wang S, Jiang H, Qiao Y, et al. The research progress of vision-based artificial intelligence in smart pig farming. *Sensors* 2022; 22(17): 6541. doi: 10.3390/s22176541
19. Diba A, Sharma V, Pazandeh A, et al. Weakly supervised cascaded convolutional networks. In: Proceedings of the 2017 IEEE Conference on Computer Vision and Pattern Recognition (CVPR); 21–26 July 2017; Honolulu, HI, USA. pp. 5131–5139. doi: 10.1109/CVPR.2017.545
20. Ronald T. Computer vision for smart farming and sustainable agriculture. In: Proceedings of the 2020 IST-Africa Conference (IST-Africa); 18–22 May 2020; Kampala, Uganda. pp. 1–8.
21. Binch A, Fox CW. Controlled comparison of machine vision algorithms for Rumex and Urtica detection in grassland. *Computers and Electronics in Agriculture* 2017; 140: 123–138. doi: 10.1016/j.compag.2017.05.018
22. Jose MR, Kaakinen H. An object detection application approach to analyze cattle under camera surveillance. Available online: https://centriabulletin.fi/object-detection/ (accessed on 26 January 2024).
23. Mediaan Conclusion. Using computer vision in the calving process. Available online: https://mediaan.com/mediaan-blog/computer-vision-calving (accessed on 26 January 2024).
24. Nye J, Zingaretti LM, Pérez-Enciso M. Estimating conformational traits in dairy cattle with DeepAPS: A two-step deep learning automated phenotyping and segmentation approach. *Frontiers in Genetics* 2020; 11. doi: 10.3389/fgene.2020.00513
25. Moore KL, Mrode R, Coffey MP. Genetic parameters of Visual Image Analysis primal cut carcass traits of commercial prime beef slaughter animals. *Animal* 2017; 11(10): 1653–1659. doi: 10.1017/s1751731117000489
26. Gupta H, Jindal P, Verma OP, et al. Computer vision-based approach for automatic detection of dairy cow breed. *Electronics* 2022; 11(22): 3791. doi: 10.3390/electronics11223791
27. Deng J, Dong W, Socher R, et al. ImageNet: A large-scale hierarchical image database. In: Proceedings of the 2009 IEEE Conference on Computer Vision and Pattern Recognition; 20–25 June 2009; Miami, FL, USA. pp. 248–255. doi: 10.1109/cvpr.2009.5206848
28. Everingham M, Van Gool L, Williams CKI, et al. The pascal visual object classes (VOC) challenge. *International Journal of Computer Vision* 2009; 88(2): 303–338. doi: 10.1007/s11263-009-0275-4
29. Lin TY, Maire M, Belongie S, et al. Microsoft COCO: Common objects in context. In: Fleet D, Pajdla T, Schiele B, Tuytelaars T (editors). *Computer Vision—ECCV 2014. ECCV 2014. Lecture Notes in Computer Science.* Springer, Cham; 2014. doi: 10.1007/978-3-319-10602-1_48
30. Bhole A, Udmale SS, Falzon O, et al. CORF3D contour maps with application to Holstein cattle recognition from RGB and thermal images. *Expert Systems with Applications* 2022; 192: 116354. doi: 10.1016/j.eswa.2021.116354
31. Andrew W, Greatwood C, Burghardt T. Visual localisation and individual identification of holstein friesian cattle via deep learning. In: Proceedings of the 2017 IEEE International Conference on Computer Vision Workshops (ICCVW); 22–29 October 2017; Venice, Italy. pp. 2850–2859. doi: 10.1109/ICCVW.2017.336
32. Andrew W, Greatwood C, Burghardt T. Aerial animal biometrics: Individual friesian cattle recovery and visual identification via an autonomous UAV with onboard deep inference. 2019 IEEE/RSJ International Conference on Intelligent Robots and Systems (IROS); 3–8 November 2019; Macau, China. pp. 237–243. doi: 10.1109/IROS40897.2019.8968555
33. Li G, Huang Y, Chen Z, et al. Practices and applications of convolutional neural network-based computer vision systems in animal farming: A review. *Sensors* 2021; 21(4): 1492. doi: 10.3390/s21041492
34. Arulmozhi E, Bhujel A, Moon BE, et al. The application of cameras in precision pig farming: An overview for swine-keeping professionals. *Animals* 2021; 11(8): 2343. doi: 10.3390/ani11082343
35. Albernaz-Gonçalves R, Olmos G, Hötzel MJ. My pigs are ok, why change?—Animal welfare accounts of pig farmers. *Animal* 2021; 15(3): 100154. doi: 10.1016/j.animal.2020.100154
36. Rauw WM, Rydhmer L, Kyriazakis I, et al. Prospects for sustainability of pig production in relation to climate change and novel feed resources. *Journal of the Science of Food and Agriculture* 2020; 100(9): 3575–3586. doi: 10.1002/jsfa.10338
37. Chijioke Ojukwu C, Feng Y, et al. Development of a computer vision system to detect inactivity in group-housed pigs. *International Journal of Agricultural and Biological Engineering* 2020; 13(1): 42–46. doi: 10.25165/j.ijabe.20201301.5030

38. Haladjian J, Ermis A, Hodaie Z, et al. *iPig: Towards Tracking the Behavior of Free-roaming Pigs*. Association for Computing Machinery; 2017. doi: 10.1145/3152130.3152145
39. Zhu W, Guo Y, Jiao P, et al. Recognition and drinking behaviour analysis of individual pigs based on machine vision. *Livestock Science* 2017; 205: 129–136. doi: 10.1016/j.livsci.2017.09.003
40. Shao H, Pu J, Mu J. Pig-posture recognition based on computer vision: Dataset and exploration. *Animals* 2021; 11(5): 1295. doi: 10.3390/ani11051295
41. Wongsriworaphon A, Arnonkijpanich B, Pathumnakul S. An approach based on digital image analysis to estimate the live weights of pigs in farm environments. *Computers and Electronics in Agriculture* 2015; 115: 26–33. doi: 10.1016/j.compag.2015.05.004
42. Li J, Green-Miller AR, Hu X, et al. Barriers to computer vision applications in pig production facilities. *Computers and Electronics in Agriculture* 2022; 200: 107227. doi: 10.1016/j.compag.2022.107227
43. Hendriks WH, Verstegen MWA, Babinszky L (editors). Poultry and Pig Nutrition: Challenges of the 21st Century. Wageningen Academic; 2019. doi: 10.3920/978-90-8686-884-1
44. Sun R, Zhang S, Wang T, et al. Willingness and influencing factors of pig farmers to adopt Internet of things technology in food traceability. *Sustainability* 2021; 13(16): 8861. doi: 10.3390/su13168861
45. Krizhevsky A, Sutskever I, Hinton GE. ImageNet classification with deep convolutional neural networks. *Communications of the ACM* 2017; 60(6): 84–90. doi: 10.1145/3065386
46. Chen LC, Papandreou G, Kokkinos I, et al. DeepLab: Semantic image segmentation with deep convolutional nets, atrous convolution, and fully connected CRFs. *IEEE Transactions on Pattern Analysis and Machine Intelligence* 2018; 40(4): 834–848. doi: 10.1109/tpami.2017.2699184
47. Szegedy C, Vanhoucke V, Ioffe S, et al. Rethinking the inception architecture for computer vision. In: Proceedings of the 2016 IEEE Conference on Computer Vision and Pattern Recognition (CVPR); 27–30 June 2016; Las Vegas, NV, USA. pp. 2818–2826, doi: 10.1109/CVPR.2016.308
48. Chen C, Zhu W, Steibel J, et al. Recognition of aggressive episodes of pigs based on convolutional neural network and long short-term memory. *Computers and Electronics in Agriculture* 2020; 169: 105166. doi: 10.1016/j.compag.2019.105166
49. Riekert M, Opderbeck S, Wild A, et al. Model selection for 24/7 pig position and posture detection by 2D camera imaging and deep learning. *Computers and Electronics in Agriculture* 2021; 187: 106213. doi: 10.1016/j.compag.2021.106213
50. Gan H, Li S, Ou M, et al. Fast and accurate detection of lactating sow nursing behavior with CNN-based optical flow and features. *Computers and Electronics in Agriculture* 2021; 189: 106384. doi: 10.1016/j.compag.2021.106384
51. Ji YP, Yang Y, Liu G. Recognition of pig eating and drinking behavior based on visible spectrum and YOLOv2. *Spectroscopy and Spectral Analysis* 2020; 40(05): 1588–1594. doi: 10.3964/j.issn.1000-0593(2020)05-1588-07
52. Neethirajan, S. Automated tracking systems for the assessment of farmed poultry. *Animals* 2022; 12: 232. doi: 10.3390/ani12030232
53. Guo Y, Chai L, Aggrey SE, et al. A machine vision-based method for monitoring broiler chicken floor distribution. *Sensors* 2020; 20(11): 3179. doi: 10.3390/s20113179
54. Jerine van der E, Guzhva O, Voss A, et al. Seeing is caring—Automated assessment of resource use of broilers with computer vision techniques. *Frontiers in Animal Science* 2022; 3. doi: 10.3389/fanim.2022.945534
55. Okinda C, Nyalala I, Korohou T, et al. A review on computer vision systems in monitoring of poultry: A welfare perspective. *Artificial Intelligence in Agriculture* 2020; 4: 184–208. doi: 10.1016/j.aiia.2020.09.002
56. Abd Aziz NSN, Mohd Daud S, Dziyauddin RA, et al. A review on computer vision technology for monitoring poultry farm—Application, hardware, and software. *IEEE Access* 2021; 9: 12431–12445. doi: 10.1109/access.2020.3047818
57. Mortensen AK, Lisouski P, Ahrendt P. Weight prediction of broiler chickens using 3D computer vision. *Computers and Electronics in Agriculture* 2016; 123: 319–326. doi: 10.1016/j.compag.2016.03.011
58. Aydin A. Using 3D vision camera system to automatically assess the level of inactivity in broiler chickens. *Computers and Electronics in Agriculture* 2017; 135: 4–10. doi: 10.1016/j.compag.2017.01.024
59. Zhuang X, Bi M, Guo J, et al. Development of an early warning algorithm to detect sick broilers. *Computers and Electronics in Agriculture* 2018; 144: 102–113. doi: 10.1016/j.compag.2017.11.032
60. Karthikeyan A, Siva M, Reshma A, et al. Applications of artificial intelligence in poultry industry. Available online: https://www.pashudhanpraharee.com/applications-of-artificial-intelligence-in-poultry-industry/ (accessed on 26 January 2024).
61. Dawkins MS, Wang L, Ellwood SA, et al. Optical flow, behaviour and broiler chicken welfare in the UK and Switzerland. *Applied Animal Behaviour Science* 2021; 234: 105180. doi: 10.1016/j.applanim.2020.105180
62. Wu D, Cui D, Zhou M, et al. Information perception in modern poultry farming: A review. *Computers and Electronics in Agriculture* 2022; 199: 107131. doi: 10.1016/j.compag.2022.107131

63. George AS, George ASH. Optimizing poultry production through advanced monitoring and control systems. *Partners Universal International Innovation Journal* 2023; 1(5): 77–97. doi: 10.5281/zenodo.10050352
64. Ammad-uddin M, Ayaz M, Aggoune EH, et al. Wireless sensor network: A complete solution for poultry farming. In: Proceedings of the 2014 IEEE 2nd International Symposium on Telecommunication Technologies (ISTT); 24–26 November 2014; Langkawi, Malaysia. pp. 321–325. doi: 10.1109/istt.2014.7238228
65. Sreenivas GRN. Modern innovations in Poultry Farming. Available online: https://www.srpublication.com/modern-innovations-in-poultry-farming/ (accessed on 26 January 2024).
66. Astill J, Dara RA, Fraser EDG, et al. Smart poultry management: Smart sensors, big data, and the internet of things. *Computers and Electronics in Agriculture* 2020; 170: 105291. doi: 10.1016/j.compag.2020.105291
67. Lu Y. Industry 4.0: A survey on technologies, applications and open research issues. *Journal of Industrial Information Integration* 2017, 6: 1–10. doi: 10.1016/j.jii.2017.04.005
68. Mataragas M, Drosinos EH, Tsola E, et al. Integrating statistical process control to monitor and improve carcasses quality in a poultry slaughterhouse implementing a HACCP system. *Food Control* 2012; 28(2): 205–211. doi: 10.1016/j.foodcont.2012.05.032
69. Manshor N, Abdul Rahiman AR, Yazed MK. IoT-based poultry house monitoring. In: Proceedings of the 2019 2nd International Conference on Communication Engineering and Technology (ICCET); 12–15 April 2019; Nagoya, Japan. pp. 72–75. doi: 10.1109/ICCET.2019.8726880
70. Esteva A, Chou K, Yeung S, et al. Deep learning-enabled medical computer vision. *npj Digital Medicine* 2021; 4(1). doi: 10.1038/s41746-020-00376-2
71. Fuentes S, Gonzalez Viejo C, Chauhan SS, et al. Non-invasive sheep biometrics obtained by computer vision algorithms and machine learning modeling using integrated visible/infrared thermal cameras. *Sensors* 2020; 20(21): 6334. doi: 10.3390/s20216334
72. Bhatt C, Hassanien A, Shah NA, Thik J. Barqi breed sheep weight estimation based on neural network with regression. *ArXiv* 2018. doi: 10.48550/arXiv.1807.10568
73. Cheng M, Yuan H, Wang Q, et al. Application of deep learning in sheep behaviors recognition and influence analysis of training data characteristics on the recognition effect. *Computers and Electronics in Agriculture* 2022; 198: 107010. doi: 10.1016/j.compag.2022.107010
74. Boesch G. Top applications of computer vision in agriculture (2024 guide) Available online: https://viso.ai/applications/computer-vision-in-agriculture/ (accessed on 26 January 2024).
75. Sanibel A, Jwade, Guzzomi A, Mian A. On farm automatic sheep breed classification using deep learning. *Computers and Electronics in Agriculture* 2019; 167: 105055. doi: 10.1016/j.compag.2019.105055
76. Sarwar F, Griffin A, Periasamy P, et al. Detecting and counting sheep with a convolutional neural network. In: Proceedings of the 2018 15th IEEE International Conference on Advanced Video and Signal Based Surveillance (AVSS); 27–30 November 2018; Auckland, New Zealand. pp. 1–6, doi: 10.1109/AVSS.2018.8639306
77. Li Z, Guo R, Li M, et al. A review of computer vision technologies for plant phenotyping. *Computers and Electronics in Agriculture* 2020; 176: 105672. doi: 10.1016/j.compag.2020.105672
78. Wang YH, Su WH. Convolutional neural networks in computer vision for grain crop phenotyping: A review. *Agronomy* 2022; 12(11): 2659. doi: 10.3390/agronomy12112659
79. Sankaran S, Khot LR, Espinoza CZ, et al. Low-altitude, high-resolution aerial imaging systems for row and field crop phenotyping: A review. *European Journal of Agronomy* 2015; 70: 112–123. doi: 10.1016/j.eja.2015.07.004
80. Virlet N, Sabermanesh K, Sadeghi-Tehran P, et al. Field Scanalyzer: An automated robotic field phenotyping platform for detailed crop monitoring. *Functional Plant Biology* 2017; 44(1): 143. doi: 10.1071/fp16163
81. Frolov K, Fripp J, Nguyen CV, et al. Automated plant and leaf separation: Application in 3D meshes of wheat plants. In: Proceedings of the 2016 International Conference on Digital Image Computing: Techniques and Applications (DICTA); 2016; Gold Coast, QLD, Australia. pp. 1–7, doi: 10.1109/DICTA.2016.7797011
82. Underwood J, Wendel A, Schofield B, et al. Efficient in-field plant phenomics for row-crops with an autonomous ground vehicle. *Journal of Field Robotics* 2017; 34(6): 1061–1083. doi: 10.1002/rob.21728
83. Bauer A, Bostrom AG, Ball J, et al. Combining computer vision and deep learning to enable ultra-scale aerial phenotyping and precision agriculture: A case study of lettuce production. *Horticulture Research* 2019; 6(1). doi: 10.1038/s41438-019-0151-5
84. Rebetzke GJ, Jimenez-Berni JA, Bovill WD, et al. High-throughput phenotyping technologies allow accurate selection of stay-green. *Journal of Experimental Botany* 2016; 67(17): 4919–4924. doi: 10.1093/jxb/erw301

85. Choudhury SD, Goswami S, Bashyam S, et al. Automated stem angle determination for temporal plant phenotyping analysis. In: Proceedings of the 2017 IEEE International Conference on Computer Vision Workshops (ICCVW); 22–29 October 2017; Venice, Italy. pp. 2022–2029, doi: 10.1109/ICCVW.2017.237
86. Mochida K, Koda S, Inoue K, et al. Computer vision-based phenotyping for improvement of plant productivity: A machine learning perspective. *GigaScience* 2018; 8(1). doi: 10.1093/gigascience/giy153
87. Minervini M, Scharr H, Tsaftaris SA. Image analysis: The new bottleneck in plant phenotyping [Applications corner]. *IEEE Signal Processing Magazine* 2015; 32(4): 126–131. doi: 10.1109/msp.2015.2405111
88. Toda Y, Okura F. How convolutional neural networks diagnose plant disease. *Plant Phenomics* 2019; 2019: 1–14. doi: 10.1155/2019/9237136
89. Harandi N, Vandenberghe B, Vankerschaver J, et al. How to make sense of 3D representations for plant phenotyping: A compendium of processing and analysis techniques. *Plant Methods* 2023; 19: 60. doi: 10.1186/s13007-023-01031-z
90. Fuentes A, Yoon S, Kim S, et al. A robust deep-learning-based detector for real-time tomato plant diseases and pests recognition. *Sensors* 2017; 17(9): 2022. doi: 10.3390/s17092022
91. Maria F, Efthimios K, Eleni C, et al. Using self organising maps in applied geomorphology. In: Mwasiagi JS (editor). *Self Organizing Maps—Applications and Novel Algorithm Design*. InTech; 2011. doi: 10.5772/13265
92. Tataridas A, Kanatas P, Chatzigeorgiou A, et al. Sustainable crop and weed management in the era of the EU green deal: A survival guide. *Agronomy* 2022; 12(3): 589. doi: 10.3390/agronomy12030589
93. Pantazi XE, Tamouridou AA, Alexandridis TK, et al. Evaluation of hierarchical self-organising maps for weed mapping using UAS multispectral imagery. *Computers and Electronics in Agriculture* 2017; 139: 224–230. doi: 10.1016/j.compag.2017.05.026
94. Zhai Z, Martínez Ortega JF, Lucas Martínez N, et al. A mission planning approach for precision farming systems based on multi-objective optimization. *Sensors* 2018; 18(6): 1795. doi: 10.3390/s18061795
95. Zhang R, Wang C, Hu X, et al. Weed location and recognition based on UAV imaging and deep learning. *International Journal of Precision Agricultural Aviation* 2018; 1(1): 23–29. doi: 10.33440/j.ijpaa.20200301.63
96. Hasan ASMM, Sohel F, Diepeveen D, et al. A survey of deep learning techniques for weed detection from images. *Computers and Electronics in Agriculture* 2021; 184: 106067. doi: 10.1016/j.compag.2021.106067
97. Nayak A. The economics of applications of artificial intelligence and machine learning in agriculture. *International Journal of Pure & Applied Bioscience* 2019; 7(1): 296–305. doi: 10.18782/2320-7051.7324
98. Farooq O, Gill J. Vegetable grading and sorting using artificial intelligence. *International Journal for Research in Applied Science and Engineering Technology* 2022; 10(3): 13–21. doi: 10.22214/ijraset.2022.40407
99. Pathak AK, Kumar M, Sharma SK. Grading and sorting of fruits and vegetables for increasing farmer's income. Available online: https://krishijagran.com/featured/grading-and-sorting-of-fruits-and-vegetables-for-increasing-farmer-s-income/ (accessed on 26 January 2024).
100. Llobet E, Hines EL, Gardner JW, et al. Non-destructive banana ripeness determination using a neural network-based electronic nose. *Measurement Science and Technology* 1999; 10(6): 538–548. doi: 10.1088/0957-0233/10/6/320
101. Bennedsen BS, Peterson DL, and Tabb A. Identifying apple surface defects using principal components analysis and artificial neural networks. *Transactions of American Society of Agricultural and Biological Engineers* 2007; 50(6): 2257–2265. doi: 10.13031/2013.24078
102. Zakaria A, Shakaff AYM, Masnan MJ, et al. Improved maturity and ripeness classifications of Magnifera Indica cv. Harumanis mangoes through sensor fusion of an electronic nose and acoustic sensor. *Sensors* 2012; 12(5): 6023–6048. doi: 10.3390/s120506023
103. Nur BAM, Ahmed SK, Ali Z, et al. Agricultural produce sorting and grading using support vector machines and fuzzy logic. In: Proceedings of the 2009 IEEE International Conference on Signal and Image Processing Applications; 18–19 November 2009; Kuala Lumpur, Malaysia. pp. 391–396 doi: 10.1109/icsipa.2009.5478684
104. Yosef, Al Ohali. Computer vision-based date fruit grading system: Design and implementation. *Journal of King Saud University—Computer and Information Sciences* 2011; 23(1): 29–36. doi: 10.1016/j.jksuci.2010.03.003
105. Nandi CS, Tudu B, Koley C. An automated machine vision-based system for fruit sorting and grading. In: Proceedings of the 2012 Sixth International Conference on Sensing Technology (ICST); 18–21 December 2012; Kolkata, India. pp. 195–200. doi: 10.1109/icsenst.2012.6461669
106. Hadha A, Faris M, Utomo PG, et al. Portable smart sorting and grading machine for fruits using computer vision. In: Proceedings of the 2013 International Conference on Computer, Control, Informatics and Its Applications (IC3INA); 19–21 November 2013; Jakarta, Indonesia; pp. 71–75. doi: 10.1109/IC3INA.2013.6819151
107. Intellias. AI in agriculture—The future of farming. Available online: https://intellias.com/artificial-intelligence-in-agriculture/ (accessed on 26 January 2024).

108. Paymode AS, Mohite JN, Shinde UB, Malode VB. Artificial intelligence for agriculture: A technique of vegetables crop onion sorting and grading using deep learning. *International Journal Of Advance Scientific Research and Engineering Trends* 2021; 6(4). doi: 10.51319/2456-0774.2021.4.0004
109. Patil PU, Lande SB, Nagalkar VJ, et al. Grading and sorting technique of dragon fruits using machine learning algorithms. *Journal of Agriculture and Food Research* 2021; 4: 100118. doi: 10.1016/j.jafr.2021.100118
110. Mushiri T, Tende L. Automated grading of tomatoes using artificial intelligence: The case of Zimbabwe. In: Strydom M, Buckley S (editors). *AI and Big Data's Potential for Disruptive Innovation*. IGI Global; 2020. pp. 216–239. doi: 10.4018/978-1-5225-9687-5.ch008
111. Everaerts J. The use of unmanned aerial vehicles (UAVs) for remote sensing and mapping. *The International Archives of the Photogrammetry, Remote Sensing and Spatial Information Sciences* 2008; XXXVII: Part B1.
112. Colomina I, Molina P. Unmanned aerial systems for photogrammetry and remote sensing: A review. *ISPRS Journal of Photogrammetry and Remote Sensing* 2014; 92: 79–97. doi: 10.1016/j.isprsjprs.2014.02.013
113. Bendig J, Bolten A, Bareth G. Introducing a low-cost mini-UAV for thermal—And multispectral-imaging. *The International Archives of the Photogrammetry, Remote Sensing and Spatial Information Sciences* 2012; XXXIX-B1: 345–349. doi: 10.5194/isprsarchives-xxxix-b1-345-2012
114. Primicerio J, Di Gennaro SF, Fiorillo E, et al. A flexible unmanned aerial vehicle for precision agriculture. *Precision Agriculture* 2012; 13(4): 517–523. doi: 10.1007/s11119-012-9257-6
115. Garre P, Harish A. Autonomous agricultural pesticide spraying UAV. *IOP Conference Series: Materials Science and Engineering* 2018; 455: 012030. doi: 10.1088/1757-899X/455/1/0120
116. Malveaux C, Hall SG, Price R. Using drones in agriculture: unmanned aerial systems for agricultural remote sensing applications. *American Society of Agricultural and Biological Engineers* 2014. doi: 10.13031/aim.20141911016
117. Hogan SD, Kelly M, Stark B, et al. Unmanned aerial systems for agriculture and natural resources. *California Agriculture* 2017; 71(1): 5–14. doi: 10.3733/ca.2017a0002
118. El Bilali H, Allahyari MS. Transition towards sustainability in agriculture and food systems: Role of information and communication technologies. *Information Processing in Agriculture* 2018; 5(4): 456–464. doi: 10.1016/j.inpa.2018.06.006
119. Mogili UM, Deepak BBVL. Review on application of drone systems in precision agriculture. *Procedia Computer Science* 2018; 133: 502–509. doi: 10.1016/j.procs.2018.07.063
120. Veroustraete F. The rise of the drones in agriculture. *EC Agriculture 2.2* 2015; 325–327.
121. Puri V, Nayyar A, Raja L. Agriculture drones: A modern breakthrough in precision agriculture. *Journal of Statistics and Management Systems* 2017; 20(4): 507–518. doi: 10.1080/09720510.2017.1395171
122. Ahirwar S, Swarnkar R, Bhukya S, et al. Application of drone in agriculture. *International Journal of Current Microbiology and Applied Sciences* 2019; 8(01): 2500–2505. doi: 10.20546/ijcmas.2019.801.264
123. Ayamga M, Tekinerdogan B, Kassahun A. Exploring the challenges posed by regulations for the use of drones in agriculture in the African context. *Land* 2021; 10(2): 164. doi: 10.3390/land10020164
124. Ren Q, Zhang R, Cai W, et al. Application and development of new drones in agriculture. *IOP Conference Series: Earth and Environmental Science* 2020; 440(5): 052041. doi: 10.1088/1755-1315/440/5/052041
125. Garnot VSF, Landrieu L. Lightweight temporal self-attention for classifying satellite images time series. In: Proceedings of the International Workshop on Advanced Analytics and Learning on Temporal Data; 18 September 2020; Ghent, Belgium. pp. 171–181. doi: 10.1007/978-3-030-65742-0_12
126. Schneider M, Korner M. Harnessing administrative data inventories to create a reliable transnational reference database for crop type monitoring. In: Proceedings of the IGARSS 2022–2022 IEEE International Geoscience and Remote Sensing Symposium; 17–22 July 2022; Kuala Lumpur, Malaysia. pp. 5385–5388. doi: 10.1109/IGARSS46834.2022.9883089
127. Garnot VSF, Landrieu L. Panoptic segmentation of satellite image time series with convolutional temporal attention networks. In: Proceedings of the IEEE/CVF International Conference on Computer Vision (ICCV); 10–17 October 2021; Montreal, QC, Canada. pp. 4872–4881. doi: 10.48550/arXiv.2107.07933
128. Quinton F, Landrieu L. Crop rotation modeling for deep learning-based parcel classification from satellite time series. *Remote Sensing* 2021; 13(22): 4599. doi: 10.3390/rs13224599
129. Liu Y, Zhao W, Chen S, et al. Mapping crop rotation by using deeply synergistic optical and SAR time series. *Remote Sensing* 2021; 13(20): 4160. doi: 10.3390/rs13204160
130. Shiraly K. How computer vision in agriculture is boosting productivity and yields. Available online: https://www.width.ai/post/computer-vision-in-agriculture (accessed on 26 January 2024).
131. Stanhope TP, Adamchuk VI, Roux JD. Computer vision guidance of field cultivation for organic row crop production. *American Society of Agricultural and Biological Engineers Annual International Meeting* 2014. doi: 10.13031/aim.20141909498

132. Braeger S, Foroosh H. Curvature augmented deep learning for 3D object recognition. In: Proceedings of the 2018 25th IEEE International Conference on Image Processing (ICIP); 7–10 October 2018; Athens, Greece. pp. 3648–3652. doi: 10.1109/ICIP.2018.8451487
133. Cué La Rosa LE, Queiroz Feitosa R, Nigri Happ P, et al. Combining deep learning and prior knowledge for crop mapping in tropical regions from multitemporal SAR image sequences. *Remote Sensing* 2019; 11(17): 2029. doi: 10.3390/rs11172029
134. Niall OM, Sean C, Anderson C, et al. Deep learning vs. traditional computer vision. In: Arai K, Kapoor S (editors). *Advances in Computer Vision. CVC 2019. Advances in Intelligent Systems and Computing*. Springer, Cham; 2020. doi: 10.1007/978-3-030-17795-9_10
135. Syal A, Garg D, Sharma S. A survey of computer vision methods for counting fruits and yield prediction. *International Journal of Computer Science Engineering (IJCSE)* 2013; 2(6).
136. Boatswain Jacques AA, Adamchuk VI, Park J, et al. Towards a machine vision-based yield monitor for the counting and quality mapping of shallots. *Frontiers in Robotics and AI* 2021; 8. doi: 10.3389/frobt.2021.627067
137. Payne A, Walsh KB. Machine vision in estimation of fruit crop yield. In: *Plant Image Analysis: Fundamentals and Applications*. CRC Press; 2013. doi: 10.1201/b17441-17
138. Raphael L, Cohen O, Naor A. Determination of the number of green apples in RGB images recorded in orchards. *Computers and Electronics in Agriculture* 2012; 81: 45–57. doi: 10.1016/j.compag.2011.11.007
139. Pandit RB, Tang J, Liu F, et al. Development of a novel approach to determine heating pattern using computer vision and chemical marker (M-2) yield. *Journal of Food Engineering* 2007; 78(2): 522–528. doi: 10.1016/j.jfoodeng.2005.10.039
140. Patel HN, Jain RK, Joshi MV. Automatic segmentation and yield measurement of fruit using shape analysis. *International Journal of Computer Applications* 2012; 45(7): 19–24.
141. Yoosefzadeh-Najafabadi M, Earl HJ, Tulpan D, et al. Application of machine learning algorithms in plant breeding: Predicting yield from hyperspectral reflectance in soybean. *Frontiers in Plant Science* 2021; 11. doi: 10.3389/fpls.2020.624273
142. Kapach K, Barnea E, Mairon R, et al. Computer vision for fruit harvesting robots—State of the art and challenges ahead. *International Journal of Computational Vision and Robotics* 2012; 3(1/2): 4. doi: 10.1504/ijcvr.2012.046419
143. Chlingaryan A, Sukkarieh S, Whelan B. Machine learning approaches for crop yield prediction and nitrogen status estimation in precision agriculture: A review. *Computers and Electronics in Agriculture* 2018; 151: 61–69. doi: 10.1016/j.compag.2018.05.012
144. Kakani V, Nguyen VH, Kumar BP, et al. A critical review on computer vision and artificial intelligence in food industry. *Journal of Agriculture and Food Research* 2020; 2: 100033. doi: 10.1016/j.jafr.2020.100033
145. Boesch G. Top applications of computer vision in agriculture (2024 guide) Available online: https://viso.ai/applications/computer-vision-in-agriculture/ (accessed on 26 January 2024).
146. Ahmmed P, Reynolds J, Hamada S, et al. Novel 3D-printed electrodes for implantable biopotential monitoring. In: Proceedings of the 2021 43rd Annual International Conference of the IEEE Engineering in Medicine & Biology Society (EMBC); 1–5 November 2021; Mexico. pp. 7120–7123. doi: 10.1109/EMBC46164.2021.9630055
147. Wang Y, Mücher S, Wang W, et al. A review of three-dimensional computer vision used in precision livestock farming for cattle growth management. *Computers and Electronics in Agriculture* 2023; 206: 107687. doi: 10.1016/j.compag.2023.107687

Computing and Artificial Intelligence 2023; 1(1): 419.
Review Article

Deep insight: Navigating the horizons of deep learning in applications, challenges, and future frontiers

Rakesh Roshan[1,*], Om Prakash Rishi[2], Mothukuri Sridevi[1]

[1] *Department of Data Science, School of Engineering, Anurag University, Hyderabad, Telangana 500088, India*

[2] *Department of CSI, University of Kota, Rajasthan 324005, India*

*** Corresponding author:** Rakesh Roshan, RRoshan1980@gmail.com

ARTICLE INFO

Received: 1 November 2023
Accepted: 17 December 2023
Available online: 28 December 2023

doi: 10.59400/cai.v1i1.419

ABSTRACT: Deep learning, a powerful subset of artificial intelligence, has emerged as a transformative force shaping the landscape of technology. This research delves into the multifaceted realm of deep learning, exploring its diverse applications, confronting inherent challenges, and envisioning future prospects that beckon innovation. The journey begins with a comprehensive examination of how deep learning has catalyzed breakthroughs in various domains. In the realm of applications, the study meticulously dissects the impact of deep learning on natural language processing (NLP), computer vision, autonomous systems, medical and healthcare domains, financial forecasting, and more. From deciphering human language nuances to revolutionizing medical diagnostics and propelling autonomous vehicles, deep learning's applications redefine the possibilities of artificial intelligence. As the exploration of applications and challenges unfolds, the research pivots towards the future horizons of deep learning. It contemplates the trajectory of explainable AI (XAI), the promises held by transfer learning, the integration of deep learning with quantum computing and neuromorphic architectures, and the ethical dimensions that will shape the evolution of AI for the greater good. The abstract encapsulates a panoramic view of "Deep Insight", where deep learning transcends its current achievements, confronting challenges head-on and embracing a future characterized by responsible innovation. This research invites stakeholders, researchers, and enthusiasts to embark on a journey of exploration, discovery, and contemplation, as the realm of deep learning continues to unfold its vast and captivating horizons.

KEYWORDS: deep learning; artificial intelligence; convolutional neural networks; explainable AI

1. Introduction

In the ever-expanding universe of artificial intelligence, one paradigm stands out as a powerful force reshaping the landscape of machine learning: Deep learning. This transformative approach, inspired by the intricacies of the human brain, has propelled machines into realms of cognitive capabilities that were once the realm of science fiction. As we embark on a journey into the heart of this neural tapestry, let's unravel the fundamental concepts and applications that define the captivating world of deep learning.

1.1. The genesis of deep learning

The "Genesis of Deep Learning" refers to the origin and foundational principles that gave rise to this transformative paradigm in artificial intelligence. The term "genesis" signifies the birth or beginning, and in the context of deep learning, it encompasses the historical development and fundamental concepts that laid the groundwork for the evolution of this powerful approach.

1.1.1. Evolution of neural networks

The journey begins with the conceptualization and evolution of artificial neural networks. Neural networks draw inspiration from the structure and functioning of the human brain, were interconnected neurons process information. The idea of using mathematical constructs to mimic neural connections dates back to the mid-20th century, with early models like the perceptron.

1.1.2. Rise of multilayer neural networks

The pivotal moment in the genesis of deep learning occurred with the realization that deeper neural networks, consisting of multiple layers, could potentially capture more complex patterns and representations in data. While early neural networks were relatively shallow, the breakthrough came with the understanding that adding more layers could enhance the learning capacity of the network.

1.1.3. Backpropagation algorithm

The development of the backpropagation algorithm was a critical milestone. This algorithm, introduced in the 1970s and later refined in the 1980s, enabled efficient training of multilayer neural networks. Backpropagation involves adjusting the weights of the connections between neurons in a network to minimize the difference between the predicted and actual outcomes, allowing the network to learn from data.

1.1.4. Challenges and resurgence

Despite these advancements, the practical application of deep neural networks faced challenges, including difficulties in training deep architectures. The field experienced a period of reduced interest and attention, often referred to as the "AI winter". However, the resurgence of deep learning in the 21st century was fueled by factors such as the availability of large datasets, increased computational power, and innovative techniques like dropout regularization.

1.1.5. Convolutional neural networks (CNNs) and deep learning renaissance

The introduction of specialized architectures like Convolutional Neural Networks (CNNs) further propelled the effectiveness of deep learning, especially in image-related tasks. The success of deep learning in various competitions and benchmarks, such as the ImageNet Large Scale Visual Recognition Challenge, marked a renaissance in the field, capturing widespread attention and establishing deep learning as a dominant paradigm.

1.2. Neural networks: The building blocks

"Neural Networks: The Building Blocks" refers to the fundamental components and principles that constitute the architecture of deep learning models. Neural networks, inspired by the structure and functioning of the human brain, serve as the foundational building blocks of deep learning systems. This section outlines key concepts related to neural networks:

1.2.1. Neural network structure

- Neurons: In a neural network, the basic processing units are called neurons. Each neuron is a mathematical entity that receives input, processes it using an activation function, and produces an output.
- Layers: Neurons are organized into layers. A typical neural network consists of an input layer, one or more hidden layers, and an output layer. The input layer receives the initial data, hidden layers process this information, and the output layer produces the final results.
- Weights and Connections: Connections between neurons are represented by weights. These weights determine the strength of the connection between neurons. During training, these weights are adjusted to optimize the network's performance.

1.2.2. Neural network training

- Forward Propagation: During the training phase, data is fed into the neural network through the input layer. The data is then processed layer by layer through the hidden layers using the assigned weights. The final output is generated through the output layer.
- Loss Function: The output is compared to the actual target values using a loss function. The loss function quantifies the difference between the predicted and actual values.
- Backpropagation: The backpropagation algorithm is employed to adjust the weights in a way that minimizes the loss. It calculates the gradient of the loss function with respect to the weights and updates the weights accordingly. This iterative process is crucial for training the neural network to make accurate predictions.

1.2.3. Activation functions

- Sigmoid and Hyperbolic Tangent (tanh): These functions introduce non-linearity to the network, allowing it to model complex relationships in the data. They squash the input values to a specific range, making them suitable for classification tasks.
- Rectified Linear Unit (ReLU): ReLU is a widely used activation function that introduces non-linearity by outputting the input for positive values and zero for negative values. It helps the network learn complex patterns and speeds up training.

1.2.4. Neural network architectures

- Feedforward Neural Networks (FNN): In FNNs, information moves in one direction—from the input layer through the hidden layers to the output layer. These networks are commonly used for tasks like classification and regression.
- Recurrent Neural Networks (RNN): RNNs are designed to work with sequential data. They have connections that form cycles, allowing them to capture temporal dependencies. RNNs are often used in tasks like natural language processing and time series analysis.
- Convolutional Neural Networks (CNN): CNNs are specialized for processing grid-like data, such as images. They use convolutional layers to automatically and adaptively learn hierarchical features from the input.

1.3. Learning from data

Deep learning models learn by example. Through a process called training, these models are exposed to vast amounts of labeled data, allowing them to adjust their internal parameters to make accurate

predictions or classifications. The iterative nature of this learning process enables neural networks to generalize from the training data and perform well on new, unseen data.

1.4. Architectures shaping the future

Convolutional Neural Networks (CNNs), Recurrent Neural Networks (RNNs), and Generative Adversarial Networks (GANs) are among the architectures that have pushed the boundaries of deep learning. CNNs excel in image and video analysis, RNNs handle sequential data such as time series or natural language, and GANs unleash creativity by generating realistic data.

1.5. Applications transforming industries

Deep learning has permeated various domains, leaving an indelible mark on industries. In Natural Language Processing (NLP), machines now comprehend and generate human-like text. Computer Vision applications, from image recognition to object detection, have redefined how machines interpret visual data. Healthcare benefits from accurate medical imaging analysis, while autonomous systems navigate complex environments with enhanced precision.

1.6. Challenges and ethical considerations

The ascent of deep learning is not without challenges. Model interpretability remains a puzzle, and ethical concerns, including biases in training data and decision-making opacity, demand careful consideration. Striking a balance between innovation and ethical deployment becomes imperative as deep learning continues to evolve.

1.7. The future horizon

As we stand on the precipice of technological evolution, the future of deep learning unfolds with promises of Explainable AI (XAI), transfer learning, and the integration of deep learning with quantum computing and neuromorphic architectures. The trajectory is not only about technological advancement but also about ethical considerations that guide the responsible deployment of AI for the greater good.

In conclusion, this introduction to deep learning is a gateway into a realm where algorithms simulate the complexity of the human brain, transforming how machines perceive, learn, and make decisions. As we journey deeper into the neural tapestry, the fusion of human ingenuity and technological prowess promises to reshape the very fabric of our technological future.

2. Literature review

The exploration of deep learning and its multifaceted dimensions has been a topic of extensive research and scholarly inquiry. This literature review provides an overview of key studies, seminal works, and critical perspectives that shape the narrative of "Deep Insight: Navigating the Horizons of Deep Learning in Applications, Challenges, and Future Frontiers."

2.1. Foundational studies in deep learning

This foundational paper by LeCun, Bengio, and Hinton outlines the core principles of deep learning, emphasizing the importance of neural networks with multiple layers. It serves as a cornerstone for understanding the fundamental concepts that underpin the transformative power of deep learning[1].

2.2. Applications of deep learning

This study provides a comprehensive guide to the applications of deep learning in healthcare. It explores how deep learning models contribute to medical imaging analysis, disease diagnosis, and personalized medicine, offering insights into the transformative impact on patient care[2].

Dr. Eric Topol's work delves into the convergence of human and artificial intelligence in medicine. It explores the potential of deep learning to enhance the performance of medical practitioners, emphasizing the synergy between human expertise and machine intelligence[3].

2.3. Challenges and ethical considerations

Overfitting is a perennial challenge in deep learning. Caruana et al.'s work discusses strategies such as backpropagation and early stopping to mitigate overfitting, shedding light on one of the key challenges faced in training deep neural networks[4].

Ethical considerations and safety in AI are explored in this seminal work. The paper discusses concrete challenges in AI safety, emphasizing the importance of responsible AI development and deployment—a critical aspect when navigating the frontiers of deep learning[5].

2.4. Future prospects and innovations

As we look towards the future, the paper by Carvalho and Cohen discusses the role of regulations, such as the General Data Protection Regulation (GDPR), in safeguarding digital rights. It offers insights into the ethical and legal considerations that will shape the future of deep learning applications[6].

The concept of federated machine learning represents an innovative direction for the future. This work explores the potential and applications of federated learning, providing a glimpse into how collaborative and decentralized approaches could shape the landscape of deep learning[7].

3. Applications of deep learning

This section delves into the diverse applications of deep learning across various domains mentioned in **Figure 1**. Subsections may include:

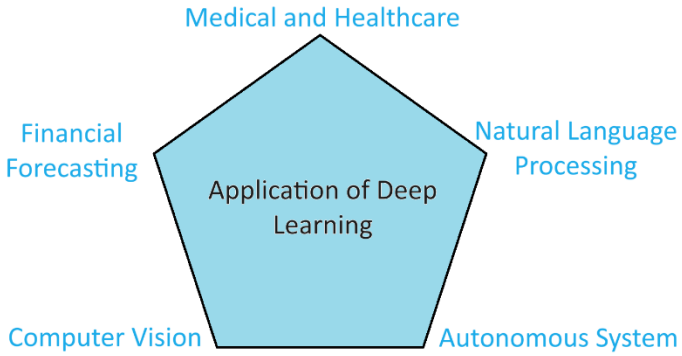

Figure 1. Applications of deep learning.

3.1. Medical and healthcare applications

3.1.1. Medical imaging

Deep learning has revolutionized medical imaging with its ability to extract complex features from images. Convolutional Neural Networks (CNNs) are widely employed for tasks such as:

MRI and CT Image Analysis: CNNs are used for segmentation, tumor detection, and classification in magnetic resonance imaging (MRI) and computed tomography (CT) scans.

X-ray and Radiography: Deep learning models aid in detecting abnormalities, fractures, and diseases in X-ray and radiography images.

Ultrasound Imaging: CNNs contribute to the analysis of ultrasound images for various applications, including fetal imaging and organ assessment[2].

3.1.2. Disease diagnosis and prediction

Deep learning models excel in diagnosing diseases and predicting patient outcomes by analyzing diverse data sources:

Pathology Image Analysis: CNNs aid pathologists in diagnosing diseases from histopathology images, improving accuracy and efficiency.

Electronic Health Records (EHRs): Recurrent Neural Networks (RNNs) analyze EHRs for disease prediction and personalized treatment planning[2].

3.1.3. Drug discovery and development

Deep learning accelerates drug discovery processes and improves drug development pipelines:

Chemoinformatics: Graph Neural Networks (GNNs) are applied to model molecular structures, aiding in drug design and discovery.

Biological Image Analysis: CNNs analyze cellular and molecular images, facilitating drug target identification and validation[3].

3.1.4. Personalized medicine

Deep learning facilitates the implementation of personalized medicine by analyzing individual patient data:

Genomic Data Analysis: Deep learning models analyze genomic data for disease risk prediction and personalized treatment strategies.

Clinical Decision Support Systems: NLP techniques powered by deep learning extract insights from unstructured clinical notes, aiding in treatment decisions[4].

3.1.5. Remote patient monitoring

Deep learning contributes to remote patient monitoring through the analysis of continuous health data:

Wearable Devices: Deep learning models process data from wearable devices, monitoring vital signs, activity levels, and health metrics in real-time.

IoT in Healthcare: Deep learning aids in analyzing data from IoT devices for preventive healthcare and early detection of anomalies[5].

3.1.6. Surgical assistance and robotics

Deep learning enhances surgical procedures and robotic interventions in healthcare:

Surgical Image Analysis: CNNs analyze surgical images for real-time decision support, improving precision and reducing errors.

Robotic Surgery: Deep learning models assist in robot-assisted surgeries by enhancing navigation, object recognition, and dexterity[6].

3.2. Natural language processing

Natural Language Processing (NLP) has witnessed a paradigm shift with the integration of deep learning, revolutionizing how machines understand and generate human language. This section provides a detailed overview of the applications of deep learning in NLP, encompassing various tasks from sentiment analysis to language translation.

3.2.1. Sentiment analysis

Deep learning models, particularly recurrent neural networks (RNNs) and long short-term memory (LSTM) networks, have proven highly effective in sentiment analysis. They can discern emotions expressed in textual data, enabling businesses to gauge customer sentiment, adapt marketing strategies, and enhance user experiences.

3.2.2. Named entity recognition (NER) and information extraction

Deep learning excels in NER tasks, extracting entities such as names, locations, and organizations from unstructured text. Models like Bidirectional LSTMs and transformer-based architectures, such as BERT (Bidirectional Encoder Representations from Transformers), have achieved state-of-the-art results in information extraction.

3.2.3. Text summarization

Abstractive and extractive text summarization benefit significantly from deep learning models. Recurrent and transformer-based architectures capture contextual information to generate concise and coherent summaries, aiding in information retrieval and comprehension.

3.2.4. Language translation

The advent of sequence-to-sequence models, notably using attention mechanisms, has revolutionized language translation. Neural machine translation (NMT) models, often based on recurrent or transformer architectures, have achieved remarkable accuracy in translating text between multiple languages.

3.2.5. Question-answering systems

Deep learning models, particularly those incorporating attention mechanisms and pre-trained language representations (e.g., BERT), have enhanced question-answering systems. These systems can understand context, infer relationships, and provide accurate responses based on diverse textual data.

3.2.6. Dialogue systems and chatbots

Recurrent and transformer-based architectures have empowered the development of intelligent dialogue systems and chatbots. These systems leverage contextual information to engage in natural and coherent conversations, enhancing user interactions in various domains.

3.2.7. Aspect-based sentiment analysis

Deep learning models are applied to extract fine-grained sentiments associated with specific aspects or features in reviews. This approach provides more nuanced insights, helping businesses understand customer feedback at a granular level.

3.2.8. Conclusions

The amalgamation of deep learning with NLP has propelled the field to unprecedented heights, enabling machines to understand and generate human-like language. From sentiment analysis to language translation, the applications outlined showcase the versatility and transformative potential of deep learning in NLP. As we navigate challenges and chart future directions, the synergy between linguistic expertise and deep learning innovations remains pivotal for advancing the frontiers of natural language processing.

3.3. Autonomous system

Autonomous systems, ranging from self-driving cars to drones and robotic platforms, have undergone a transformative evolution with the integration of deep learning. This section provides a detailed exploration of how deep learning algorithms contribute to the perception, decision-making, and control processes within autonomous systems.

3.3.1. Object detection and recognition

Deep learning, particularly convolutional neural networks (CNNs), has revolutionized object detection in autonomous systems. State-of-the-art models such as YOLO (You Only Look Once) and Faster R-CNN excel in real-time identification and localization of objects, enhancing the ability of self-driving cars and drones to navigate complex environments.

3.3.2. Semantic segmentation

In autonomous systems, understanding the semantics of the surrounding environment is crucial. Deep learning models, including fully convolutional networks (FCNs) and U-Net, enable pixel-level segmentation, distinguishing between different elements in the scene. This aids in path planning and obstacle avoidance.

3.3.3. Simultaneous localization and mapping (SLAM)

Deep learning enhances SLAM techniques by providing robust feature extraction and matching capabilities. Visual SLAM, in particular, benefits from deep neural networks in estimating the pose of the autonomous system and creating detailed maps of the environment.

3.3.4. Sensor fusion

Autonomous systems often rely on a combination of sensors such as cameras, LiDAR, and radar. Deep learning facilitates sensor fusion, integrating information from multiple sources to create a comprehensive and accurate representation of the environment. This improves the system's perception capabilities and reliability.

3.3.5. Path planning and decision-making

Reinforcement learning (RL) and deep reinforcement learning (DRL) play a crucial role in autonomous system decision-making. These models learn optimal policies through interaction with the environment, enabling self-driving cars and robots to make real-time decisions on navigation and task execution.

3.3.6. Human-robot interaction

Deep learning contributes to natural and intuitive human-robot interaction in autonomous systems. This includes understanding and responding to human gestures, speech, and intentions, enhancing the collaboration between autonomous robots and their human counterparts.

3.3.7. Conclusions

Deep learning has ushered in a new era for autonomous systems, enhancing their perception, decision-making, and interaction capabilities. From object detection to path planning and human-robot collaboration, the applications highlighted underscore the pivotal role of deep learning in shaping the future of autonomous technologies. As we navigate challenges and forge ahead, the synergy between advanced deep learning models and domain-specific expertise remains key for unlocking the full potential of autonomous systems.

3.4. Computer vision

Computer vision, propelled by deep learning, has witnessed unprecedented advancements, transforming the way machines interpret and understand visual information. This section provides an in-depth exploration of the diverse applications of deep learning in computer vision, spanning image and video analysis, object recognition, and scene understanding.

3.4.1. Image classification and recognition

Deep learning, particularly convolutional neural networks (CNNs), has revolutionized image classification tasks. Models such as AlexNet, VGG, and ResNet have achieved breakthroughs in accurately categorizing objects within images, laying the foundation for various computer vision applications.

3.4.2. Object detection

State-of-the-art object detection models, including Faster R-CNN, YOLO, and SSD, leverage deep learning to precisely locate and classify objects within images. This technology finds applications in surveillance, autonomous vehicles, and robotics, enhancing the ability to identify and track objects in real-time.

3.4.3. Image segmentation

Deep learning models, such as U-Net and Mask R-CNN, have transformed image segmentation by providing pixel-level accuracy in distinguishing object boundaries. This technology is crucial for medical image analysis, autonomous systems, and scene understanding, enabling more detailed and precise visual comprehension.

3.4.4. Video analysis and action recognition

Recurrent neural networks (RNNs) and 3D convolutional networks excel in video analysis and action recognition. Deep learning models can capture temporal dependencies in video sequences, enabling applications such as surveillance, human-computer interaction, and content analysis in video streaming platforms.

3.4.5. 3D object recognition and pose estimation

Deep learning extends its capabilities to 3D object recognition and pose estimation. Models like PointNet and PoseNet leverage neural networks to analyze point clouds and estimate the spatial orientation of objects. This is crucial in robotics, augmented reality, and manufacturing processes.

3.4.6. Cross-modal image and text understanding

Deep learning facilitates the integration of image and text data, enabling cross-modal understanding. Models like Visual Question Answering (VQA) systems leverage both visual and textual information to

comprehend and respond to queries about images, fostering more nuanced interactions between machines and users.

3.4.7. Conclusion

The integration of deep learning into computer vision has not only propelled the accuracy of visual tasks but has also broadened the scope of applications across industries. From image classification to video analysis and 3D object recognition, the versatility and transformative potential of deep learning in computer vision continue to redefine the possibilities of visual perception by machines. Navigating challenges and embracing future research directions will undoubtedly shape the evolution of computer vision powered by deep learning.

3.5. Financial forecasting

Deep learning has emerged as a powerful tool in the financial sector, transforming the landscape of forecasting, risk assessment, and decision-making. This section provides an in-depth exploration of the applications of deep learning in financial forecasting, including stock price prediction, fraud detection, and credit risk assessment.

3.5.1. Stock price prediction

Deep learning models, particularly recurrent neural networks (RNNs) and long short-term memory (LSTM) networks, have shown promise in predicting stock prices. By analyzing historical price data, these models capture temporal dependencies and patterns, providing insights for traders and investors. Notable architectures such as Gated Recurrent Units (GRUs) and attention mechanisms enhance the accuracy of predictions.

3.5.2. Time series analysis

Deep learning models, including various recurrent and convolutional architectures, contribute to accurate time series analysis in financial markets. They enable the identification of trends, seasonality, and irregularities, facilitating more informed decision-making in areas such as algorithmic trading and portfolio management.

3.5.3. Fraud detection

Deep learning plays a crucial role in fraud detection by analyzing patterns and anomalies in financial transactions. Models employing autoencoders, recurrent neural networks, and deep belief networks can identify unusual behaviors, potentially indicating fraudulent activities. This application enhances the security and integrity of financial systems.

3.5.4. Credit scoring and risk assessment

Deep learning models contribute to more accurate credit scoring and risk assessment in financial institutions. By analyzing diverse data sources, including credit history, transaction records, and social media data, these models provide a comprehensive evaluation of an individual's or a company's creditworthiness, thereby improving lending decisions.

3.5.5. Portfolio optimization

Deep learning facilitates portfolio optimization by analyzing historical market data and identifying optimal asset allocations. Reinforcement learning techniques, such as deep Q-networks, contribute to dynamic and adaptive portfolio management, considering changing market conditions and risk preferences.

3.5.6. Conclusions

The application of deep learning in financial forecasting has reshaped traditional approaches, providing enhanced accuracy and insights. From predicting stock prices to fraud detection and credit risk assessment, the integration of deep learning in finance continues to evolve. As the financial industry embraces these innovations, addressing challenges and exploring future directions will be instrumental in unlocking the full potential of deep learning for robust and reliable financial forecasting.

4. Challenges in deep learning

Deep learning, while powerful and versatile, comes with its set of challenges mentioned in **Figure 2**. Here are some of the prominent challenges in deep learning:

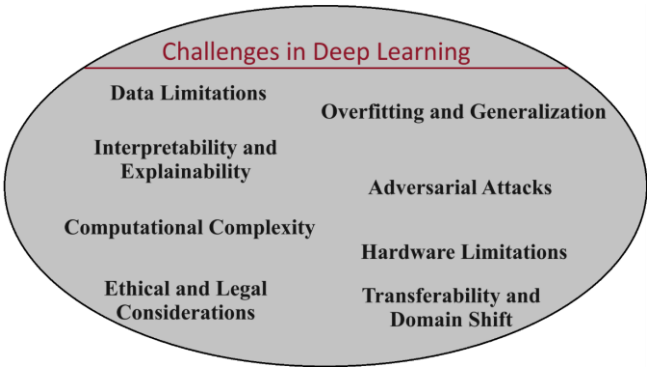

Figure 2. Challenges in deep learning.

4.1. Data limitations

One significant challenge in deep learning is the requirement for large amounts of labeled data for training robust models. Acquiring and annotating massive datasets can be expensive and time-consuming. Transfer learning and data augmentation are techniques used to mitigate this challenge, allowing models to generalize from limited labeled data[1].

The requirement for a vast amount of labeled medical data poses a challenge, particularly when dealing with rare conditions or diseases with diverse manifestations. In this scenario, the deep learning model may struggle to generalize to different cases due to insufficient data representation of certain conditions. Acquiring a diverse and representative dataset is crucial for training a robust model that can accurately identify a spectrum of respiratory anomalies.

To address the data limitations, practitioners often resort to transfer learning and data augmentation strategies. Transfer learning involves leveraging pre-trained models on larger datasets (e.g., general image datasets) and fine-tuning them on the specific task with the limited medical dataset. This approach allows the model to benefit from knowledge gained in unrelated domains.

Additionally, data augmentation involves artificially expanding the dataset by applying transformations to the existing images, such as rotations, flips, and slight variations in brightness or contrast. This technique enhances the model's ability to recognize patterns and features, even when trained on a smaller set of labeled data.

4.2. Interpretability and explainability

Deep learning models are often viewed as "black boxes" due to their complexity, making it challenging to interpret and understand their decision-making processes. Ensuring the interpretability

and explainability of models is crucial, especially in applications where trust and accountability are paramount[4].

4.3. Computational complexity

Training deep learning models, especially large architectures like deep neural networks, can be computationally intensive and require substantial resources. High computational demands can limit the accessibility of deep learning to researchers and organizations with significant computing power[8].

4.4. Ethical and legal considerations

Ethical challenges in deep learning include issues related to bias in training data, fairness, accountability, and transparency. Addressing these concerns is crucial to prevent discriminatory outcomes and ensure that deep learning systems are deployed ethically[9].

4.5. Overfitting and generalization

Deep learning models may suffer from overfitting, where they perform well on the training data but fail to generalize to new, unseen data. Techniques such as regularization, dropout, and cross-validation are employed to address overfitting and improve model generalization[10].

4.6. Adversarial attacks

Deep learning models are vulnerable to adversarial attacks, where carefully crafted input data can mislead the model's predictions. Robustness against adversarial attacks is a critical concern, particularly in applications where security and safety are paramount[11].

4.7. Hardware limitations

The efficient training and deployment of deep learning models require powerful hardware, such as Graphics Processing Units (GPUs) or specialized accelerators. Access to and affordability of such hardware can be a limiting factor for researchers and smaller organizations[12].

4.8. Transferability and domain shift

Deep learning models trained on one dataset may not perform well when applied to a different distribution or domain. Adapting models to new domains, known as domain adaptation, is a challenge that arises in scenarios where the training and deployment environments differ[13].

Addressing these challenges requires ongoing research and collaboration across the deep learning community, as well as advancements in algorithmic approaches and model architectures.

5. Future prospects of deep learning: Navigating towards innovation

5.1. Explainable AI (XAI)

The quest for more interpretable and transparent deep learning models is a burgeoning area of research. Explainable AI (XAI) aims to enhance the interpretability of complex models, making their decisions more understandable and trustworthy for users and stakeholders[6].

Consider the deployment of a deep learning model for credit scoring in a financial institution. The model is designed to assess the creditworthiness of loan applicants based on a variety of features, including financial history, income, and debt-to-income ratio.

One of the challenges with deep learning models, especially complex ones like neural networks, is their inherent lack of interpretability. In the financial sector, understanding the decision-making process

of a model is crucial for regulatory compliance, risk assessment, and building trust with customers. The black-box nature of deep neural networks can be a barrier to adoption in sensitive domains like finance.

To address this challenge, an Explainable AI (XAI) approach is implemented. Instead of relying solely on a complex neural network for credit scoring, an interpretable model, such as a decision tree or rule-based system, is employed alongside the deep learning model.

5.2. Transfer learning and few-shot learning

The evolution of transfer learning and few-shot learning promises to improve the generalization capabilities of deep learning models. This includes the ability to leverage knowledge gained from one task or domain to enhance performance on new, related tasks with limited labeled data[7].

5.3. Hybrid models and integrative approaches

The integration of deep learning with other AI paradigms, such as symbolic reasoning and knowledge representation, is gaining attention. Hybrid models that combine the strengths of deep learning with rule-based systems could lead to more robust and versatile AI systems[14].

5.4. AI for good

The application of deep learning for societal benefits, often termed "AI for Good", is an emerging trend. This includes leveraging deep learning in healthcare for disease diagnosis and drug discovery, in environmental monitoring for climate modeling, and in education for personalized learning[3].

5.5. Quantum computing and neuromorphic architectures

The intersection of deep learning with quantum computing and neuromorphic architectures holds promise for overcoming current computational limitations. Quantum computing may enable faster training and inference, while neuromorphic computing architectures seek to mimic the brain's structure for more efficient and brain-inspired learning[15].

5.6. AI Ethics and responsible AI

As deep learning systems become more pervasive, addressing ethical considerations becomes imperative. The future involves integrating principles of fairness, accountability, transparency, and ethical use into the development and deployment of deep learning models[16].

5.7. Edge computing for deep learning

The integration of deep learning with edge computing aims to bring computation closer to the data source, reducing latency and enhancing privacy. This is particularly important in applications such as IoT, where real-time processing is crucial[17].

As the field of deep learning continues to advance, these future prospects highlight the multifaceted directions that researchers and practitioners are exploring. The synergy of technological innovation, ethical considerations, and interdisciplinary collaboration will play a pivotal role in shaping the future of deep learning.

6. Conclusion

The journey through the realms of deep learning reveals a transformative landscape, where innovation converges with challenges, and the future beckons with promising horizons. Deep learning,

characterized by the ascendancy of neural networks with multiple layers, has evolved into a cornerstone of artificial intelligence, revolutionizing diverse domains and applications.

In the domain of natural language processing (NLP), deep learning has propelled machines into realms of linguistic comprehension once deemed insurmountable. From sentiment analysis and language translation to question-answering systems, the versatility of deep learning models has endowed machines with a nuanced understanding of human language. Yet, challenges persist, including the need for interpretability and the ethical considerations inherent in the development of language models.

The foray into computer vision unveils a world where deep learning is the linchpin of visual perception. Image classification, object detection, and video analysis showcase the prowess of convolutional neural networks (CNNs) and recurrent architectures. Deep learning in computer vision, however, grapples with challenges of interpretability and ethical implications, necessitating a delicate balance between innovation and responsible deployment.

Autonomous systems, guided by deep learning algorithms, are poised to redefine the future of transportation, robotics, and beyond. Object detection, simultaneous localization and mapping (SLAM), and human-robot interaction underscore the transformative potential of deep learning in autonomous technologies. Nevertheless, challenges such as safety concerns, adaptability to dynamic environments, and the ethical dimensions of decision-making loom large on the horizon.

Venturing into the intricate domain of medical and healthcare applications, deep learning emerges as a beacon of hope for accurate diagnostics, personalized medicine, and remote patient monitoring. From medical imaging to natural language processing in healthcare, the integration of deep learning augurs well for improved patient outcomes. Challenges, however, encompass data privacy, interpretability, and the need for robust models in the face of evolving medical landscapes.

In financial forecasting, deep learning charts a course towards enhanced predictive analytics, fraud detection, and risk assessment. The future promises innovations in explainable AI (XAI), transfer learning, and ethical considerations, ensuring that financial systems harness the power of deep learning responsibly.

As we navigate these applications, the future prospects of deep learning unveil a tapestry woven with threads of innovation and responsibility. Explainable AI strives to demystify complex models, while transfer learning and hybrid approaches promise to enhance model generalization. The trajectory towards "AI for Good" underscores the societal impact of deep learning, where technology serves as a force for positive change.

In the realm of quantum computing and neuromorphic architectures, the fusion of deep learning with cutting-edge technologies offers a glimpse into a future where computational boundaries are pushed beyond conventional limits. Ethical considerations stand as sentinels, guarding against biases and ensuring that the ethical dimensions of AI are woven into the fabric of technological advancements.

Edge computing heralds a future where deep learning converges with the decentralized power of computation, ushering in a new era of real-time processing and privacy preservation. Responsible AI becomes the lodestar, guiding the ethical deployment of deep learning models in a world where the impacts of technology are far-reaching.

In conclusion, the Odyssey through deep learning is a testament to the ever-evolving synergy between human ingenuity and technological prowess. Challenges are the crucibles that refine innovation, and ethical considerations are the compasses that steer us towards responsible deployment. As we

navigate the depths of deep learning, the future promises not just technological advancements but a harmonious balance between innovation and ethical stewardship, shaping a future where deep learning serves as a catalyst for positive transformation across diverse facets of human life.

Conflict of interest

We declare that there are no conflicts of interest associated with this review article.

References

1. LeCun Y, Bengio Y, Hinton G. Deep learning. *Nature* 2015; 521: 436–444. doi: 10.1038/nature14539
2. Esteva A, Robicquet A, Ramsundar B, et al. A guide to deep learning in healthcare. *Nature Medicine* 2019; 25: 24–29. doi: 10.1038/s41591-018-0316-z
3. Topol EJ. High-performance medicine: The convergence of human and artificial intelligence. *Nature Medicine* 2019; 25: 44–56. doi: 10.1038/s41591-018-0300-7
4. Caruana R, Lawrence S, Giles C. Overfitting in neural nets: backpropagation, conjugate gradient, and early stopping. In: Leen T, Dietterich T, Tresp V (editors). *Advances in Neural Information Processing Systems*. MIT Press; 2000. pp. 402–408.
5. Amodei D, Olah C, Steinhardt J, et al. Concrete problems in AI safety. Available online: https://arxiv.org/abs/1606.06565 (accessed on 25 December 2023).
6. Carvalho VF, Cohen IG. The general data protection regulation as a guardian of digital rights. *Science* 2019; 364(6439): 1235–1237.
7. Yang Q, Liu Y, Chen T, et al. Federated machine learning. *ACM Transactions on Intelligent Systems and Technology* 2019; 10(2): 1–19. doi: 10.1145/3298981
8. Chen XW, Lin X. Big data deep learning: Challenges and perspectives. *IEEE Access* 2014; 2: 514–525. doi: 10.1109/access.2014.2325029
9. Amodei D, Olah C, Steinhardt J, et al. Concrete problems in AI safety. Available online: https://arxiv.org/abs/1606.06565 (accessed on 25 December 2023).
10. Goodfellow I, Bengio Y, Courville A. *Deep Learning*. MIT Press; 2016.
11. Szegedy C, Zaremba W, Sutskever I, et al. Intriguing properties of neural networks. Available online: https://arxiv.org/abs/1312.6199 (accessed on 25 December 2023).
12. Dean J, Corrado G, Monga R, et al. Large scale distributed deep networks. In: Pereira F, Burges CJ, Bottou L, Weinberger KQ (editors). *Advances in Neural Information Processing Systems 25: 26th Annual Conference on Neural Information Processing Systems 2012*. Curran Associates, Inc.; 2013. pp. 1223–1231.
13. Pan SJ, Yang Q. A survey on transfer learning. *IEEE Transactions on Knowledge and Data Engineering* 2010; 22(10): 1345–1359. doi: 10.1109/tkde.2009.191.
14. Marcus G. Deep learning: A critical appraisal. Available online: https://arxiv.org/abs/1801.00631 (accessed on 25 December 2023).
15. Aaronson S. Read the fine print. *Nature Physics* 2015; 11: 291–293. doi: 10.1038/nphys3272.
16. Floridi L, Cowls J. A unified framework of five principles for AI in society. *Harvard Data Science Review* 2019; 1(1). doi: 10.1162/99608f92.8cd550d1
17. Satyanarayanan M. The emergence of edge computing. *Computer* 2017; 50(1): 30–39. doi: 10.1109/mc.2017.9

Academic Publishing Pte. Ltd.

Add: 73 Upper Paya Lebar Road #07-02B-01 Centro Bianco Singapore 534818

Tel: +65 83184869

E-mail: editorial_office@acad-pub.com

Web: http://ojs.acad-pub.com/